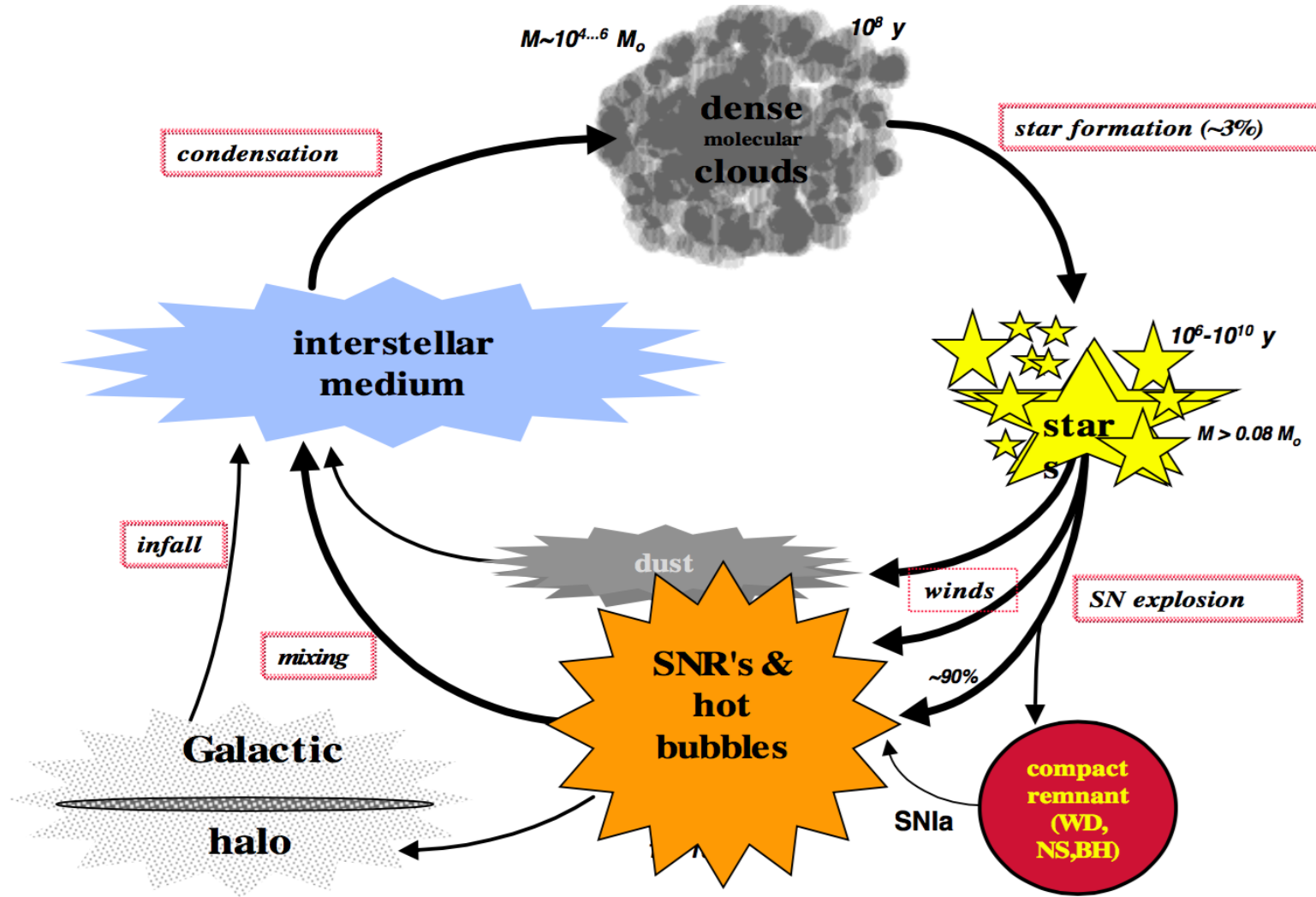


# Astrofisica Nucleare e Subnucleare

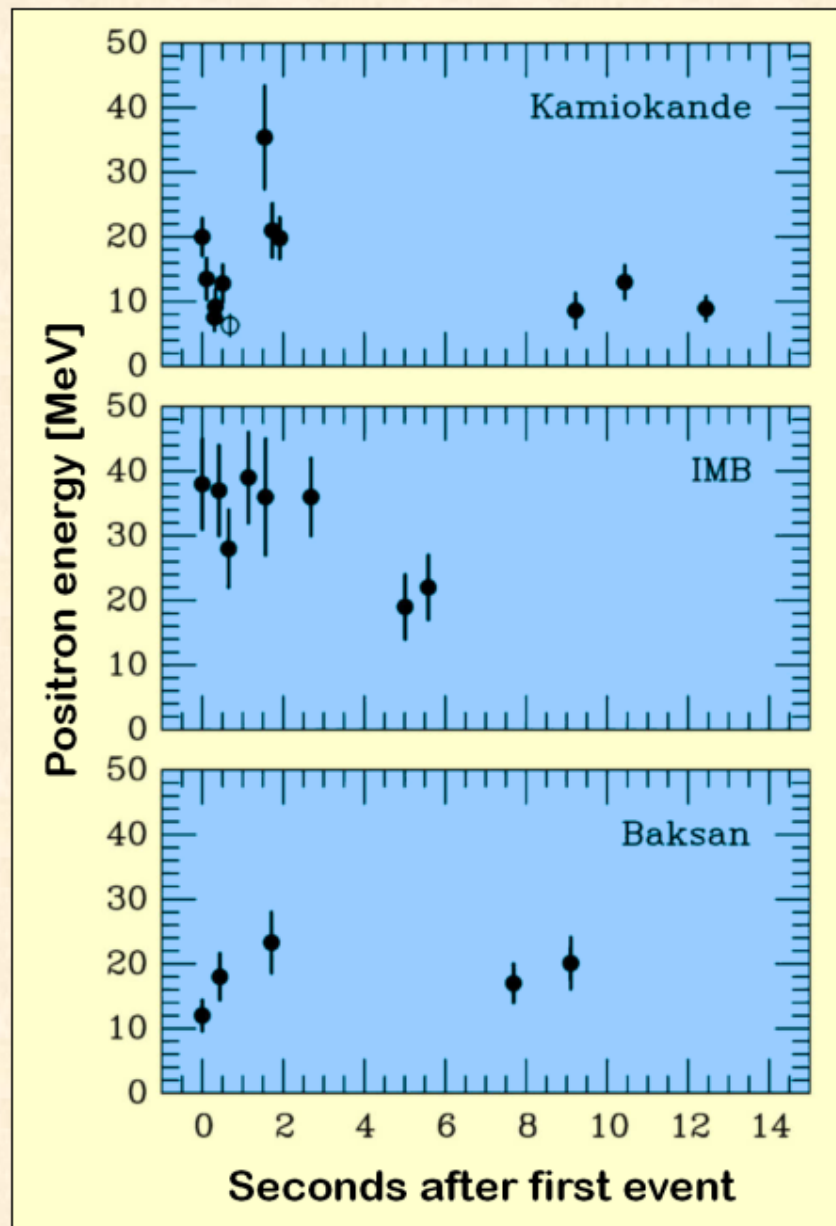
## Neutrino Astrophysics

# Cosmic Cycle





# Neutrino Signal of Supernova 1987A



Kamiokande (Japan)  
Water Cherenkov detector  
Clock uncertainty  $\pm 1$  min

Irvine-Michigan-Brookhaven  
(USA)  
Water Cherenkov detector  
Clock uncertainty  $\pm 50$  ms

Baksan Scintillator Telescope  
(Soviet Union)  
Clock uncertainty  $+2/-54$  s

Within clock uncertainties,  
signals are contemporaneous

# Astrofisica Nucleare e Subnucleare

## Supernovae Neutrinos

# SuperNovae Remnants

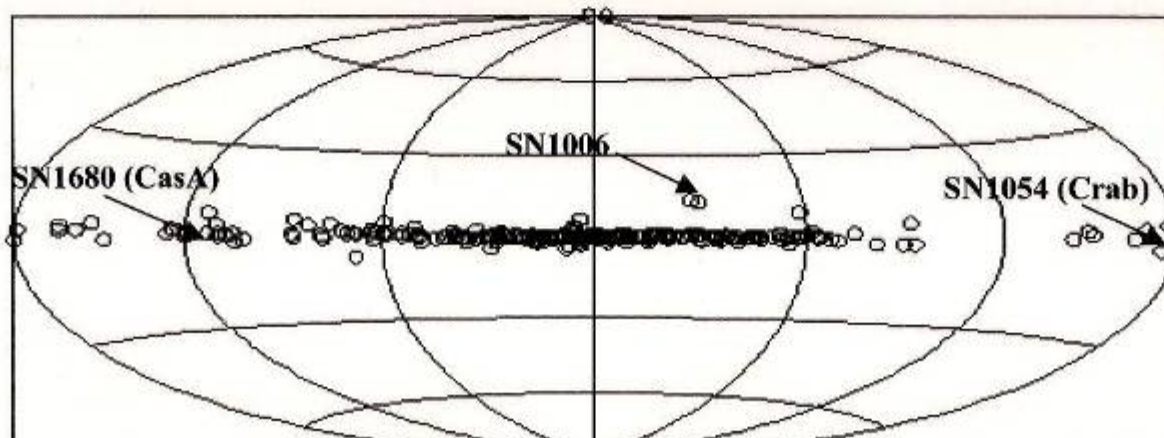
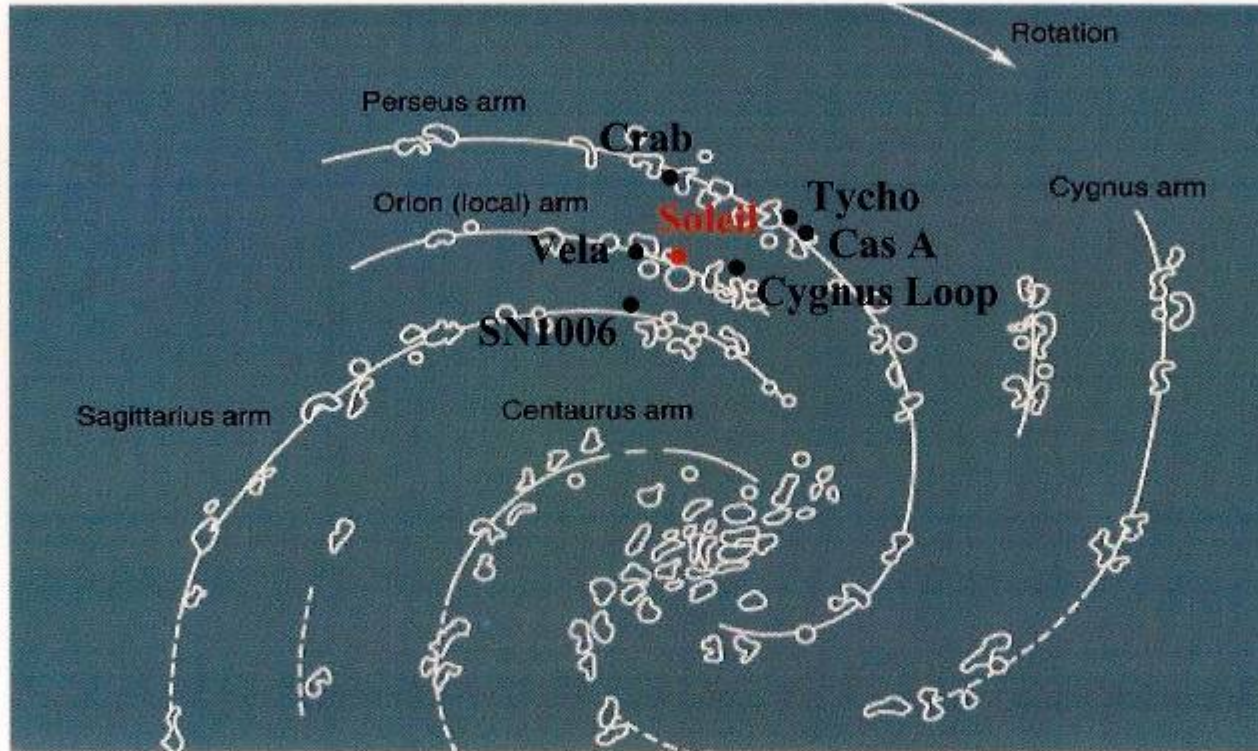
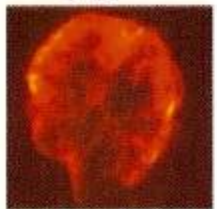
Vela



Tycho



Cygnus



Crab



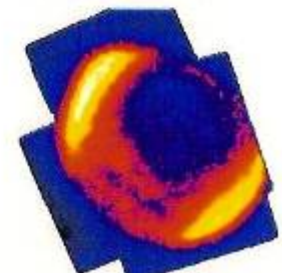
Kepler



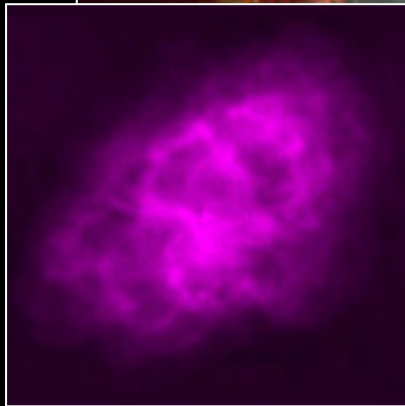
Cas A



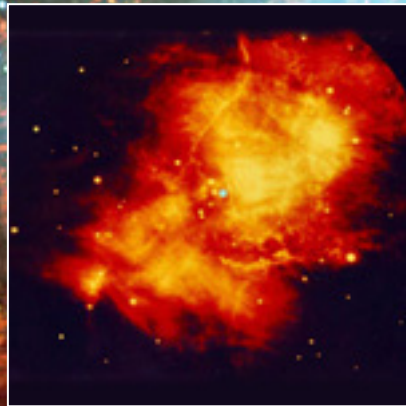
SN1006



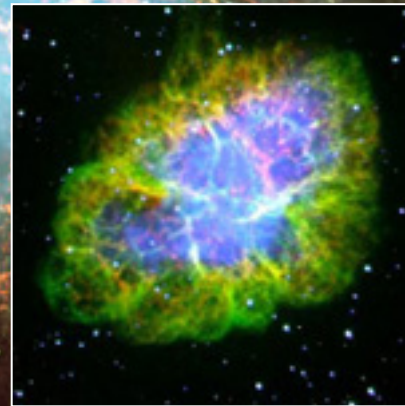
# The Crab in Multi-Wavelengths Photons



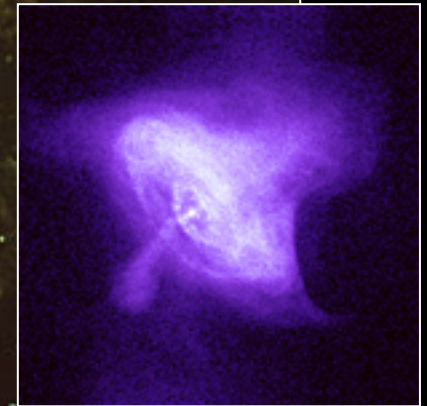
Radio



Infrared

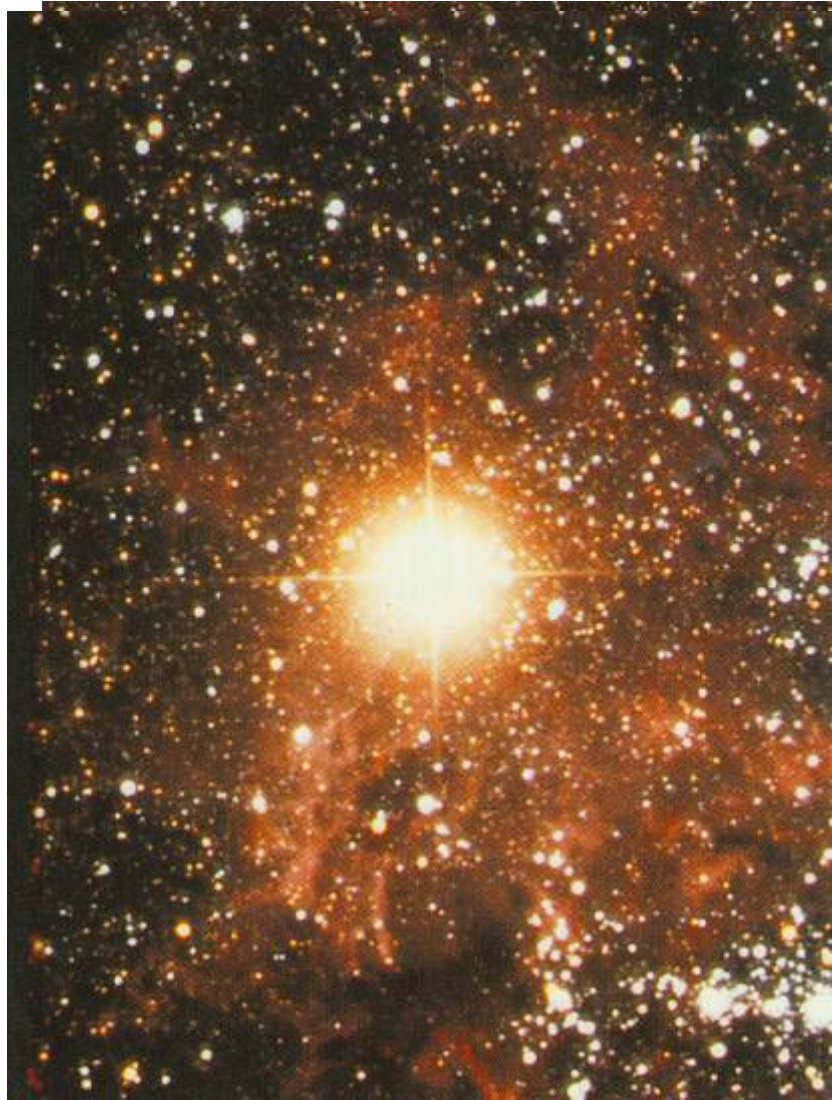


Optical



X-ray

# Supernovae



The field of the  
supernova SN1987A  
after 23 February 1987.

This picture shows a  
small area of sky in the  
**Large Magellanic Cloud**,  
the nearby dwarf  
companion galaxy to  
our own Galaxy.

Anglo-Australian Telescope



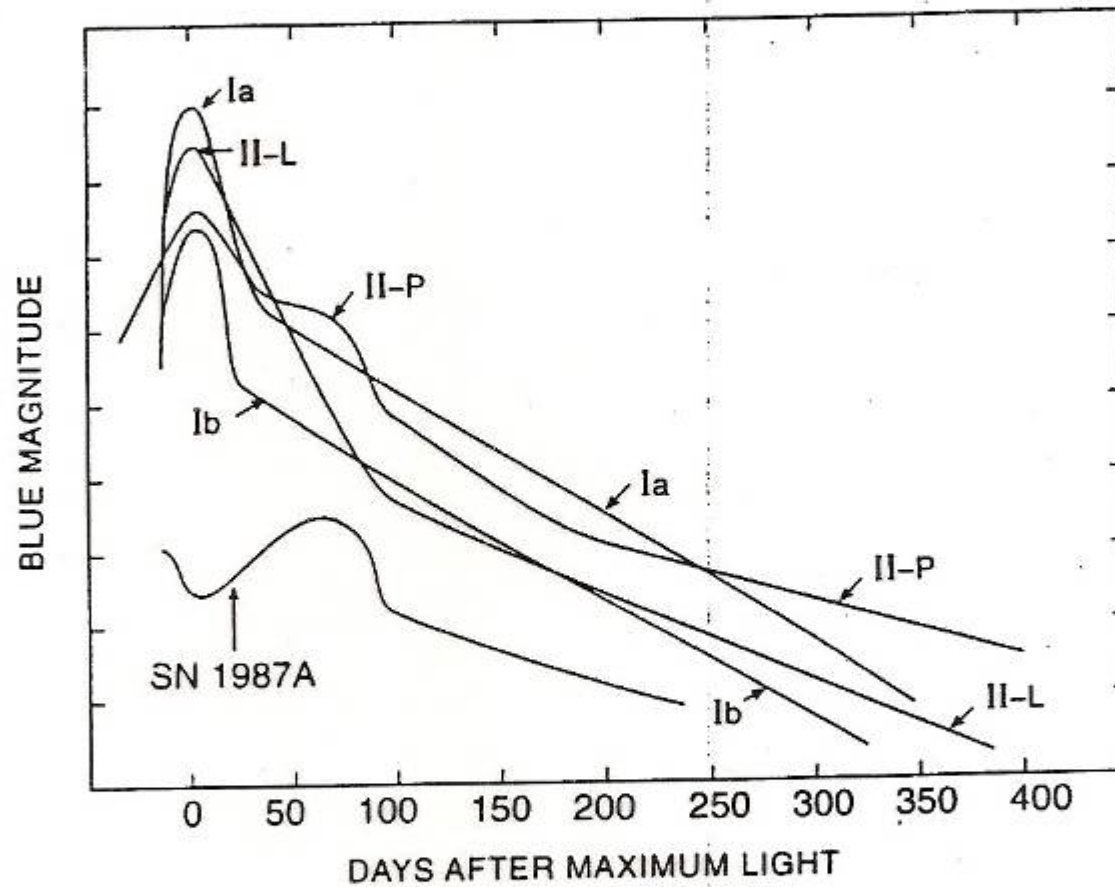
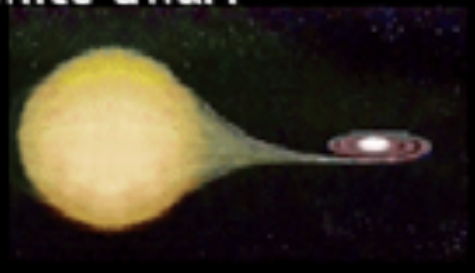


**Figure 13.3.** Brightness in the B-band for different supernova types. The deviation of supernova 1987a from the standard schemes can clearly be seen. Type II supernovae which have an almost linear decline after the maximum (II-L) are distinguished from those which remain almost constant over a longer time and display a form of plateau (II-P). SN 1987a appears from its characteristics to be a new form (from [Whe90]).

## Type Ia vs. Core-Collapse Supernovae

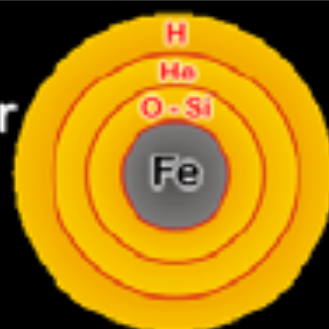
### Type Ia

- Carbon-oxygen white dwarf (remnant of low-mass star)
- Accretes matter from companion



### Core collapse (Type II, Ib/c)

- Degenerate iron core of evolved massive star
- Accretes matter by nuclear burning at its surface



Chandrasekhar limit is reached –  $M_{Ch} \approx 1.5 M_{sun} (2Y_e)^2$

**COLLAPSE SETS IN**

Nuclear burning of C and O ignites  
→ Nuclear deflagration  
("Fusion bomb" triggered by collapse)

Collapse to nuclear density  
Bounce & shock  
Implosion → Explosion

Powered by nuclear binding energy

Powered by gravity

Gain of nuclear binding energy  
- 1 MeV per nucleon

Gain of gravitational binding energy  
- 100 MeV per nucleon  
99% into neutrinos

# Classification of Supernovae

Spectral Type	Ia	Ib	Ic	II
Spectrum	No Hydrogen			Hydrogen
	Silicon	No Silicon		
		Helium	No Helium	
Physical Mechanism	Nuclear explosion of low-mass star	Core collapse of evolved massive star (may have lost its hydrogen or even helium envelope during red-giant evolution)		
Light Curve	Reproducible	Large variations		
Neutrinos	Insignificant	~ 100 × Visible energy		
Compact Remnant	None	Neutron star (typically appears as pulsar) Sometimes black hole?		
Rate / h <sup>2</sup> SNU	0.36 ± 0.11	0.14 ± 0.07		0.71 ± 0.34
Observed	Total ~ 2000 as of today (nowadays ~200/year)			

# Supernova types

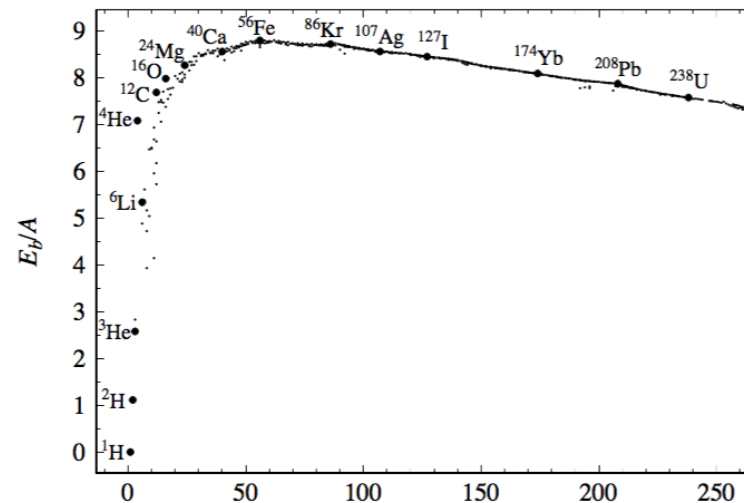
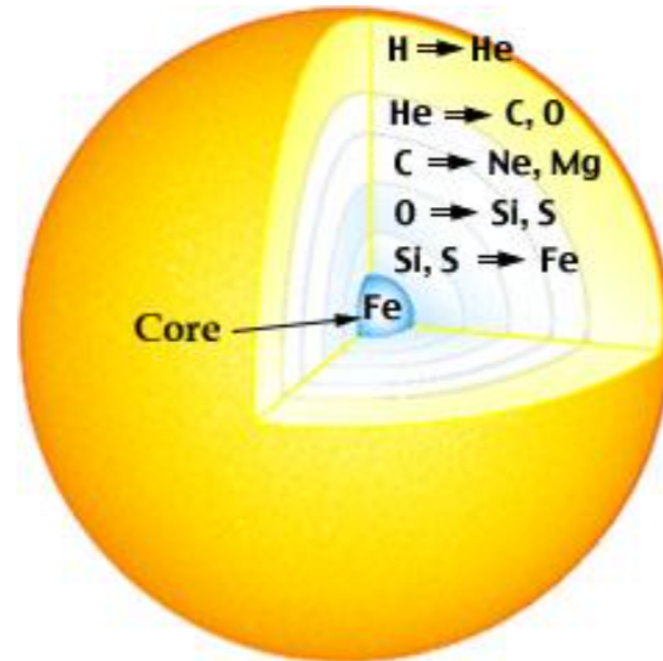
<p><b>(a) Type Ia supernova</b></p> <ul style="list-style-type: none"> <li>The spectrum has no hydrogen or helium lines, but does have a strong absorption line of ionized silicon (Si II).</li> <li>Produced by runaway carbon fusion in a white dwarf in a close binary system (the ionized silicon is a by-product of carbon fusion).</li> </ul>	<p>SN 1987N (Type Ia)</p> <p>Si II</p>	<p>Red giant    White dwarf explodes</p> <p>White dwarf</p>
<p><b>(b) Type Ib supernova</b></p> <ul style="list-style-type: none"> <li>The spectrum has no hydrogen lines, but does have a strong absorption line of un-ionized helium (He I).</li> <li>Produced by core collapse in a massive star that lost the hydrogen from its outer layers.</li> </ul>	<p>SN 1984L (Type Ib)</p> <p>He I</p>	<p>Supergiant star with outer hydrogen removed</p> <p>Core collapse, explosion</p>
<p><b>(c) Type Ic supernova</b></p> <ul style="list-style-type: none"> <li>The spectrum has no hydrogen lines or helium lines.</li> <li>Produced by core collapse in a massive star that lost the hydrogen and the helium from its outer layers.</li> </ul>	<p>SN 1987M (Type Ic)</p>	<p>Supergiant star with outer hydrogen, helium removed</p> <p>Core collapse, explosion</p>
<p><b>(d) Type II supernova</b></p> <ul style="list-style-type: none"> <li>The spectrum has prominent hydrogen lines such as <math>H_{\alpha}</math>.</li> <li>Produced by core collapse in a massive star whose outer layers were largely intact.</li> </ul>	<p>SN 1992H (Type II)</p> <p><math>H_{\alpha}</math></p>	<p>Supergiant star with outer layers largely intact</p> <p>Core collapse, explosion</p>

Wavelength (nm)



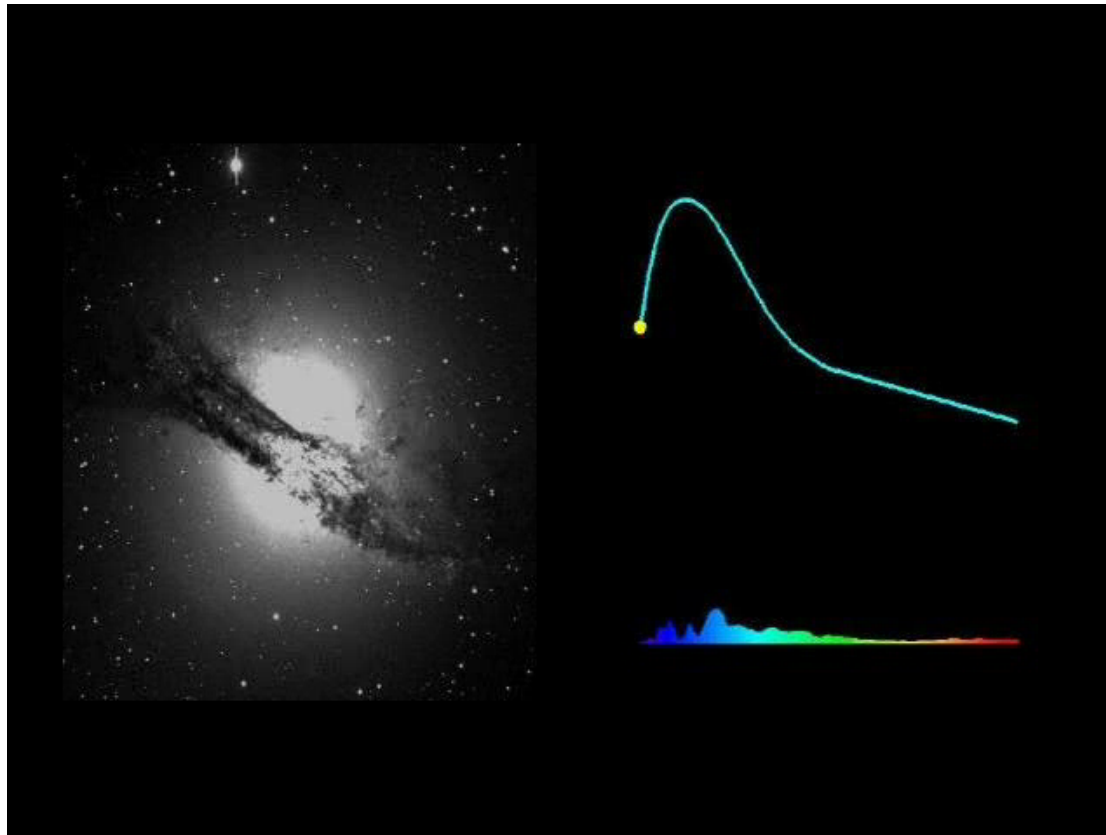
# Presupernova Star

- Star has an onion like structure.
- Iron is the final product of the different burning processes.
- As the mass of the iron core grows it becomes unstable and collapses when it reaches around  $1.4 M_{\odot}$ .





# Neutrinos from a Stellar Gravitational Collapse



Una supernova nella Galassia Centaurus A. Il clip è stato preparato dal "Supernova Cosmology Project" (P. Nugent, A. Conley) con l'aiuto del Lawrence Berkeley National Laboratory's Computer Visualization Laboratory (N. Johnston: animazione) al "National Energy Research Scientific Computing Center"

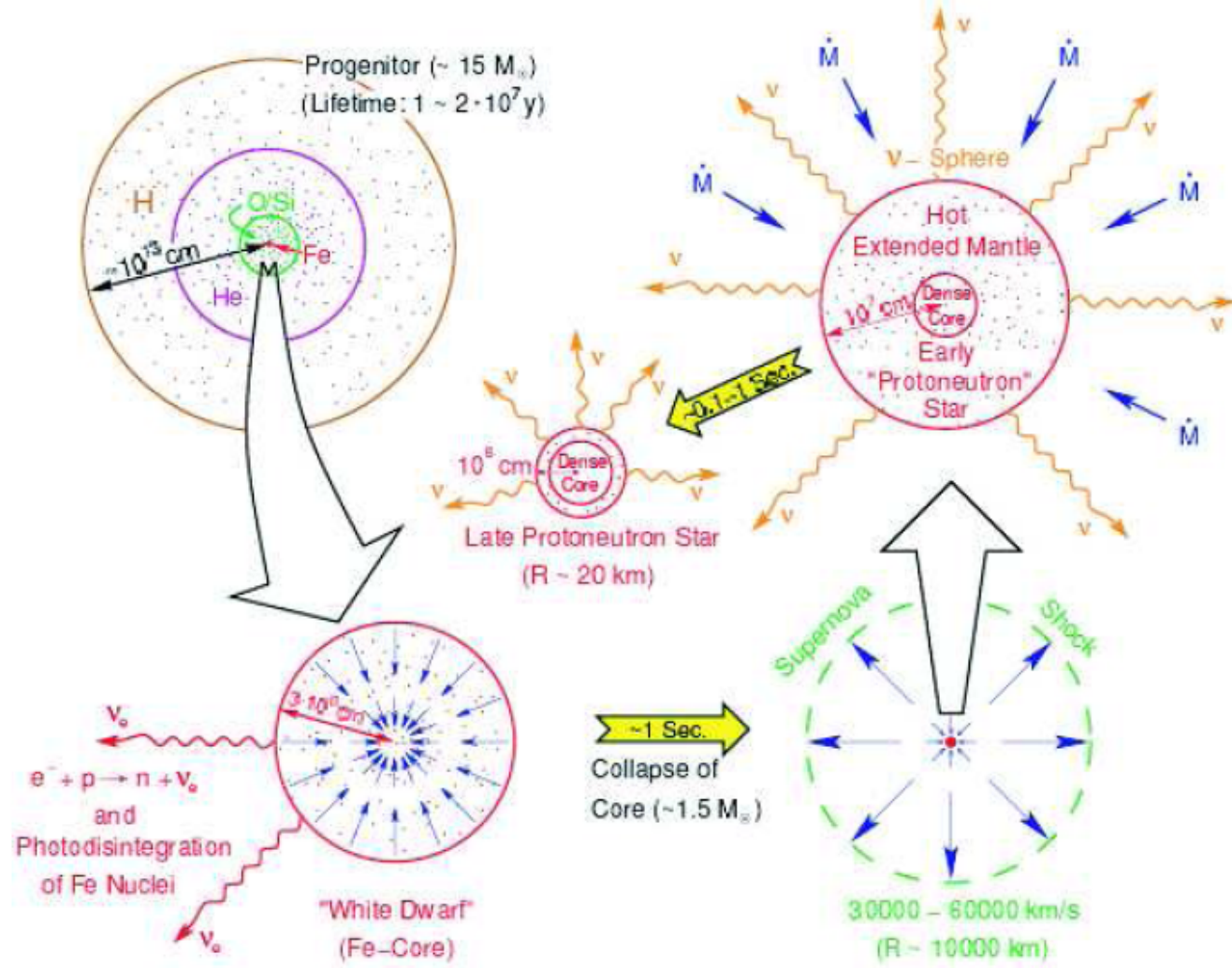
<http://supernova.lbl.gov>



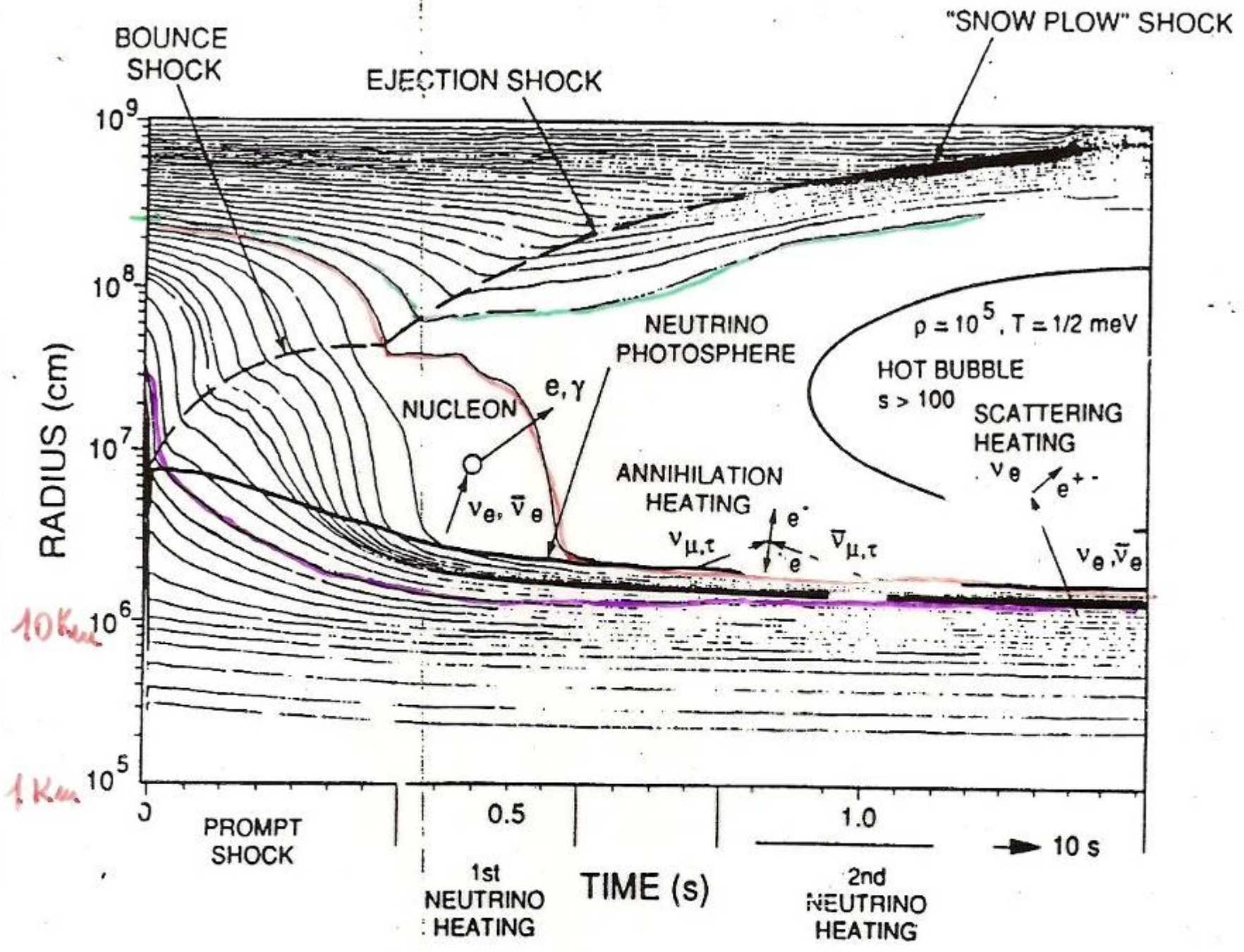
- Stars with masses above eight solar masses undergo ***gravitational collapse***.
- Once the core of the star becomes constituted primarily of iron, further compression of the core does not ignite nuclear fusion and the star is unable to thermodynamically support its outer envelope.
- As the surrounding matter falls inward under gravity, the temperature of the core rises and iron dissociates into  $\alpha$  particles and nucleons.
- Electron capture on protons becomes heavily favored and electron neutrinos are produced as the core gets neutronized (a process known as ***neutronization***).
- When the core reaches densities above  $10^{12}$  g/cm<sup>3</sup>, neutrinos become trapped (in the so-called *neutrinosphere*).
- The collapse continues until 3 – 4 times nuclear density is reached, after which the inner core rebounds, sending a shock-wave across the outer core and into the mantle.
- This shock-wave loses energy as it heats the matter it traverses and incites further electron-capture on the free protons left in the wake of the shock.
- During the few milliseconds in which the shock-wave travels from the inner core to the *neutrinosphere*, electron neutrinos are released in a pulse. This neutronization burst carries away approximately  **$10^{51}$  ergs of energy**.



- 99% of the binding energy  $E_b$ , of the protoneutron star is released in the following  $\sim 10$  seconds primarily via  $\beta$ -decay (providing a source of electron antineutrinos),  $\nu_e$ , anti- $\nu_e$  and  $e^+e^-$  annihilation and nucleon bremsstrahlung (sources for all flavors of neutrinos including  $\nu_\mu$ , anti- $\nu_\mu$ ,  $\nu_\tau$  and anti- $\nu_\tau$ ), in addition to electron capture.



Schematic illustration of a SN explosion. The dense Fe core collapses in a fraction of a second and gets neutronized (lower-left). The inner core rebounds and gives rise to a shock-wave (lower-right). The protoneutron star cools by the emission of neutrinos.





## Initial conditions

The dominant contribution to the pressure comes from the electrons. They are degenerate and relativistic:

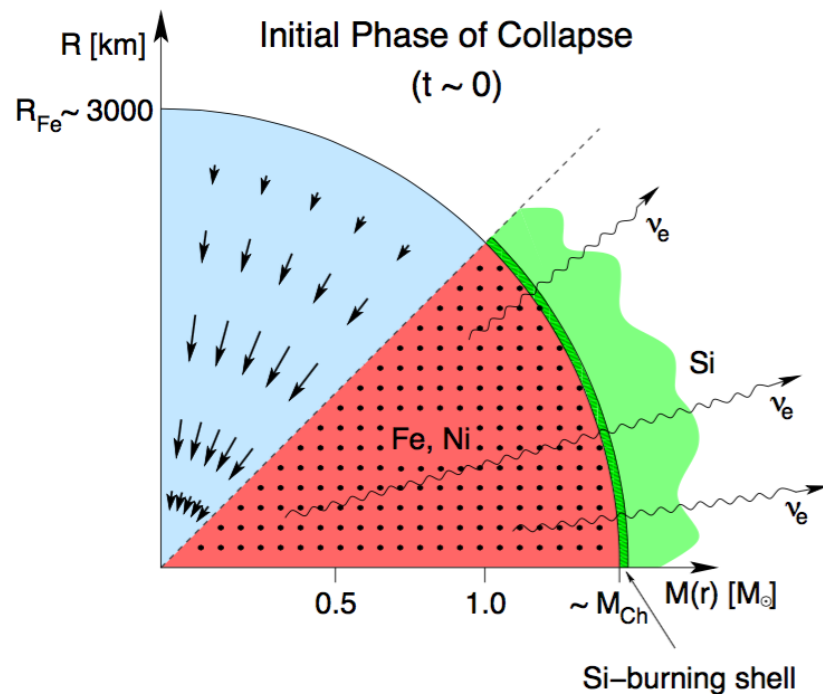
$$P \approx n_e \mu_e = n_e \mathcal{E}_F$$

$\mu_e$  is the chemical potential, fermi energy, of the electrons:

$$\mu_e \approx 1.11(\rho_7 Y_e)^{1/3} \text{ MeV}, \quad \frac{\rho Y_e}{m_u} = n_e$$

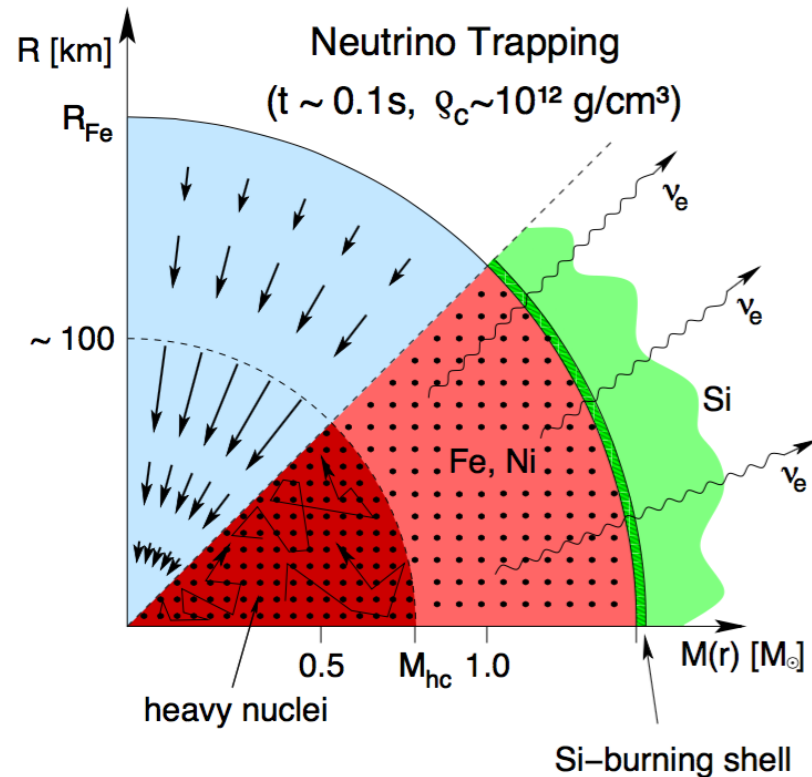
For  $\rho_7 = 1$  ( $\rho = 10^7 \text{ g cm}^{-3}$ ) the chemical potential is 1 MeV, reaching the nuclear energy scale. At this point is energetically favorable to capture electrons by nuclei.

# Presupernova evolution



- $T = 0.1\text{--}0.8$  MeV,  
 $\rho = 10^7\text{--}10^{10}$  g cm $^{-3}$ .  
Composition of iron group nuclei.
- Important processes:
  - electron capture:  
 $e^- + (N, Z) \rightarrow (N+1, Z-1) + \nu_e$
  - $\beta^-$  decay:  
 $(N, Z) \rightarrow (N-1, Z+1) + e^- + \bar{\nu}_e$
- Dominated by allowed transitions (Fermi and Gamow-Teller)
- Evolution decreases number of electrons ( $Y_e$ ) and Chandrasekar mass ( $M_{\text{ch}} \approx 1.4(2Y_e)^2 M_{\odot}$ )

# Collapse phase



## Important processes:

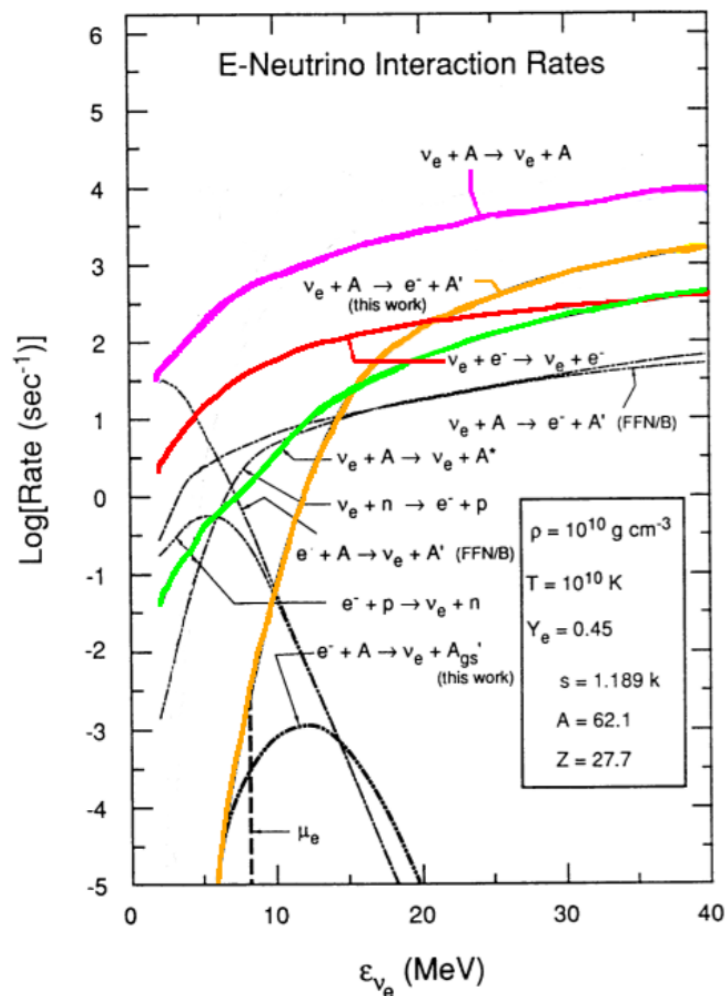
- Neutrino transport  
(Boltzmann equation):  
 $\nu + A \rightleftharpoons \nu + A$  (trapping)  
 $\nu + e^- \rightleftharpoons \nu + e^-$  (thermalization)  
 cross sections  $\sim E_{\nu}^2$
- electron capture on protons:  
 $e^- + p \rightleftharpoons n + \nu_e$
- electron capture on nuclei:  
 $e^- + A(Z, N) \rightleftharpoons A(Z-1, N+1) + \nu_e$



# Neutrino interactions in the collapse

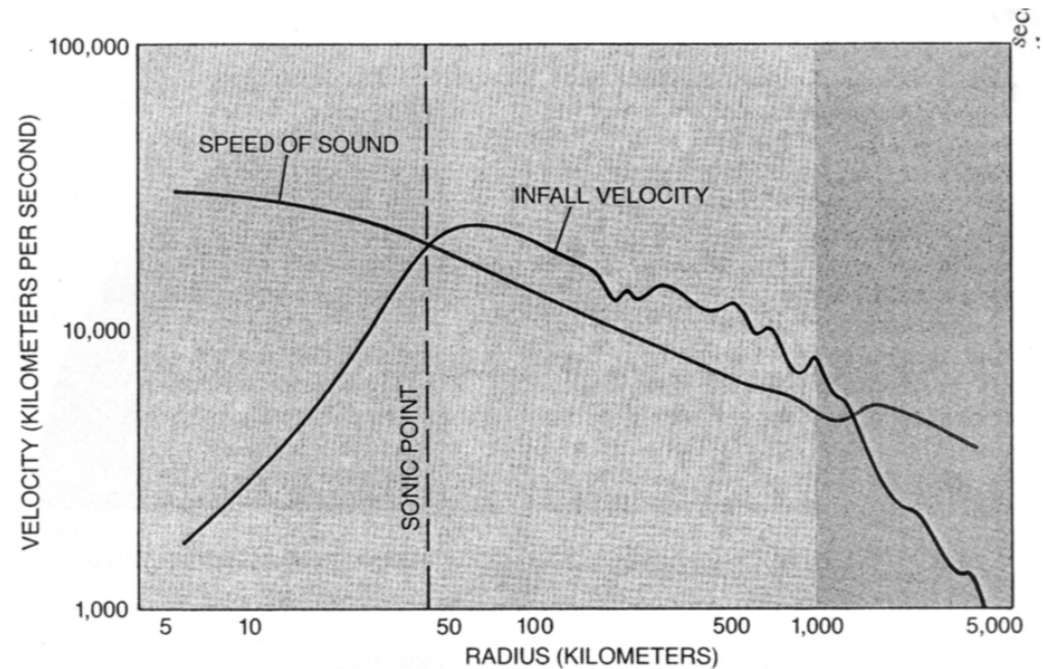
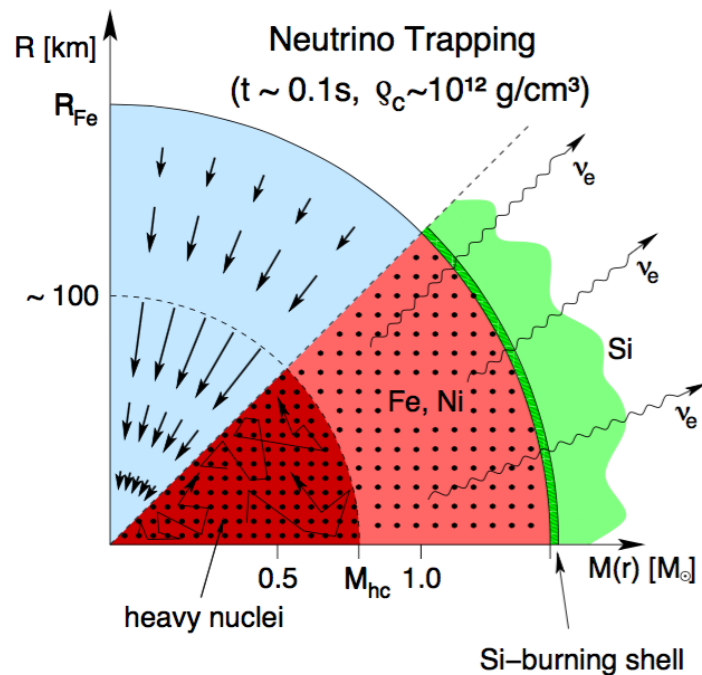
Bruenn and Haxton (1991)

Based on results for  $^{56}\text{Fe}$



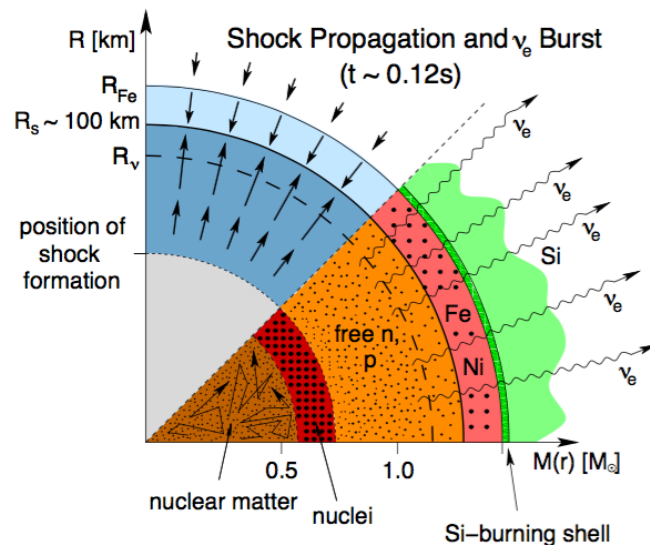
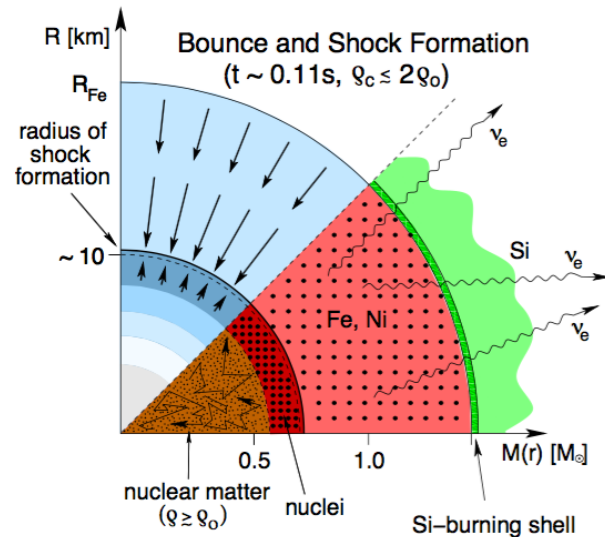
- **Elastic scattering:**  
 $\nu + A \rightleftharpoons \nu + A$  (trapping)
- **Absorption:**  
 $\nu_e + (N, Z) \rightleftharpoons e^- + (N - 1, Z + 1)$
- **$\nu$ - $e$  scattering:**  
 $\nu + e^- \rightleftharpoons \nu + e^-$  (thermalization)
- **Inelastic  $\nu$ -nuclei scattering:**  
 $\nu + A \rightleftharpoons \nu + A^*$

# Homologous collapse



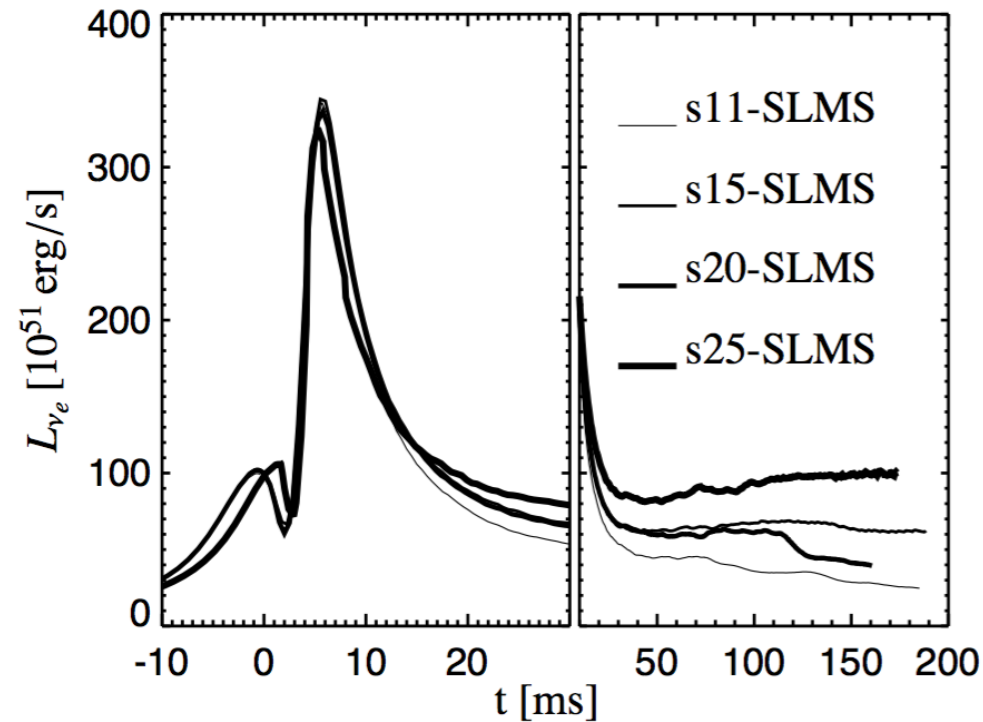
- After thermalization an inner homologous core forms in which the local sound velocity is larger than the infall velocity.
- Matter in the outer core falls at supersonic velocities.

# Bounce and $\nu_e$ burst



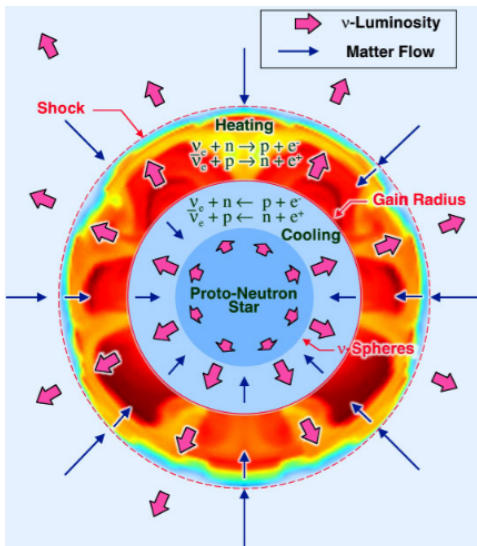
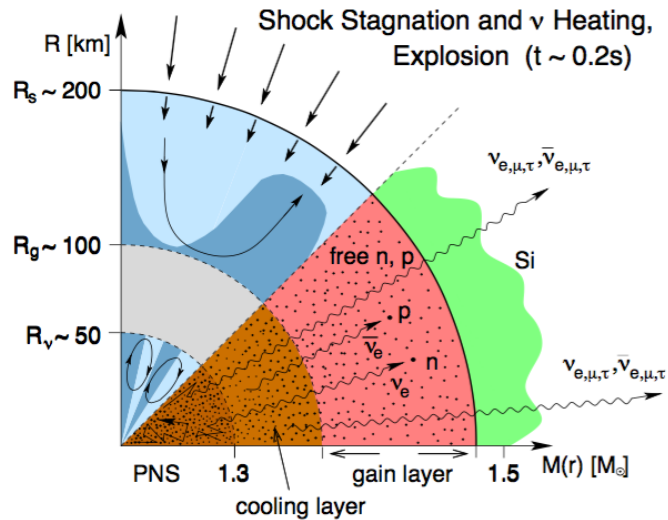
- Collapse continues until central density becomes around twice nuclear matter density.
- Sudden increase in nuclear pressure stops the collapse and a shock wave is launched at the sonic point. The energy of the shock depends on the Equation of State.
- The passage of the shock dissociates nuclei into free nucleons which costs  $\sim 8$  MeV/nucleon. Additional energy is lost by neutrino emission produced by electron capture ( $\nu_e$  burst).
- Shock stalls at a distance of around 100 km.

# Neutrino burst

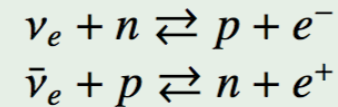


- Burst is produced when shock wave reaches regions with densities low enough to be transparent to neutrinos
- Burst structure does not depend on the progenitor star.
- Future observation by a supernova neutrino detector. Standard neutrino candles.

# Delayed explosion mechanism: neutrino heating



## Main processes:



Concept of gain radius due to Bethe.  
Corresponds to the region where cooling  
(electron positron capture) and heating  
(neutrino antineutrino absorption) are equal.

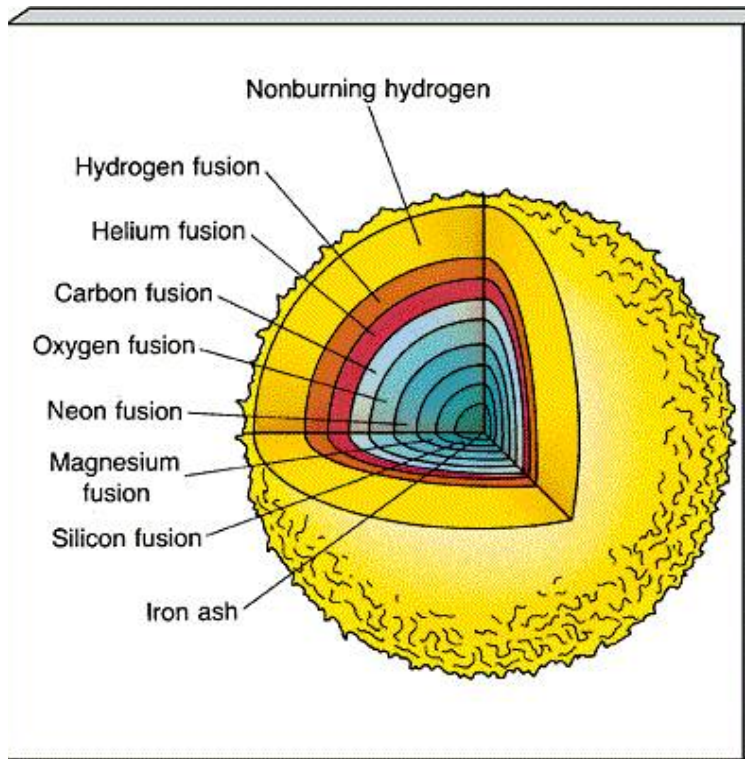
$$\text{Cooling: } 143 \left( \frac{kT}{2 \text{ MeV}} \right)^6 \text{ MeV/s}$$

$$\text{Heating: } 110 \left( \frac{L_{\nu_e, 52} \epsilon_{\nu_e}^2}{r_7^2} Y_n + \frac{L_{\bar{\nu}_e, 52} \epsilon_{\bar{\nu}_e}^2}{r_7^2} Y_p \right) \text{ MeV/s}$$

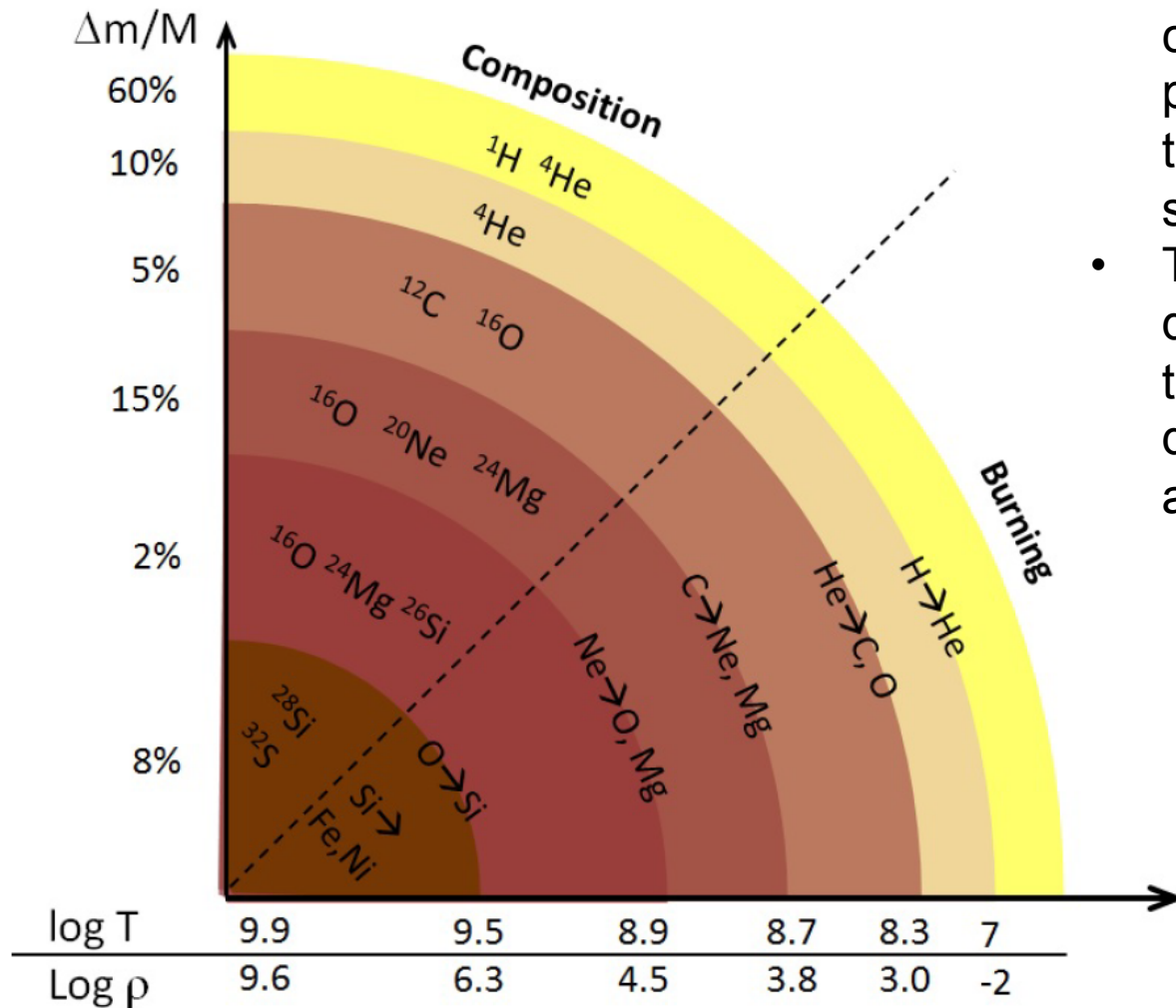
Gravitational energy of a nucleon at 100 km: 14 MeV  
Energy transfer induces convection and requires  
multidimensional simulations.

# Pre supernovae

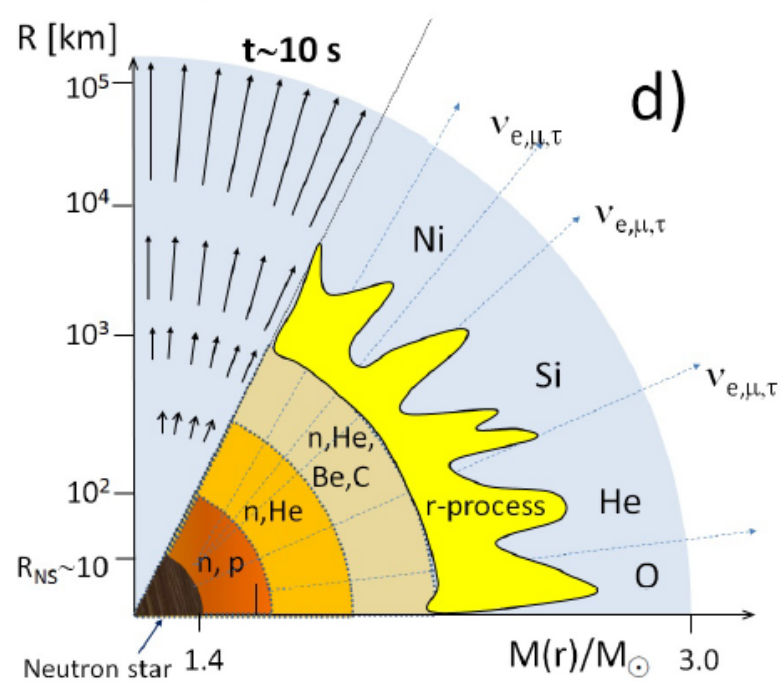
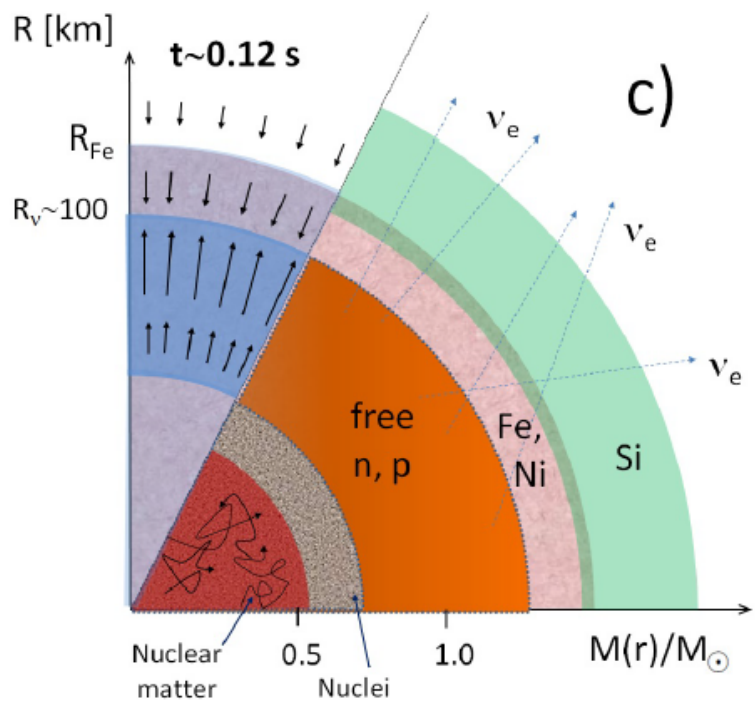
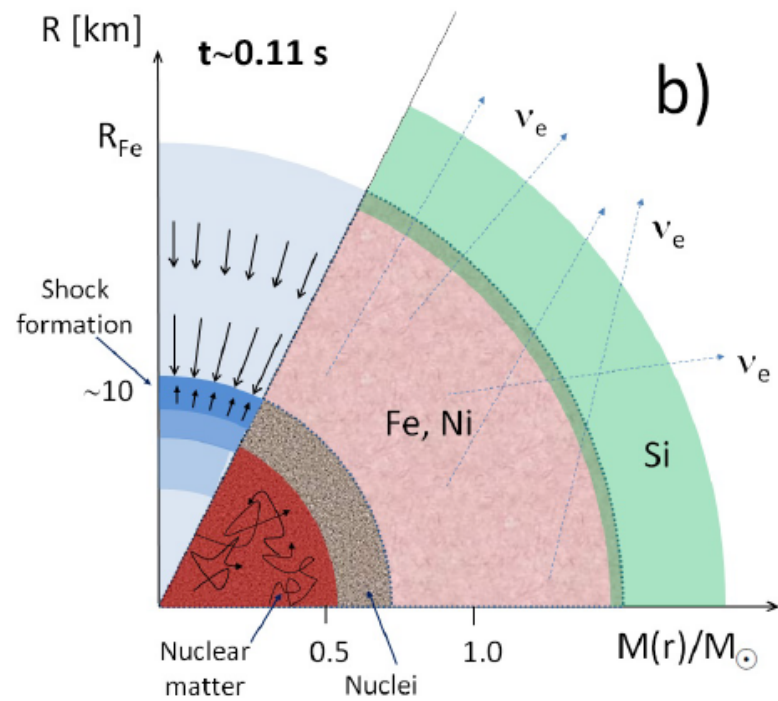
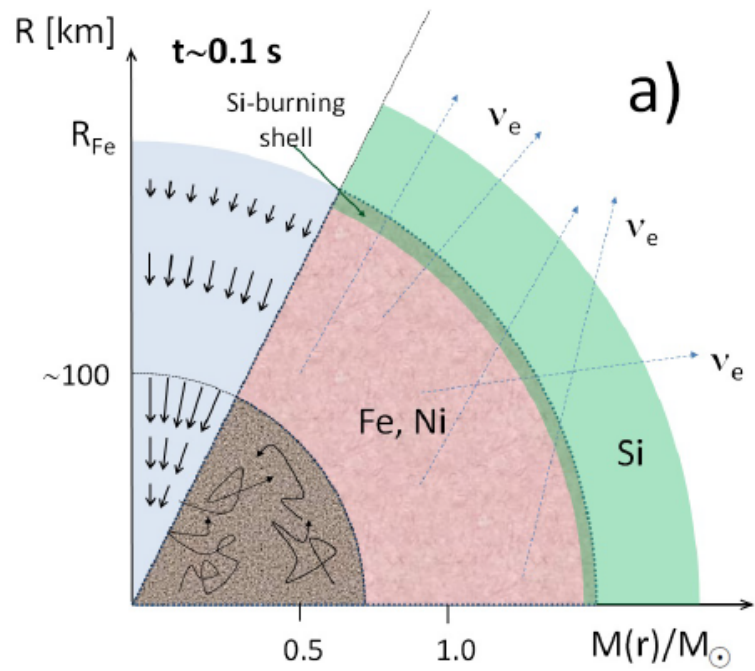
## Evolutionary stages of a 25 MSUN star:



Stage	Temperature (K)	Duration of stage
Hydrogen burning	$4 \times 10^7$	$7 \times 10^6$ years
Helium burning	$2 \times 10^8$	$5 \times 10^5$ years
Carbon burning	$6 \times 10^8$	600 years
Neon burning	$1.2 \times 10^9$	1 year
Oxygen burning	$1.5 \times 10^9$	6 months
Silicon burning	$2.7 \times 10^9$	1 day
Core collapse	$5.4 \times 10^9$	1/4 second



- The onion-like structure in the final stage of a massive star (25M).
- The outermost envelope is composed of H and He, and progressively heavier nuclei (up to Fe) are layered, due to successive fusion reactions.
- Typical values of the mass, density  $\rho$  (in  $\text{g/cm}^3$ ) and temperature  $T$  (in K) of the different shells are indicated along the axes





# Naked eye Supernovae



SN1987A

## Recorded explosions visible to naked eye:

Year (A.D.)	Where observed	Brightness
185	Chinese	Brighter than Venus
369	Chinese	Brighter than Mars or Jupiter
1006	China, Japan, Korea, Europe, Arabia	Brighter than Venus
1054	China, SW India, Arabia	Brighter than Venus
1572	Tycho	Nearly as bright as Venus
1604	Kepler	Brighter than Jupiter
1987	Ian Shelton (Chile)	

# Core Collapse Supernova Energetics

Liberated gravitational binding energy of neutron star:

$$E_b \approx 3 \times 10^{53} \text{ erg} \approx 17\% M_{\text{SUN}} c^2$$

This shows up as

- 99% Neutrinos**
- 1% Kinetic energy of explosion  
(1% of this into cosmic rays)**
- 0.01% Photons (outshine host galaxy)**

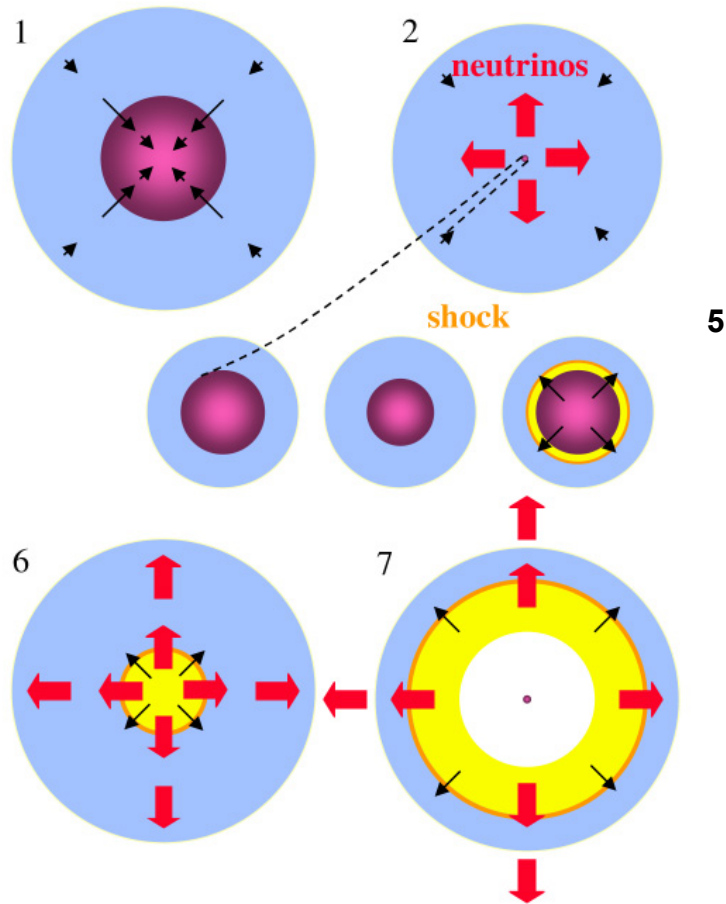
Neutrino luminosity

$$L_\nu \approx 3 \times 10^{53} \text{ erg} / 3 \text{ sec} \approx 3 \times 10^{19} L_{\text{SUN}}$$

While it lasts, outshines the photon  
luminosity of the entire visible universe!

# Explosion

## Core Collapse and Explosion

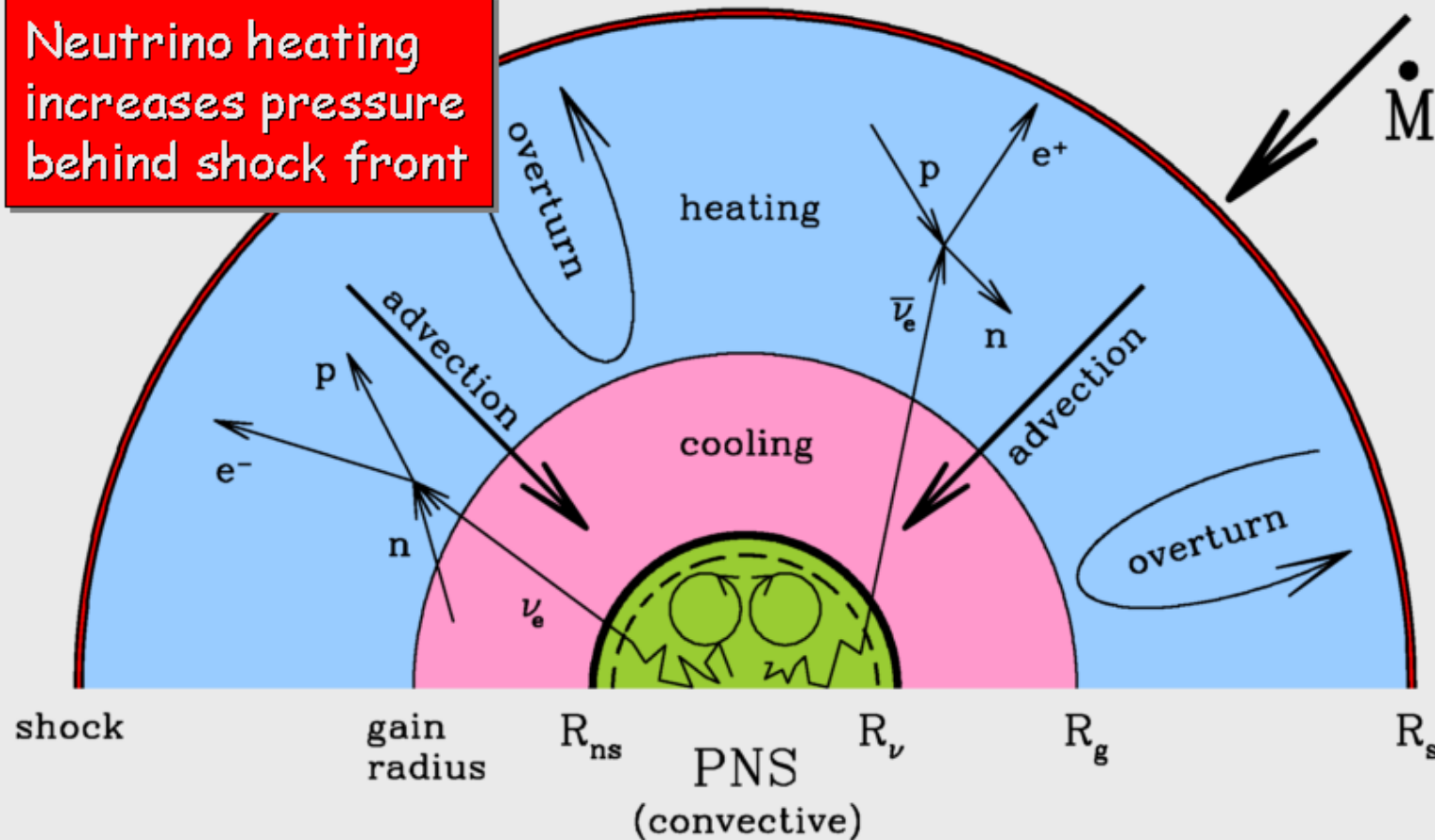


- **Collapse and re-bound(1-4) creates a shock wave(5) propagating outward from center of core(6) , meeting in falling outer core material**
- **Shock stalls due to neutrino escape & nuclear dissociation**
- **Deleptonisation of the core creates intensive neutrino flux (99% of energy)**
- **Neutrino interactions behind the shock reheat the shock and drive it outwards(7)**
- **Measuring  $^{56}\text{Fe}(\nu_e, e^-) ^{56}\text{Co}$  provides valuable data to guide shock formation models.**
- **Other cross sections,  $^{28}\text{Si}$ , should also play an important role.**

# Neutrinos to the Rescue

Adapted from Janka, astro-ph/0008432

Neutrino heating  
increases pressure  
behind shock front

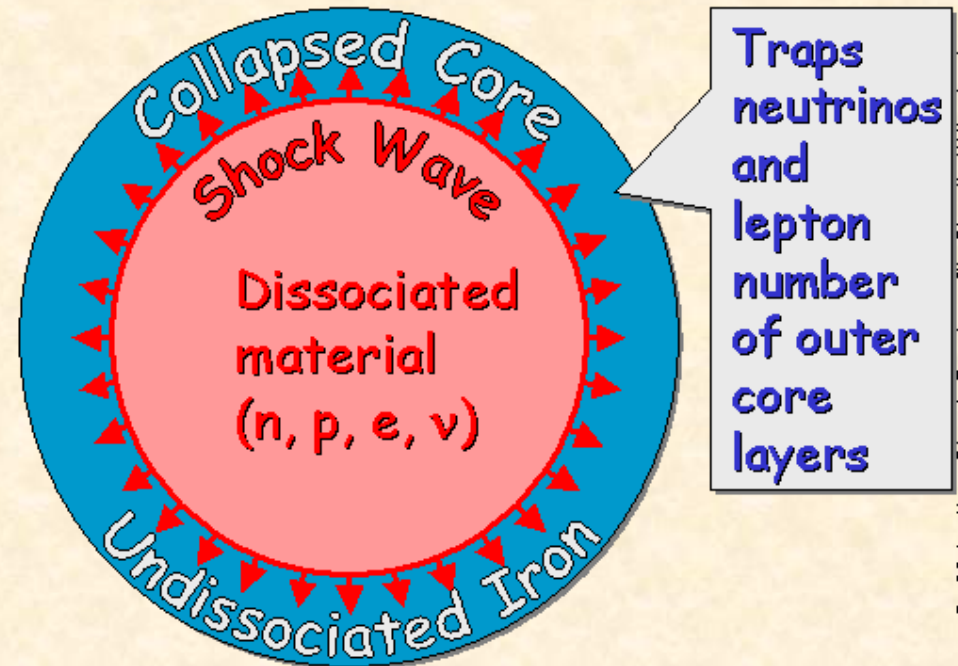
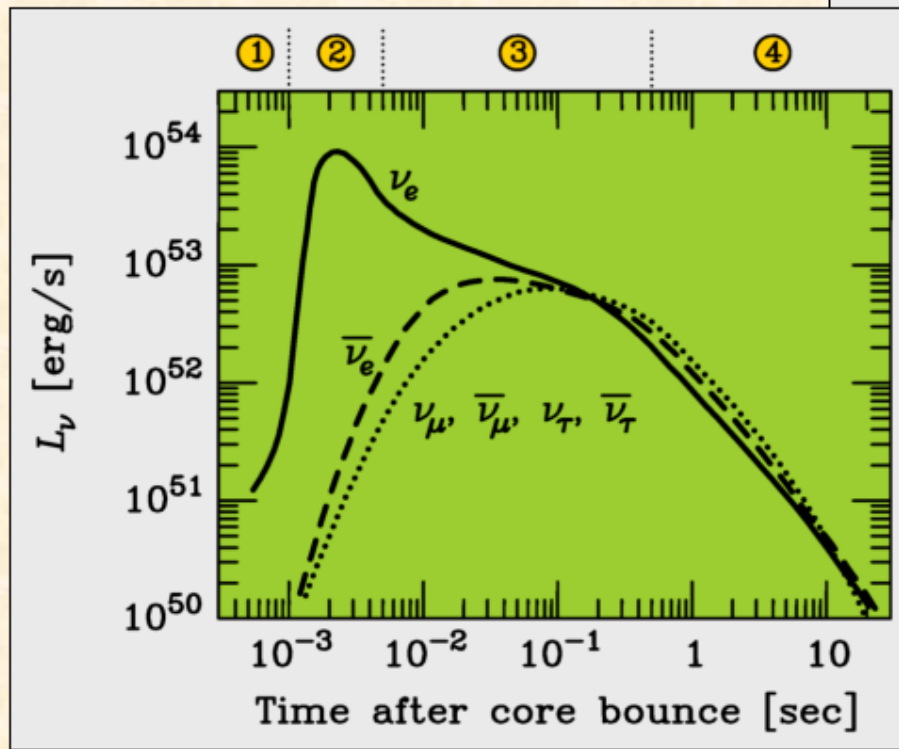
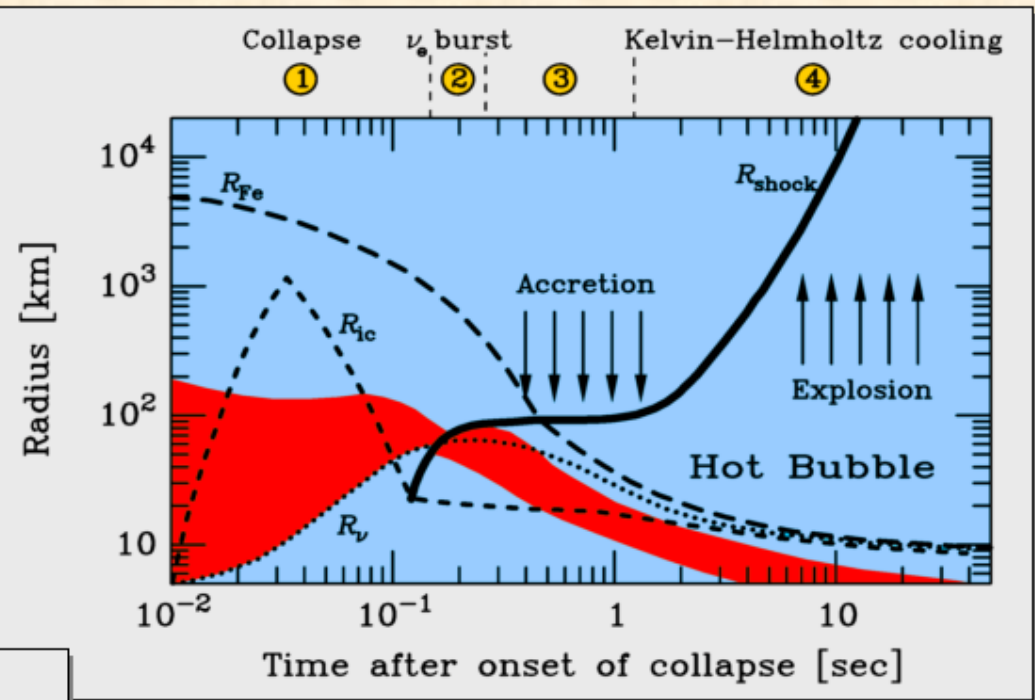


Heating mostly by  $\beta$  processes ( $\nu_e + n \rightarrow p + e^-$  and  $\bar{\nu}_e + p \rightarrow n + e^+$ )  
Pair annihilation ( $\nu + \bar{\nu} \rightarrow e^- + e^+$ ) negligible

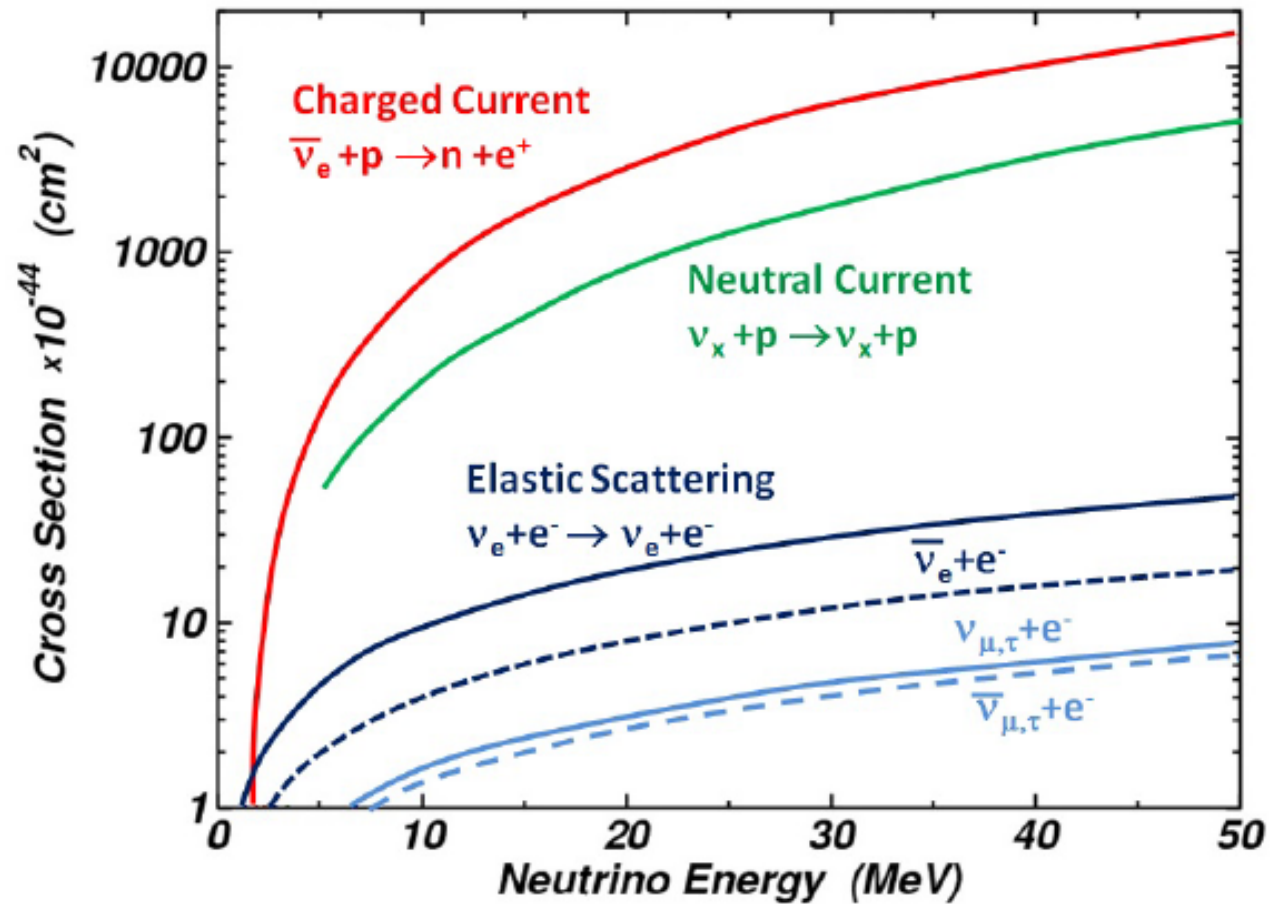
Mu- and tau-neutrino fluxes and spectra not crucial for explosion

# Supernova Neutrino Signal

1. Collapse (infall phase)
2. Shock break out
3. Matter accretion
4. Kelvin-Helmholtz cooling

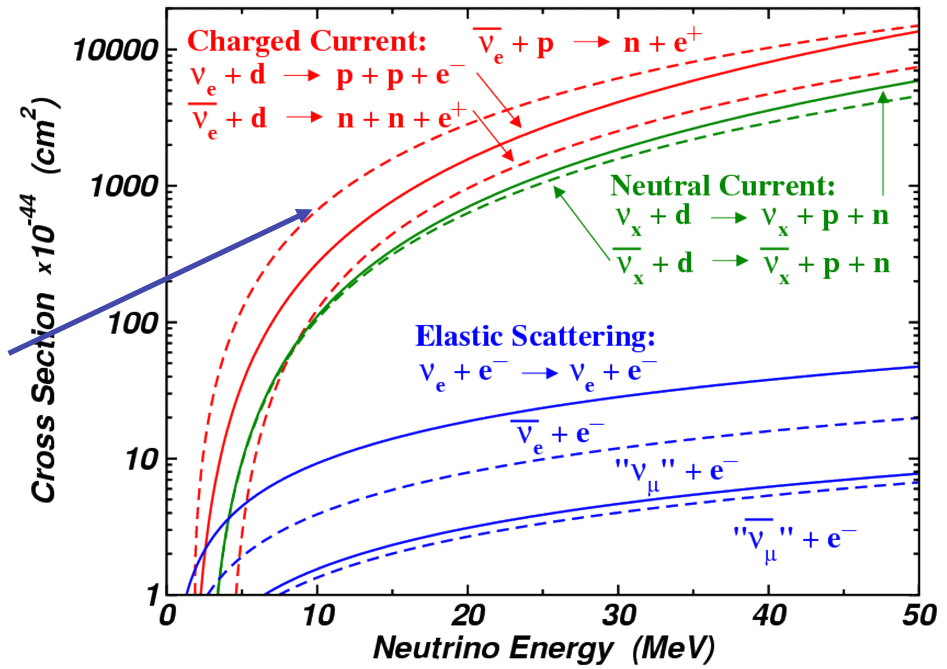


# The SN neutrino signal



# 8.6 The SN1987A

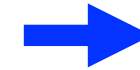
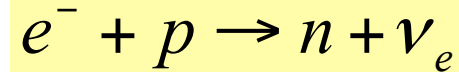
Neutrino cross sections:



Distance: 52 kpc (LMC)

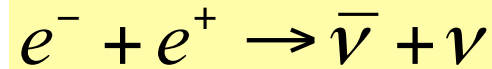
## Introduction: Core collapse of type-II SN

- *Neutronization*, ~10 ms
- $10^{51}$  erg,  $\nu_e$  only

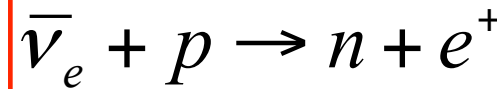


t=0

- *Thermalization*: ~10 s
- $3 \times 10^{53}$  erg
- $L_{\nu_e}(t) \approx L_{\text{anti-}\nu_e}(t) \approx L_{\nu_x}(t)$



Detection: mainly through

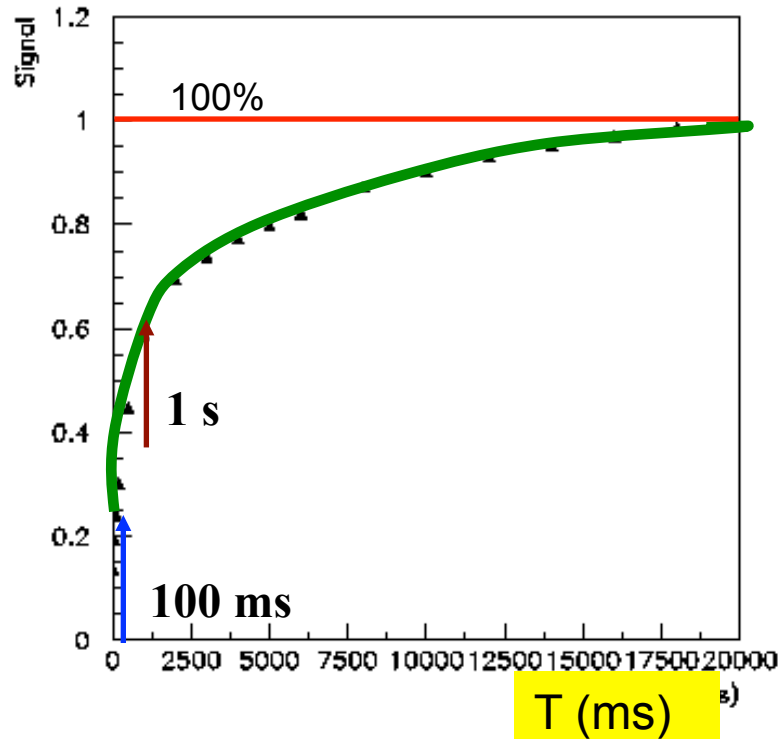


~300 events/kt (@GC)

**Supernovae explode in Nature, but non  
in computers** (J. Beacom, v2002)

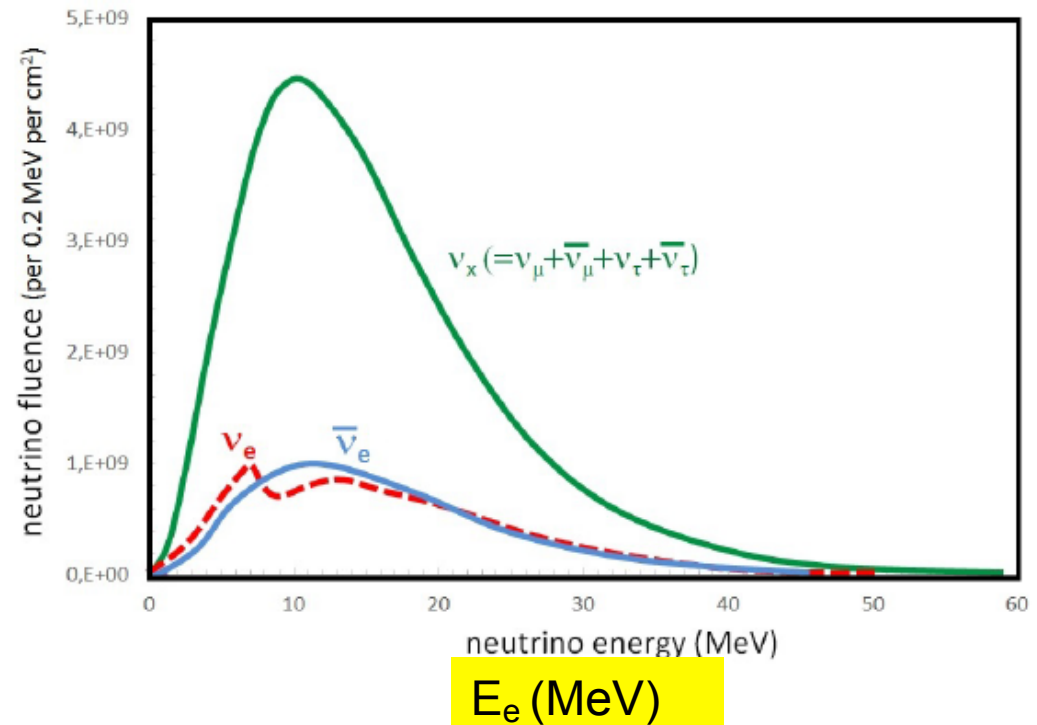


# Time-energy



(a)

(a) Time-integrated fraction of the SN positrons produced in the detector versus time. 24% of the signal it is produced in the first 100 ms after the *neutronization* burst. It is 60% after 1 second.



(b) Differential energy spectrum (arbitrary units) of positrons. A SN1987A-like stellar collapse was assumed.

# The SN1987A: how many events?

1- Energy released  $2.5 \cdot 10^{53}$  erg

2- Average  $\nu_e$  energy  $\approx 16$  MeV =  $2.5 \cdot 10^{-5}$  erg

3-  $N_{\text{source}} = (1/6) \times 2.5 \cdot 10^{53} / (2.5 \cdot 10^{-5}) = 1.7 \cdot 10^{57} \nu_e$

4- LMC Distance :

$D = 52$  kpc =  $1.6 \cdot 10^{23}$  cm

5- Fluency at Earth:

$F = N_{\text{source}} / 4\pi D^2 = 0.5 \cdot 10^{10} \text{ cm}^{-2}$

6- Targets in 1 Kt water:

$N_{\dagger} = 0.7 \cdot 10^{32}$  protons

7- cross section:

$\sigma(\text{antineutr}_e + p) \sim 2 \cdot 10^{-41} \text{ cm}^2$

8-  $N_{e^+} = F (\text{cm}^{-2}) \times \sigma (\text{cm}^2) \times N_{\dagger} (\text{kt}^{-1}) = 0.5 \cdot 10^{10} \times 2 \cdot 10^{-41} \times 0.7 \cdot 10^{32}$   
 $= 7$  positrons/kt

9 - M(Kam II) = 2.1 kt, efficiency  $\varepsilon \sim 80\%$

10 - Events in Kam II =  $7 \times 2.1 \times \varepsilon \sim 12$  events

For a SN @ Galactic Center (8.5 kpc) :

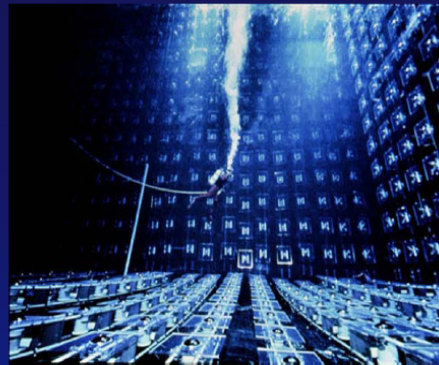
$N_{\text{events}} = 7 \times (52/8.5)^2 = 260 \text{ e}^+/\text{kt}$

# The Detectors

- Water Cherenkov detectors
  - Kamiokande (Japan)
  - IMB (Ohio)
- Liquid scintillation telescopes
  - Baksan – USSR Academy of Sciences, in North Caucasus Mountains, Russia
  - Mont Blanc – Italian Soviet collaboration, in Mont Blanc Laboratory, France

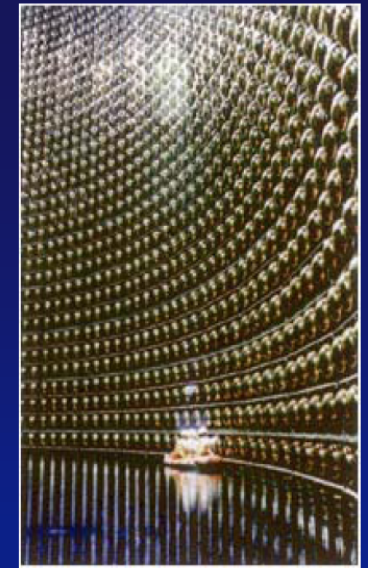
## IMB

- Located in the Morton Thiokol mine in Ohio
- 580m underground
- Rectangular tank
  - 18 by 17 by 23 m
- 2048 8” photomultipliers
- 2.5 million gallons of water
- Compared to Kamiokande II: Larger volume, but not as deep



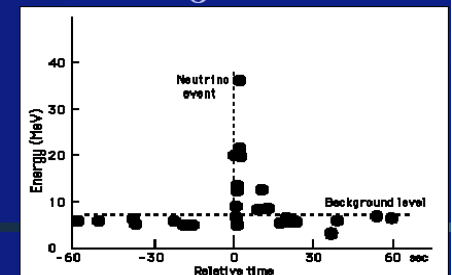
## Kamiokande II

- Located in the Kamioka mine in Japan
- 1000m underground
- Cylindrical tank
  - $d = 15.6\text{m}$ ,  $h = 16\text{m}$
- Large ( $D = 20$  inches) photomultipliers
- Volume of water weighs 3000 metric tons



## Results

- Feb 23, 7:36 UT:
  - K II records 9 neutrinos within 2 sec, 3 more neutrinos 9-13 seconds later
  - IMB records 8 neutrinos within 6 seconds
  - Baksan records 5 neutrinos within 5 seconds
- 25 neutrinos detected!



# Neutrino mass from SN

- The observation of supernova neutrinos should bring a better understanding of the core collapse mechanism from the feature of the time and energy spectra, and constraints the supernova models.
- Moreover, an estimation of the neutrino masses could be done in the following manner. The velocity of a particle of energy  $E$  and mass  $m$ , with  $E \gg m$ , is given by (with  $c = 1$ ):

$$v = \frac{p}{E} = \frac{(E^2 - m^2)^{1/2}}{E} \approx 1 - \frac{m^2}{2E} .$$

- Thus, for a supernova at distance  $d$ , the delay of a neutrino due to its mass is, expressed in the proper units:

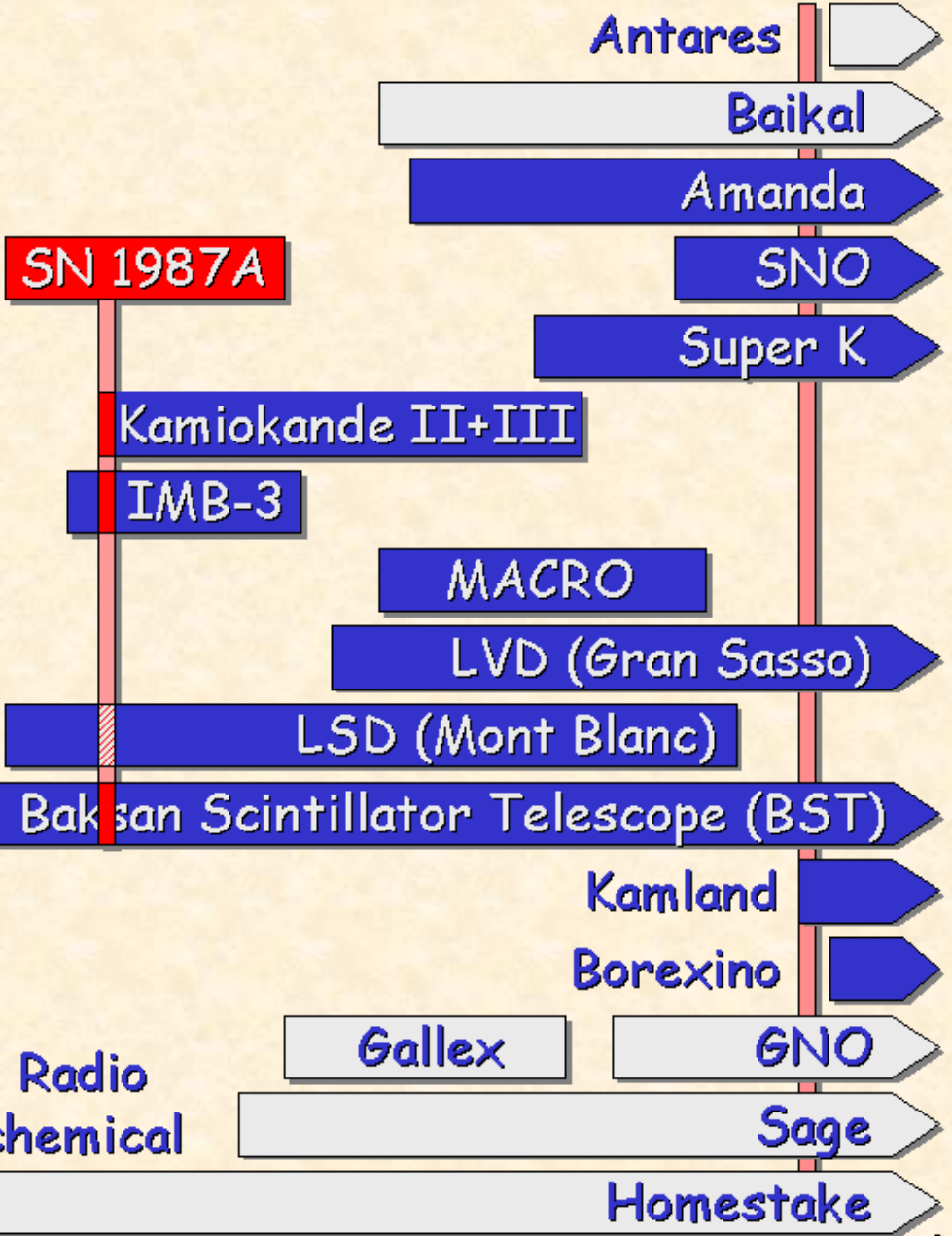
$$\Delta t_{[s]} \approx 0.05 \frac{m_{[eV]}^2}{E_{[MeV]}} d_{[kpc]} .$$

- Therefore, neutrinos of different energies released at the same instant should show a spread in their arrival time.

# Neutrino Astronomy

Events from a Supernova at 10 kpc

- many  $\sigma$
- 800
- 8000
- 370
- 940
- 240
- 400
- 20
- 70
- 330
- 80



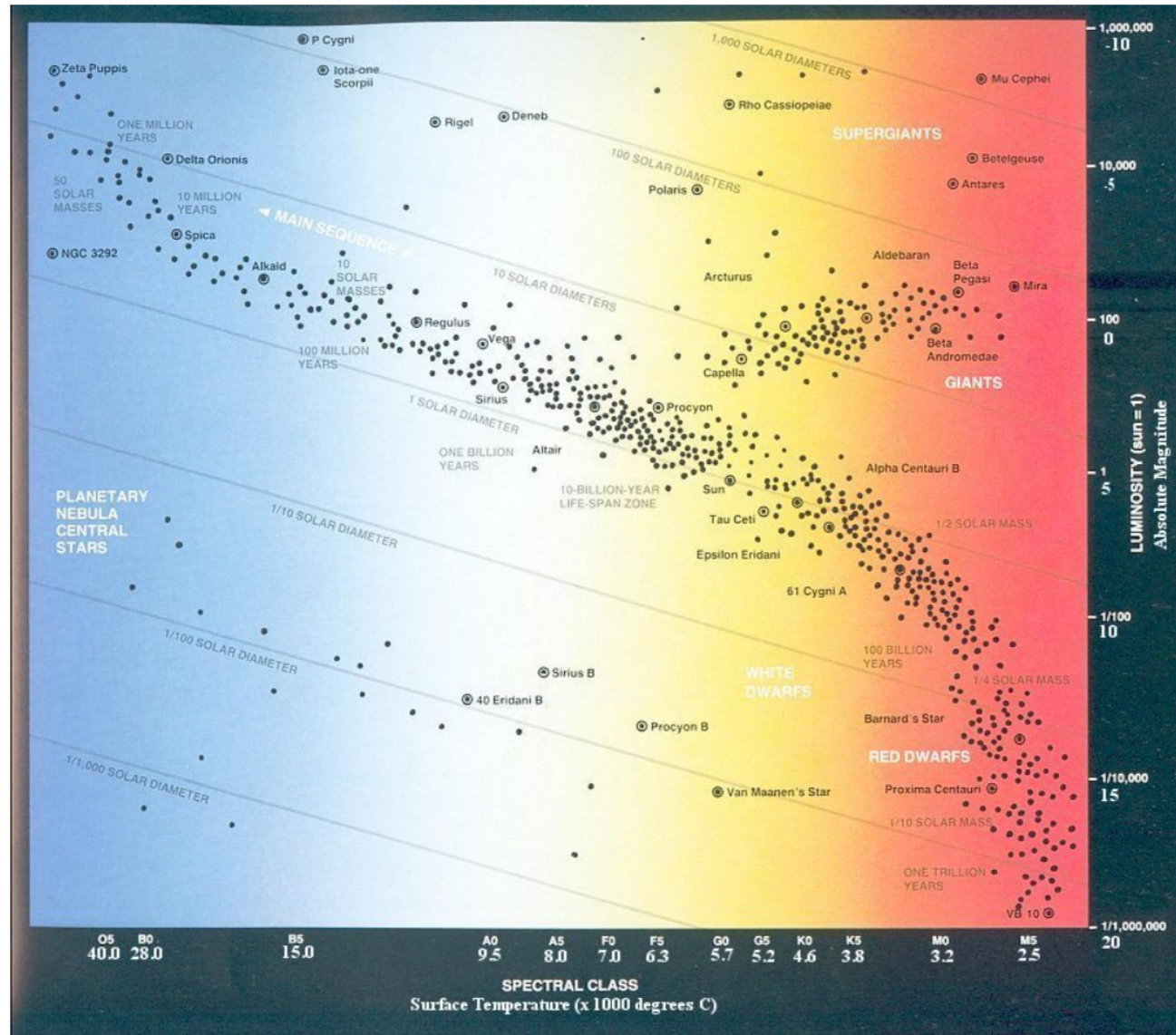
# Neutrino Astrophysics

- The only SN seen with neutrino was SN1987a
- Small experiments, small statistics
- Qualitative agreement with the SN models
- Wait for the next near SN with the new larger experiments (SK, SNO, Borexino, LVD...)
- → neutrino properties (mass, lifetime, magnetic moment) from astrophysics

# Astrofisica Nucleare e Subnucleare

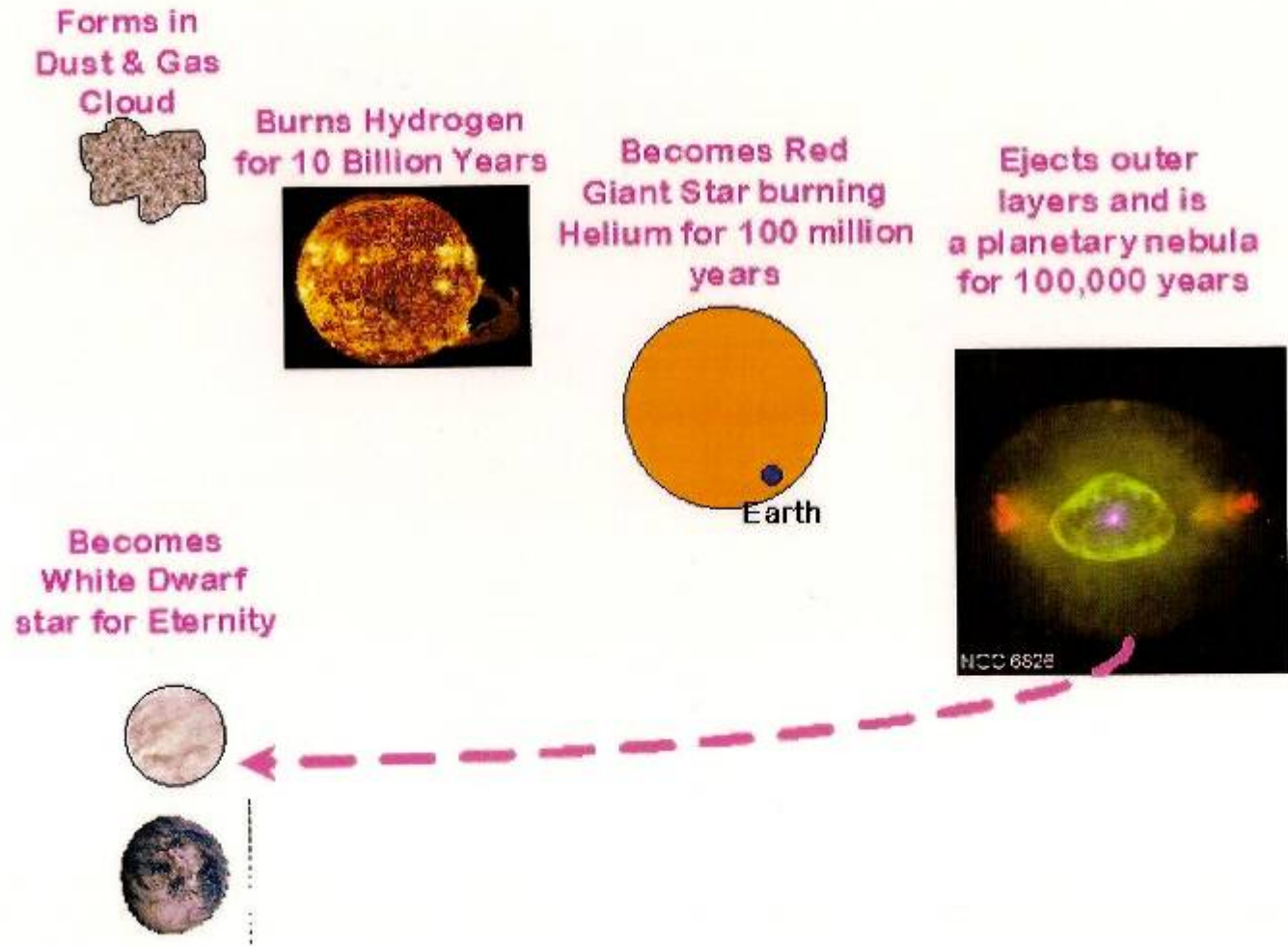
## Nuclear Astrophysics - 1

# Hertzspung-Russell diagram





# Life of small star ( $< 1,4 M_{\odot}$ )

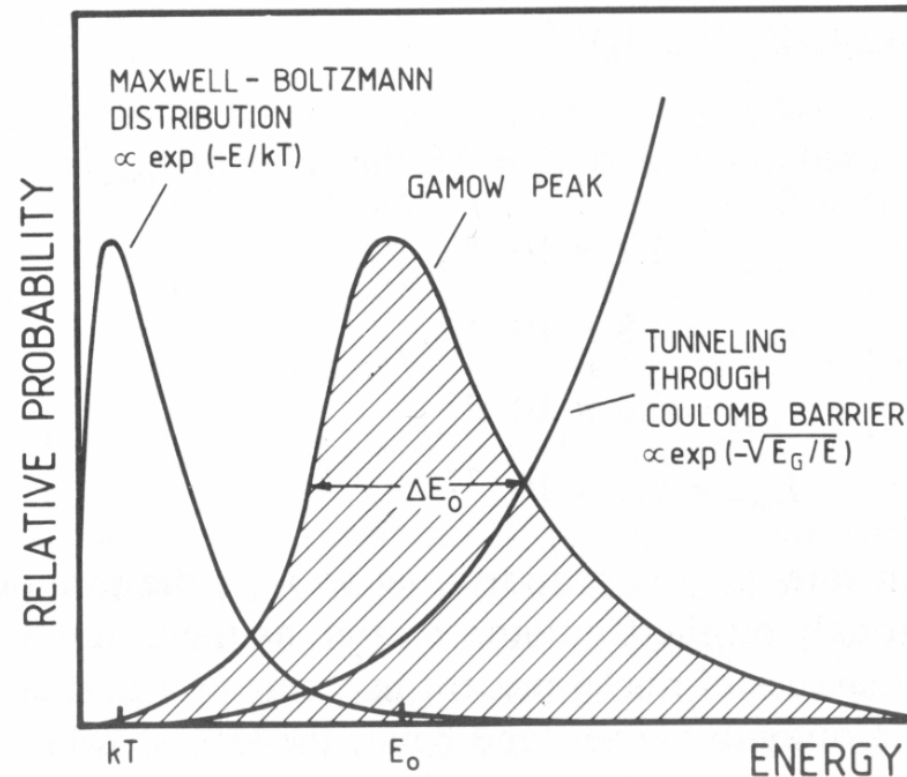




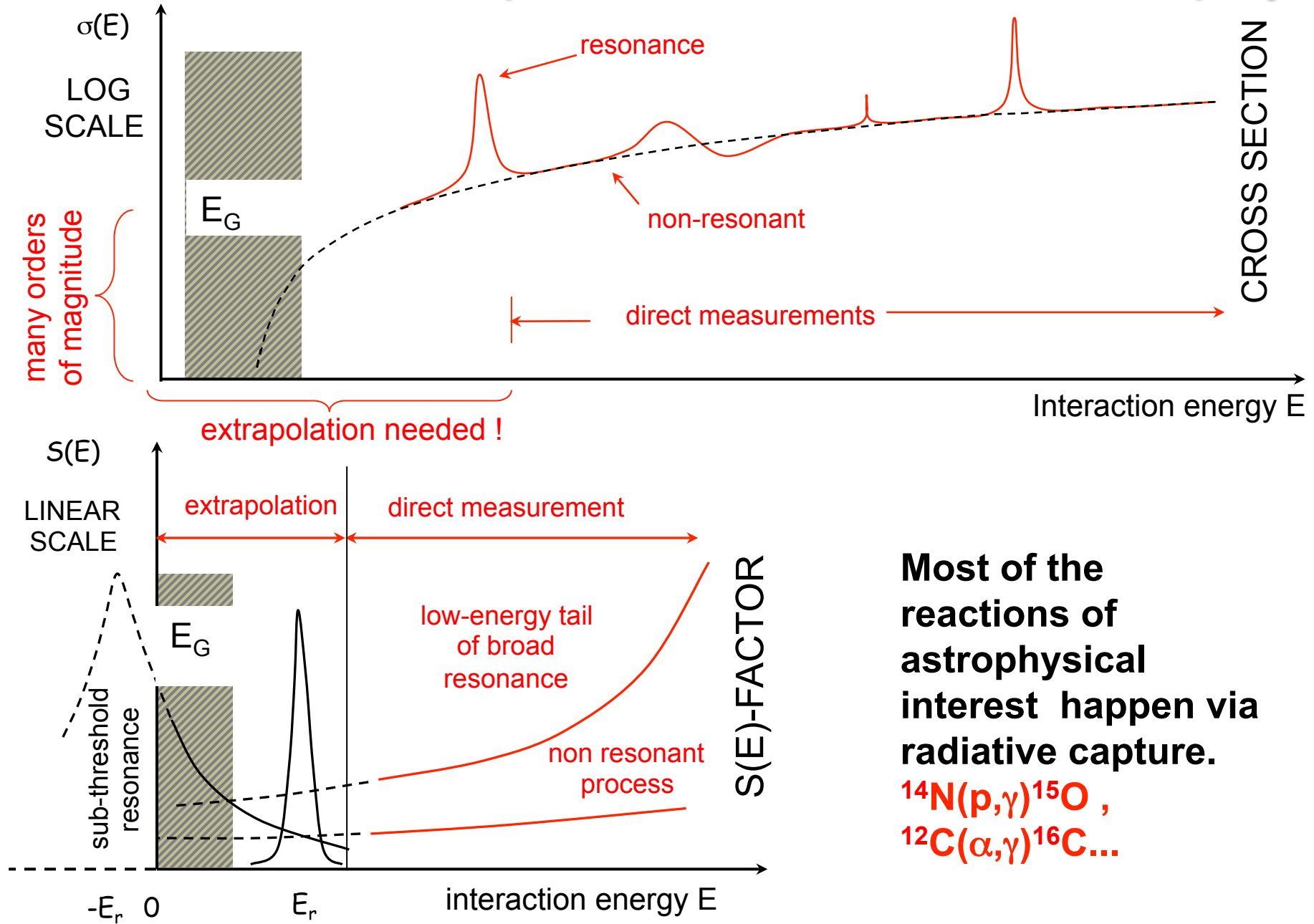
# Gamow window

Using definition S factor:

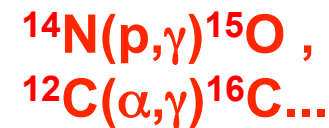
$$\langle \sigma v \rangle = \left( \frac{8}{\pi m} \right)^{1/2} \frac{1}{(kT)^{3/2}} \int_0^{\infty} S(E) \exp \left[ -\frac{E}{kT} - \frac{b}{E^{1/2}} \right] dE$$



# Problem of extrapolation in nuclear astrophysics



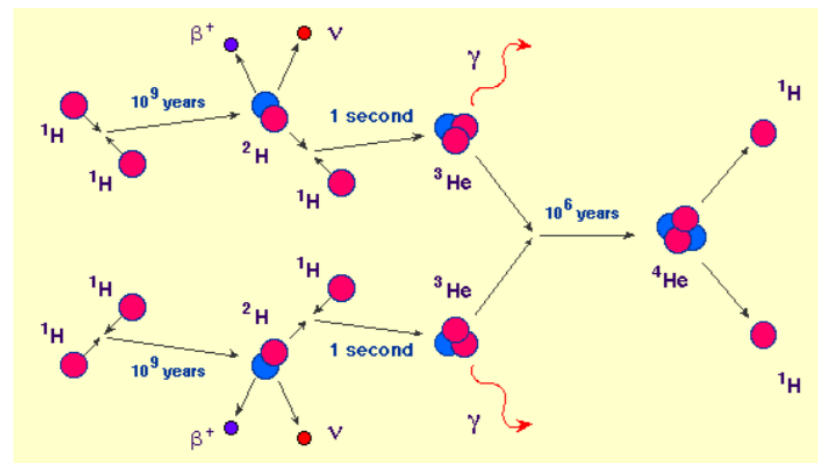
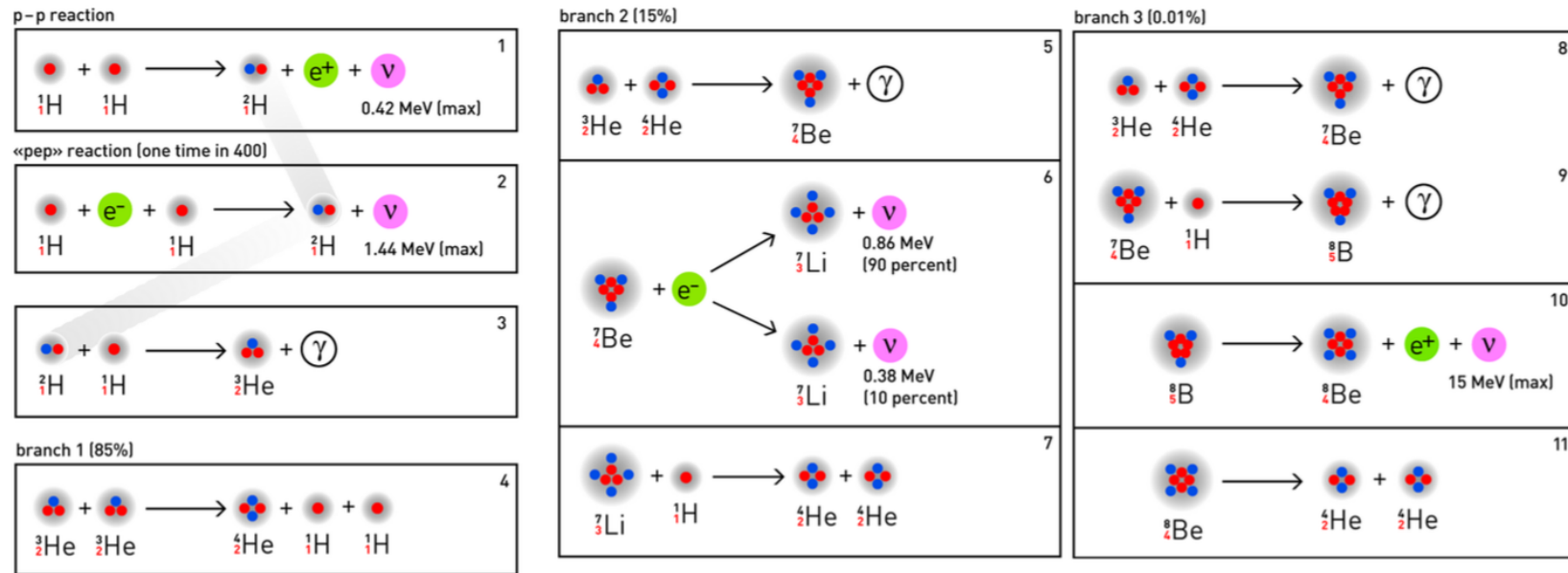
**Most of the reactions of astrophysical interest happen via radiative capture.**





## pp chains

Once  ${}^4\text{He}$  is produced can act as catalyst initializing the ppII and ppIII chains.





## The relevant S-factors

$p(p, e^+ \nu_e)d$ :  $S_{11}(0) = (4.00 \pm 0.05) \times 10^{25} \text{ MeV b}$   
**calculated**

$p(d, \gamma)^3\text{He}$ :  $S_{12}(0) = 2.5 \times 10^{-7} \text{ MeV b}$   
**measured at LUNA**

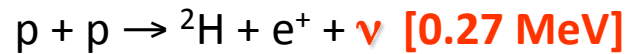
$^3\text{He}(^3\text{He}, 2p)^4\text{He}$ :  $S_{33}(0) = 5.4 \text{ MeV b}$   
**measured at LUNA**



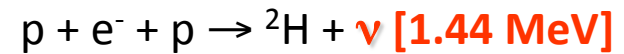
Laboratory Underground for Nuclear Astrophysics (Gran Sasso).



# LUNA program: pp chain



99.75%



0.25%

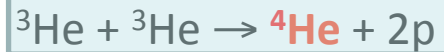


86%

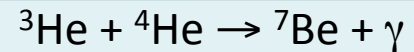
14%

50 kV 2001

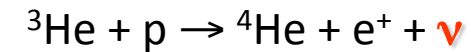
$2 \cdot 10^{-5}\%$



50 kV 1999

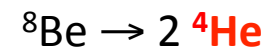
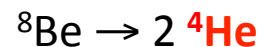
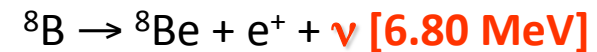
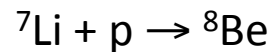
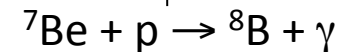
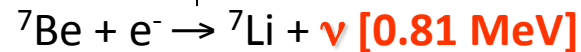


400 kV 2006



99.89%

0.11%



CHAIN I

$Q_{\text{eff}} = 26.20 \text{ MeV}$

CHAIN II

$Q_{\text{eff}} = 25.66 \text{ MeV}$

CHAIN III

$Q_{\text{eff}} = 19.67 \text{ MeV}$

CHAIN IV

$Q_{\text{eff}} = 16.84 \text{ MeV}$

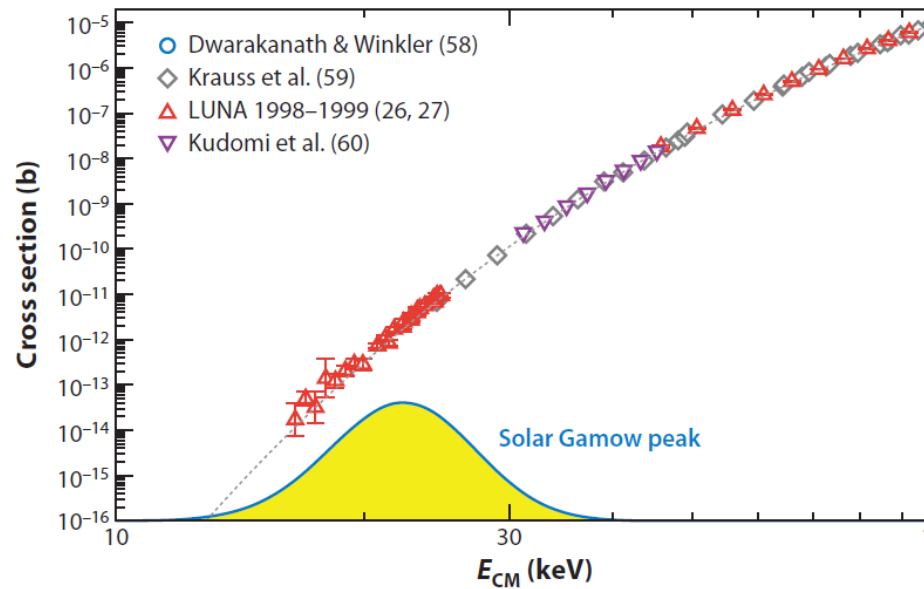
# LUNA (Laboratory Underground for Nuclear Astrophysics)

50 kV accelerator @ Gran Sasso – Italy

(1400 m rock ->  $10^6$  shielding factor)



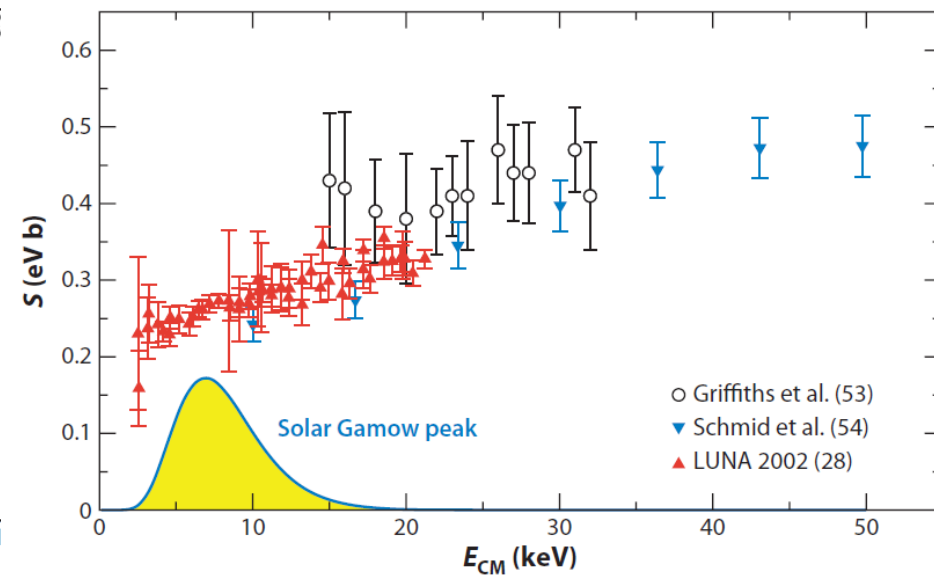
R. Bonetti et al.: Phys. Rev. Lett. 82 (1999) 5205



At lowest energy:  $\sigma \sim 20$  fb  $\rightarrow$  1 event/month



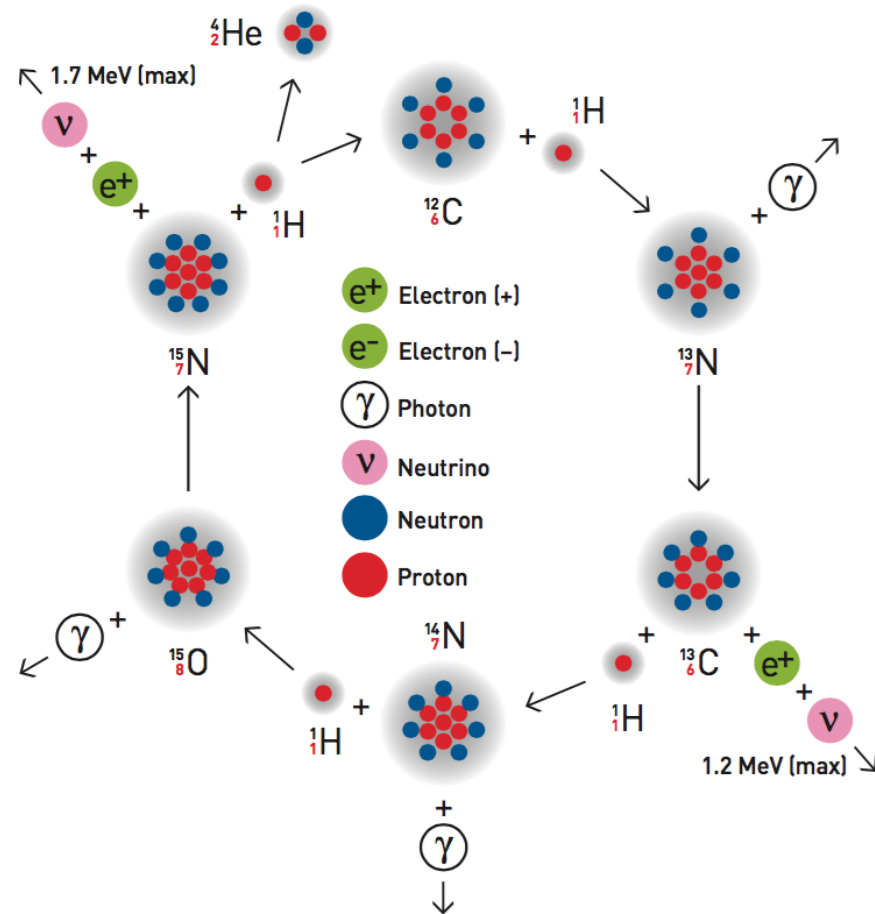
C. Casella et al.: Nucl. Phys. A706 (2002) 203-216



At lowest energy:  $\sigma \sim 9$  pb  $\rightarrow$  50 counts/day

**No extrapolation needed!**

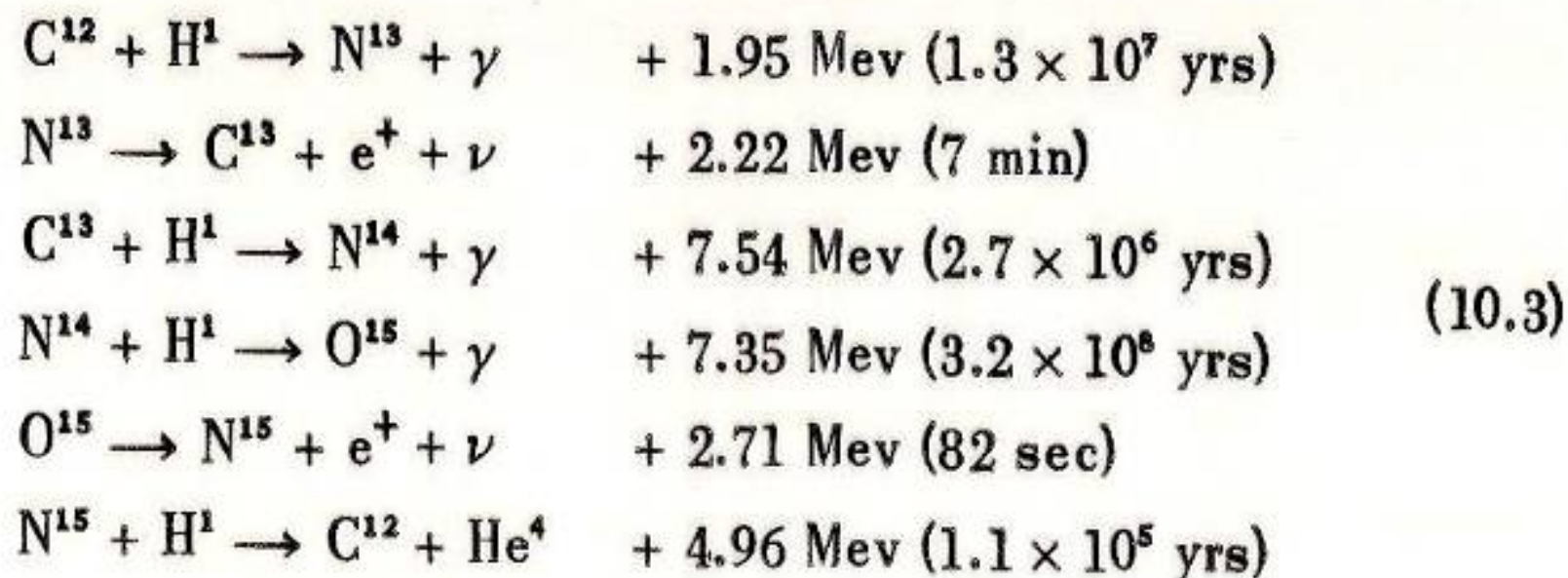
# The other hydrogen burning: CNO cycle



requires presence of  $^{12}\text{C}$  as catalyst.

## The Carbon Cycle

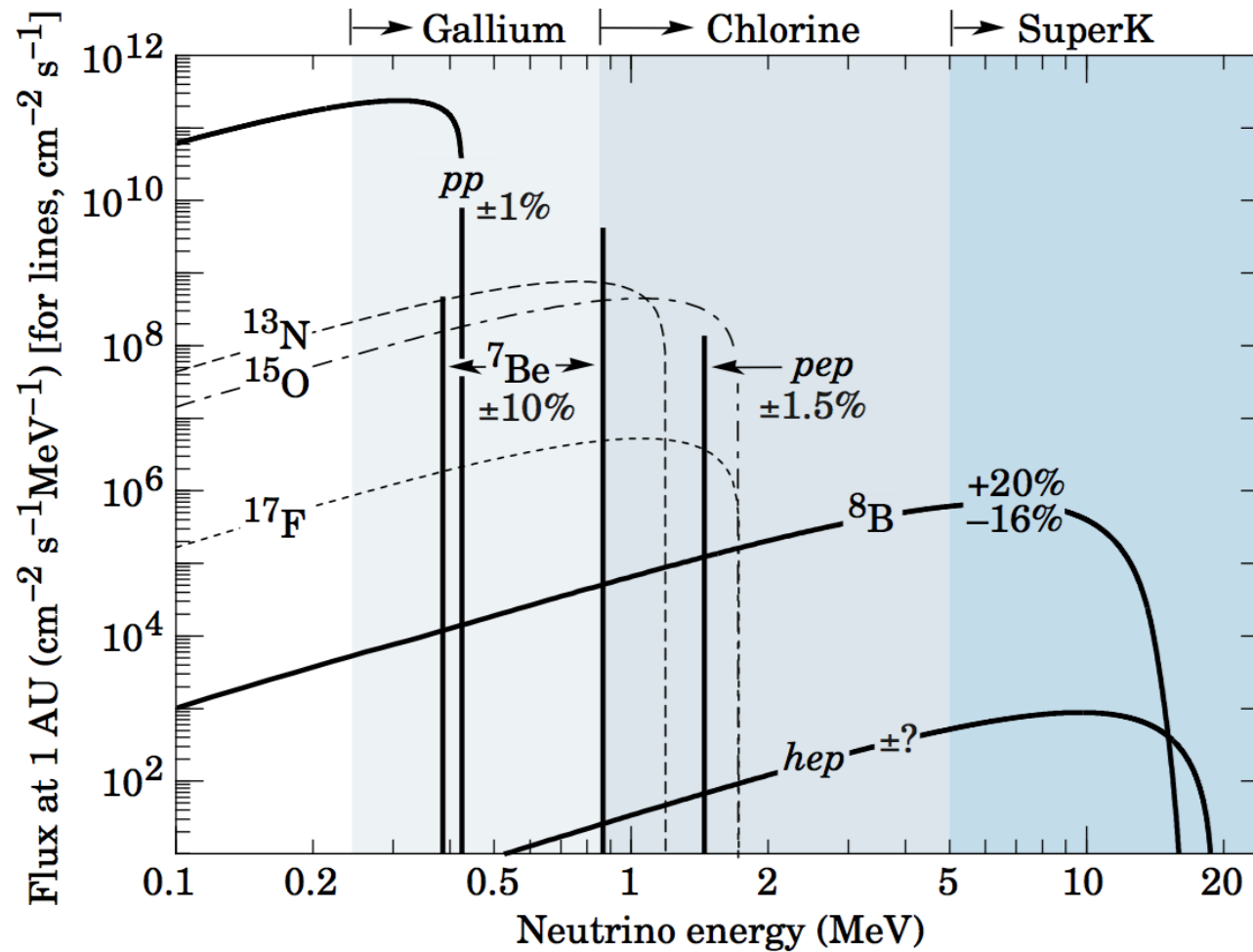
An alternative way of transmuting hydrogen into helium exists in the carbon cycle, which consists of the following six reactions



To start with, the collision of a proton with a common carbon nucleus produces a  $\text{N}^{13}$  particle with emission of a gamma ray. The  $\text{N}^{13}$  particle is not stable but decays—in seven minutes, on the average—into the heavy carbon isotope with the emission of a positron and a neutrino. Again, the positron disappears together with an electron and the neutrino leaves the star. The next build-up step is taken when a second proton collides with the heavy carbon isotope, forming a common nitrogen nucleus.

# Neutrino spectrum (Sun)

This is the predicted neutrino spectrum





# Life of big star ( $> 1,4 M_{\odot}$ )

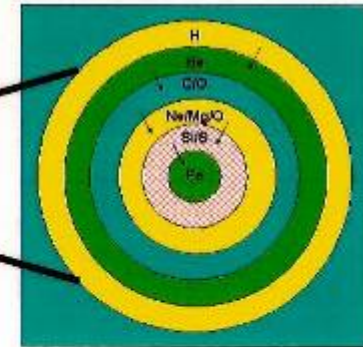
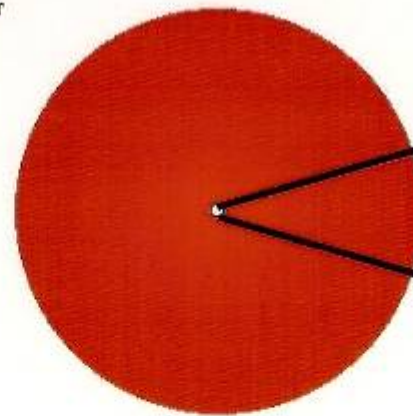
Forms in  
Dust & Gas  
Cloud



Burns Hydrogen  
for 50 Million Years



Becomes Red  
SuperGiant Star for  
1 Million Years



End in Supernovae of type Ib, Ic et II



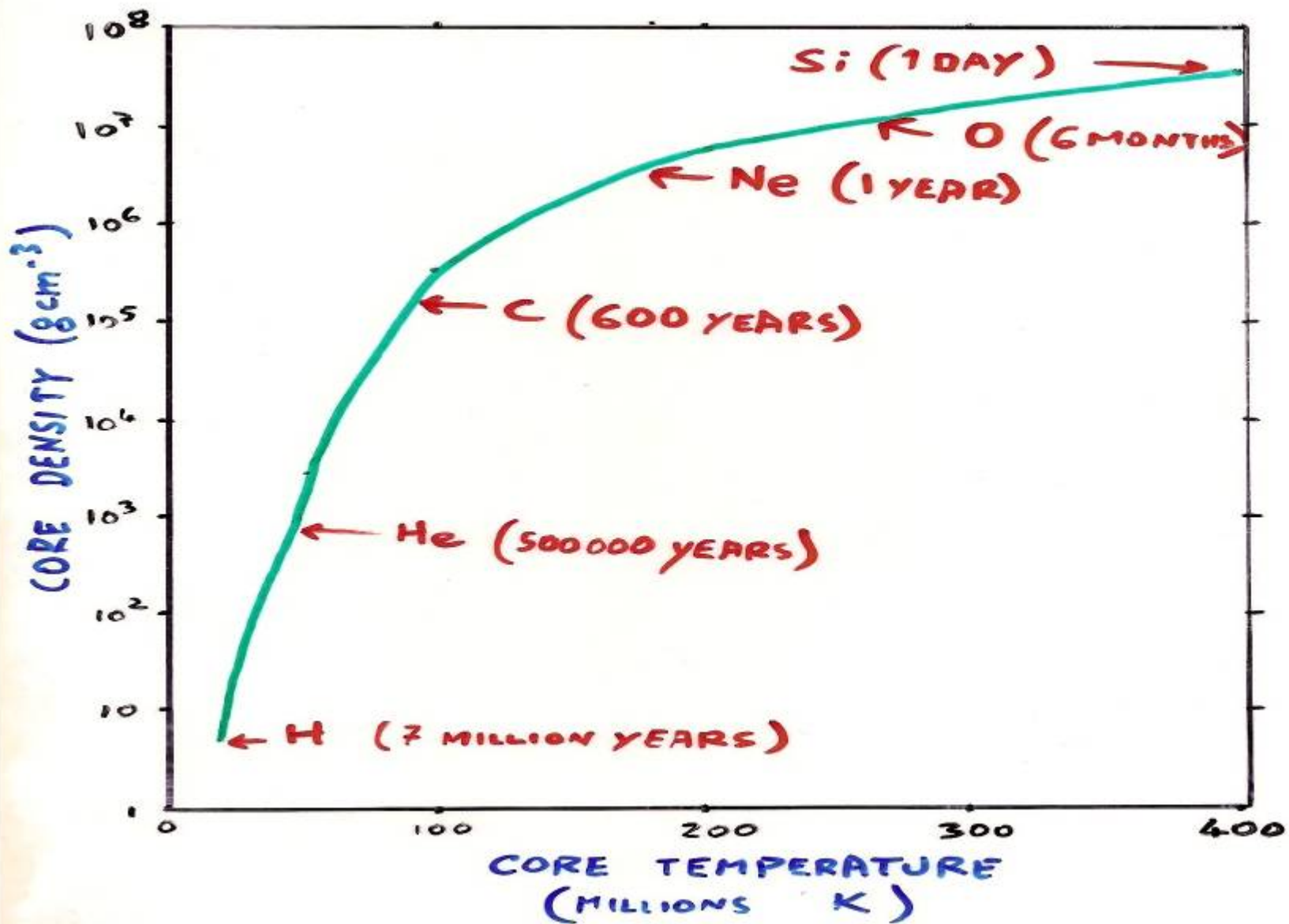


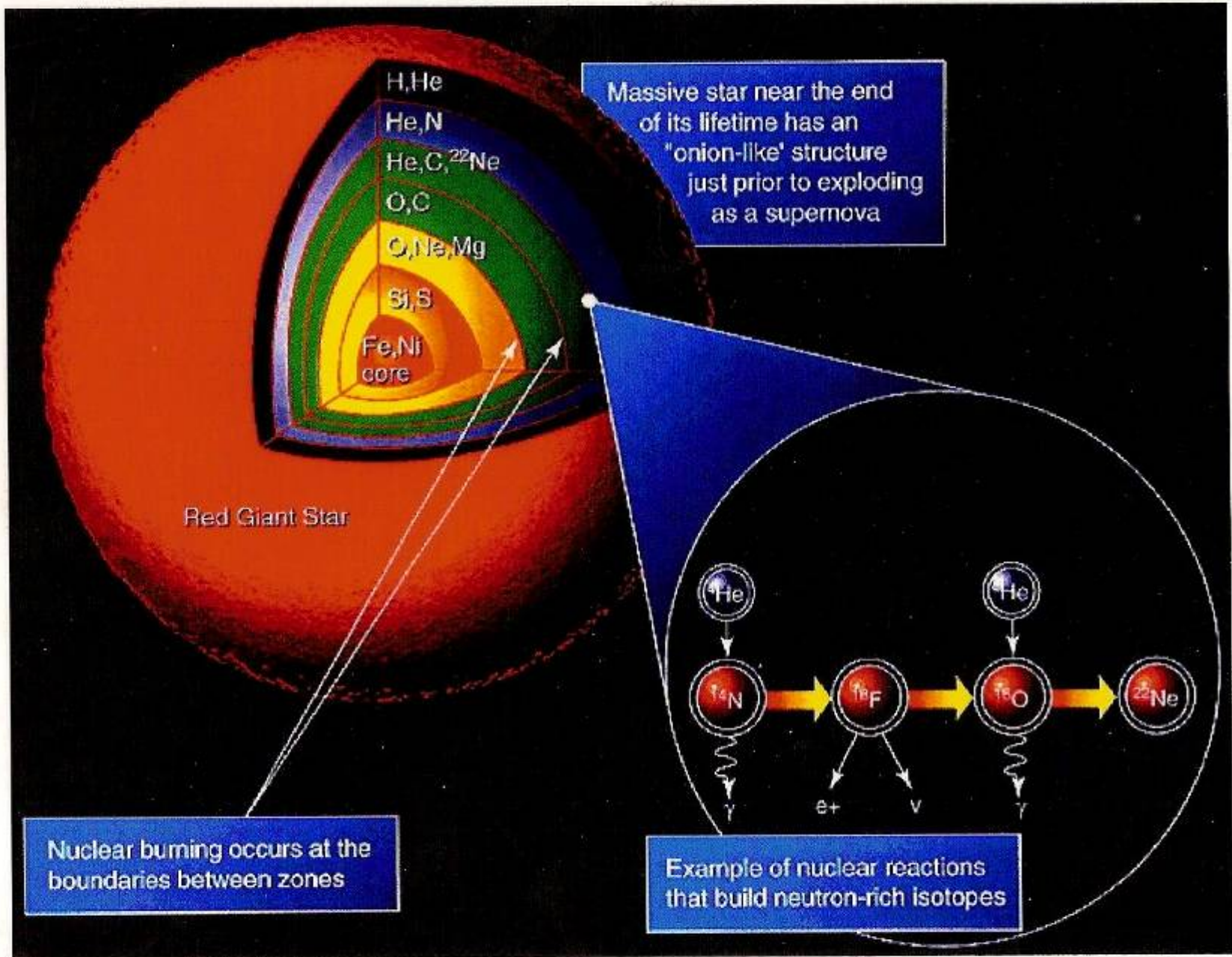


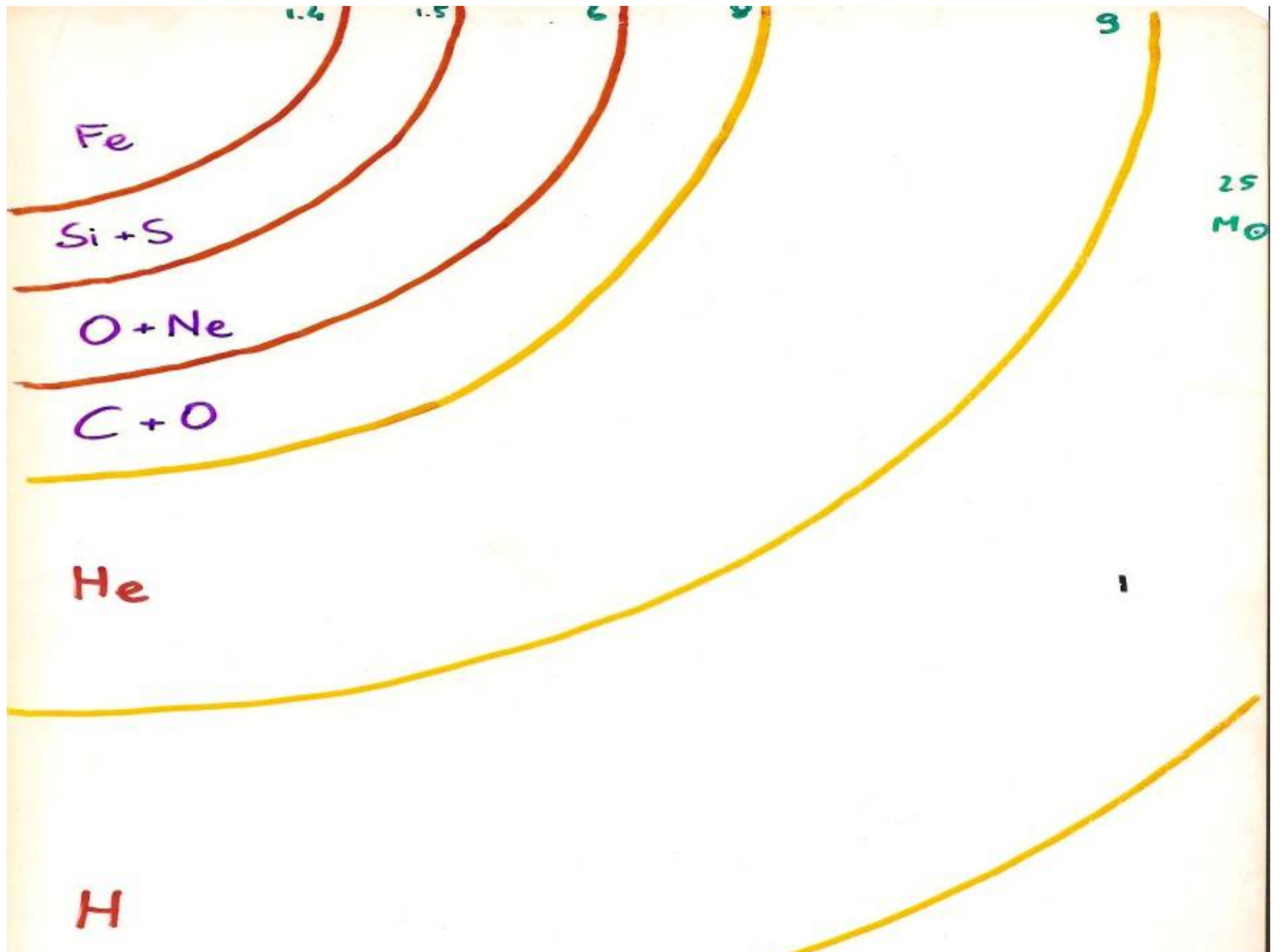




# MASSIVE STAR EVOLUTION : $M = 25 M_{\odot}$







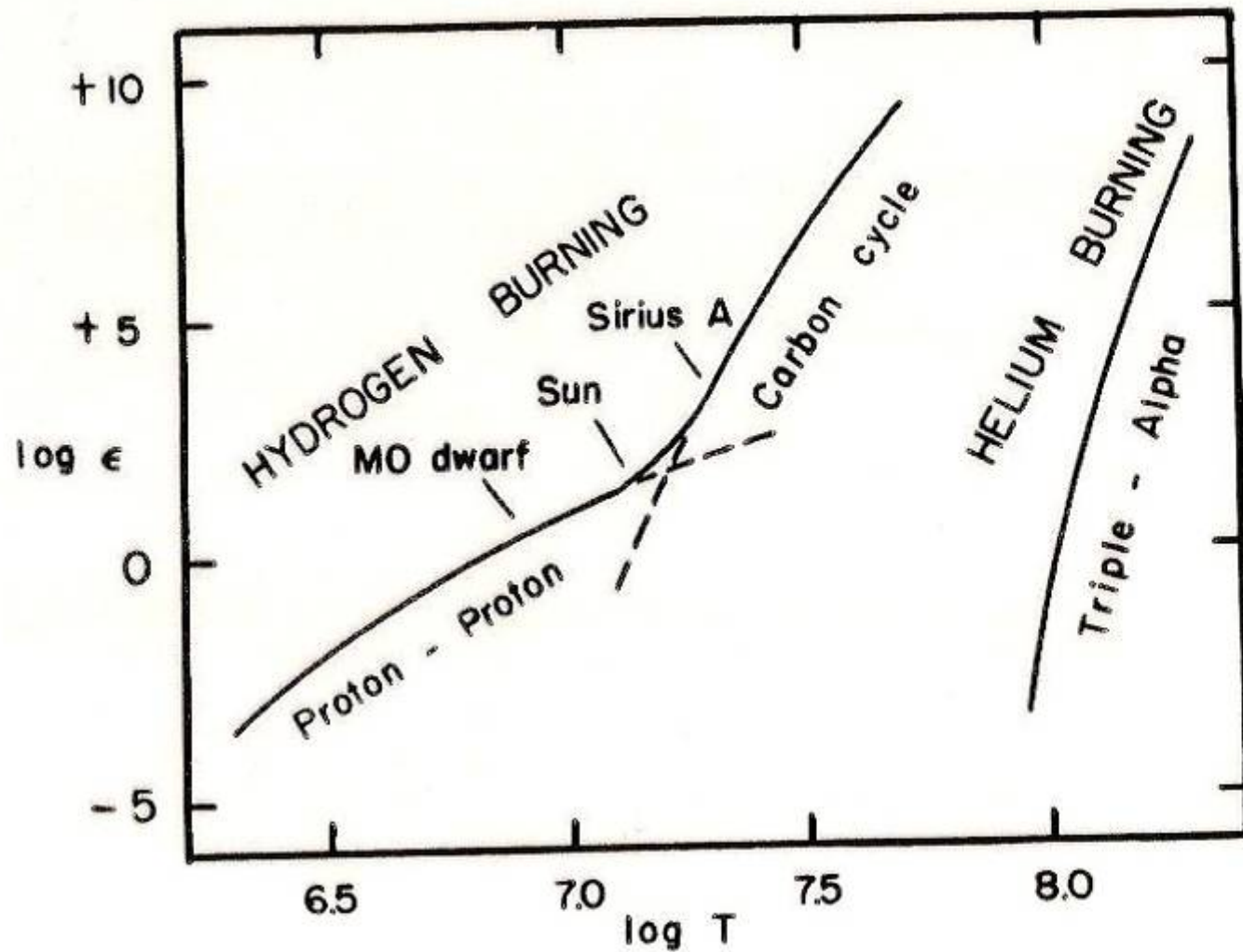


Fig. 10.1. Nuclear energy generation as a function of temperature (with  $\rho X^2 = 100$  and  $X_{CN} = 0.005X$  for the proton-proton reaction and the carbon cycle, but  $\rho^2 Y^3 = 10^8$  for the triple-alpha process).

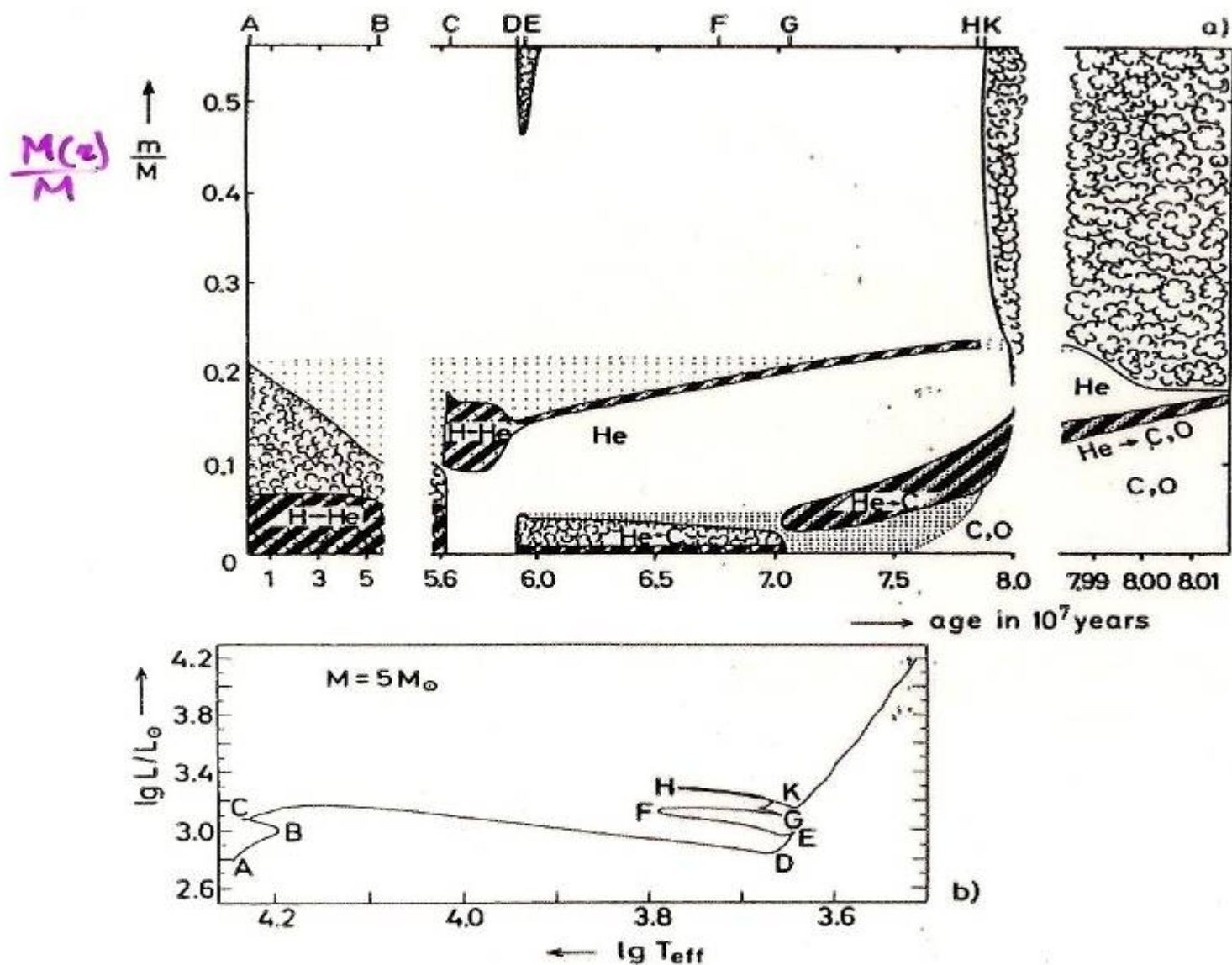
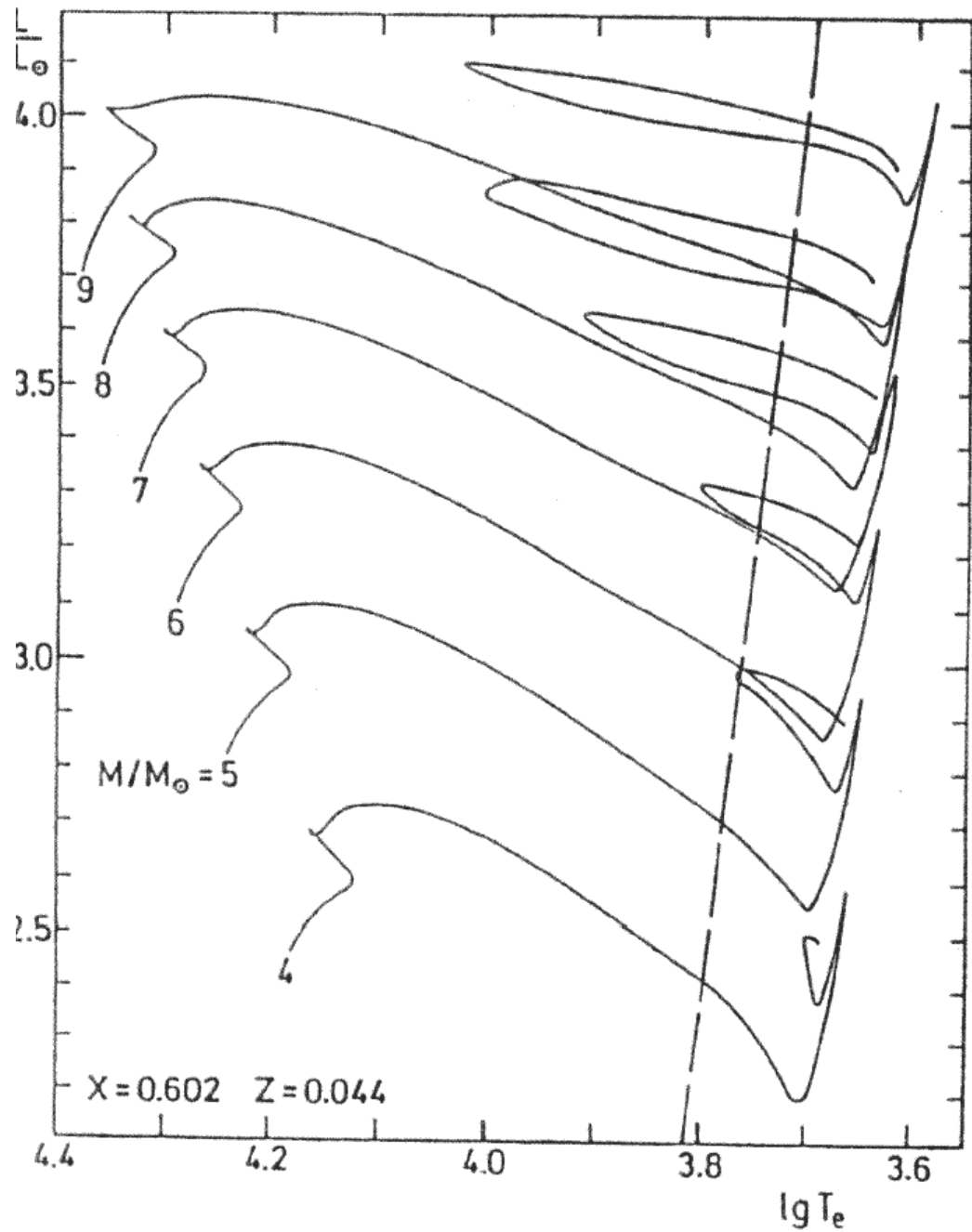


Fig. 31.2. (a) The evolution of the internal structure of a star of  $5M_{\odot}$  of extreme population I. The abscissa gives the age after the ignition of hydrogen in units of  $10^7$  years; each vertical line corresponds to a model at a given time. The different layers are characterized by their values of  $m/M$ . "Cloudy" regions indicate convective areas. Heavily hatched regions indicate where the nuclear energy generation ( $\epsilon_{\text{H}}$  or  $\epsilon_{\text{He}}$ ) exceeds  $10^3 \text{ erg g}^{-1} \text{ s}^{-1}$ . Regions of variable chemical composition are dotted. The letters A ... K above the upper abscissa indicate the corresponding points in the evolutionary track, which is plotted in Fig. 31.2 (b). (After KIPPENHAHN et al., 1965)





**Fig. 31.6.** Hertzsprung–Russell diagram with evolutionary tracks for stars in the mass range from  $4 M_{\odot}$  to  $9 M_{\odot}$  from the main sequence through helium burning (after MATRAKA et al., 1982). The broken line indicates the Cepheid strip

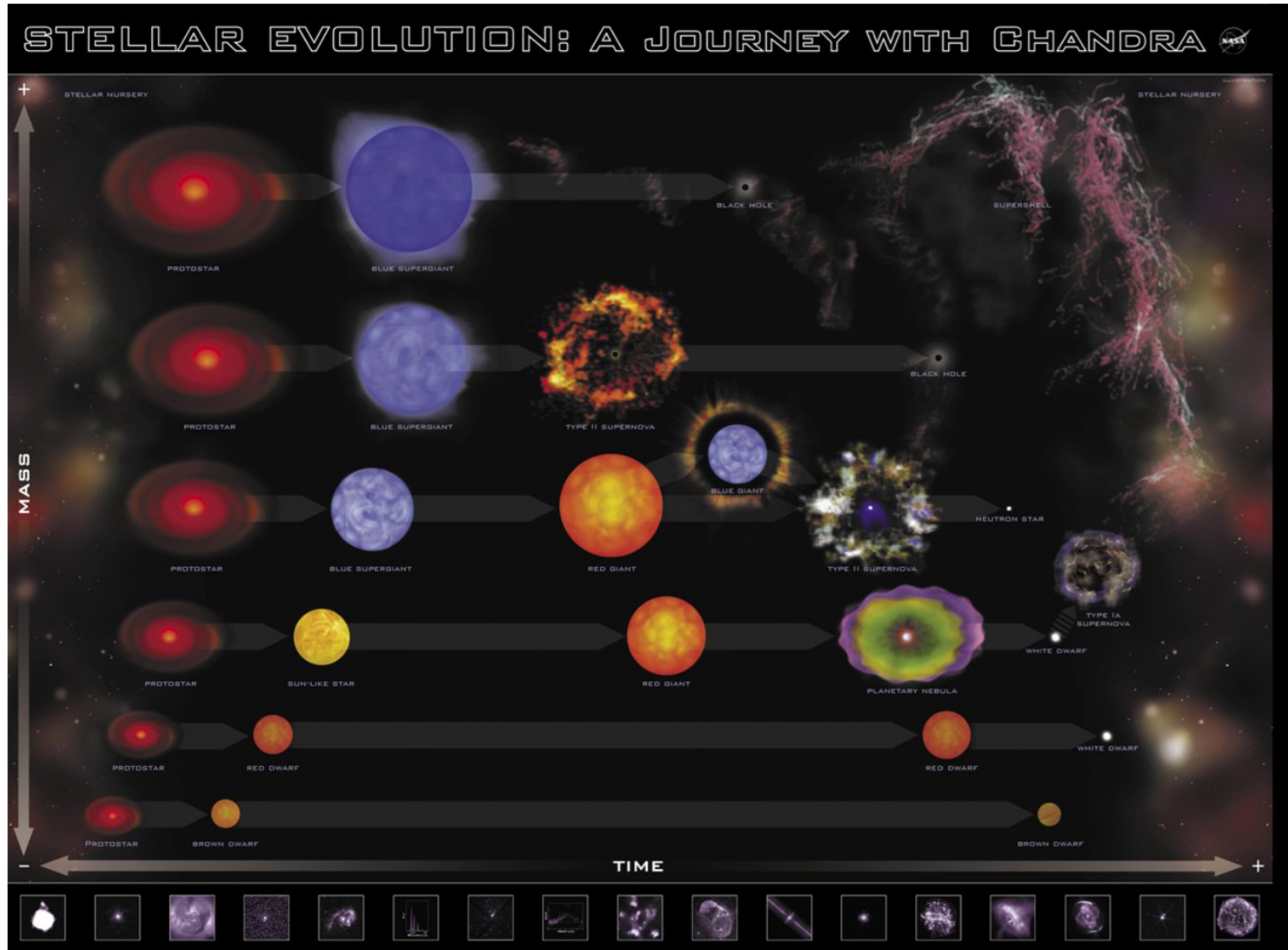
## Stellar life

## Nuclear burning stages

(e.g., 20 solar mass star)

Fuel	Main Product	Secondary Product	T ( $10^9$ K)	Time (yr)	Main Reaction
H	He	$^{14}\text{N}$	0.02	$10^7$	$4\text{H} \xrightarrow{\text{CNO}} ^4\text{He}$
He	O, C	$^{18}\text{O}$ , $^{22}\text{Ne}$ s-process	0.2	$10^6$	$3\text{He}^4 \rightarrow ^{12}\text{C}$ $^{12}\text{C}(\alpha, \gamma)^{16}\text{O}$
C	Ne, Mg	Na	0.8	$10^3$	$^{12}\text{C} + ^{12}\text{C}$
Ne	O, Mg	Al, P	1.5	3	$^{20}\text{Ne}(\gamma, \alpha)^{16}\text{O}$ $^{20}\text{Ne}(\alpha, \gamma)^{24}\text{Mg}$
O	Si, S	Cl, Ar, K, Ca	2.0	0.8	$^{16}\text{O} + ^{16}\text{O}$
Si	Fe	Ti, V, Cr, Mn, Co, Ni	3.5	0.02	$^{28}\text{Si}(\gamma, \alpha)\dots$

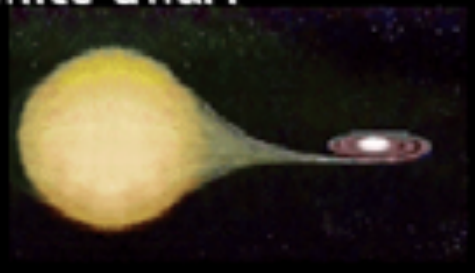
# Stellar Evolution



## Type Ia vs. Core-Collapse Supernovae

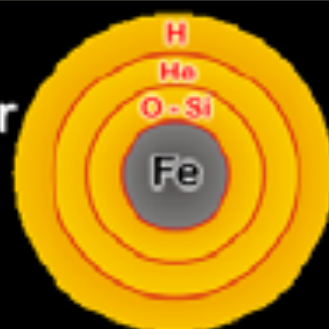
### Type Ia

- Carbon-oxygen white dwarf (remnant of low-mass star)
- Accretes matter from companion



### Core collapse (Type II, Ib/c)

- Degenerate iron core of evolved massive star
- Accretes matter by nuclear burning at its surface



Chandrasekhar limit is reached –  $M_{Ch} \approx 1.5 M_{sun} (2Y_e)^2$

**COLLAPSE SETS IN**

Nuclear burning of C and O ignites  
→ Nuclear deflagration  
("Fusion bomb" triggered by collapse)

Collapse to nuclear density  
Bounce & shock  
Implosion → Explosion

Powered by nuclear binding energy

Powered by gravity

Gain of nuclear binding energy  
- 1 MeV per nucleon

Gain of gravitational binding energy  
- 100 MeV per nucleon  
99% into neutrinos

## Classification of Supernovae

Spectral Type	Ia	Ib	Ic	II
Spectrum	No Hydrogen			Hydrogen
	Silicon	No Silicon		
		Helium	No Helium	
Physical Mechanism	Nuclear explosion of low-mass star	Core collapse of evolved massive star (may have lost its hydrogen or even helium envelope during red-giant evolution)		
Light Curve	Reproducible	Large variations		
Neutrinos	Insignificant	~ 100 × Visible energy		
Compact Remnant	None	Neutron star (typically appears as pulsar) Sometimes black hole?		
Rate / h <sup>2</sup> SNU	0.36 ± 0.11	0.14 ± 0.07		0.71 ± 0.34
Observed	Total ~ 2000 as of today (nowadays ~200/year)			



# SuperNovae Remnants

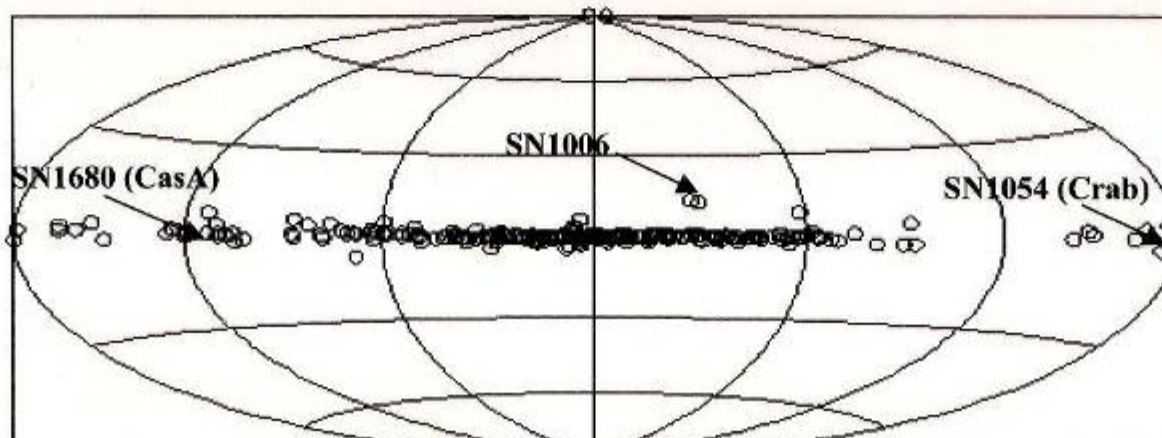
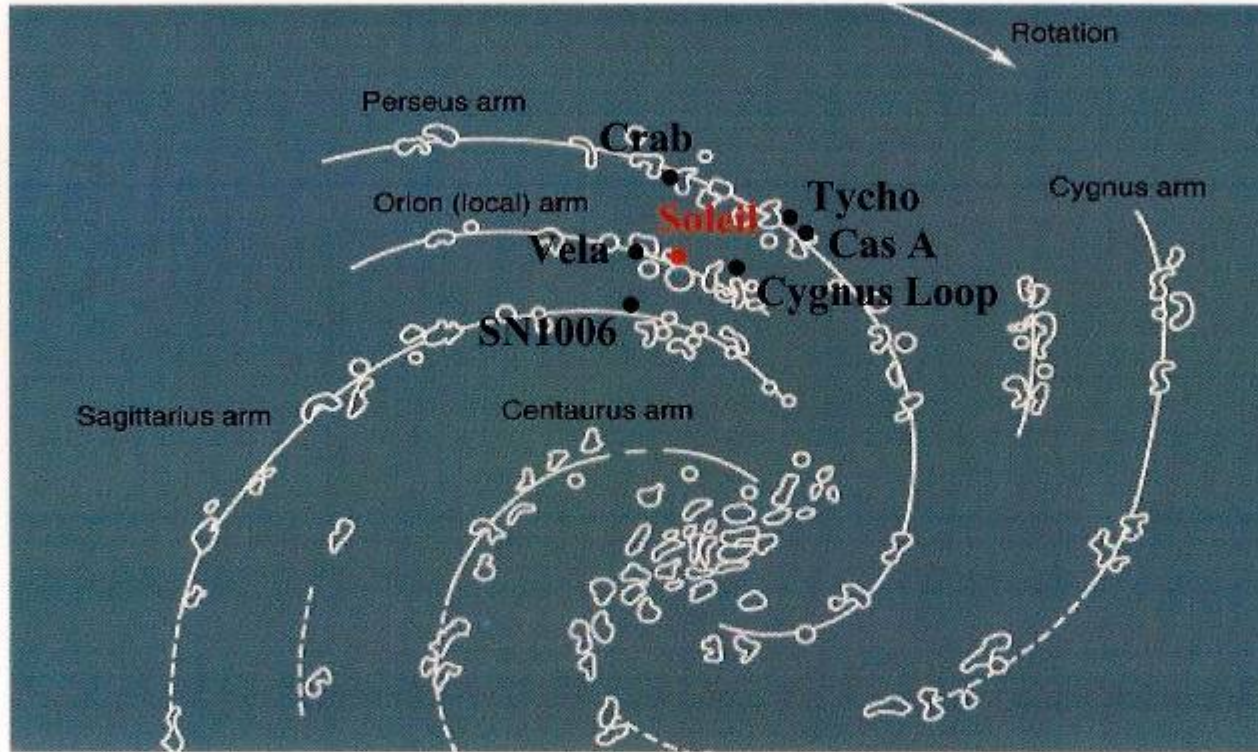
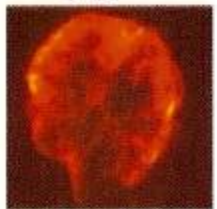
Vela



Tycho



Cygnus



Crab



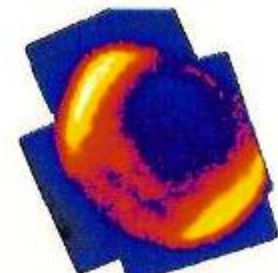
Kepler



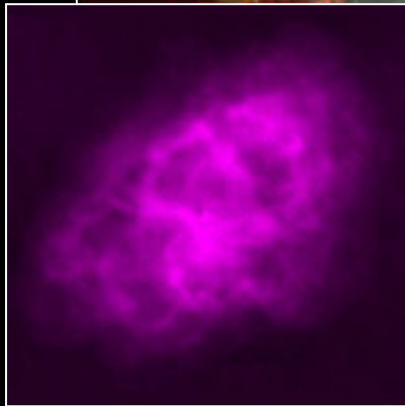
Cas A



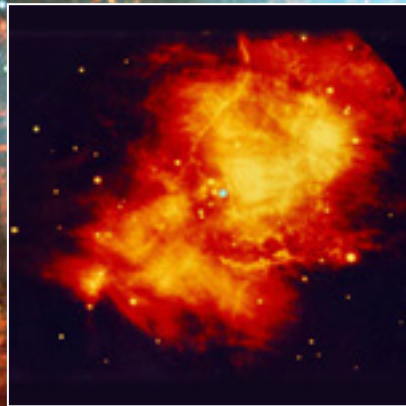
SN1006



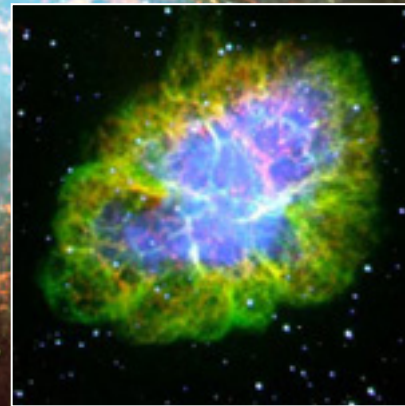
# The Crab in Multi-Wavelengths Photons



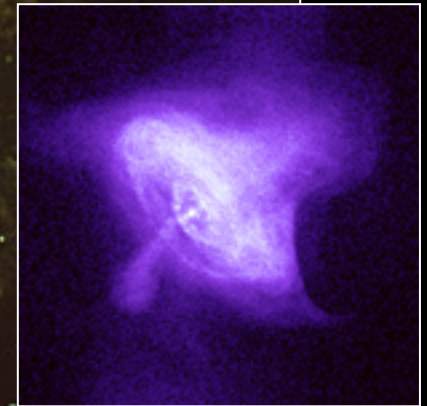
Radio



Infrared



Optical



X-ray



# Astrofisica Nucleare e Subnucleare

## Solar Neutrinos

# The 2002 Nobel Prize for the Solar Neutrino Physics



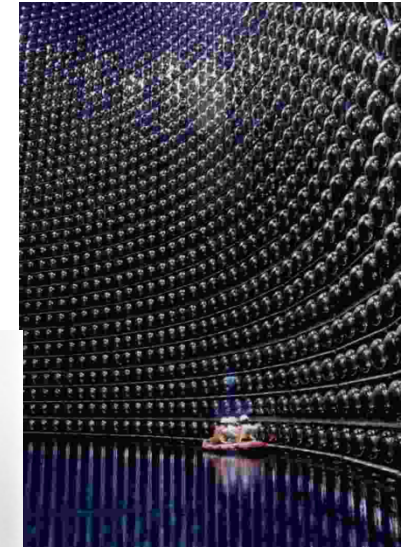
Raymond Davis Jr.

[http://nobelprize.org/nobel\\_prizes/physics/laureates/2002/davis-lecture.pdf](http://nobelprize.org/nobel_prizes/physics/laureates/2002/davis-lecture.pdf)

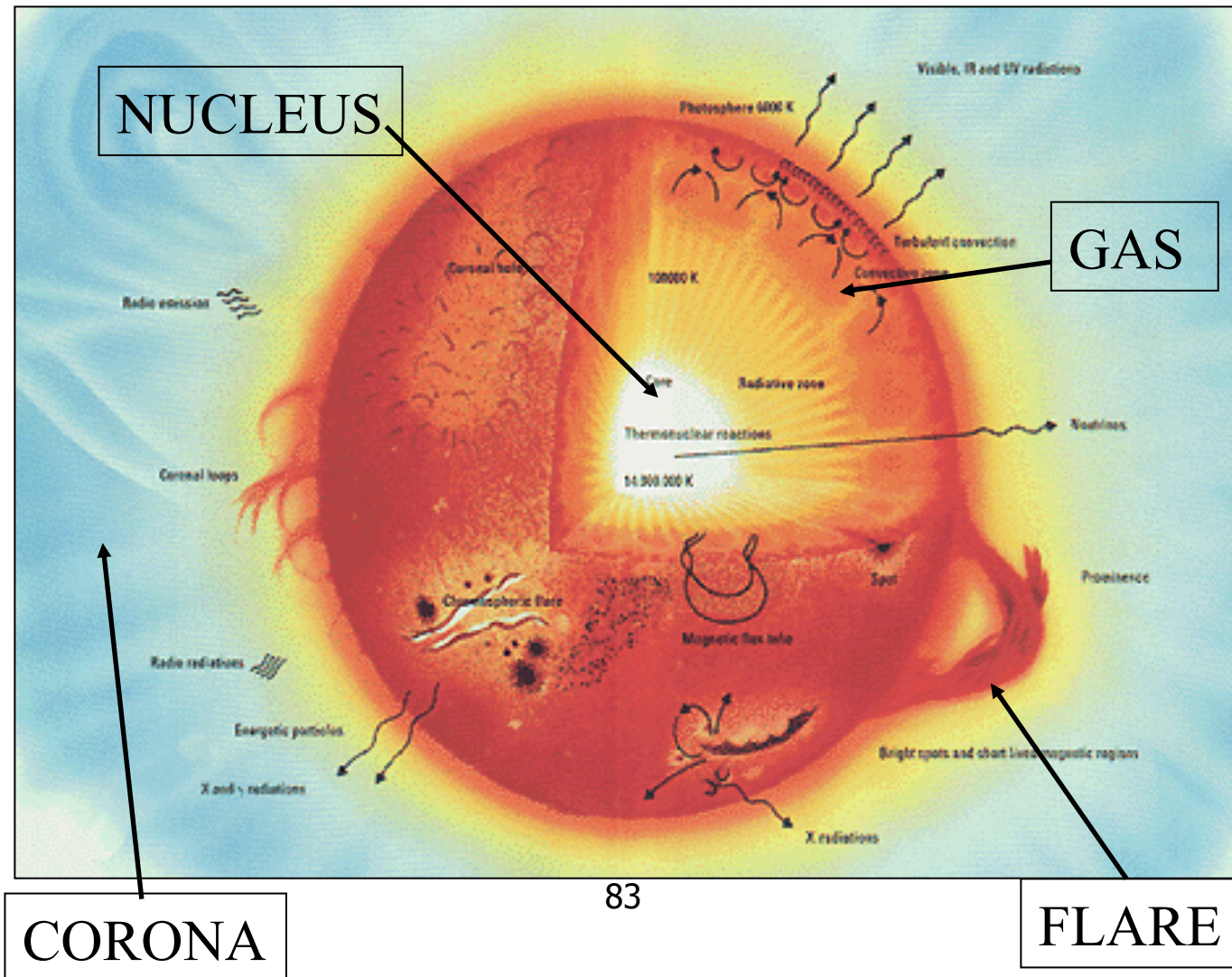


Masatoshi Koshihara

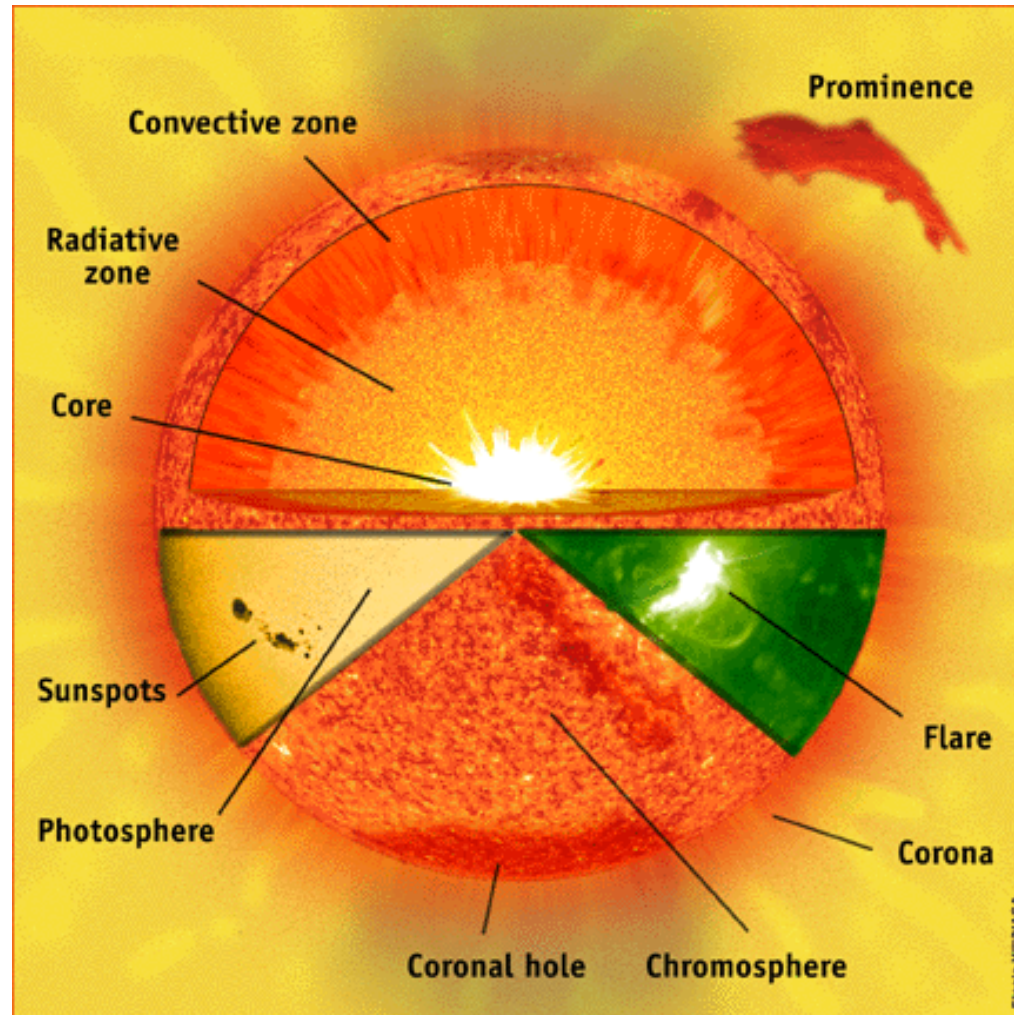
[http://nobelprize.org/nobel\\_prizes/physics/laureates/2002/koshihara-lecture.pdf](http://nobelprize.org/nobel_prizes/physics/laureates/2002/koshihara-lecture.pdf)



# The Standard Solar Model



# The Standard Solar Model



# The Standard Solar Model

<http://www.sns.ias.edu/~jnb/>

- J. Bahcall: The main author of the SSM
- The standard solar model is derived from the conservation laws and energy transport equations of physics, applied to a spherically symmetric gas (plasma) sphere
- Constrained by the luminosity, radius, age and composition of the Sun
- Inputs for the Standard Solar Model
  - Mass
  - Age
  - Luminosity
  - Radius
- No free parameters
- Tested by helioseismology
- Fusion  $\Rightarrow$  neutrinos



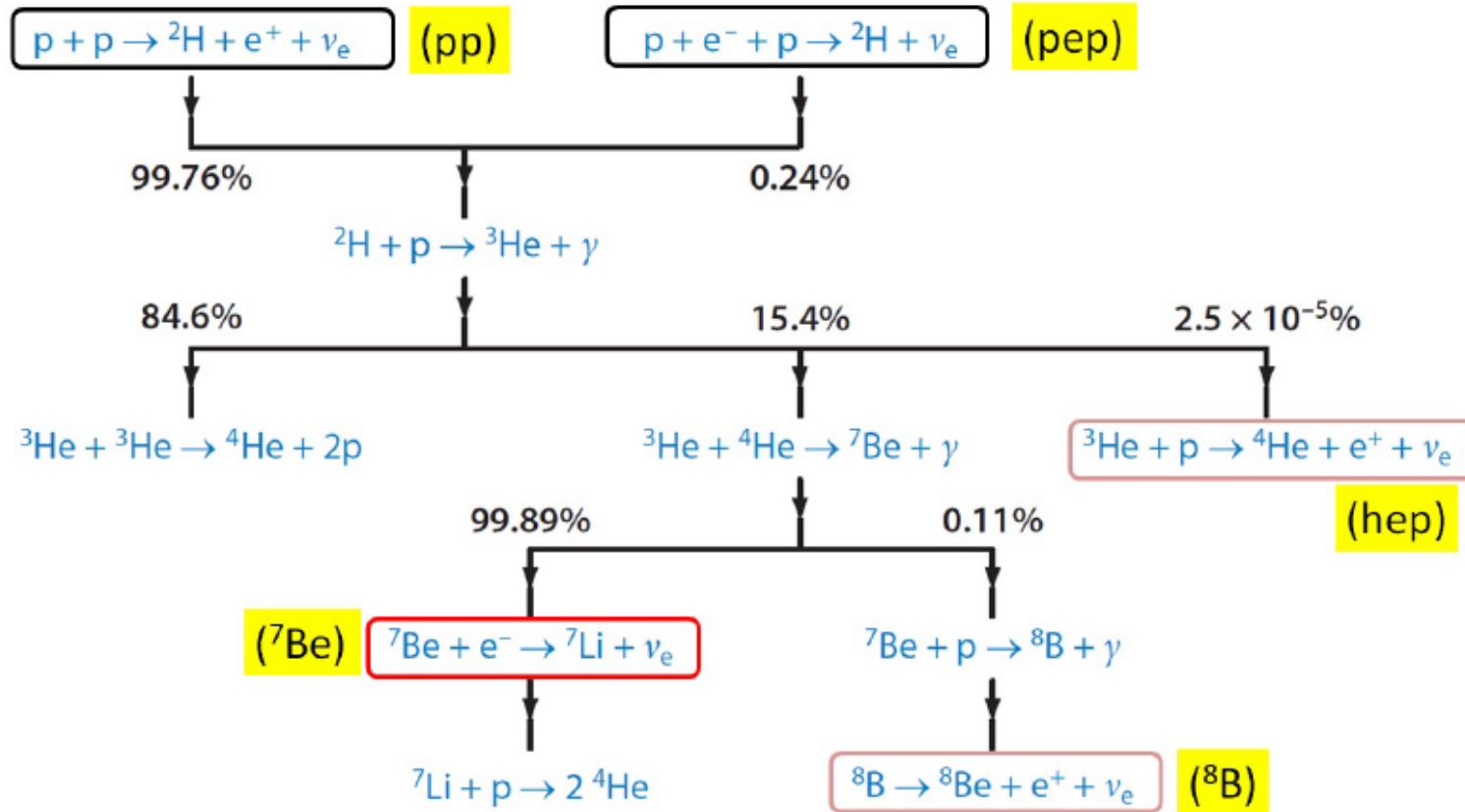
**Nota: Leggere l'articolo (tradotto anche in italiano)**

<http://www.sns.ias.edu/~jnb/Papers/Popular/Nobelmuseum/italianmystery.pdf>

# The predictions of the SSM

- Most of the neutrinos produced in the sun come from the first step of the pp chain.
- Their energy is so low ( $<0.425$  MeV)  $\rightarrow$  very difficult to detect.
- A rare side branch of the pp chain produces the "boron-8" neutrinos with a maximum energy of roughly 15 MeV
- These are the easiest neutrinos to observe, because the neutrino cross section increases with energy.
- A very rare interaction in the pp chain produces the "hep" neutrinos, the highest energy neutrinos produced in any detectable quantity by our sun.
- All of the interactions described above produce neutrinos with a spectrum of energies. The inverse beta decay of  $\text{Be}^7$  produces mono-energetic neutrinos at either roughly 0.9 or 0.4 MeV.

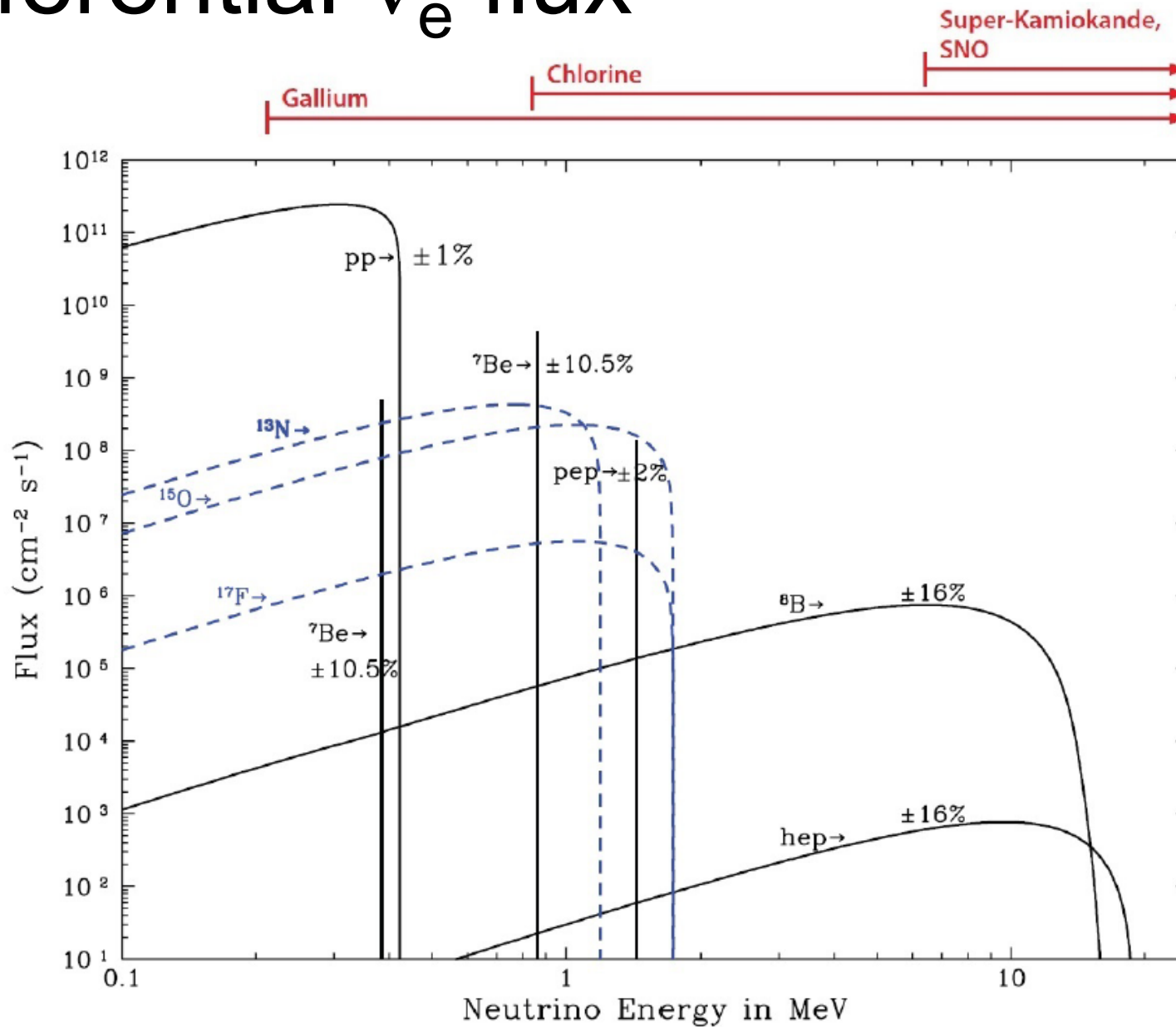
# $\nu$ from the Sun: the proton cycle



$$4p \rightarrow {}^4\text{He} + 2e^+ + 2\nu_e \quad Q = 26.73 \text{ MeV} \quad \langle E_\nu \rangle \simeq 0.3 \text{ MeV}$$

$$\Phi_{\nu_e} \simeq \frac{1}{4\pi D_\odot^2} \frac{2L_\odot}{(Q - \langle E_\nu \rangle)} = 6 \times 10^{10} \text{ cm}^{-2} \text{ s}^{-1}$$

# Differential $\nu_e$ flux





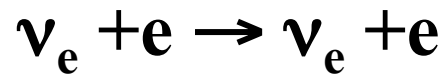
# Neutrino Emission

Source $r$	Reaction	Average Neutrino Energy $\langle E \rangle_r$ (MeV)	Maximum Neutrino Energy (MeV)
$pp$	$p + p \rightarrow d + e^+ + \nu_e$	0.2668	$0.423 \pm 0.03$
$pep$	$p + e^- + p \rightarrow d + \nu_e$	1.445	1.445
${}^7\text{Be}$	$e^- + {}^7\text{Be} \rightarrow {}^7\text{Li} + \nu_e$	0.3855 0.8631	0.3855 0.8631
${}^8\text{B}$	${}^8\text{B} \rightarrow {}^8\text{Be}^* + e^+ + \nu_e$	$6.735 \pm 0.036$	$\sim 15$
$hep$	${}^3\text{He} + p \rightarrow {}^4\text{He} + e^+ + \nu_e$	9.628	18.778
${}^{13}\text{N}$	${}^{13}\text{N} \rightarrow {}^{13}\text{C} + e^+ + \nu_e$	0.7063	$1.1982 \pm 0.0003$
${}^{15}\text{O}$	${}^{15}\text{O} \rightarrow {}^{15}\text{N} + e^+ + \nu_e$	0.9964	$1.7317 \pm 0.0005$
${}^{17}\text{F}$	${}^{17}\text{F} \rightarrow {}^{17}\text{O} + e^+ + \nu_e$	0.9977	$1.7364 \pm 0.0003$

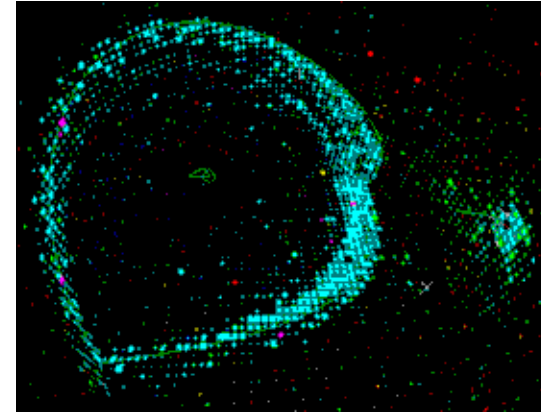
# Experimental Techniques

Two detection techniques for the solar neutrinos:

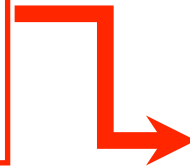
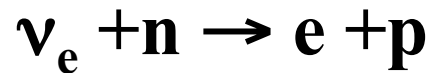
1- elastic scattering



SK



2- Neutron capture



No free neutrons in nature:



Example:  ${}^{71}\text{Ga} + \nu \rightarrow {}^{71}\text{Ge} + e$

3- The SNO way:

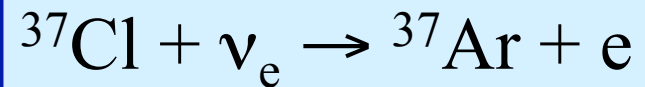
- $\nu_e + d \rightarrow e + p + p$
- $\nu_x + d \rightarrow \nu_x + n + p$

# Solar Neutrino Detectors

- Neutrino Absorption Experiments
  - $^{37}\text{Cl}$
  - $^{71}\text{Ga}$
- Neutrino Scattering Experiments
  - SuperKamiokande
- Direct Counting experiments
  - SNO

- 'Davis'
- GALLEX/GNO < (radiochemical)
- SAGE
- SuperKamiokande (elastic scattering)
- SNO

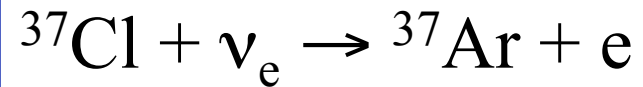
## • The Chlorine or 'Davis' experiment



- Pioneering experiment by Ray Davis at Homestake mine began in 1967
- Consisted of a 600 ton chlorine tank
- Experiment was carried out over a 20 year period, in an attempt to measure the flux of neutrinos from the Sun
- Measured flux was only one third the predicted value !!

# $^{37}\text{Cl}$ experiment

## • The Chlorine or 'Davis' experiment

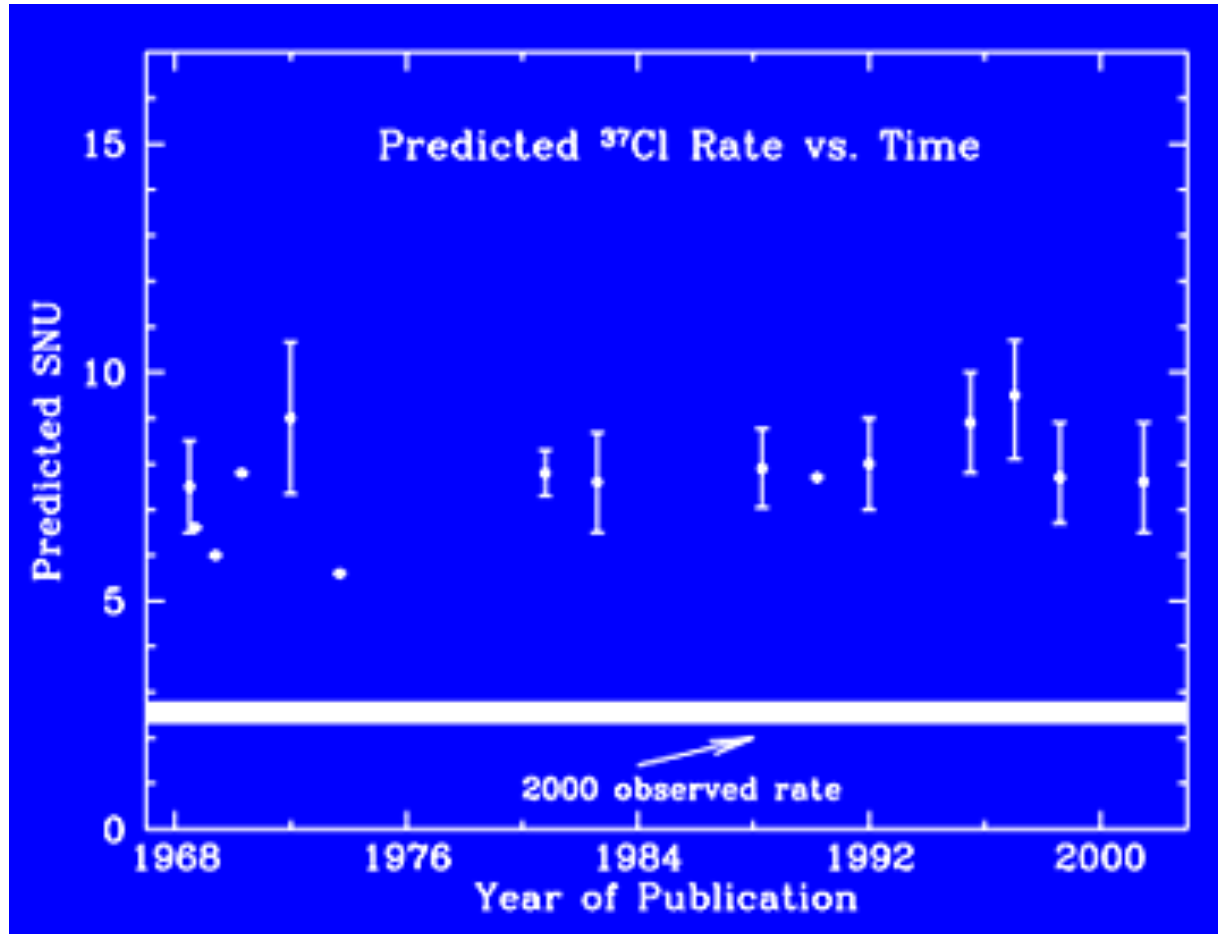


- Pioneering experiment by Ray Davis at Homestake mine began in 1967
- Consisted of a 600 ton chlorine tank
- Threshold  $E = 0.814$  MeV
- Experiment was carried out over a 20 year period, in an attempt to measure the flux of neutrinos from the Sun
- Chemical extraction of Argon and direct counting of Argon decays (15 atoms over 130 tons of Cl every month!)
- Measured flux was only one third the predicted value

# $^{37}\text{Cl}$ experiment

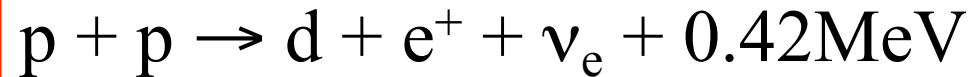


# $^{37}\text{Cl}$ experiment



# Radiochemical experiments: GALLEX/GNO and SAGE

- The main solar neutrino source is from the p-p reaction:



- Solar neutrino experiment based on the reaction:

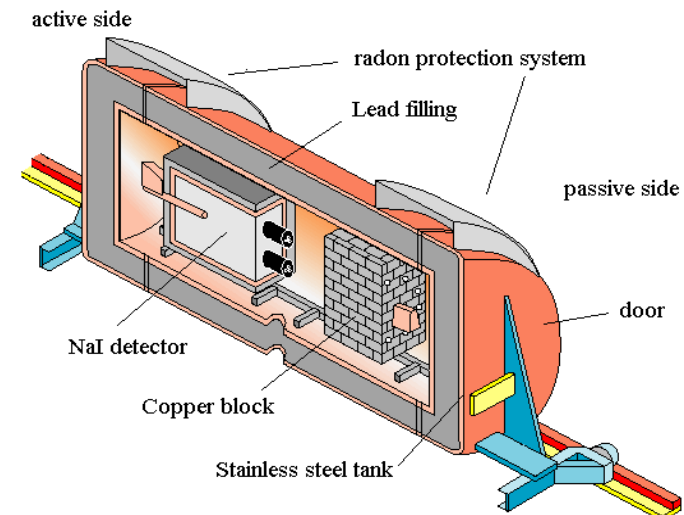
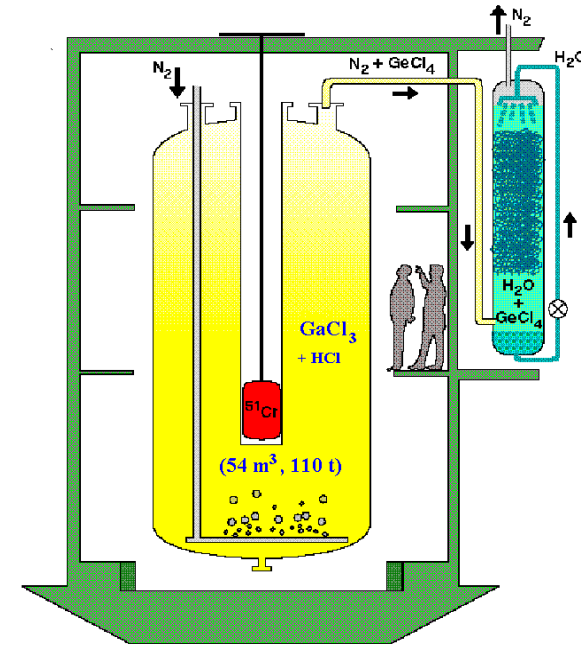


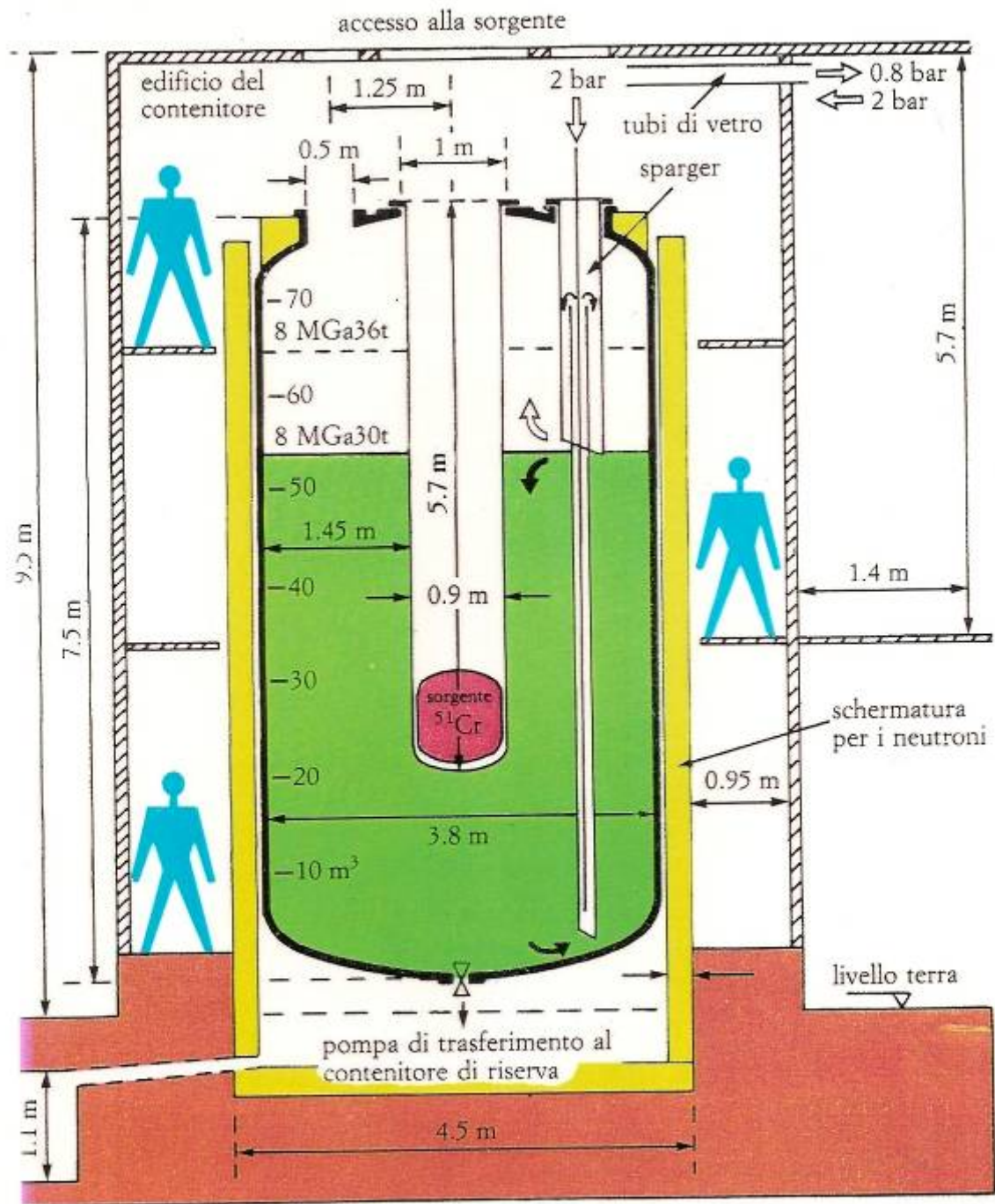
- Ability to detect the low-energy neutrinos from p-p fusion
- **SAGE**: Located at the Baksan Neutrino Observatory in the northern Caucasus mountains of Russia (1990-2000)
- **GALLEX/GNO**: Located at the Gran Sasso
- Energy threshold:  $233.2 \pm 0.5$  keV, below that of the p-p  $\nu_e$  (420 keV)



# • GALLEX/GNO

- 30.3 tons of gallium in form of a concentrated  $\text{GaCl}_3\text{-HCl}$  solution exposed to solar  $\nu$ 's
- Neutrino induced  $^{71}\text{Ge}$  forms the volatile compound  $\text{GeCl}_4$
- Nitrogen gas stream sweeps  $\text{GeCl}_4$  out of solution
- $\text{GeCl}_4$  is absorbed in water  $\text{GeCl}_4 \rightarrow \text{GeH}_4$  and introduced into a proportional counter
- Number of  $^{71}\text{Ge}$  atoms evaluated by their radioactive decay





# GALLEX

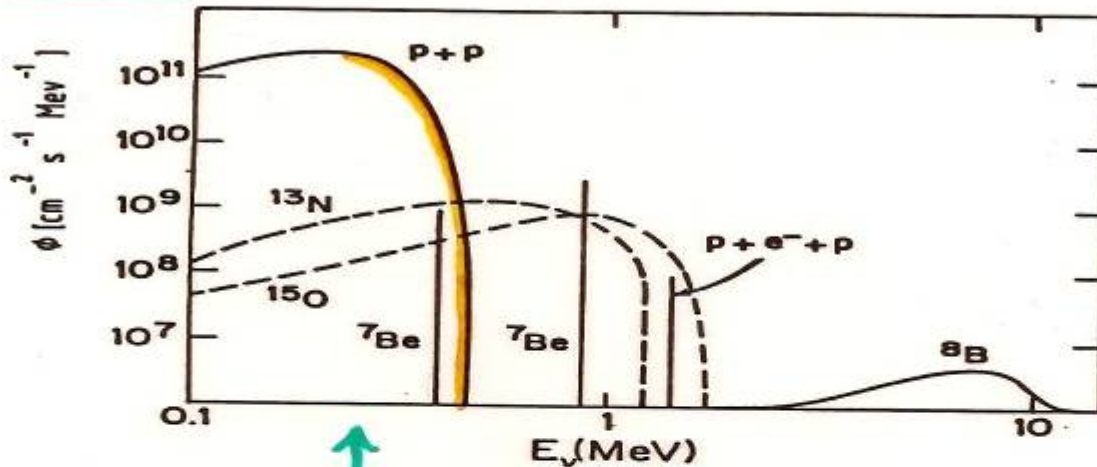
GALLIUM EUROPEAN COLLABORATION

30 TONS OF GALLIUM IN  $\text{GaCl}_3$

12 Tons  ${}^{71}\text{Ga}$

NEUTRINO FLUX FROM SUN (BACHALL et al.)

(IN  $\text{HCl}$ )



↑  
THRESHOLD

$E > 233 \text{ KeV}$



LIQUIDO  $\text{GaCl}_3 \Rightarrow \text{GeCl}_4$  GASSOSO

$T_{1/2} = 11.43 \text{ d}$



# SAGE – Russian American Gallium Experiment

- radiochemical Ga experiment at Baksan Neutrino Observatory with 50 tons of metallic gallium
- running since 1990-present

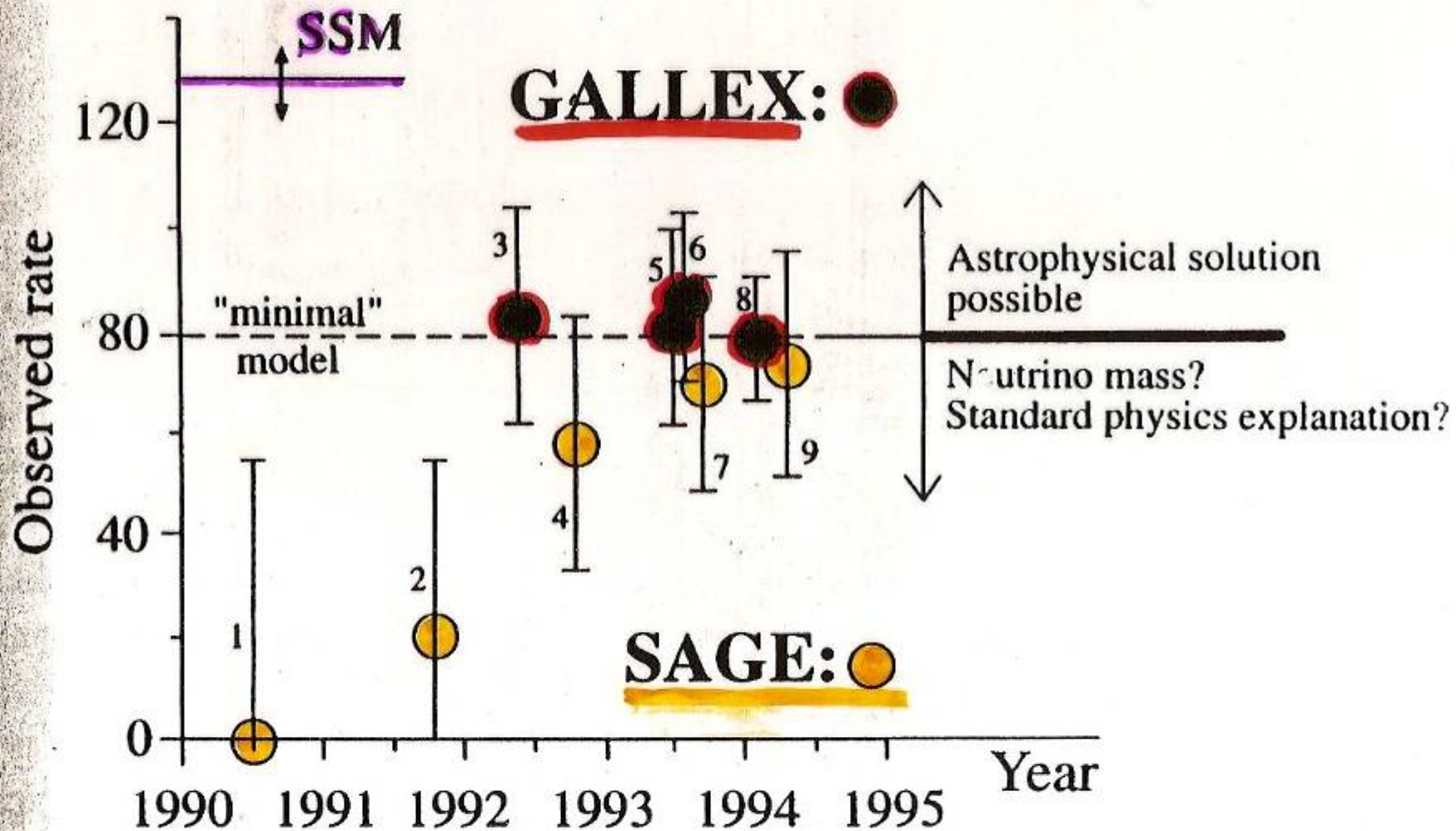
$66.2^{+3.3}_{-3.2} \text{ }^{+3.5}_{-3.2} \text{ SNU}$

measures *pp* solar flux in agreement with SSM when oscillations are included – the predicted signal is

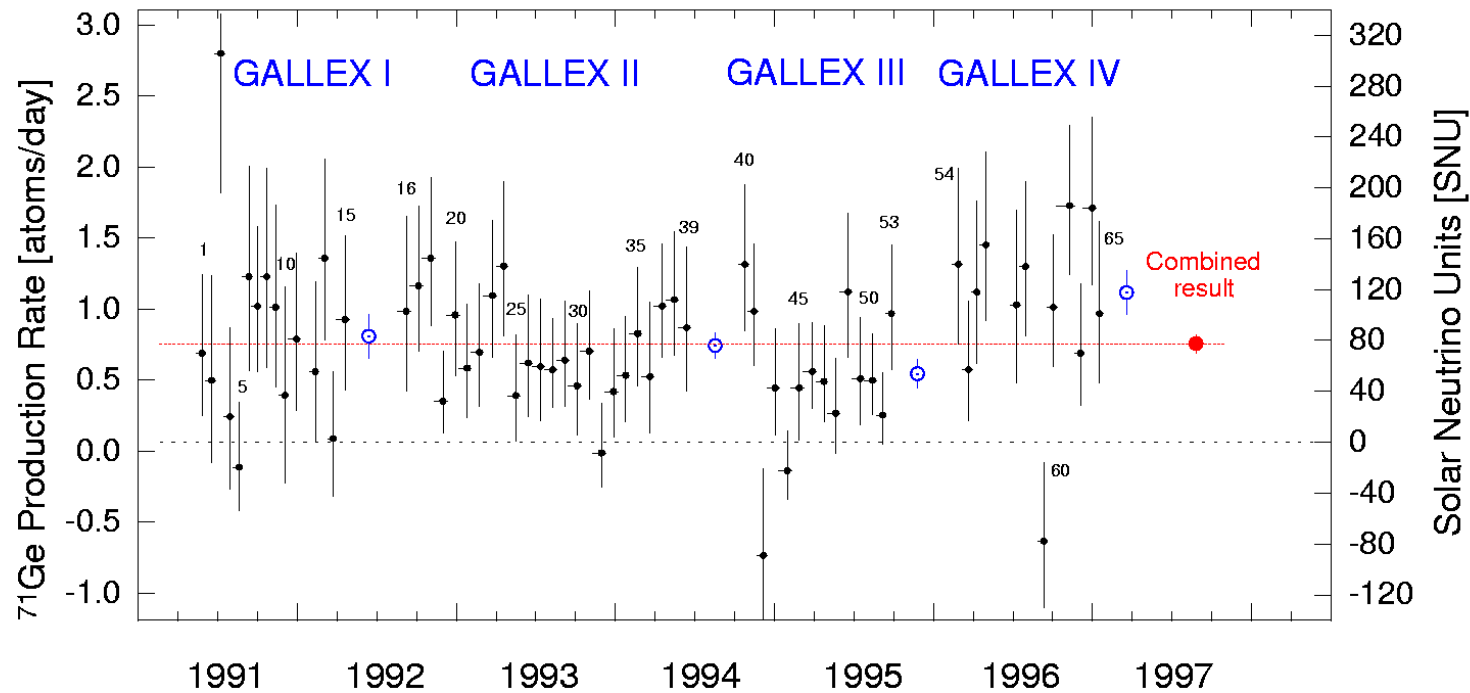
$67.3^{+3.9}_{-3.5} \text{ SNU}$

- latest result from 157 runs (1990-2006)

**Figure 12.17.** The SAGE experiment in the Baksan underground laboratory in the Caucasus. The 10 so-called reactors can be seen, 8 of which contain a total of 57 tons of metallic gallium (with kind permission, of the SAGE collaboration).



# GALLEX-SAGE results



	GALLEX+GNO (SNU)	SAGE (SNU)
Measured	$71 \pm 5$	$66 \pm 5$
Expected	$128 \pm 8$	$128 \pm 8$

SNU=  $10^{-36}$  (interactions/s · nucleus)

# Solar Neutrino Problem

Experiment	Result	Theory	$\frac{\text{Result}}{\text{Theory}}$
Homestake [38]	$2.56 \pm 0.16 \pm 0.16$ ( $2.56 \pm 0.23$ )	$7.7^{+1.2}_{-1.0}$	$0.33^{+0.06}_{-0.05}$
GALLEX [322]	$77.5 \pm 6.2^{+4.3}_{-4.7}$ ( $78 \pm 8$ )	$129^{+8}_{-6}$	$0.60 \pm 0.07$
SAGE [323]	$66.6^{+6.8+3.8}_{-7.1-4.0}$ ( $67 \pm 8$ )	$129^{+8}_{-6}$	$0.52 \pm 0.07$
Kamiokande [41]	$2.80 \pm 0.19 \pm 0.33$ ( $2.80 \pm 0.38$ )	$5.15^{+1.0}_{-0.7}$	$0.54 \pm 0.07$
Super-Kamiokande [48]	$2.44 \pm 0.05^{+0.09}_{-0.07}$ ( $2.44^{+0.10}_{-0.09}$ )	$5.15^{+1.0}_{-0.7}$	$0.47^{+0.07}_{-0.09}$

# The Solar Neutrino Problem

How can this deficit be explained?

1. The Sun's reaction mechanisms are not fully understood

***NO!*** *new measurements (~1998) of the sun resonant cavity frequencies*

2. The experiment is wrong –

***NO!*** *All the forthcoming new experiments confirmed the deficit!*

3. Something happens to the neutrino as it travels from the Sun to the Earth

***YES! Oscillations of electron neutrinos!***

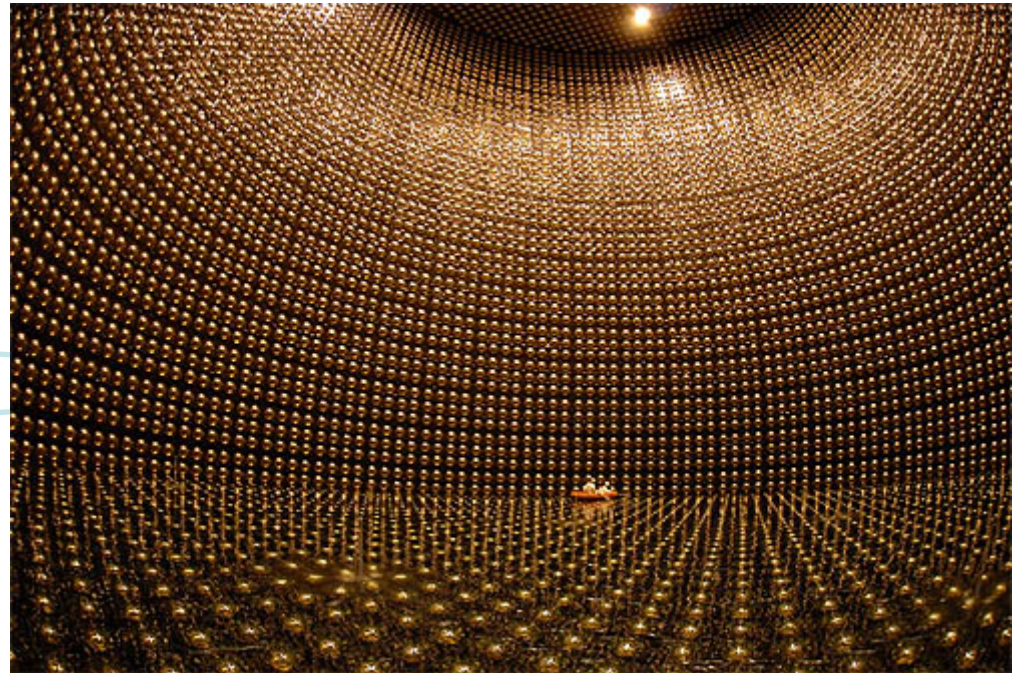
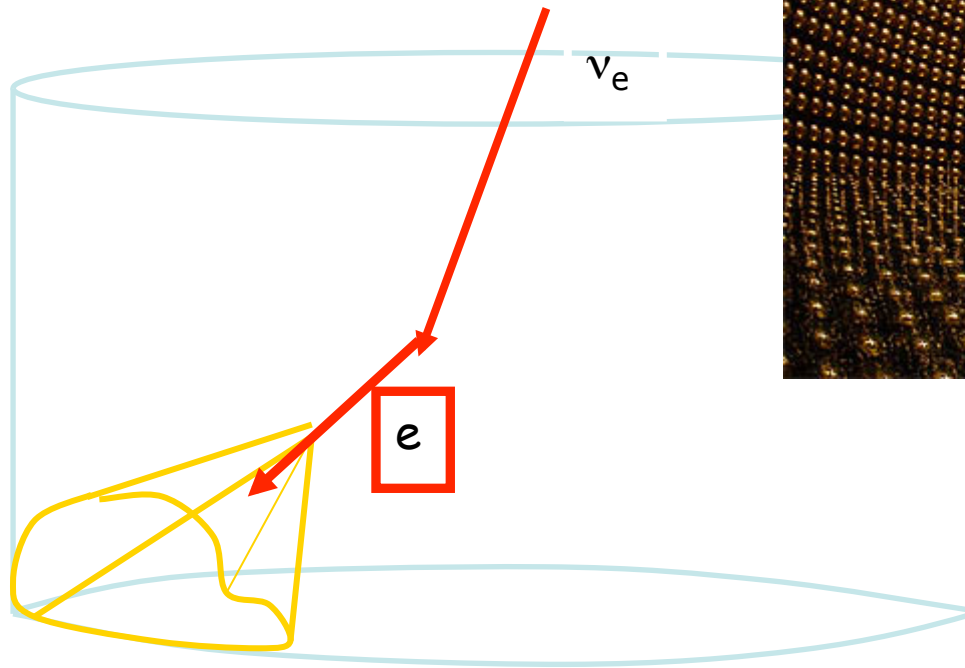


# Solar Neutrino Problem

- Astrophysical solutions?:
  - Low metallicity
  - Burnt out core
  - Rapid Rotation
  - High mass loss rate
  - Pure CNO cycle
  - WIMP
  - Central BH

# The SK way- The elastic scattering of neutrinos on electrons

- Real-time detector
- Elastic scattering  
 $\nu_e \rightarrow \nu_e$



# Neutrino Scattering Experiments

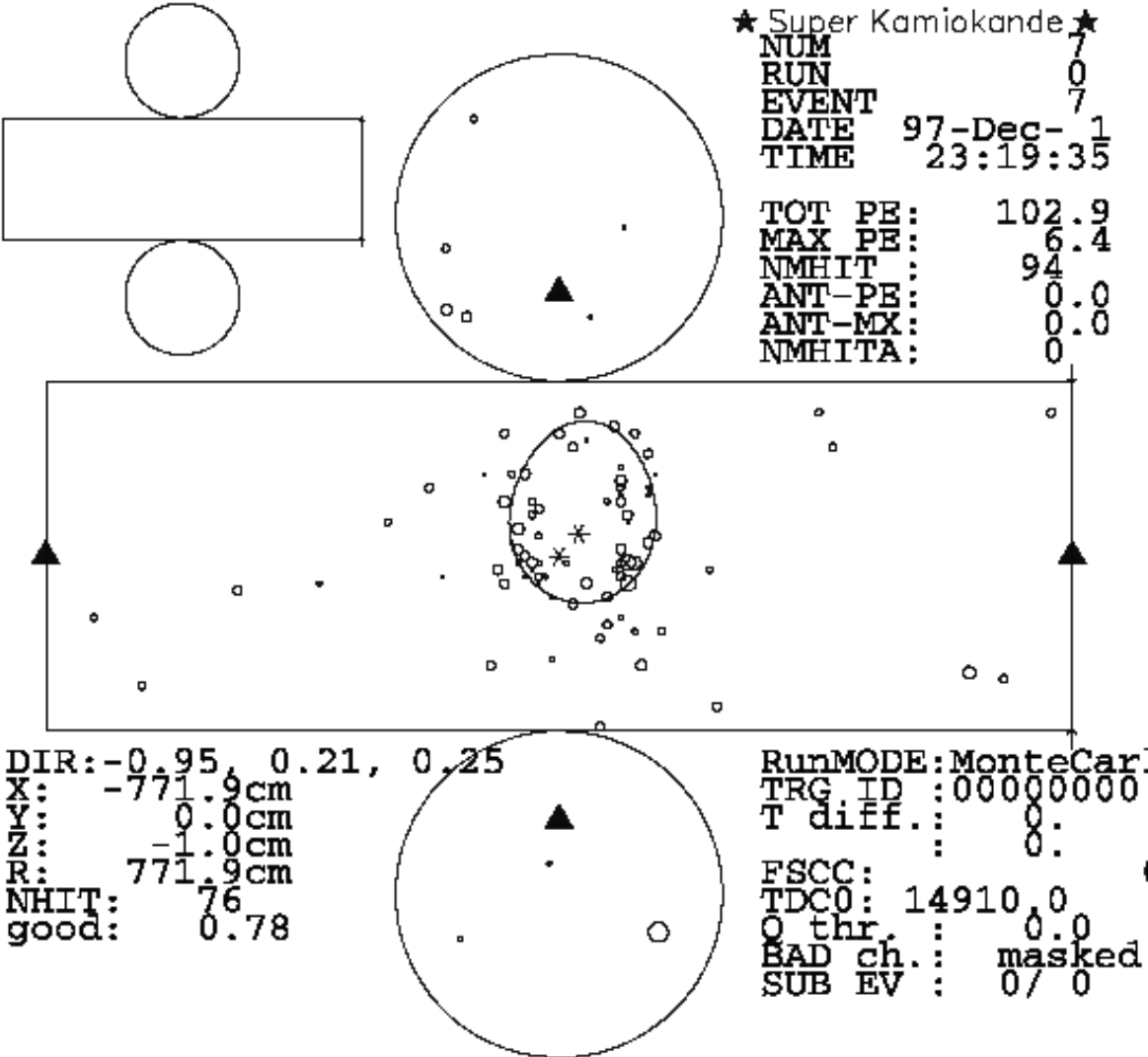
Particle	Cherenkov threshold in total Energy
$e^\pm$	0.768(MeV)
$\mu^\pm$	158.7
$\pi^\pm$	209.7

Cherenkov threshold energies of various particles.

$$\cos \theta = \frac{1}{n\beta'}$$

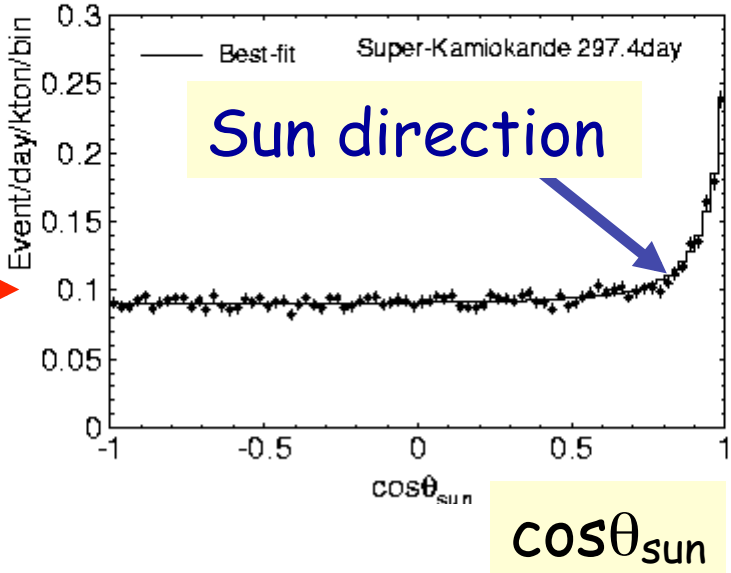
Cherenkov light is emitted in a cone of half angle  $\theta$  from the direction of the particle track

# Neutrino Scattering Experiments

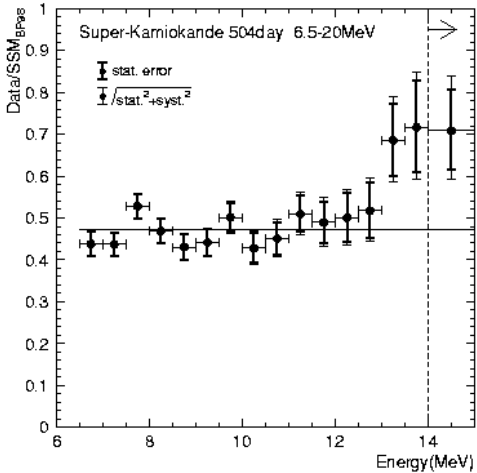


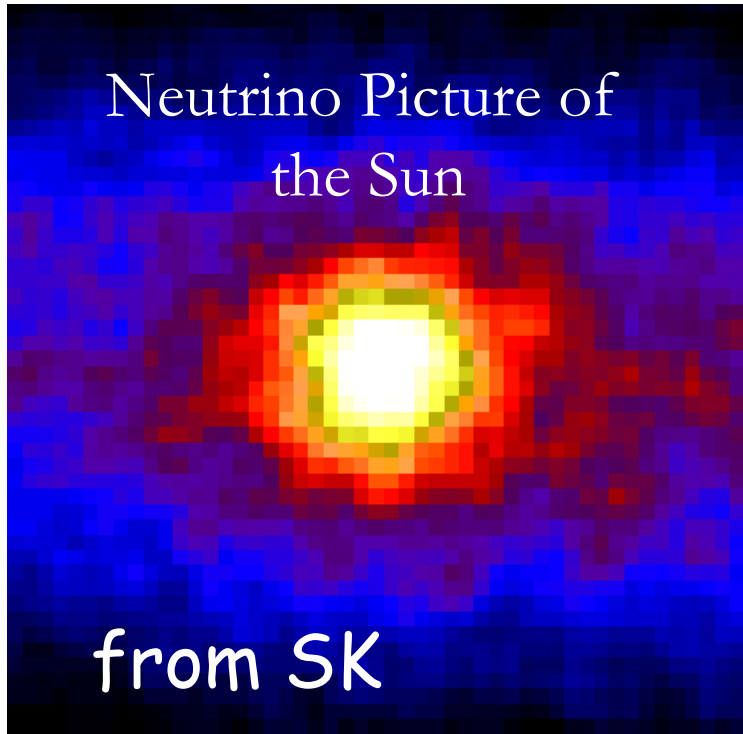
# Neutrino Scattering Experiments

Radioactivity Background



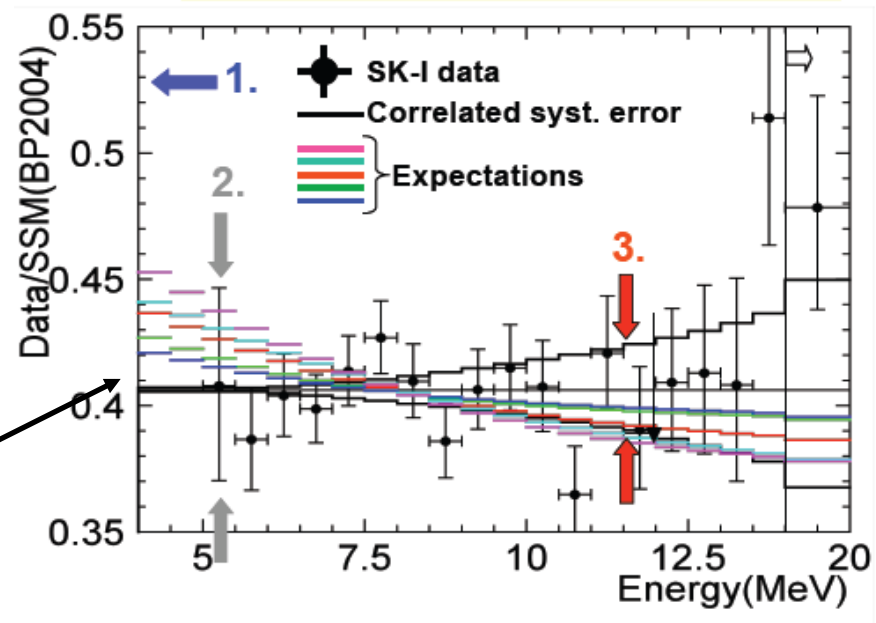
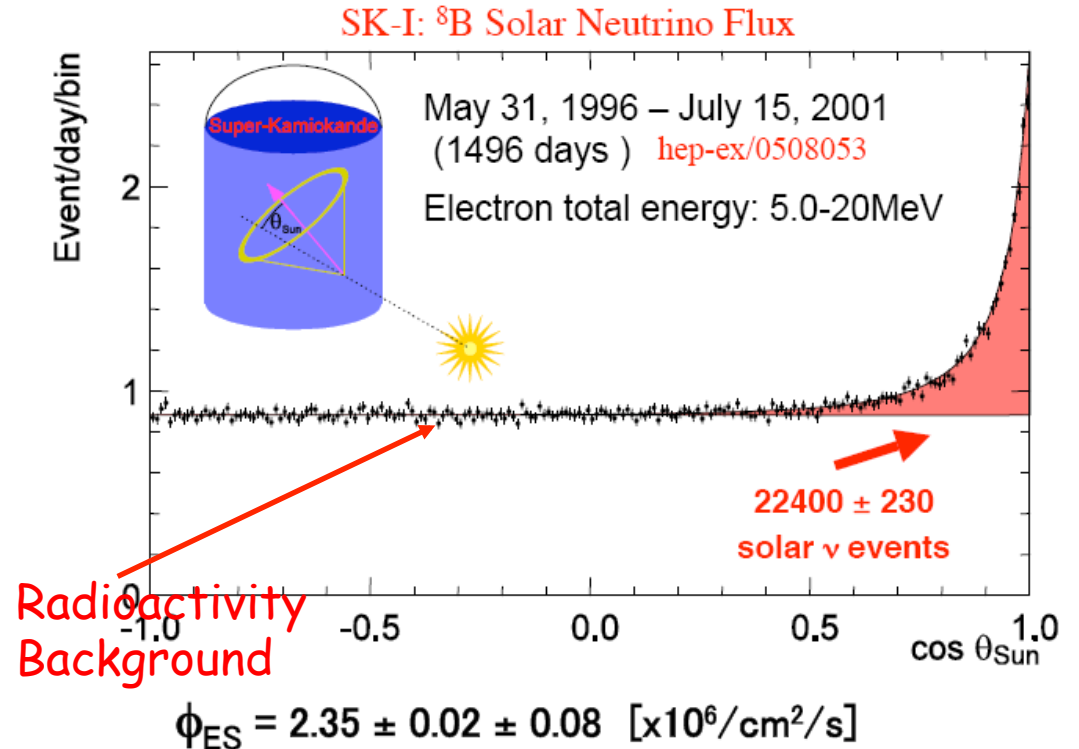
Ratio of observed electron energy spectrum and expectation from SSM





- SK measured a flux of solar neutrinos with energy  $> 5$  MeV (from  $B^8$ ) about 40% of that predicted by the SSM
- The reduction is almost constant up to 18 MeV

Ratio of observed electron energy spectrum and expectation from SSM



# The decisive results: SNO ( $\alpha$ : 1999 – $\Omega$ :2006)

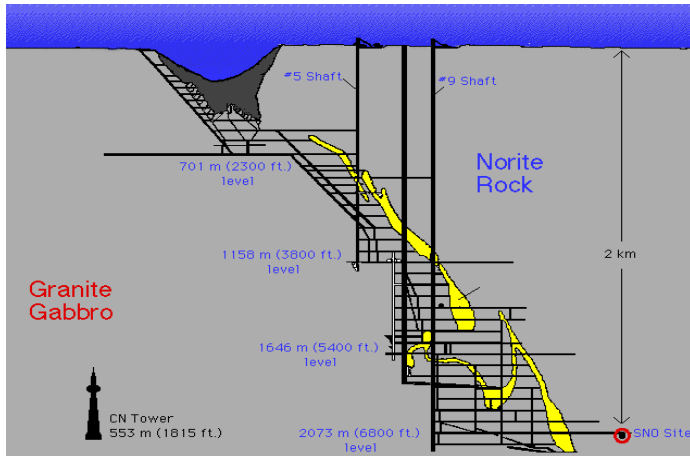
- 18m sphere, situated underground at about 2.5km underground, in Ontario
- 10,000 photomultiplier tubes (PMT)
- Each PMT collect Cherenkov light photons
- Heavy water ( $D_2O$ ) inside a transparent acrylic sphere (12m diameter)
- Pure salt is added to increase sensitivity of NC reactions (2002)
- It can measure the flux of all neutrinos ' $\Phi(\nu_x)$ ' and electron neutrinos ' $\Phi(\nu_e)$ '
- The flux of non-electron neutrinos

$$\Phi(\nu_\mu, \nu_\tau) = \Phi(\nu_x) - \Phi(\nu_e)$$

■ These fluxes can be measured via the 3 different ways in which neutrinos interact with heavy water



# Sudbury Neutrino Observatory



1000 tonnes  $D_2O$

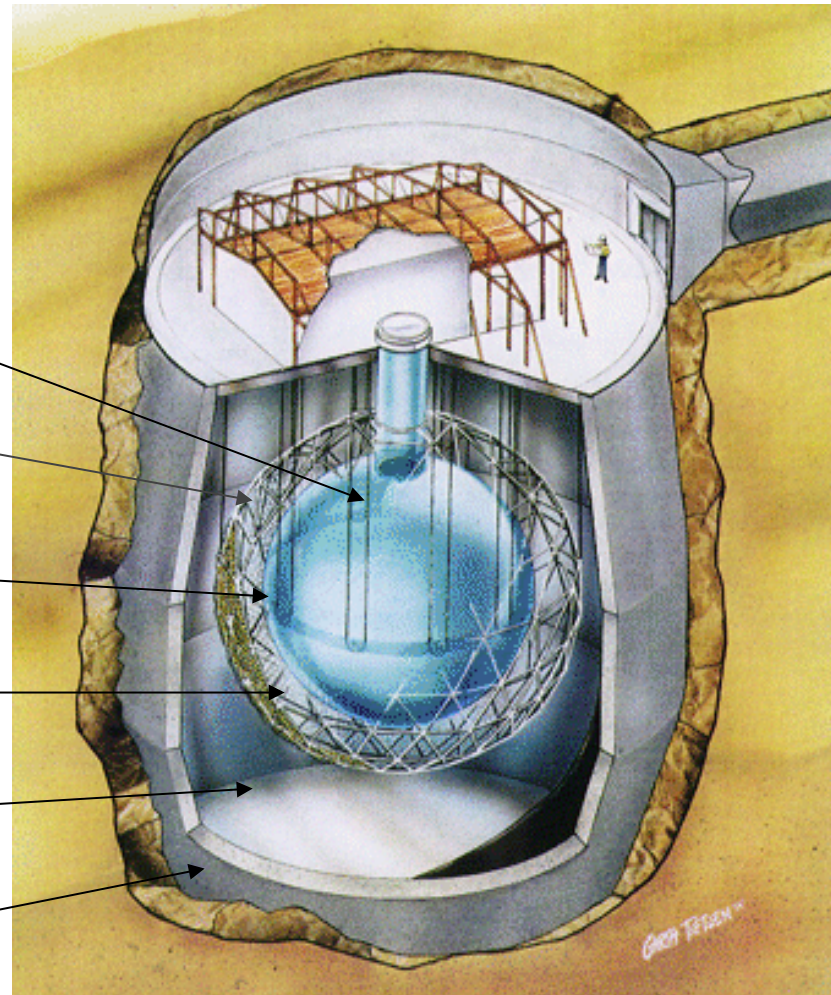
Support Structure for 9500 PMTs, 60% coverage

12 m Diameter Acrylic Vessel

1700 tonnes Inner Shielding  $H_2O$

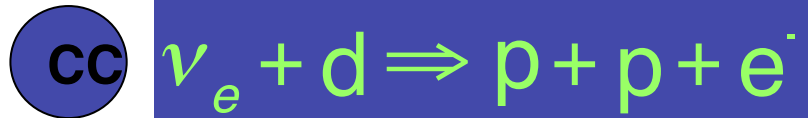
5300 tonnes Outer Shield  $H_2O$

Urylon Liner and Radon Seal

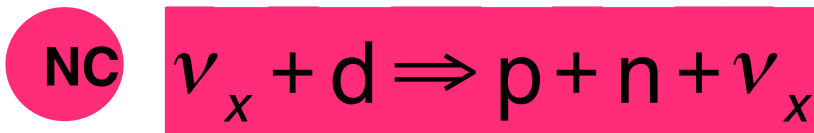




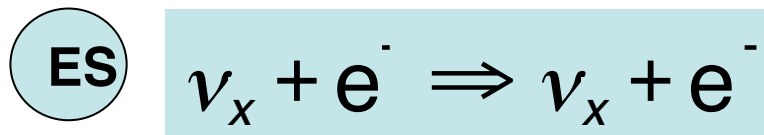
# $\nu$ Reactions in SNO



- Gives  $\nu_e$  energy spectrum well
- Weak direction sensitivity  $\propto 1 - 1/3 \cos(\theta)$
- $\nu_e$  only.
- SSM: 30 CC events day<sup>-1</sup>



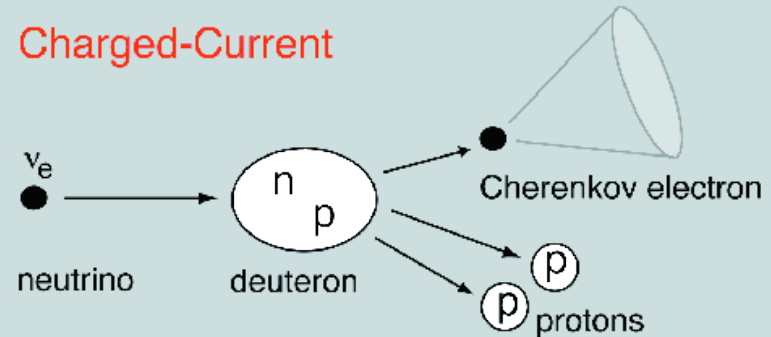
- Measure total <sup>8</sup>B  $\nu$  flux from the sun.
- Equal cross section for all  $\nu$  types
- SSM: 30/day



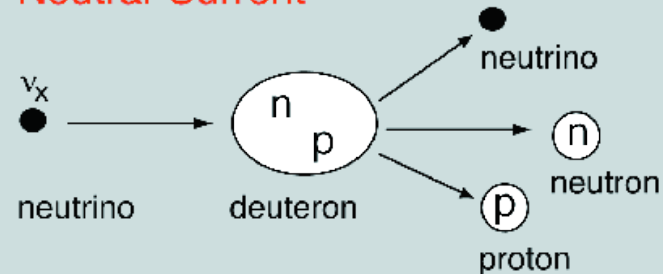
- Low Statistics (3/day)
- Mainly sensitive to  $\nu_e$ , some
  - sensitivity to  $\nu_\mu$  and  $\nu_\tau$
- Strong direction sensitivity

## Neutrino Reactions on Deuterium

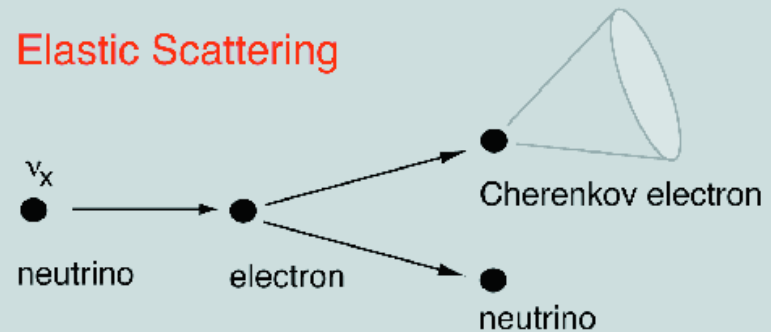
### Charged-Current



### Neutral-Current



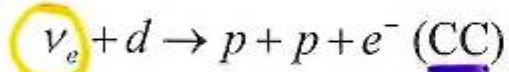
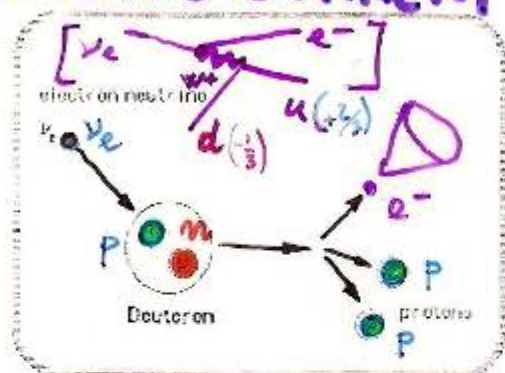
### Elastic Scattering



# OBSERVABLE REACTIONS IN S.N.O.

## Le Reazioni Osservabili in SNO

### CHARGED CURRENT

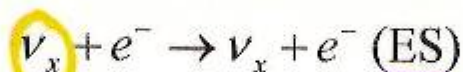
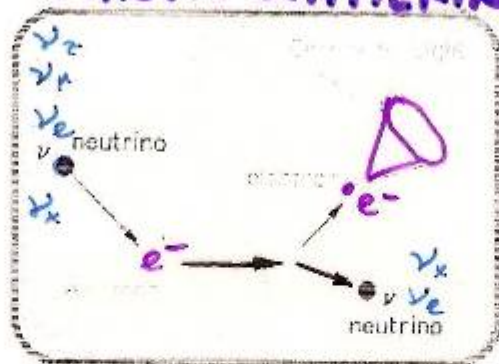


Solo neutrini elettronici  
 $\nu_e$  ONLY

Neutrini prodotti da  $^8\text{B}$  ( $E_\nu < 15 \text{ MeV}$ )

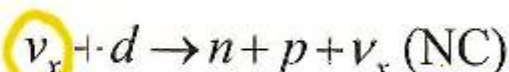
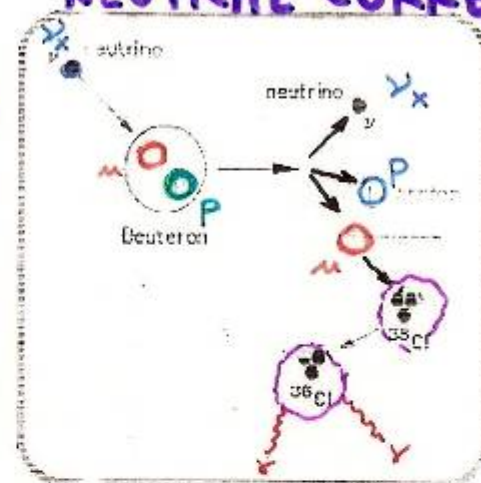
Soglia Rivelatore 6.75 MeV

### ELASTIC SCATTERING



Tutti i neutrini  
 $\nu_x = \text{ALL NEUTRINOS}$

### NEUTRAL CURRENT



Tutti i neutrini  
 $\nu_x = \text{ALL NEUTRINOS}$

**THRESHOLD @ 6.75 MeV**

Può essere separato il contributo dei diversi neutrini

**IT IS POSSIBLE TO SEPARATE  $\nu_x$  CONTRIBUTIONS**



Indipendenza dalle previsioni del modello Solare

**INDIPENDENT FROM S. SOLAR MODEL**

## □ The 2001 results

□ The  $\nu_e$ 's flux from  ${}^8\text{B}$  decay is measured by the CC (1) reaction:  $\phi^{\text{CC}}(\nu_e)$   
 $= (1.75 \pm 0.24) \times 10^6 \text{ cm}^{-2}\text{s}^{-1}$

□ Assuming no oscillations, the total  $\nu$  flux inferred from the ES (3) reaction rate is:

$$\square \phi^{\text{ES}}(\nu_x) = (2.39 \pm 0.50) \times 10^6 \text{ cm}^{-2}\text{s}^{-1} \quad (\text{SNO})$$

$$\square \phi^{\text{ES}}_{\text{SK}}(\nu_x) = (2.32 \pm 0.08) \times 10^6 \text{ cm}^{-2}\text{s}^{-1} \quad (\text{SK})$$

□ The difference between the  ${}^8\text{B}$  flux deduced from the ES and the CC rate at SNO and SK is:

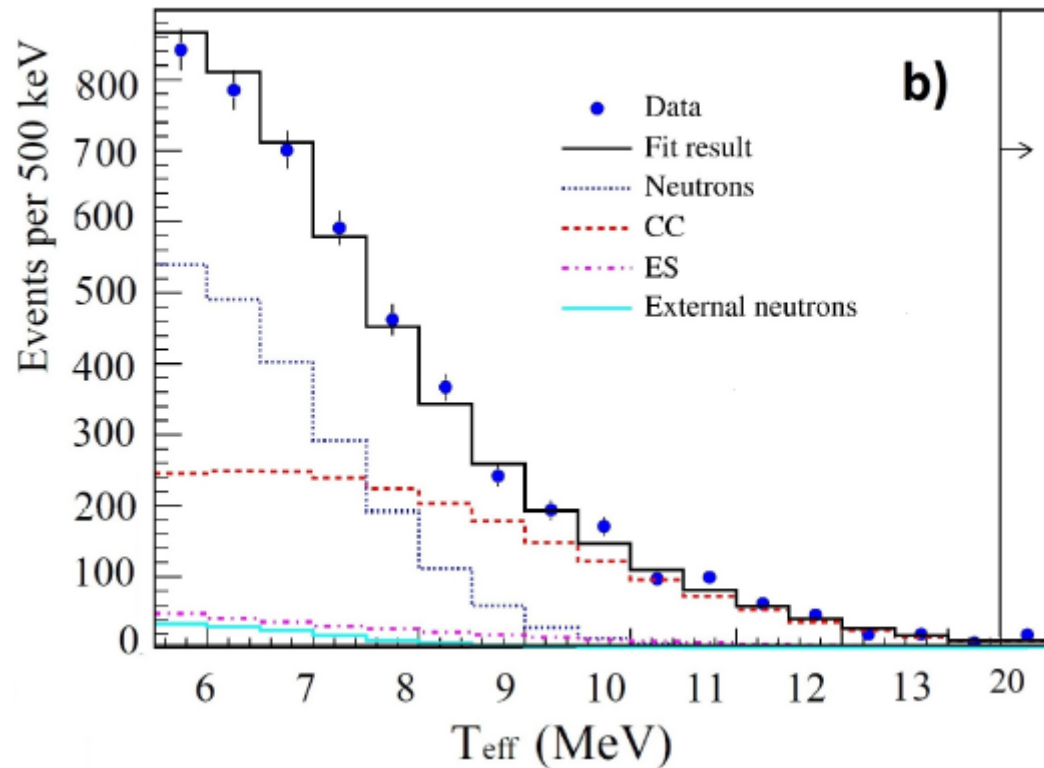
$$\square \Phi(\nu_\mu, \nu_\tau) = (0.57 \pm 0.17) \times 10^6 \text{ cm}^{-2}\text{s}^{-1} \quad (3.3 \sigma)$$

□ This difference first shows that **there is a non-electron** flavour active neutrino component in the solar flux !

UNITS:  
 $\times 10^6 \text{ cm}^{-2} \text{ s}^{-1}$

$$\left\{ \begin{array}{l} \phi_{\text{CC}}^{\text{SNO}} = 1.59_{-0.07}^{+0.08}(\text{stat})_{-0.08}^{+0.06}(\text{syst}) \\ \phi_{\text{ES}}^{\text{SNO}} = 2.21_{-0.26}^{+0.31}(\text{stat}) \pm 0.10(\text{syst}) \\ \phi_{\text{NC}}^{\text{SNO}} = 5.21 \pm 0.27(\text{stat}) \pm 0.38(\text{syst}) \end{array} \right.$$

ATTESO: Bahcall et al. – SSM=  $5.05 \pm 0.8$



Electron kinetic energy

**2003 SNO**  
**Energy spectra**  
**(Salt data)**

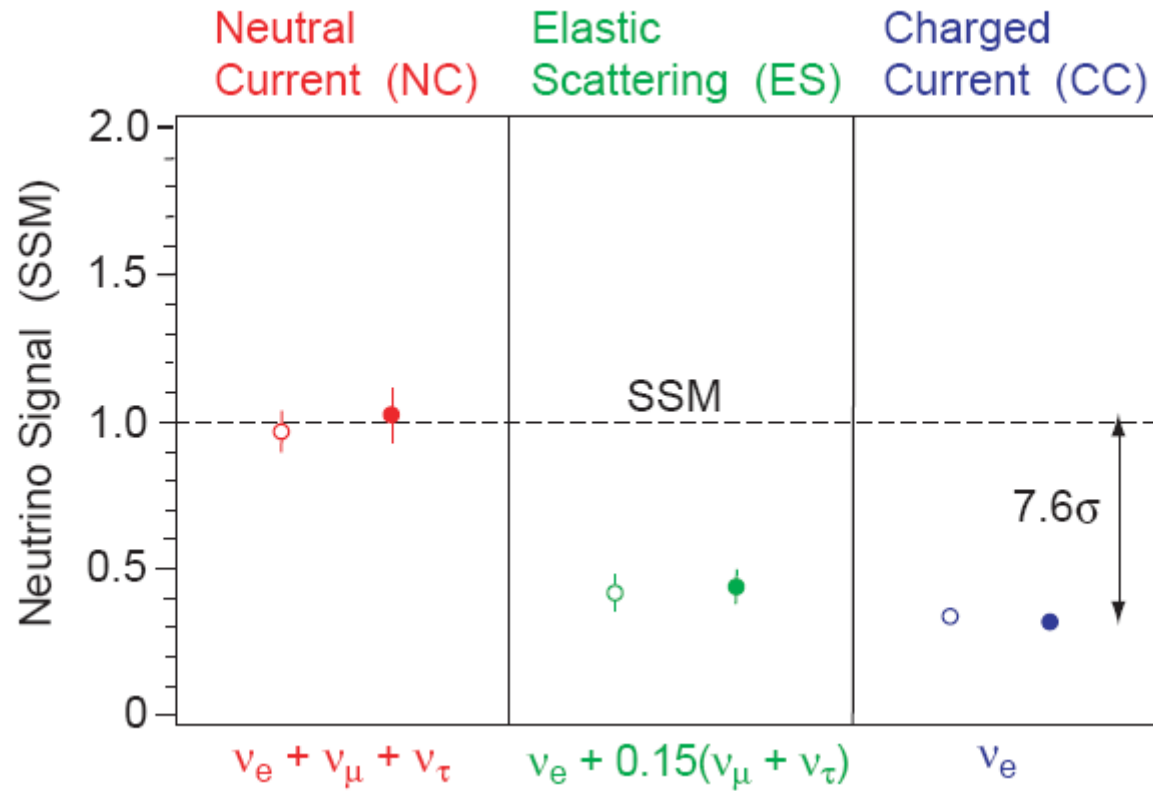
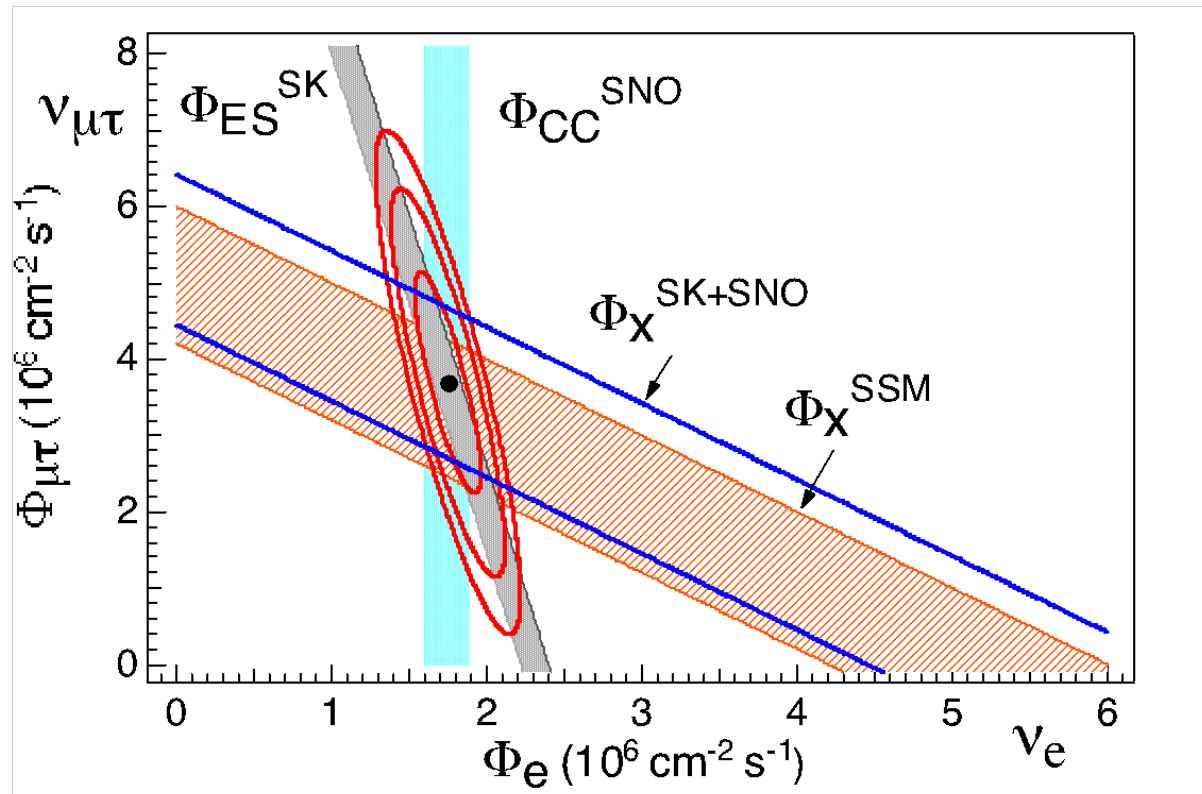


Figure 8: Evidence for neutrino flavor change seen by SNO. The open (filled) circles represent the 2003 SNO flux results, relative to the SSM, under the assumption of an undistorted (unconstrained)  $^8\text{B}$  neutrino energy spectrum.

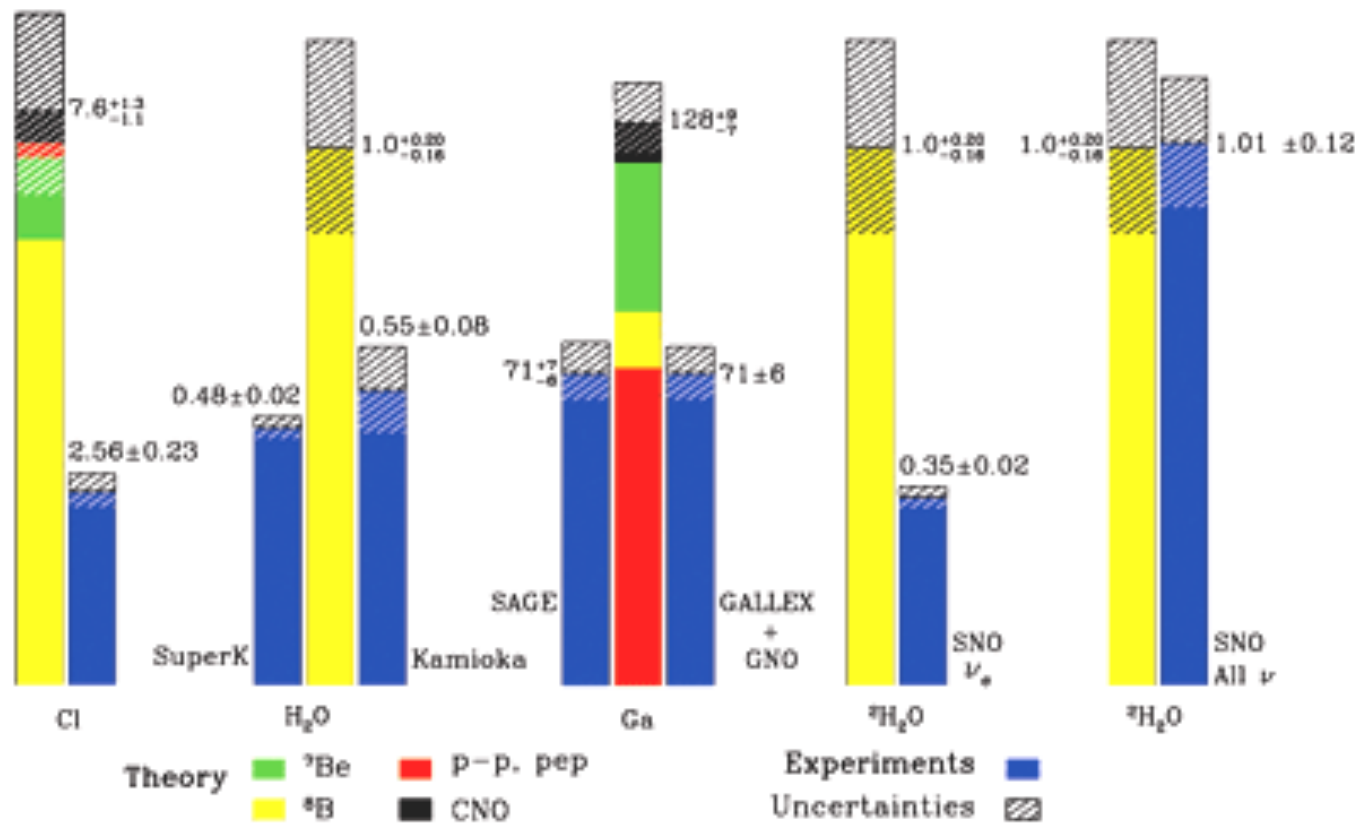
# Solar Neutrino Problem



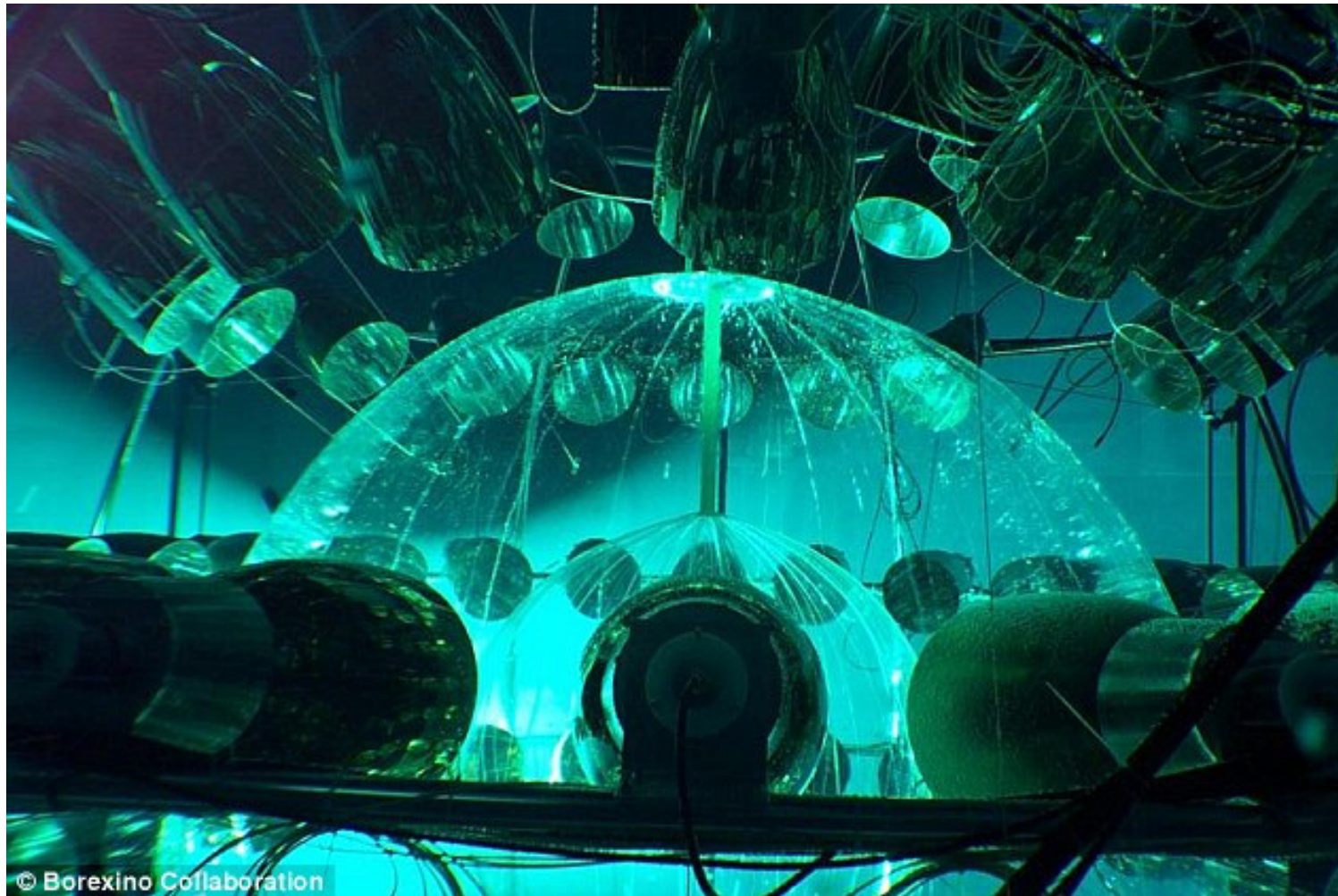
- The total flux of active  ${}^8\text{B}$  neutrinos is:  
 $(5.44 \pm 0.99) \times 10^6 \text{ cm}^{-2}\text{s}^{-1}$  , in agreement with SSM

# Solar Neutrino Problem

Total Rates: Standard Model vs. Experiment  
Bahcall-Pinsonneault 2000

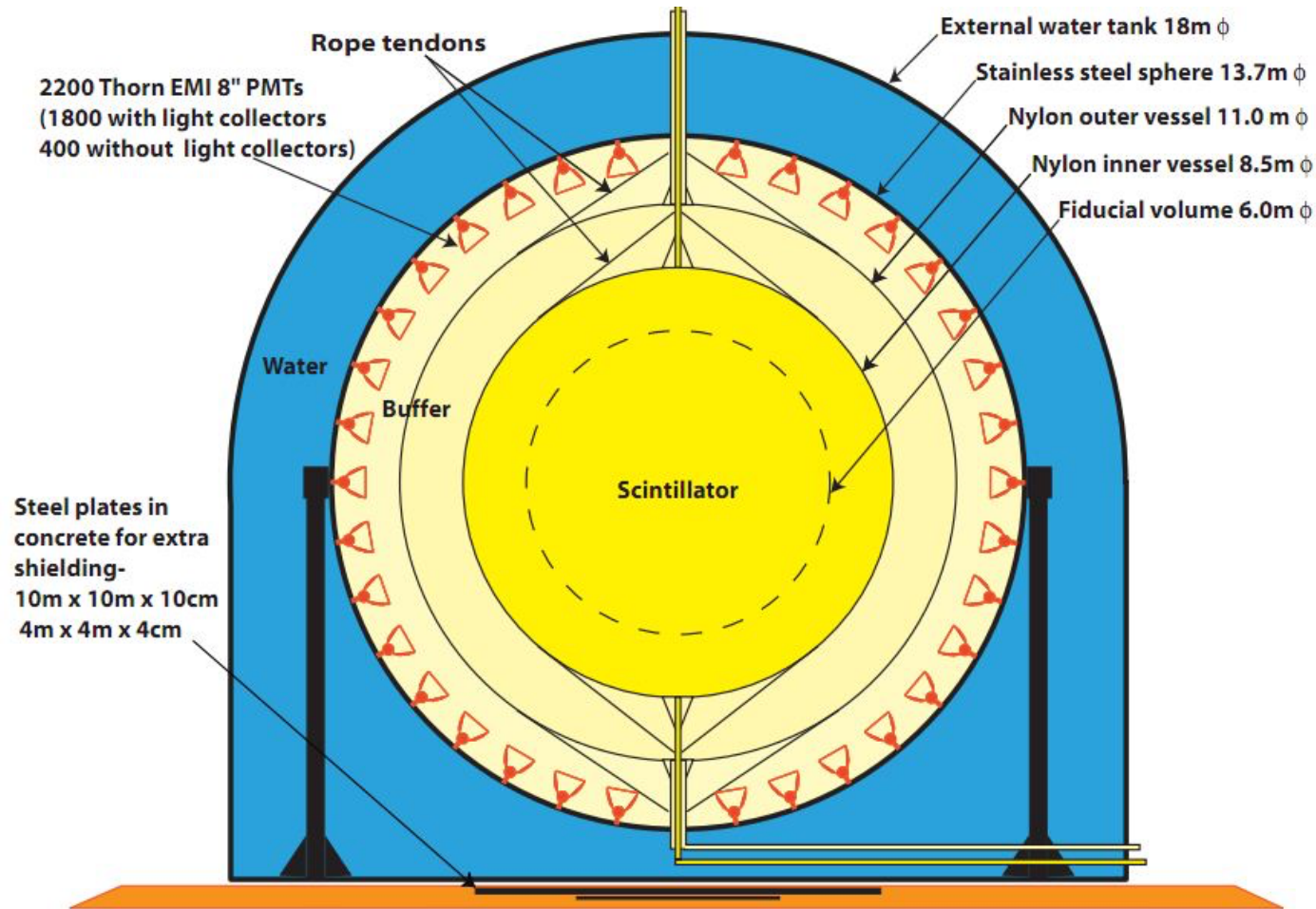


# Borexino @LNGS



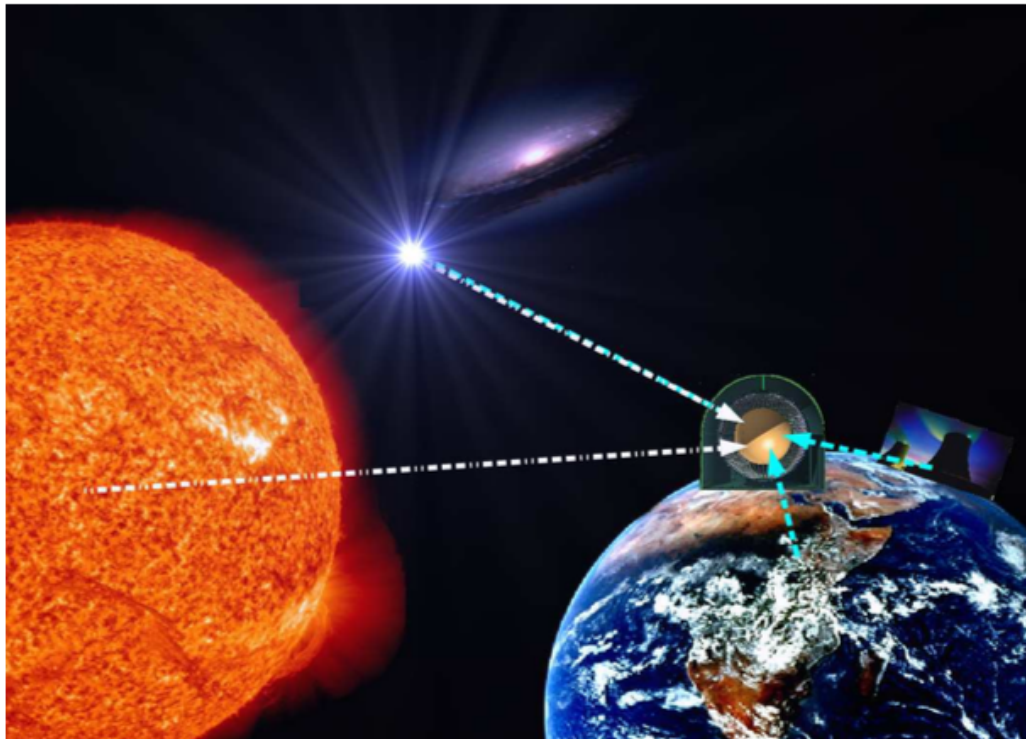


# Borexino @LNGS



# BOREXINO

## Recent Solar And Terrestrial Neutrino Results



Werner Maneschg  
on behalf of the Borexino Collaboration

# Borexino: detector properties & design, and physics goals

## Main properties:

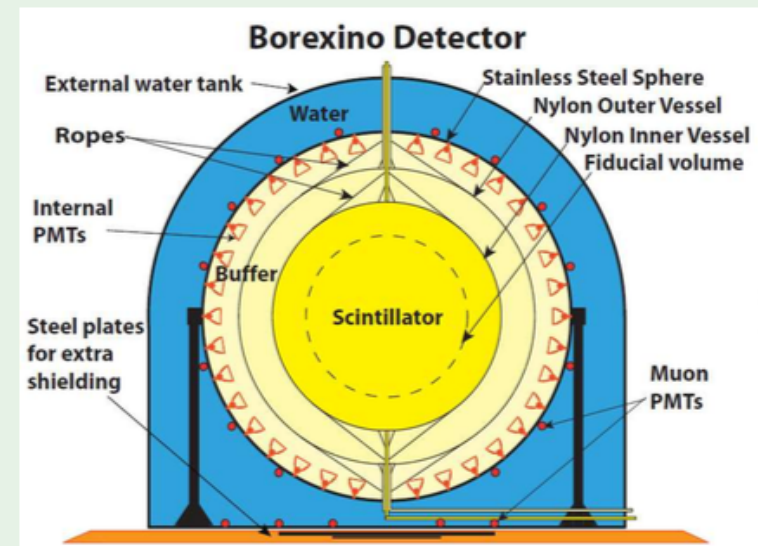
- Large volume organic liquid scintillator detector:
  - at LNGS (1.4 km overburden)
  - operational since May 2007
- Ultra low background (radiopurest environment ever measured)
- Real-time detection (time stamp and pulse shape for every event)
- Spectroscopy at low energies, typically between 0.1-15 MeV
- 3D position reconstruction

## Main physics goals:

- Neutrinos from Sun
- Antineutrinos from Earth & reactors
- Sterile neutrinos (TH 23-07-15:13.5)
- SN-(anti)neutrinos & other exotic particles and processes

## Nut shell profile:

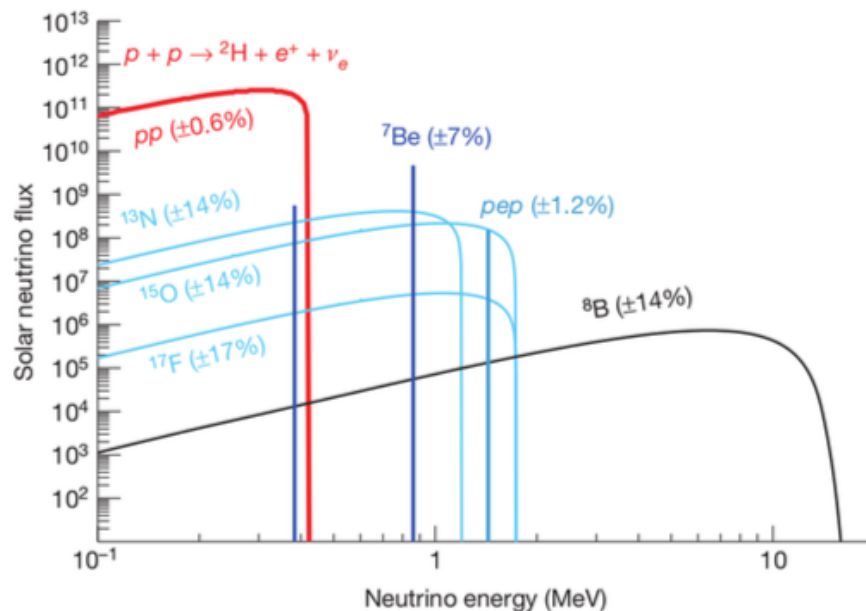
- 1 Water tank (2100 m<sup>3</sup>):
  - Absorption of environmental  $\gamma$  rays and neutrons
  - $\mu$  Cherenkov detector (208 PMTs)
- 2 Stainless Steel Sphere:
  - 2212 PMTs, 1350 m<sup>3</sup>, R=6.85 m
- 3 2 buffer layers: PC+DMP
  - Outer R<sub>2</sub>=5.50 m, Inner R<sub>1</sub>=4.25 m
  - Shielding from external  $\gamma$  rays
- 4 Scintillator: 270 tons of PC+PPO



# Solar neutrino fluxes (according to Standard Solar Model predictions)

## Neutrino fluxes at 1 AU:

from simulations by A. Serenelli et al., *Astrophys. J.* 743, 24 (2011)



**Units:** [ $\text{cm}^{-2}\text{s}^{-1}\text{MeV}^{-1}$ ] for continuum neutrino sources, [ $\text{cm}^{-2}\text{s}^{-1}$ ] for mono-energetic neutrino sources.

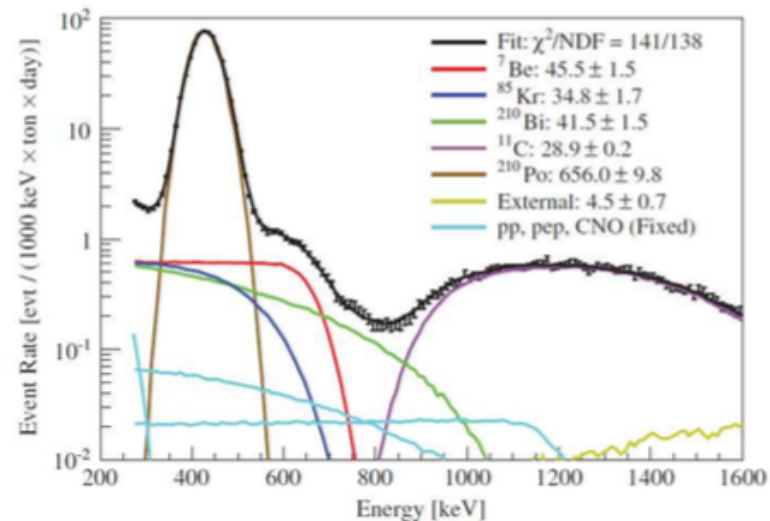
$\nu$ flux	GS98	AGSS09
pp	5.98(1±0.006)	6.03(1±0.006)
$^7\text{Be}$	5.00(1±0.07)	4.56(1±0.07)
pep	1.44(1±0.012)	1.47(1±0.012)
$^{13}\text{N}$	2.96(1±0.14)	2.17(1±0.14)
$^{15}\text{O}$	2.23(1±0.15)	1.56(1±0.15)
$^{17}\text{F}$	5.52(1±0.17)	3.40(1±0.16)
$^8\text{B}$	5.58(1±0.14)	4.59(1±0.14)

**Factors:**  $10^{10}$  (pp),  $10^9$  ( $^7\text{Be}$ ),  
 $10^8$  (pep,  $^{13}\text{N}$ ,  $^{15}\text{O}$ ),  $10^6$  ( $^8\text{B}$ ,  $^{17}\text{F}$ );  
**Units:**  $\text{cm}^{-2}\text{s}^{-1}$ .

**Solar neutrino measurements:**  
**different obstacles:** diff. background, detector response, energy threshold  
**sensitivity for different phenomena:** neutrino osc. (incl. matter effects (MSW)), SSM metallicity scenarios

# Solar $^7\text{Be}$ neutrino rate measurement

Averaged  $^7\text{Be}-\nu$  rate fitted with MC (ROI: 0.2-0.7 MeV)

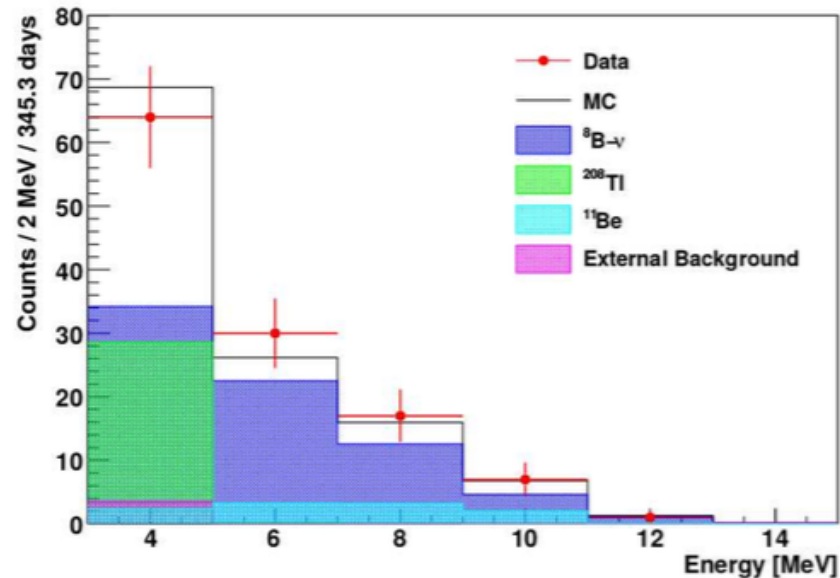


## Results and remarks:

- **Averaged rate:**  $R = (46 \pm 1.5(\text{stat})_{-1.6}^{+1.5}(\text{sys})) \text{ c/d/100 ton}$  (**uncertainty  $\pm 5\%$** )  
Comparison to SSM predictions:
  - Without osc.:  $(74 \pm 5) \text{ c/d/100 ton}$  ( **$5\sigma$  exclusion**)
  - With osc.: 44 (High-met.) and 48 (Low-met.) c/d/100 ton
- **Day-Night asymmetry:**  $(N-D)/((N+D)/2) = 0.001 \pm 0.012(\text{stat}) \pm 0.007(\text{sys})$   
( **$8.5\sigma$  exclusion of LOW osc. solution**)
- **7% Annual modulation:** according to rate-vs-time analysis:  $T = (1.01 \pm 0.07) \text{ yr}$ ;  
 $\epsilon = 0.0398 \pm 0.0102 \rightarrow$  **expected value within  $2\sigma$**

# Solar $^8\text{B}$ neutrino rate measurement

Data vs. MC of  $^8\text{B}$  recoil energy spectrum (ROI: 3-15 MeV)



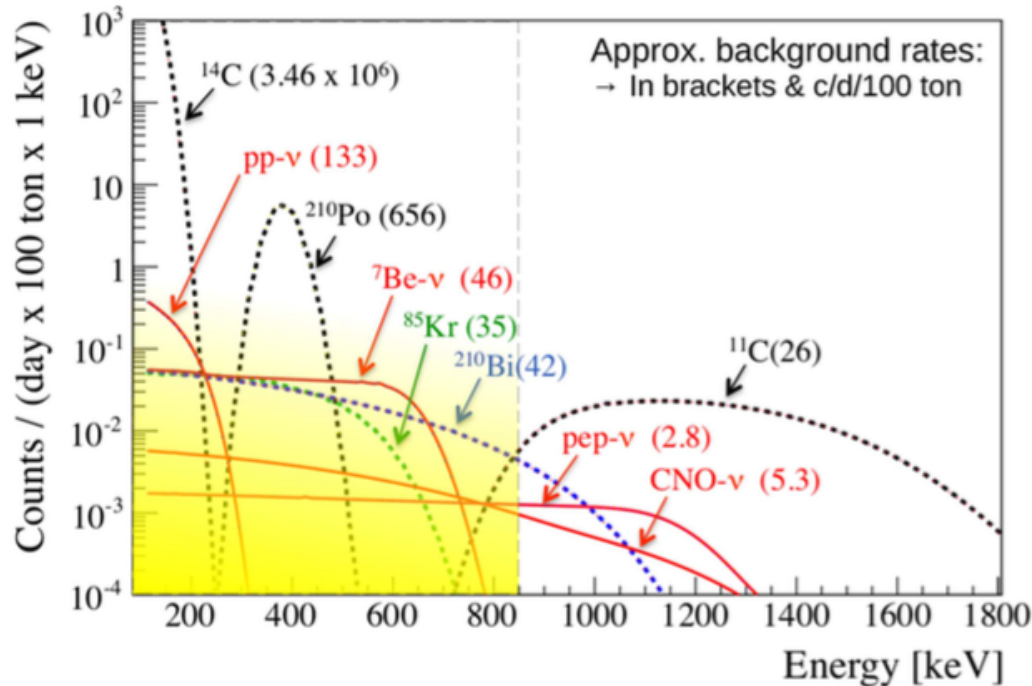
## Results and remarks:

- **Challenging:** low neutrino rate, many small background components
- **Rate above 3 MeV:**  $0.217 \pm 0.038(\text{stat}) \pm 0.008(\text{syst})$  c/d/100ton
- **Flux at 1 AU:**  $(2.7 \pm 0.4 \pm 0.1) \times 10^6 \text{ cm}^{-2} \text{ s}^{-1}$ 
  - **good agreement** with SuperKamiokaNDE and SNO
  - **confirmation** of MSW-LMA solution for oscillation in vacuum/matter
- **Data set:** used 488 d; new analysis with multiple statistics ongoing



# Towards the detection of solar pp neutrinos

pp recoil energy spectrum (ROI: 0.05-0.27 MeV)



pp neutrinos:

Endpoint energy  $E_{mx}$ :

$0 < E_{mx} < 420 \text{ keV}$

$\rightarrow E_{rec} < 264 \text{ keV}$

Energy threshold  $E_{th}$ :

Borexino:  $E_{th} \sim 50 \text{ keV}$

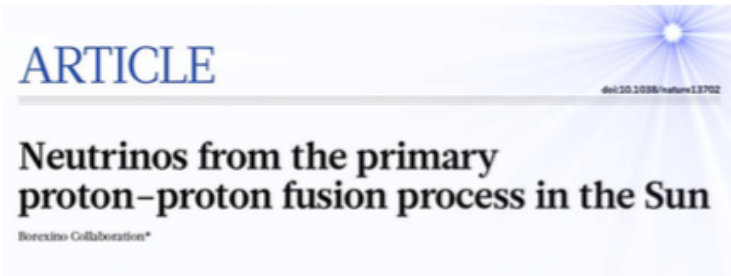
Radiochem. experiments:

$E_{th} \sim 233 \text{ keV}$

## Main obstacles:

- Above  $\sim 240 \text{ keV}$ : decays of  $^{85}\text{Kr}$ ,  $^{210}\text{Bi}$  ( $^{210}\text{Pb}$  daughter)
- Below  $\sim 240 \text{ keV}$ : decays of  $^{14}\text{C}$ ,  $^{14}\text{C}$  pile-ups

# Solar pp neutrino rate measurement (August 2014)



Nature, Vol. 512, August 28, 2014

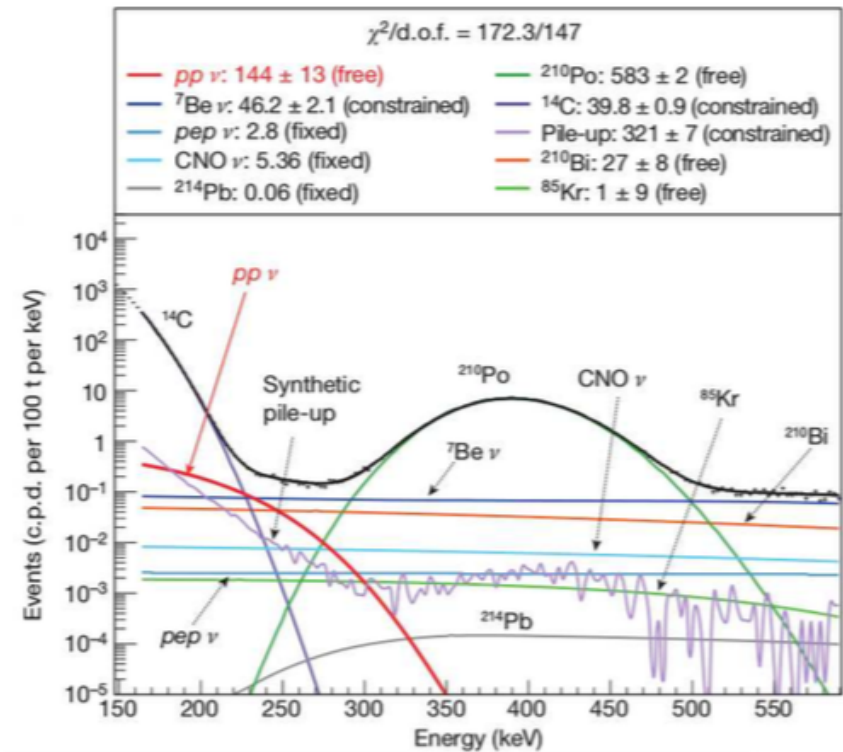
## Results and remarks:

- **Rate:**  
 $144 \pm 13(\text{stat}) \pm 10(\text{sys})$  c/d/100 ton  
 ( $10\sigma$  exclusion of pp  $\nu$  absence)
- **Robustness of analysis:**

Parameter	Systematics:
energy estimator	$\pm 7\%$
fit energy range	
data selection	
pile-up evaluation	
fiducial mass	$\pm 2\%$

- **Check of residual background**

## Measured recoil energy spectrum Fit in (165-590) keV



Rates in [c/d/100 ton], except for  $^{14}\text{C}$  [c/s/100 ton]



# Astrofisica Nucleare e Subnucleare

## Neutrino Oscillations

# Scoperta graduale

## 1964. Homestake + Modello Solare di J. Bahcall

flusso di  $\nu_e$  dal sole  $\approx 1/3$  dell'aspettato ha  
colpa il sole, la fisica nucleare, il neutrino?



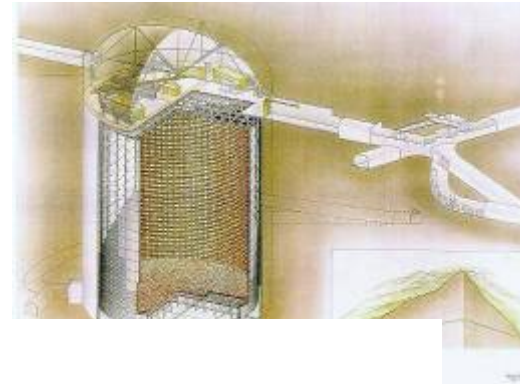
## 1997. GALLEX + LUNA

il colpevole è il neutrino



## 1998. SuperKAMIOKANDE

scoperta oscillazioni: scomparsa nei  
 $\nu_\mu$  da atmosfera

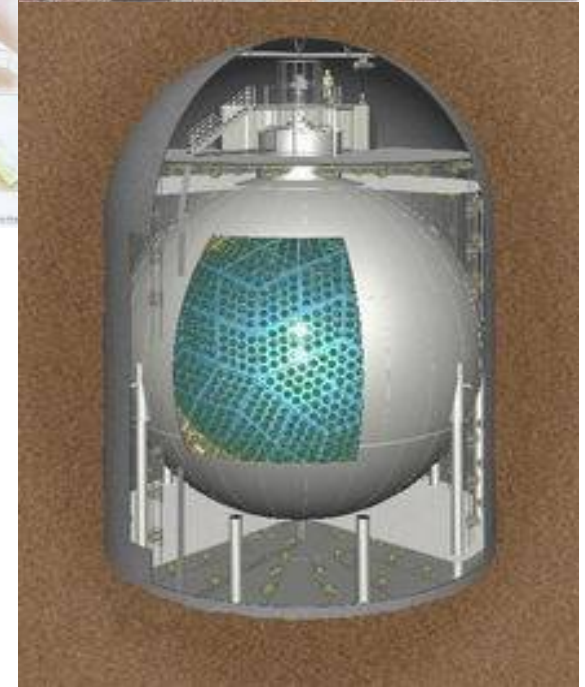


## 2002. SNO

osservazione di comparsa di  $\nu_\mu$  e  $\nu_\tau$  dal sole, tanti  
quanti sono i  $\nu_e$  scomparsi

## 2002. KamLAND

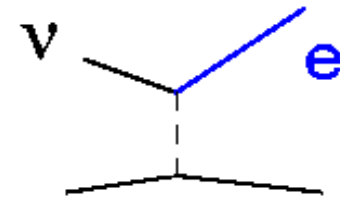
osservazione dell'oscillazione "solare" su  $\nu_e$   
nel vuoto



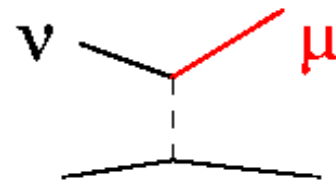
# Comparsa/Appearance



"Appearance Experiments"  
see the new neutrino type  
in the detector



A "Disappearance Experiment" observes  
fewer



than expected



# Scomparsa/Desappearance

# Oscillazioni dei Neutrini

- Idea della massa dei neutrini suggerita per la prima volta da Bruno Pontecorvo

**I Neutrini Interagiscono  
(Produzione o Rivelazione) come  
Autostati dell'Interazione Debole**

$|\nu_e\rangle, |\nu_\mu\rangle, |\nu_\tau\rangle$  = Autostati dell' Interazione Debole

$|\nu_1\rangle, |\nu_2\rangle, |\nu_3\rangle$  = Autostati di Massa (H  $\rightarrow$  Evoluzione t)

• I Neutrini si propagano (evolvono) come  
sovrapposizione di autostati di massa:  
**MESCOLAMENTO**

## Mescolamento tra neutrini: p.es. due famiglie

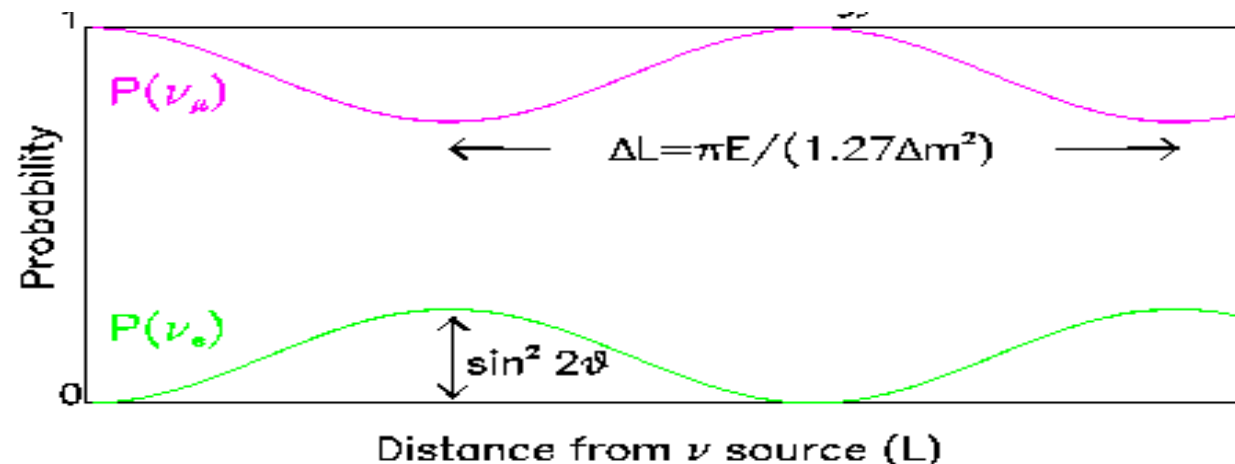
$$|\nu_e\rangle = \cos\theta |\nu_1\rangle + \sin\theta |\nu_2\rangle$$

$$|\nu_\mu\rangle = -\sin\theta |\nu_1\rangle + \cos\theta |\nu_2\rangle$$

$\theta$  = mixing angle  
Angolo di  
mescolamento

$$P_{\nu_\mu\nu_\mu} = 1 - \sin^2 2\theta \cdot \sin^2 \left[ 1.27 \frac{\Delta m^2 \cdot L}{E_\nu} \right]$$

- Distanza percorsa  $L=ct$  (Km)
- Differenza di massa quadra  $\Delta m^2 = m_2^2 - m_1^2$  (eV<sup>2</sup>)
- Energia del neutrino  $E_\nu$  (GeV)



## Vacuum flavor oscillations: mass and weak eigenstates

$$\begin{array}{|c|} \hline \text{flavor} \\ \hline \text{states} \\ \hline \end{array}
 \begin{array}{l} |\nu_e\rangle \\ |\nu_\mu\rangle \end{array}
 \leftrightarrow
 \begin{array}{l} |\nu_L\rangle \\ |\nu_H\rangle \end{array}
 \begin{array}{|c|} \hline m_L \\ m_H \\ \hline \text{mass} \\ \hline \text{states} \\ \hline \end{array}$$

Noncoincident bases  $\Rightarrow$  oscillations down stream:

$$\begin{aligned} |\nu_e\rangle &= \cos\theta |\nu_L\rangle + \sin\theta |\nu_H\rangle \\ |\nu_\mu\rangle &= -\sin\theta |\nu_L\rangle + \cos\theta |\nu_H\rangle \end{aligned}
 \quad \begin{array}{l} \text{vacuum mixing} \\ \text{angle} \end{array}$$

$$\begin{aligned} |\nu_e^k\rangle &= |\nu^k(x=0, t=0)\rangle \quad E^2 = k^2 + m_i^2 \\ |\nu^k(x \sim ct, t)\rangle &= e^{ikx} [e^{-iE_L t} \cos\theta |\nu_L\rangle + e^{-iE_H t} \sin\theta |\nu_H\rangle] \\ |\langle \nu_\mu | \nu^k(t) \rangle|^2 &= \sin^2 2\theta \sin^2 \left( \frac{\delta m^2}{4E} t \right), \quad \delta m^2 = m_H^2 - m_L^2 \end{aligned}$$

$\nu_\mu$  appearance downstream  $\Leftrightarrow$  vacuum oscillations

Can slightly generalize this

$$|\nu(0)\rangle \rightarrow a_e(0)|\nu_e\rangle + a_\mu(0)|\nu_\mu\rangle$$

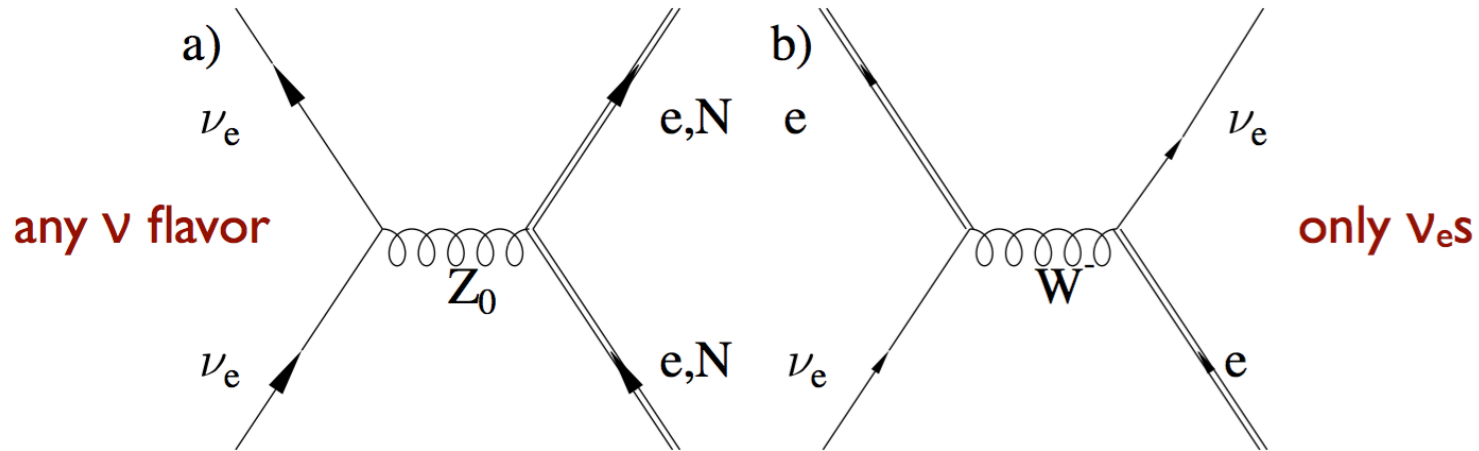
with the subsequent evolution downstream governed by

$$i \frac{d}{dx} \begin{pmatrix} a_e(x) \\ a_\mu(x) \end{pmatrix} = \frac{1}{4E} \begin{pmatrix} -\delta m^2 \cos 2\theta & \delta m^2 \sin 2\theta \\ \delta m^2 \sin 2\theta & \delta m^2 \cos 2\theta \end{pmatrix} \begin{pmatrix} a_e(x) \\ a_\mu(x) \end{pmatrix}$$

vacuum  $m_\nu^2$  matrix

This problem familiar from hadronic physics: the Cabibbo angle and CKM matrix.

# solar matter generates a flavor asymmetry

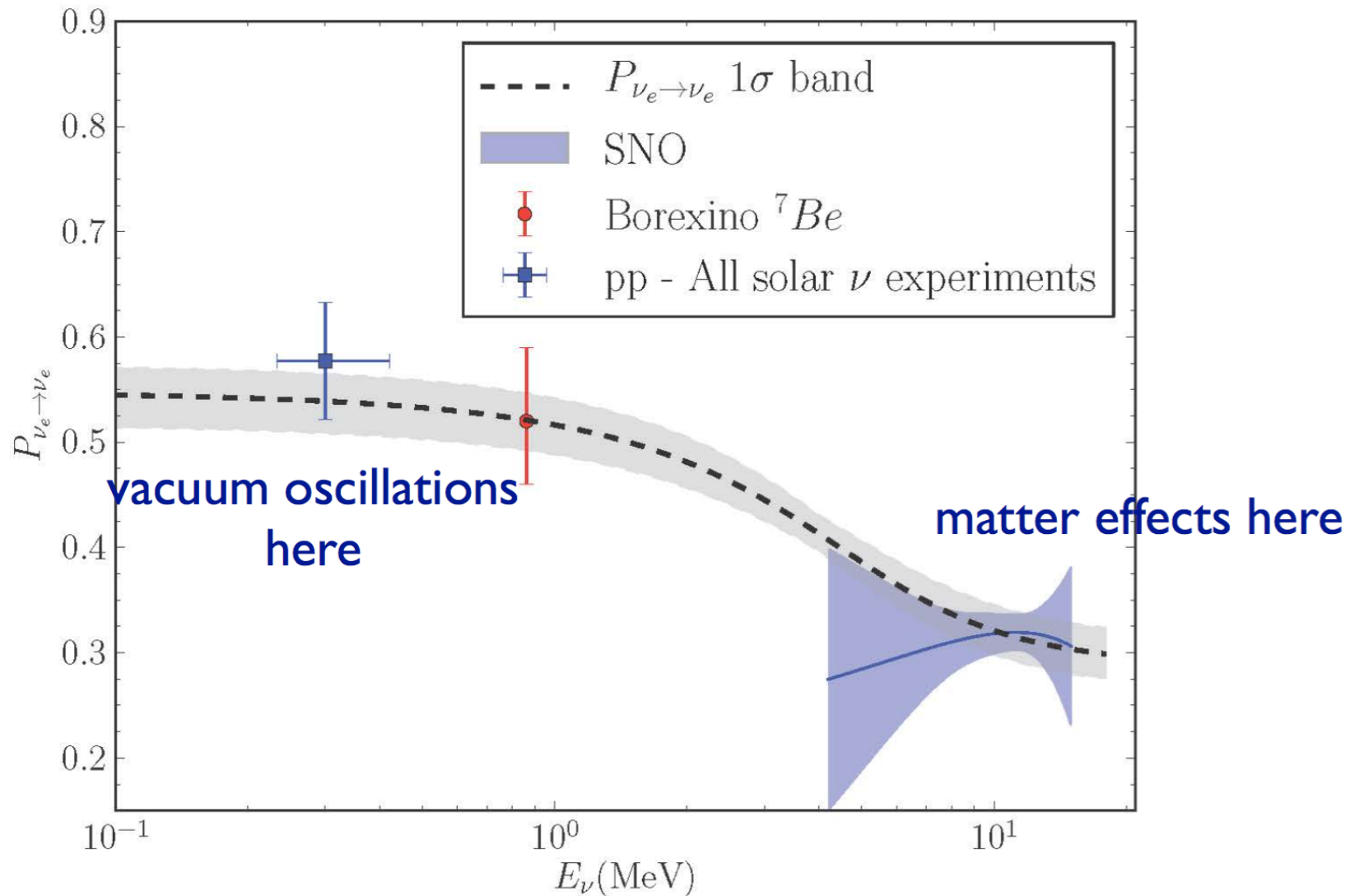


- modifies forward scattering amplitude: flavor-dependent index of refraction
- the affect is proportional to the (changing) solar electron density
- makes the electron neutrino heavier at high density

$$m_{\nu_e}^2 = 4E\sqrt{2}G_F \rho_e(x)$$

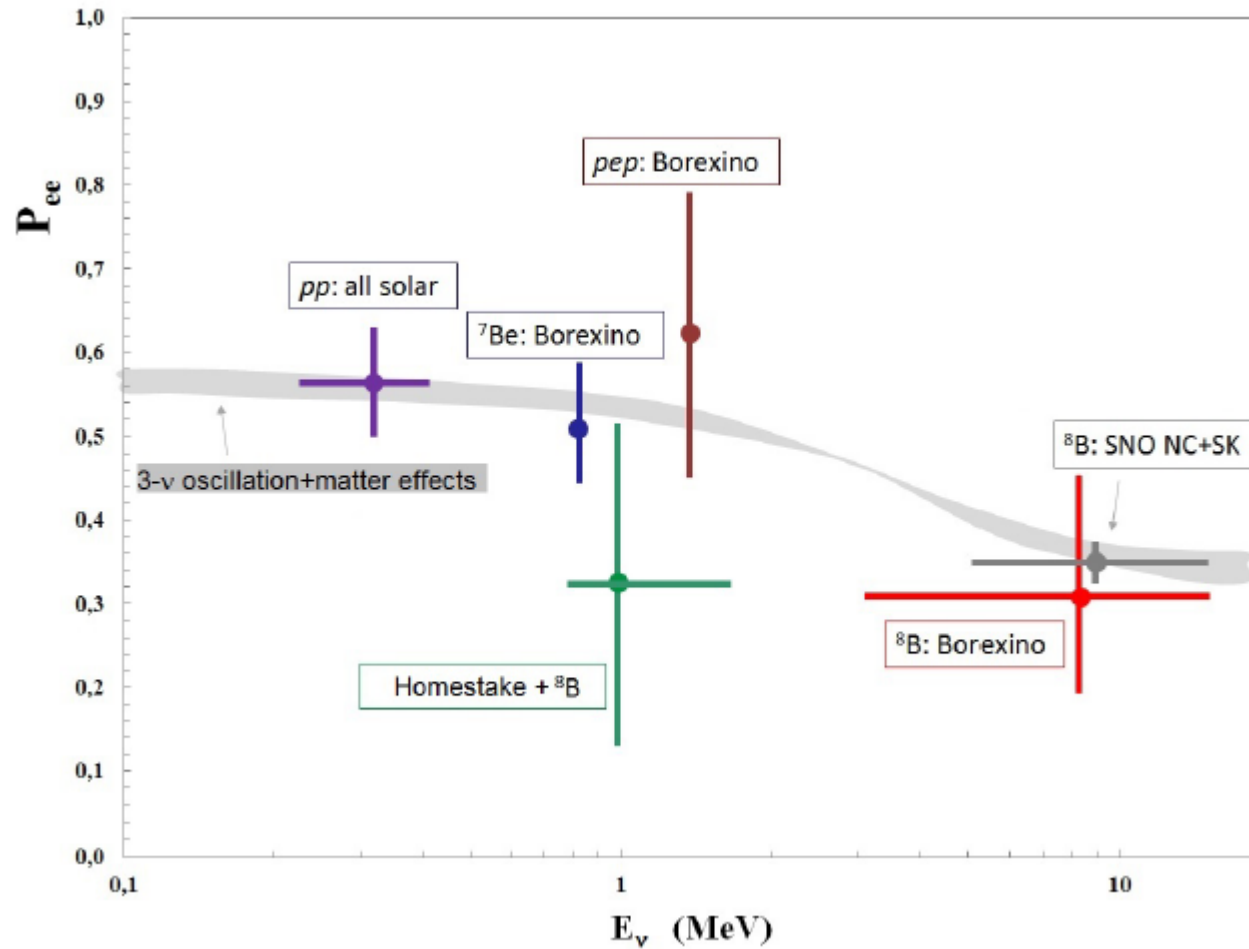


from Art McDonald



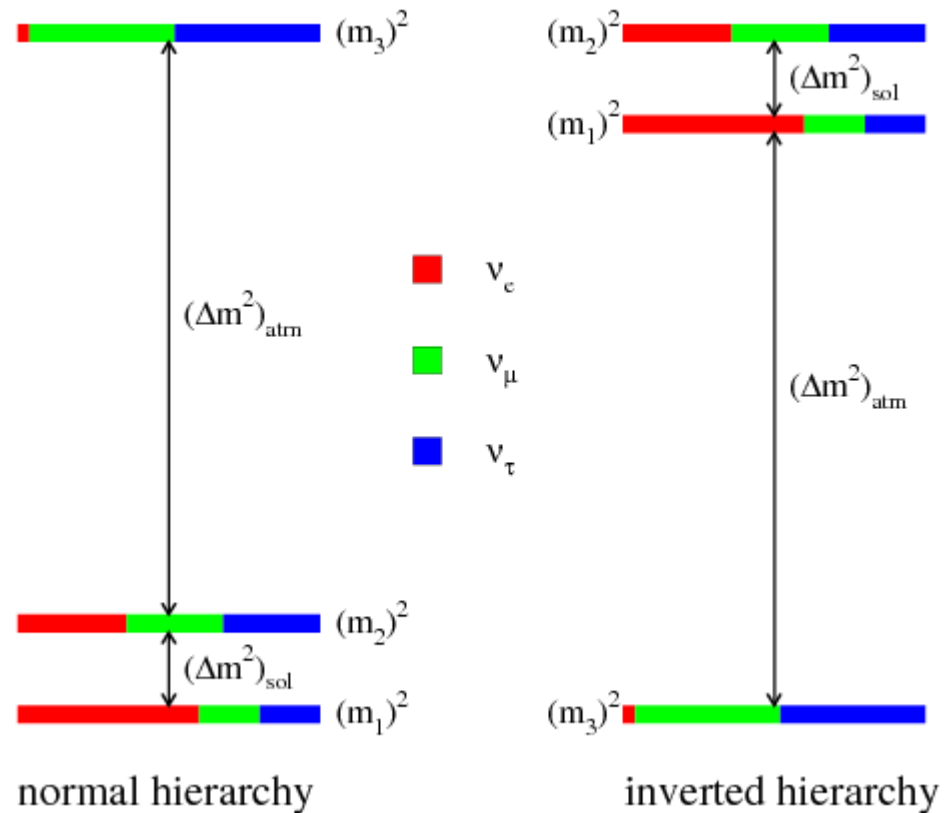
Matter effects produce a characteristic energy-dependence in the  $\nu_e$  survival probability, in accord with experiments

# Neutrino oscillations and the Sun



# Neutrino parameters

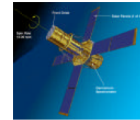
Parameter	best-fit value ( $\pm 1\sigma$ )
$\Delta m_{\odot}^2$	$(7.58^{+0.22}_{-0.26}) \times 10^{-5} \text{ eV}^2$
$\Delta m_{atm}^2$	$(2.35^{+0.12}_{-0.09}) \times 10^{-3} \text{ eV}^2$
$\sin^2 \theta_{12}$	$0.306^{+0.018}_{-0.015}$
$\sin^2 \theta_{23}$	$0.42^{+0.08}_{-0.03}$
$\sin^2 \theta_{13}$	$0.0251 \pm 0.0034$



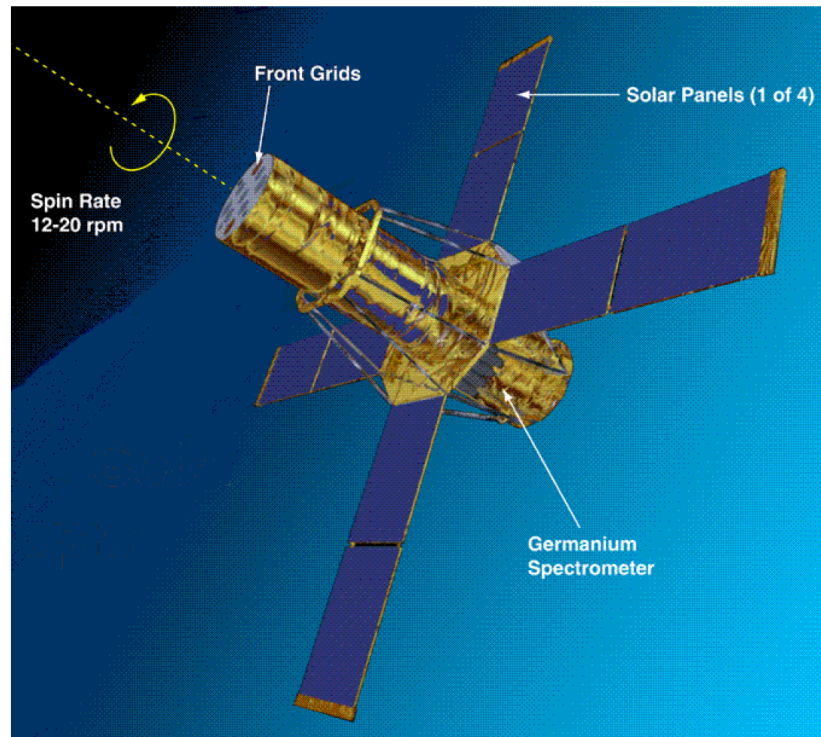
Astrofisica Nucleare e Subnucleare  
The Sun in Gamma-rays

# Solar Flares in Gamma-rays

Solar  $\gamma$ -Ray Physics Comes of Age

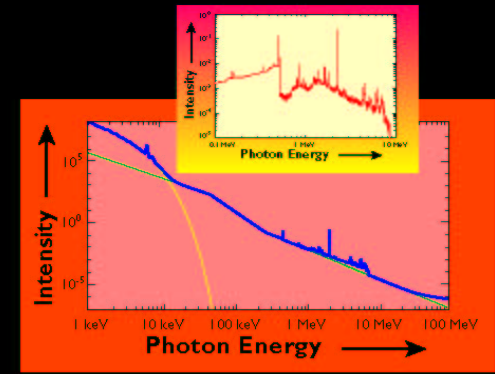


## The High Energy Solar Spectroscopic Imager



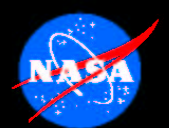
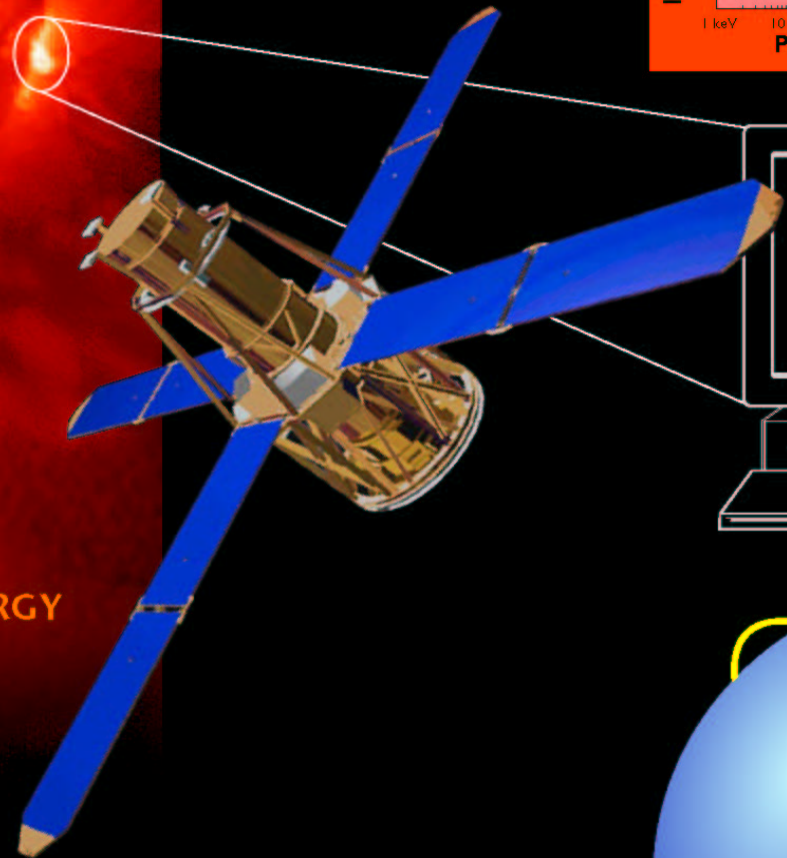
Share 2001

High-Resolution Spectroscopic Imaging of Solar Flares in X Rays and Gamma Rays



# RHESSI

THE REUVEN RAMATY HIGH ENERGY SOLAR SPECTROSCOPIC IMAGER



*To explore the basic physics of particle acceleration and explosive energy release in solar flares*

Lin 2002

DenB0201794\_001



# HESSI Science Objective

To explore the basic physics of particle acceleration and explosive energy release in solar flares

- Impulsive Energy Release in the Corona
- Acceleration of Electrons, Protons, and Ions
- Plasma Heating to Tens of Millions of degrees
- Energy and Particle Transport and Dissipation



Lin 2002

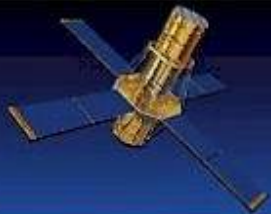
# HESSI Primary Observations

- Hard X-ray Images
  - Angular resolution as fine as 2 arcseconds
  - Temporal resolution as fine as 10 ms
  - Energy resolution of  $<1$  keV to  $\sim 3$  keV (FWHM)
- High Resolution X-ray and Gamma-ray Spectra
  - $\sim$ keV energy resolution
  - To energies as high as 15 MeV



Lin 2002



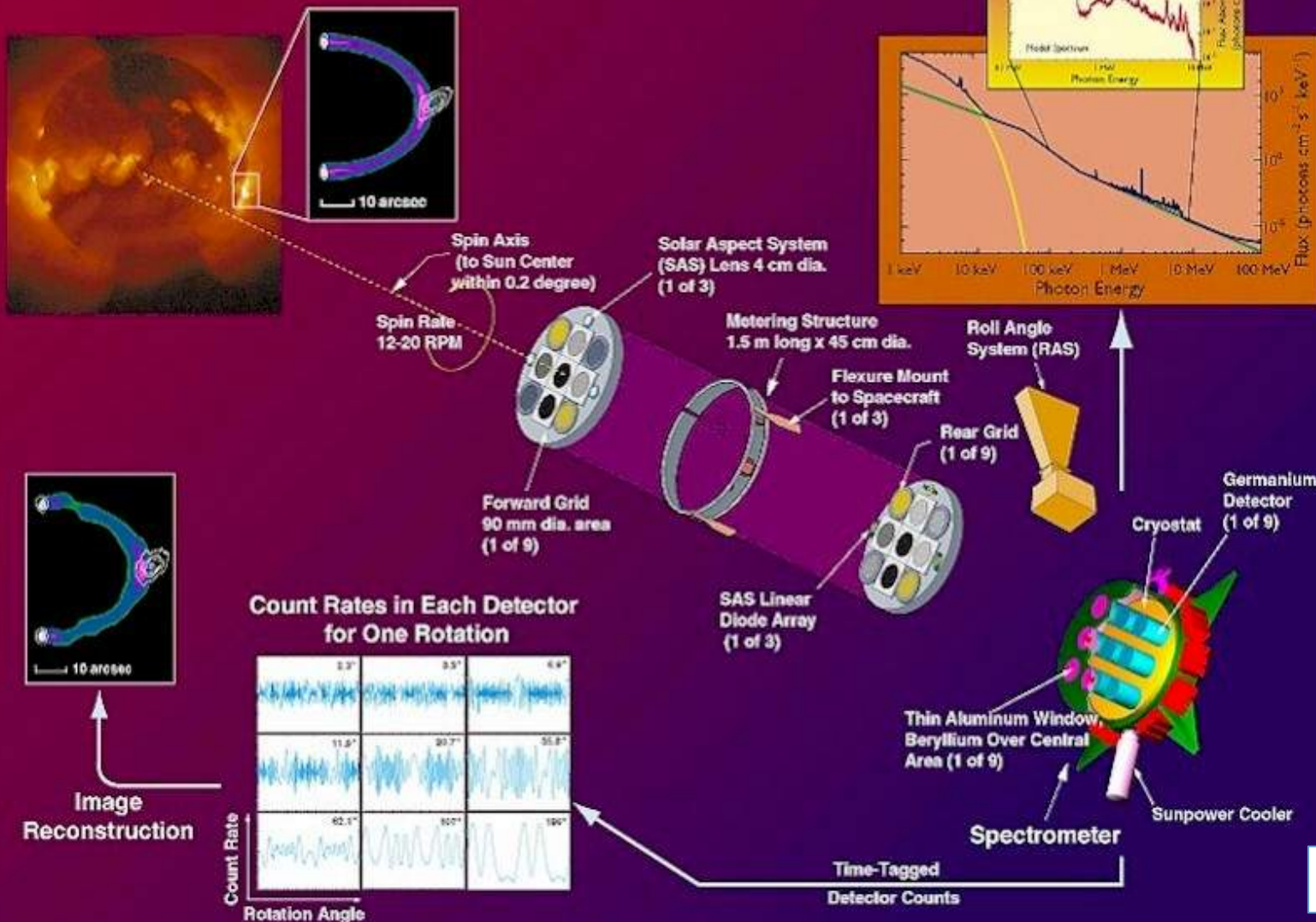


# HESSI: The High Energy Solar Spectroscopic Imager



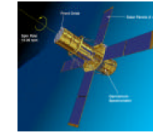
Web Site: <http://hesperia.gsfc.nasa.gov/hessi/>

## High-Resolution Spectroscopic Imaging of Solar Flares from 3 keV X-Rays to 20 MeV Gamma Rays

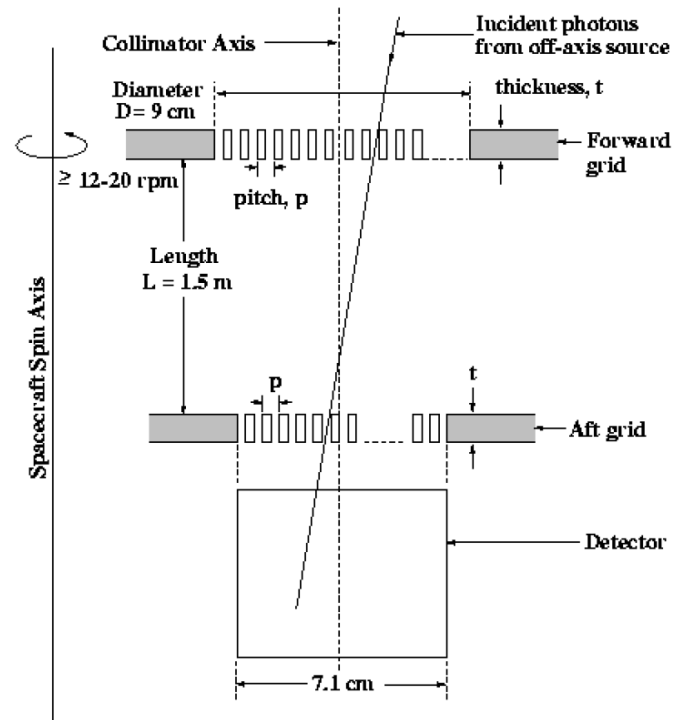


# Solar Flares in Gamma-rays

Solar  $\gamma$ -Ray Physics Comes of Age



## HESSI IMAGING SYSTEM

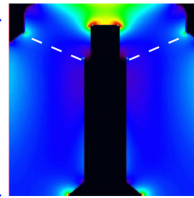
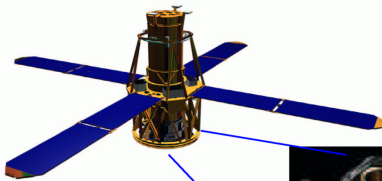


Share 2001



# RHessi

## THE RHessi SPECTROMETER

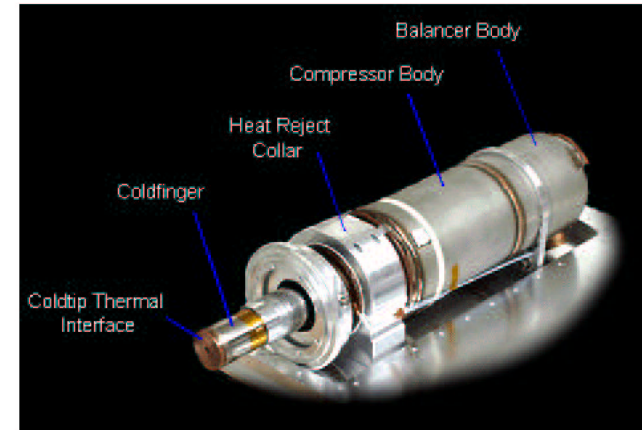


9 segmented coaxial Ge detectors, 7cm x 8.5cm

- Energy range:** Front segments: 3 keV - 2.8 MeV  
Rear segments: 20 keV - 17 MeV
- Resolution:** Front segments: 1 keV @ 100 keV  
Rear segments: 2.9 keV @ 1 MeV
- Throughput:** 25,000+ counts/segment/second
- Shielding:** NONE (4mm Al sides, 2cm Al rear)

Other important subsystems:

Sunpower Stirling-cycle cryocooler, keeps detectors at 75K with 52W of power:

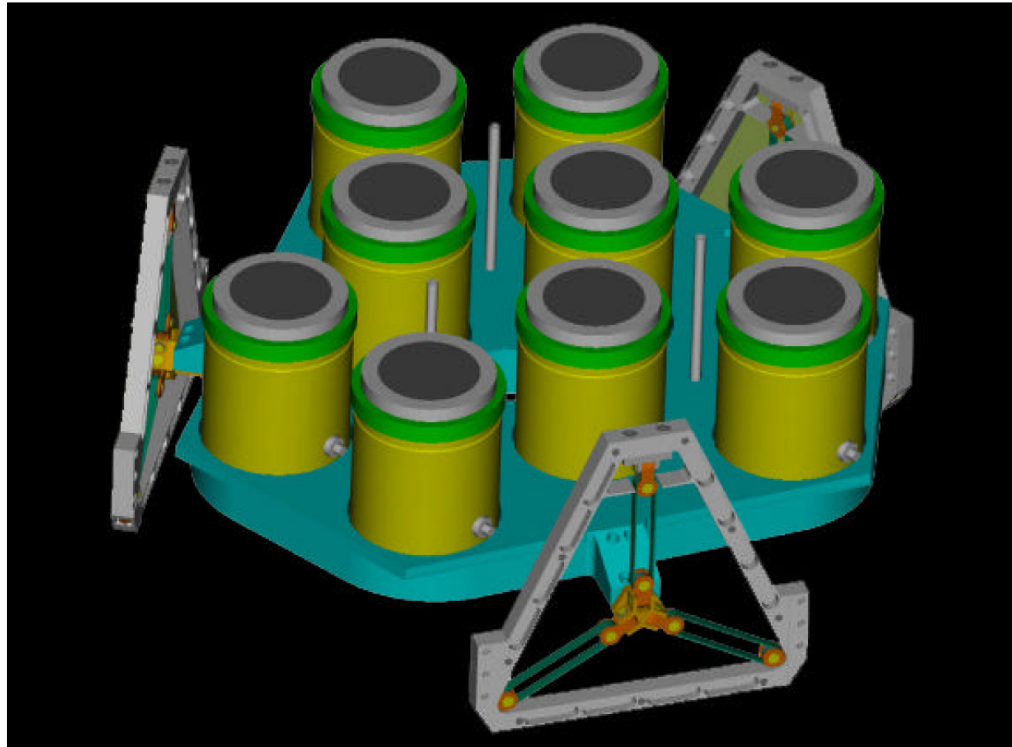
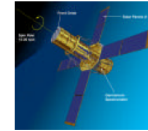


Attenuators: two sets of aluminum disks (thick and thin) that can be manually or automatically moved in front of the detectors to reduce the count rates from large flares.

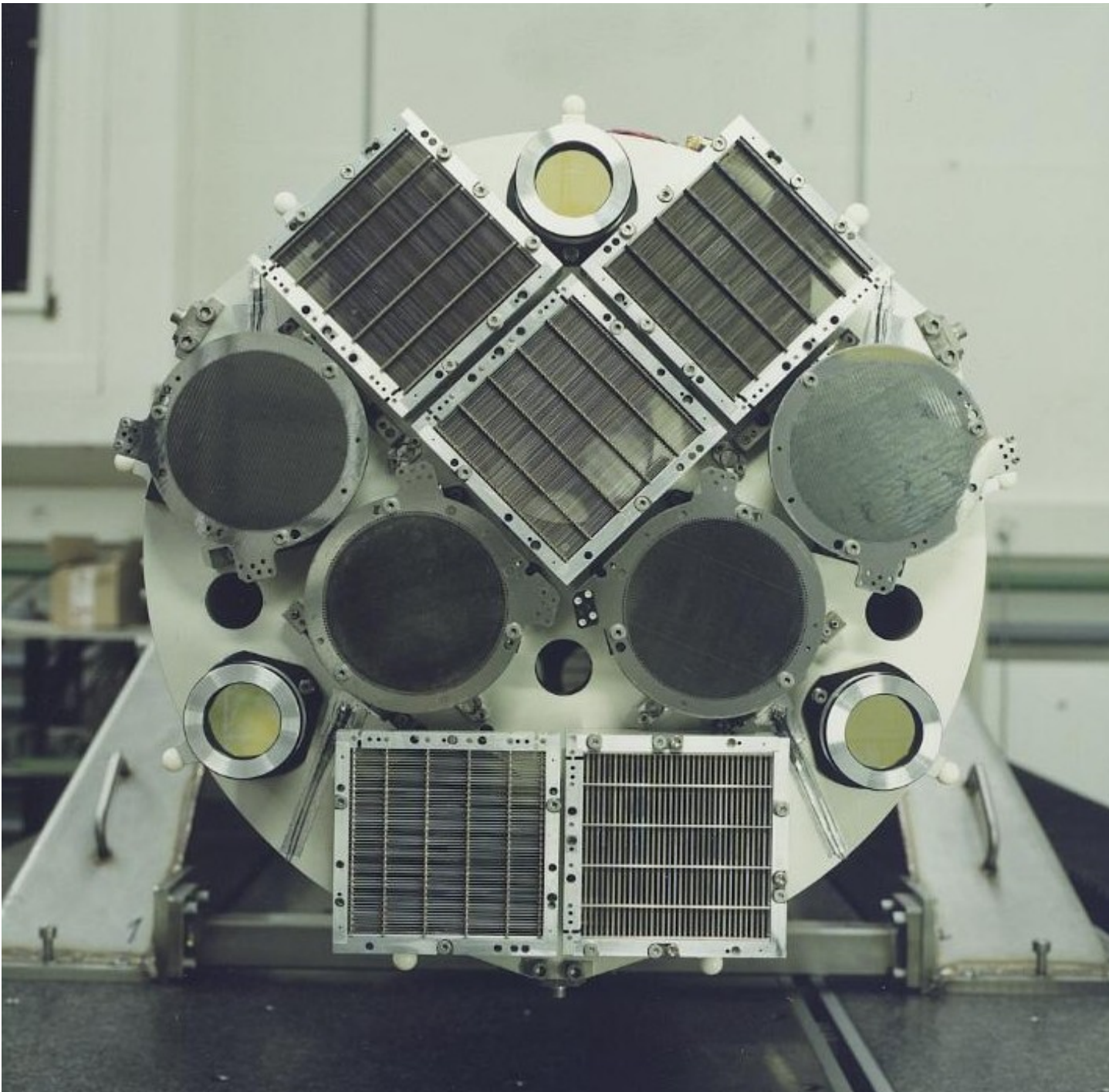
# Solar Flares in Gamma-rays

Solar  $\gamma$ -Ray Physics Comes of Age

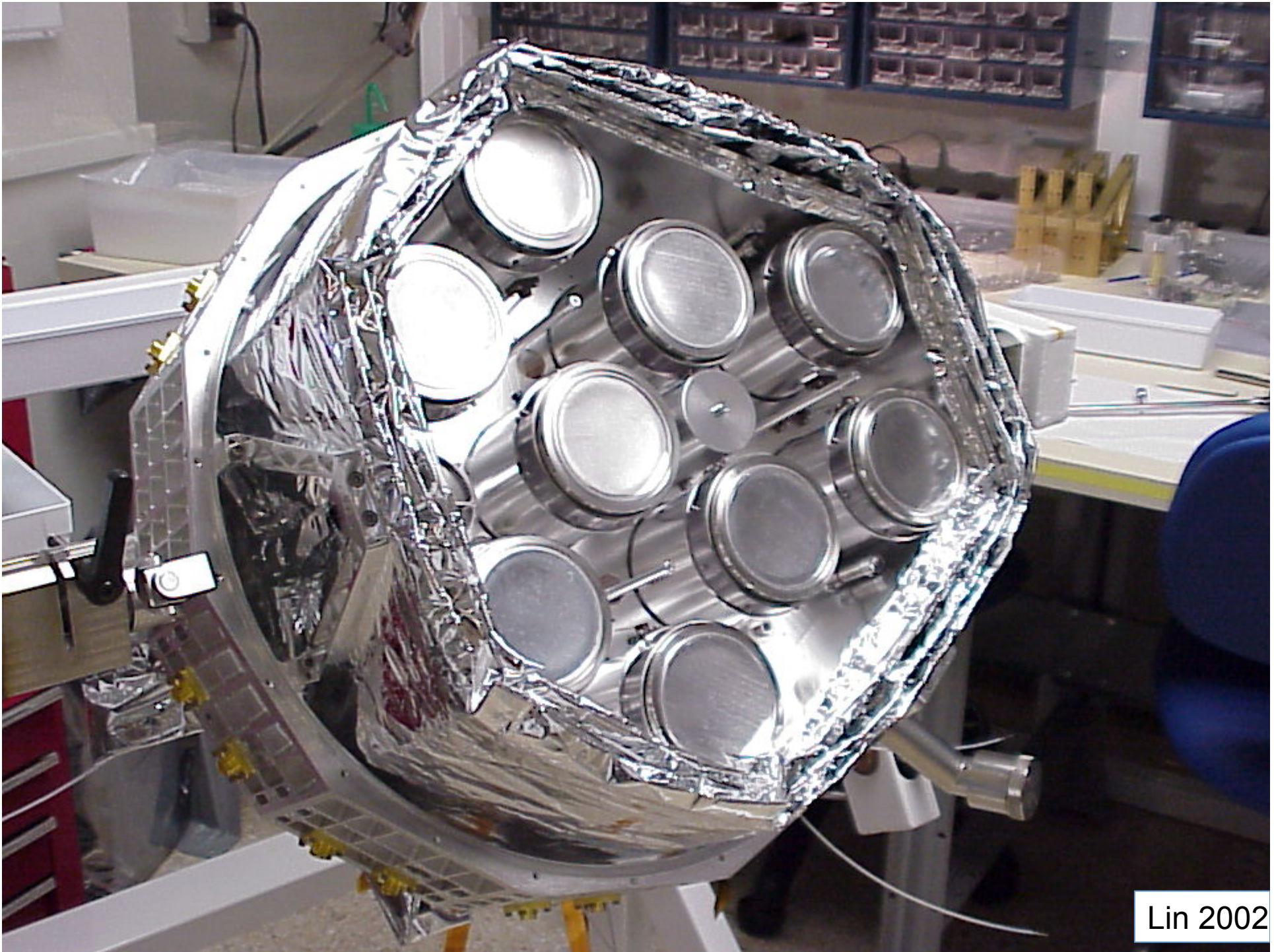
HESSI Germanium Detector Array



Share 2001



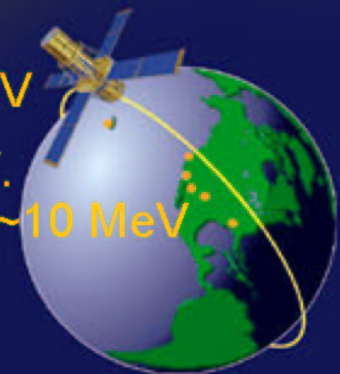
Lin 2002



Lin 2002

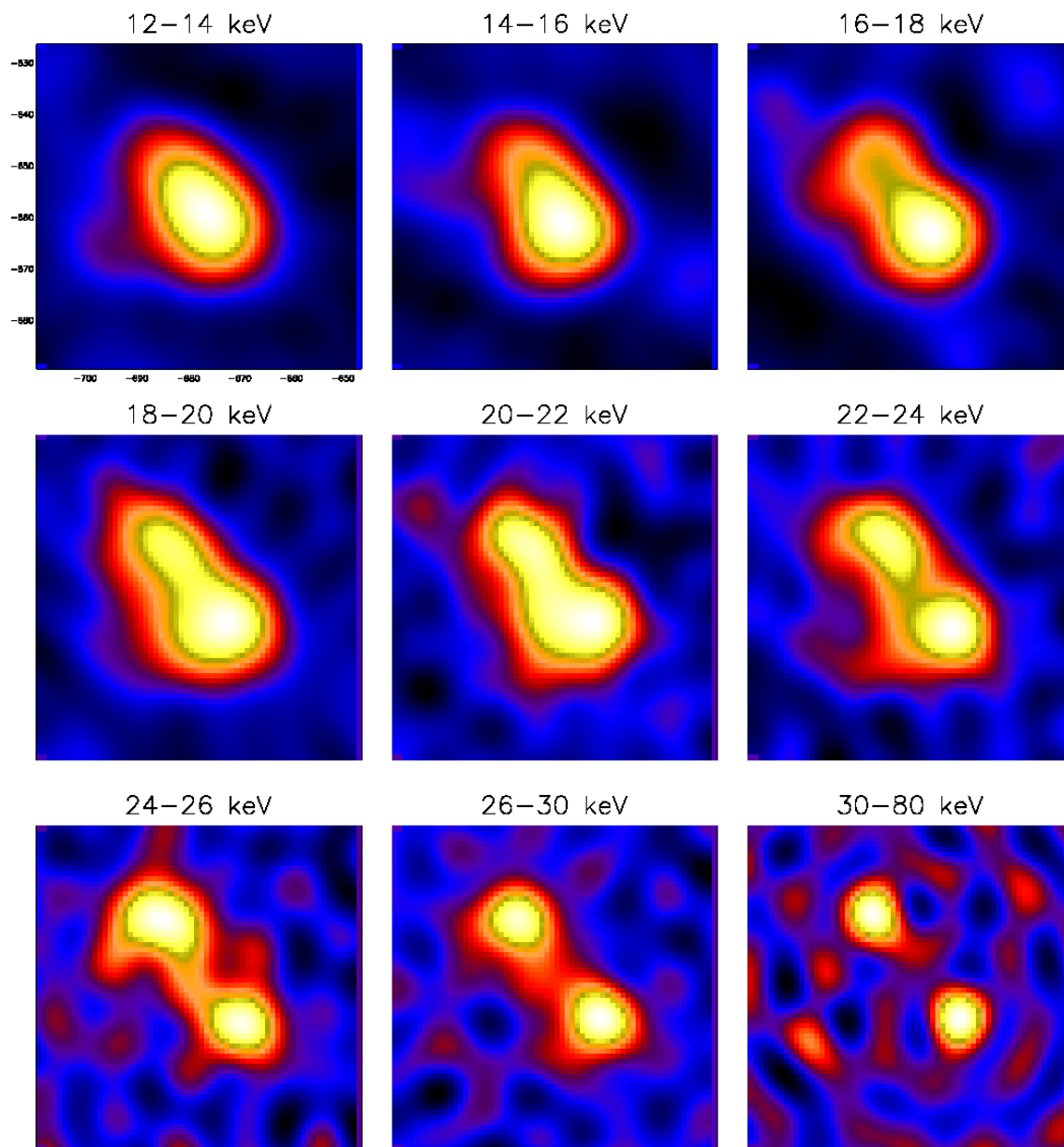
# HESSI Observational Characteristics

- Energy Range 3 keV to 15 MeV
- Energy Resolution (FWHM) <1 keV FWHM at 3 keV  
increasing to 5 keV at 15 MeV
- Angular Resolution 2 arcseconds to 100 keV  
7 arcseconds to 400 keV  
36 arcseconds to 15 MeV
- Temporal Resolution Tens of ms for basic image  
2 s for detailed image
- Field of View Full Sun
- Effective Area - cm<sup>2</sup>  
(with attenuators out) 10<sup>-3</sup> at 3 keV, 50 at 10 keV  
60 at 100 keV, 20 at 10 MeV
- Numbers of flares ~1000 imaged to >100 keV.  
~100 with spectroscopy to ~10 MeV



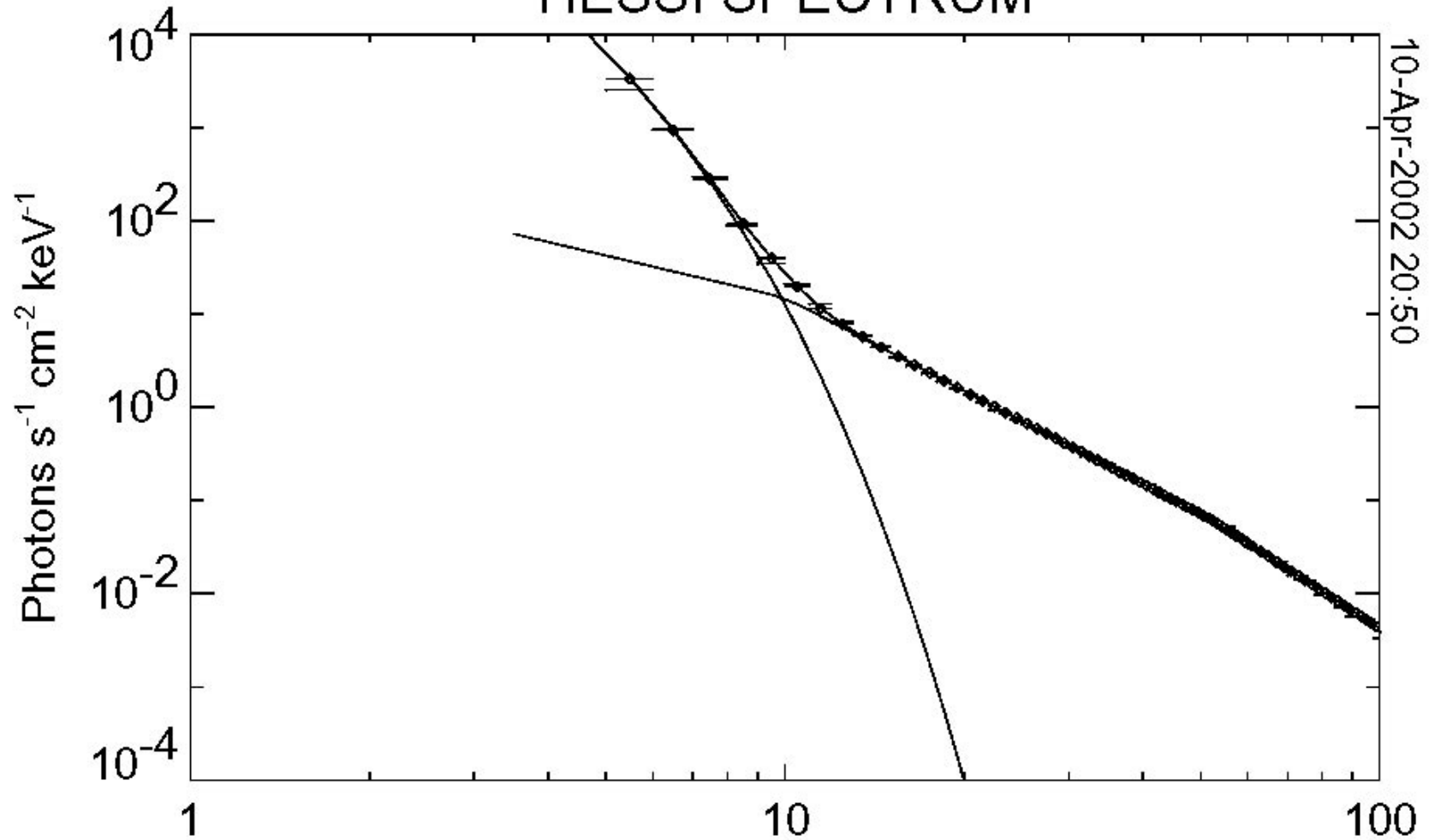
02/02/20, 11:06:00.6 – 11:06:39.6

cleaned maps





# HESSI SPECTRUM



Interval 0  
11:06:11.99 - 11:06:24.00

f\_vth\_bpow parameters: 0.4495, 0.9123, 0.07185, 3.319, 52.00, 4.121

# RHESSI DATA ANALYSIS

Documentation and details at  
**RHESSI SOFTWARE AND DATA ANALYSIS CENTER**

<http://hesperia.gsfc.nasa.gov/rhessidatcenter/>

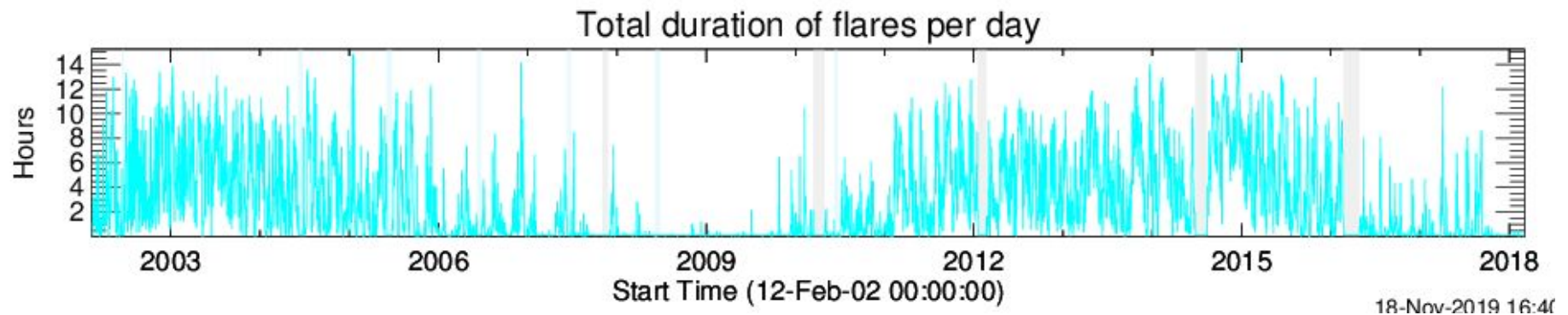
# Status of the RHESSI Mission Archive

**Target 2020**

7-July-2020

R. A. Schwartz A. K. Tolbert

Contributing: B Dennis, A Shih, A Inglis, M Fivian, D Smith, M.  
Abdallaoui



# Overview of the Archive

- **Mission Archive Web Page:**  
<https://hesperia.gsfc.nasa.gov/rhessi3/mission-archive/index.html>
- Image Archive – so much information
- Visibility Archive – coarse and fine
- Energy Spectra – ready for stand-alone spectroscopy
- Detector Health – you have wanted this
- Calibrated SAS data – a select few
- GRB & TGF – in progress
- Calibration and Roll Aspect Databases – in progress
- Ancillary missions – MESSENGER, FERMI, GOES, SMM, AIA

# Flare Image Archive

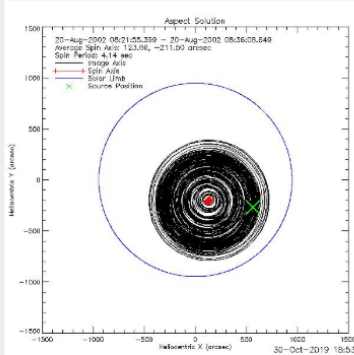
[RHESSI Image Archive Strategy](#) [Guide to RHESSI Image Archive](#)

2002 February Load

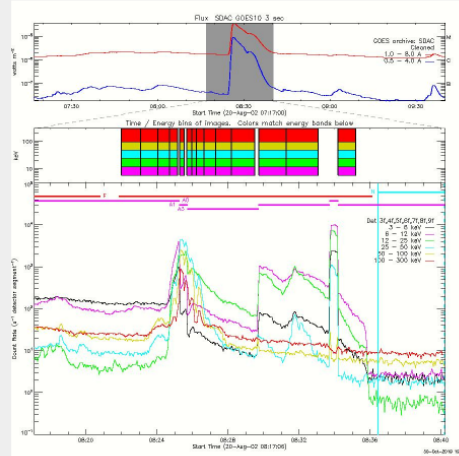
## RHESSI Flare Images February 2002

<a href="#">12-Feb-2002 21:30:00 - 21:41:00</a>	6tx2e	<a href="#">Browser</a>	<a href="#">Aspect Plot</a>	<a href="#">Profile Plot</a>	Panels	Image Movies:	-	6-12	12-25	-	-	-
<a href="#">12-Feb-2002 21:44:00 - 21:48:00</a>	-	<a href="#">Browser</a>	<a href="#">Aspect Plot</a>	-	-	-	-	-	-	-	-	-
<a href="#">13-Feb-2002 00:53:00 - 00:57:00</a>	-	<a href="#">Browser</a>	<a href="#">Aspect Plot</a>	-	-	-	-	-	-	-	-	-
<a href="#">13-Feb-2002 04:22:00 - 04:26:00</a>	1tx1e	<a href="#">Browser</a>	<a href="#">Aspect Plot</a>	<a href="#">Profile Plot</a>	Panels	Image Movies:	-	6-12	-	-	-	-
<a href="#">13-Feb-2002 07:03:00 - 07:30:00</a>	18tx2e	<a href="#">Browser</a>	<a href="#">Aspect Plot</a>	<a href="#">Profile Plot</a>	Panels	Image Movies:	-	6-12	12-25	-	-	-

Flare 20820140, 20-Aug-2002 08:21:52 - 08:36:08 Peak: 08:26:22 Duration: 856 s Peak: 1424 c/s Total Counts: 2876159  
Highest Energy: 100-300 keV Flare Position: 569,-264 asec AR: 69



[Movie of Aspect Solution in Image Time Bins](#)



[BACK\\_PROJECTION Images](#)  
[CLEAN Images](#)  
[CLEAN\\_59 Images](#)  
[MEM\\_GE Images](#)  
[VIS\\_CS Images](#)  
[VIS\\_FWDFIT Images](#)

[RHESSI Browser](#)  
[AIA-movies](#)  
[Direct Link to Plot Folder](#)

Download files:

[BACK\\_PROJECTION Image Cube FITS](#)  
[CLEAN Image Cube FITS](#)  
[CLEAN\\_59 Image Cube FITS](#)  
[MEM\\_GE Image Cube FITS](#)  
[VIS\\_CS Image Cube FITS](#)  
[VIS\\_FWDFIT Image Cube FITS](#)

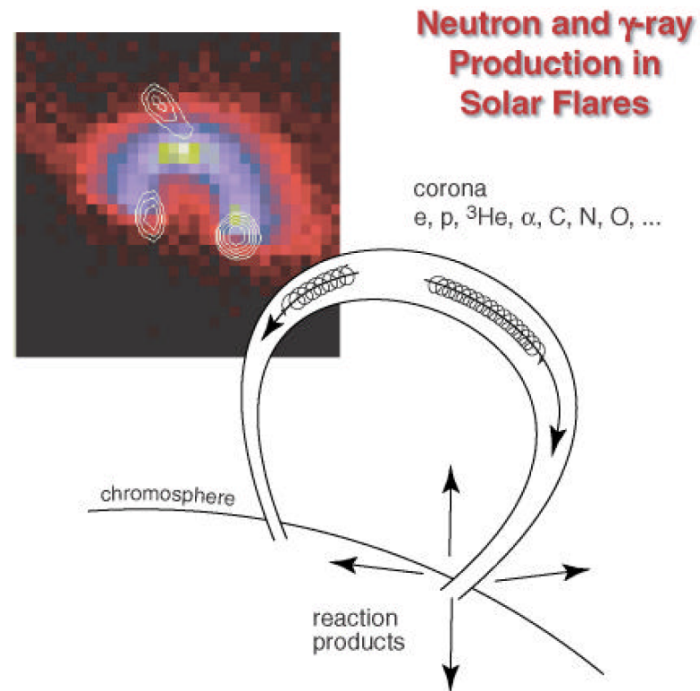
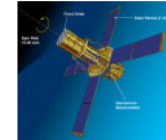
[Visibility FITS](#)  
[Eventlist FITS](#)

Image Creation Scripts:

[BACK\\_PROJECTION](#) [\\_non-default\\_params](#) [all\\_params](#)  
[CLEAN](#) [\\_non-default\\_params](#) [all\\_params](#)  
[CLEAN\\_59](#) [\\_non-default\\_params](#) [all\\_params](#)  
[MEM\\_GE](#) [\\_non-default\\_params](#) [all\\_params](#)  
[VIS\\_CS](#) [\\_non-default\\_params](#) [all\\_params](#)  
[VIS\\_FWDFIT](#) [\\_non-default\\_params](#) [all\\_params](#)

# Solar Flares in Gamma-rays

Solar  $\gamma$ -Ray Physics Comes of Age



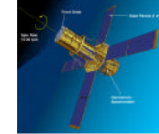
electrons: X- and  $\gamma$ -ray bremsstrahlung

ions: radioactive nuclei  $\rightarrow e^+ \rightarrow \gamma_{511}$   
 $\pi \rightarrow \gamma$  (decay,  $e^\pm$  bremsstrahlung)  
excited nuclei  $\rightarrow \gamma$ -ray line radiation  
neutrons  $\rightarrow$   $\left\{ \begin{array}{l} \text{escape to space} \\ 2.223 \text{ MeV capture line} \end{array} \right.$

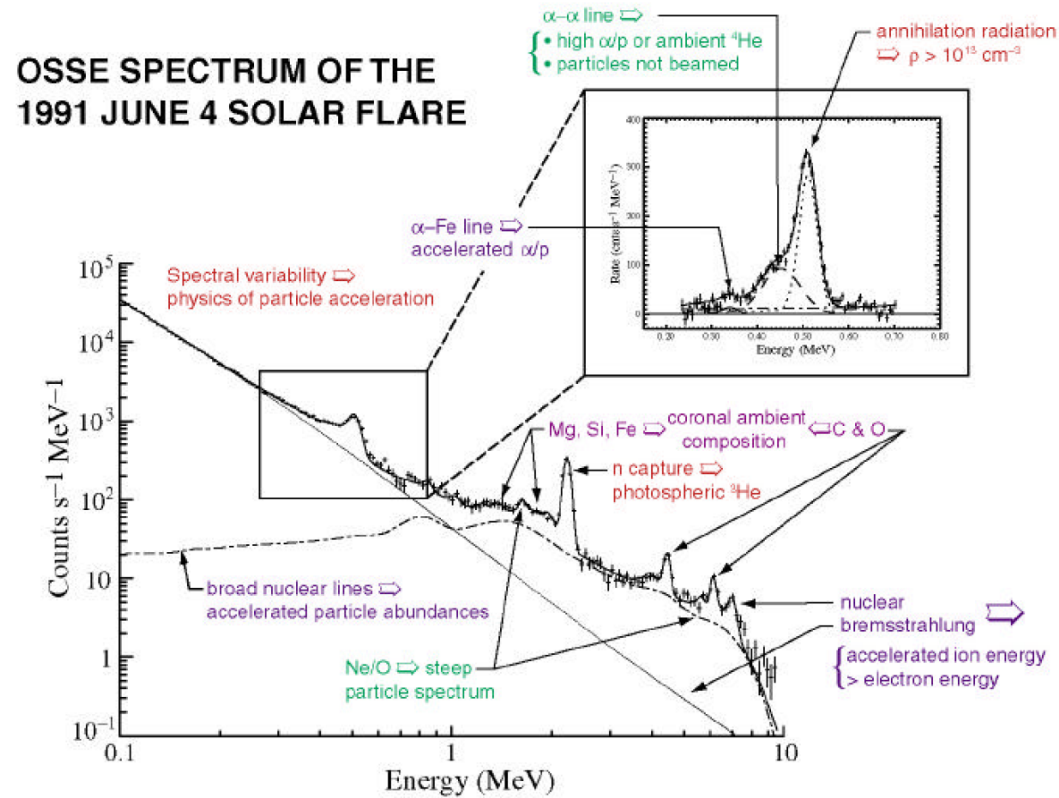
Share 2001

# Solar Flares in Gamma-rays

Solar  $\gamma$ -Ray Physics Comes of Age



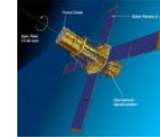
## The Physics of Flares Revealed by $\gamma$ -Ray Spectroscopy



Share 2001

# Solar Flares in Gamma-rays

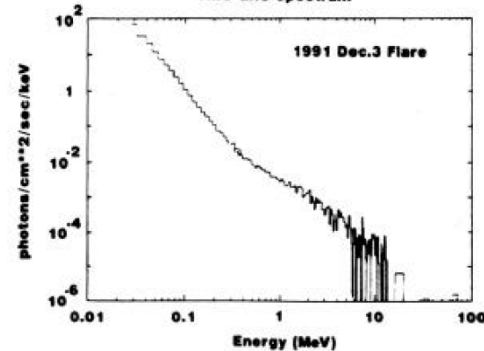
Solar  $\gamma$ -Ray Physics Comes of Age



## Shape of Bremsstrahlung Continuum >100 keV

Yohkoh

HXS-GRS Spectrum



Hardening found in spectra >100 keV by combined analysis of *SMM* GRS/HXRBS spectra.

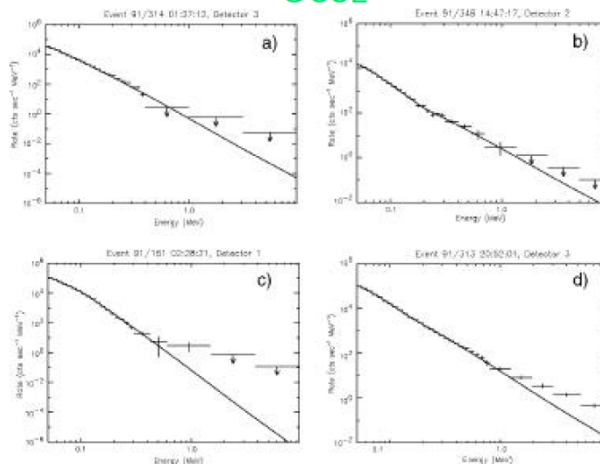
Similar hardening observed in combined spectrum from *Yohkoh* HRS/GRS.

Important for measurements to be made with the same instrument.

Best instruments BATSE, OSSE, and HESSI.

OSSE continuum spectra exhibit: single power laws, broken power laws with hardening and softening between  $\sim 100$  and 200 keV, and additional hardening above  $\sim 1$  MeV.

OSSE

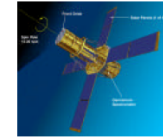


Share 2001

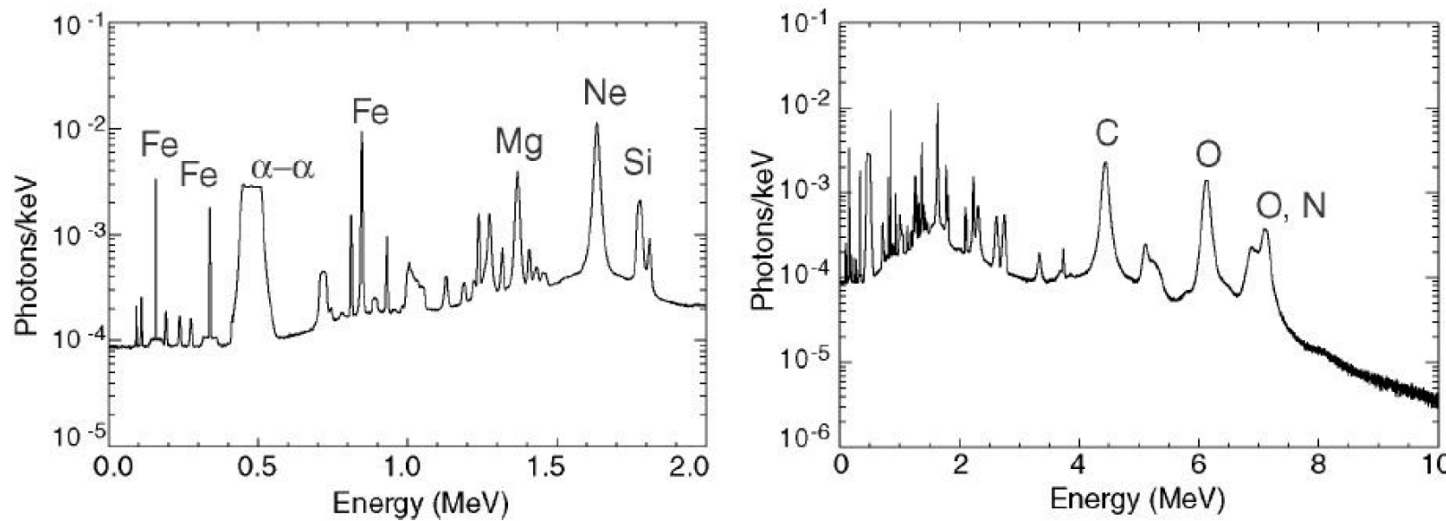


# Solar Flares in Gamma-rays

Solar  $\gamma$ -Ray Physics Comes of Age



## Theoretical Nuclear Line Spectrum

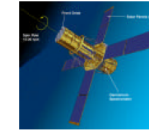


Ramaty, Kozlovsky, Lingenfelter, and Murphy

Share 2001

# Solar Flares in Gamma-rays

Solar  $\gamma$ -Ray Physics Comes of Age



## Narrow $\gamma$ -Ray Lines Observed in Flare Spectra

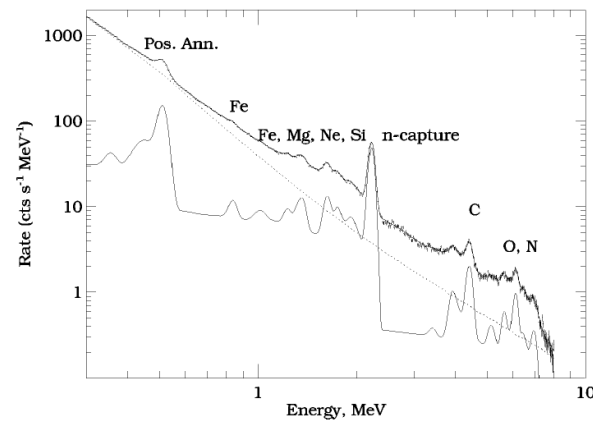
Produced by  $p$  and  $\alpha$  interactions with ambient material.

At least 30% of flares with emission  $>0.3$  MeV exhibit  $\gamma$ -ray line features. *HESSI* will make more definitive measurement.

At least 19 de-excitation lines have been identified in fits to flare spectra.

Widths of de-excitation lines measured to be  $\sim 2$ -4% in the summed spectrum. This exceeds theory in some cases suggesting presence of blended lines (e.g.  $^{14}\text{N}$  near  $^{20}\text{Ne}$ ) or different Doppler shifts in the flares (see later discussion).

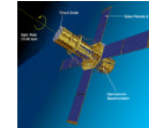
*HESSI* can resolve these lines and determine intrinsic widths.



Share 2001

# Solar Flares in Gamma-rays

Solar  $\gamma$ -Ray Physics Comes of Age



## Narrow $\gamma$ -Ray Lines in Solar-Flare Spectra

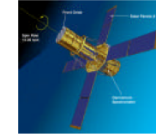
### Sum of 19 SMM Flares

Energy, MeV	Width (% FWHM)	Identification
$0.357 \pm 0.002$	$3.7 \pm 3.1$	$^{59}\text{Ni}$ (0.339 MeV)
0.454	--	$^7\text{Be}$ , $^7\text{Li}$ (0.429, 0.478 MeV)
$0.513 \pm 0.001$	< 2	$e^+ - e^-$ annihilation (0.511 MeV)
$0.841 \pm 0.003$	--	$^{56}\text{Fe}$ (0.847 MeV)
0.937	--	$^{18}\text{F}$ (0.937 MeV)
$\sim 1.020$	--	$^{18}\text{F}$ , $^{58}\text{Co}$ , $^{58}\text{Ni}$ , $^{59}\text{Ni}$ (1.00/4/5/8)
1.234	$3.3 \pm 3.9$	$^{56}\text{Fe}$ (1.238 MeV)
1.317	--	$^{55}\text{Fe}$ (1.317 MeV)
$1.366 \pm 0.003$	$3.0 \pm 1.1$	$^{24}\text{Mg}$ (1.369 MeV)
$1.631 \pm 0.002$	$2.9 \pm 0.6$	$^{20}\text{Ne}$ (1.633 MeV)
1.785	$4.3 \pm 1.5$	$^{28}\text{Si}$ (1.779 MeV)
$2.226 \pm 0.001$	< 1.5	n-capture on H (2.223 MeV)
$3.332 \pm 0.030$	--	$^{20}\text{Ne}$ (3.334 MeV)
$4.429 \pm 0.004$	$3.3 \pm 0.3$	$^{12}\text{C}$ (4.439 MeV)
5.200	--	$^{14}\text{N}$ , $^{15}\text{N}$ , $^{15}\text{O}$
$6.132 \pm 0.005$	$2.6 \pm 0.3$	$^{16}\text{O}$ (6.130 MeV)
6.43	--	$^{11}\text{C}$ (6.337, 6.476 MeV)
$6.983 \pm 0.015$	$4.0 \pm 0.5$	$^{14}\text{N}$ , $^{16}\text{O}$ (7.028, 6919 MeV)

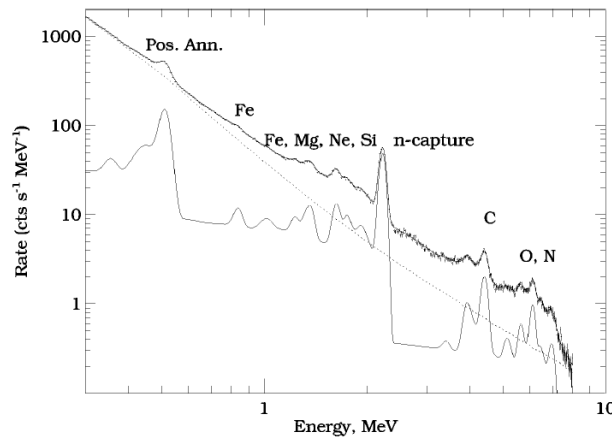
Share 2001

# Solar Flares in Gamma-rays

Solar  $\gamma$ -Ray Physics Comes of Age



## Revealing the Spectrum from Accelerated Heavy Ions



Accelerated heavy ions are excited by interaction with ambient H.

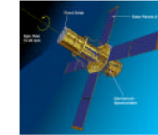
De-excitation lines from these ions are expected to be Doppler broadened by  $\sim 25\%$ .

Broad line spectrum is revealed by subtracting best fitting narrow-line and bremsstrahlung components shown for sum of 19 flares observed by the *SMM*/GRS.

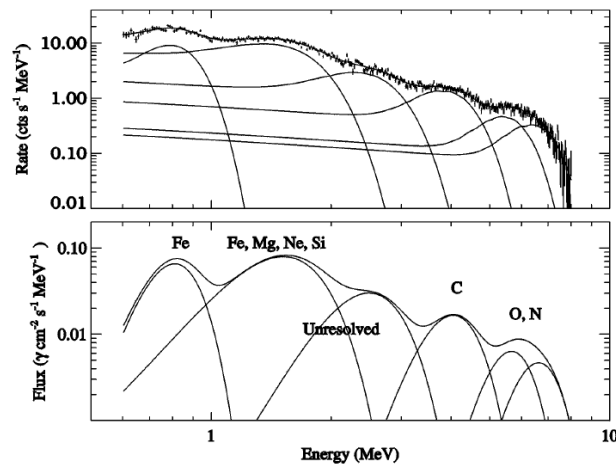
Share 2001

# Solar Flares in Gamma-rays

Solar  $\gamma$ -Ray Physics Comes of Age



## Gamma-Ray Spectrum from Accelerated Heavy Ions



Residual spectrum after subtracting contributions from bremsstrahlung and narrow lines reveals broadened lines from accelerated ions.

Best fit to spectrum contains six Gaussian features that can be identified with different ions.

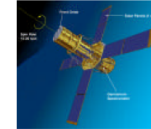
Fe and C are resolved. The Fe, Mg, Ne, and Si lines between 1 - 2 MeV cannot be resolved.

Major uncertainty is the shape of the 'unresolved line' component that is expected to peak in the 1 - 3 MeV region.

Share 2001

# Solar Flares in Gamma-rays

Solar  $\gamma$ -Ray Physics Comes of Age



## Broadened Lines Identified in $\gamma$ -Ray Spectra

Energy, MeV	Width, MeV	Identification	Enhancement	
			$\gamma$ -Rays	SEP's
$0.81 \pm 0.01$	$0.25 \pm 0.02$	$^{56}\text{Fe}$	$7.8 \pm 1.9$	$6.7 \pm 0.8$
$1.52 \pm 0.02$	$0.78 \pm 0.05$	Unresolved, $^{56}\text{Fe}$ , $^{24}\text{Mg}$ , $^{20}\text{Ne}$ , $^{28}\text{Si}$	$2.4 \pm 0.4$	
		$^{24}\text{Mg}$ , $^{20}\text{Ne}$ , $^{28}\text{Si}$		$\sim 2.7$
$2.49 \pm 0.07$	$1.05 \pm 0.17$	Unresolved lines		
$4.04 \pm 0.05$	$1.26 \pm 0.15$	$^{12}\text{C}$	1	1
$5.67 \pm 0.19$	1.5	$^{16}\text{O}$	$0.9 \pm 0.2$	$1.1 \pm 0.1$
$6.63 \pm 0.16$	1.7	$^{14}\text{N}$ , $^{16}\text{O}$	$1.3 \pm 0.4$	

Lines appear to be red-shifted by  $\sim 5 - 9 \%$ .

Lines are broadened by  $\sim 30\%$ .

Some shift and broadening may be due to summing of 19 spectra.

Enhancement ( $\gamma$ -ray) =  $(\text{Fe}_{\text{brd}}/\text{Fe}_{\text{nar}})/(\text{C}_{\text{brd}}/\text{C}_{\text{nar}}) * Z^2/A$ .

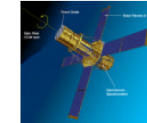
O and Fe enhancements in good agreement with SEPs.

Mg, Si, Ne enhancement is upper limit due to unknown contribution from unresolved lines. This suggests higher temperatures than inferred from SEP's.

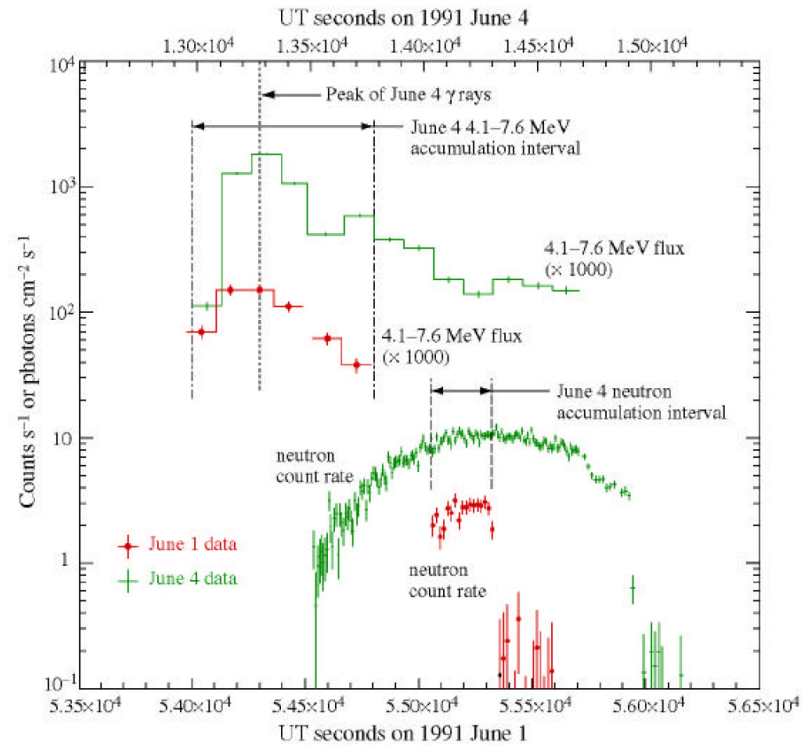
Share 2001

# Solar Flares in Gamma-rays

Solar  $\gamma$ -Ray Physics Comes of Age



$\gamma$  Rays and Neutrons Observed from the 1 & 4 June 1991 Flares

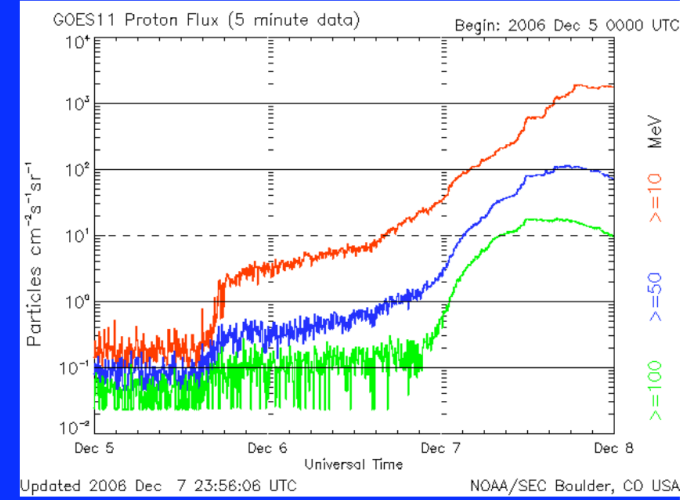
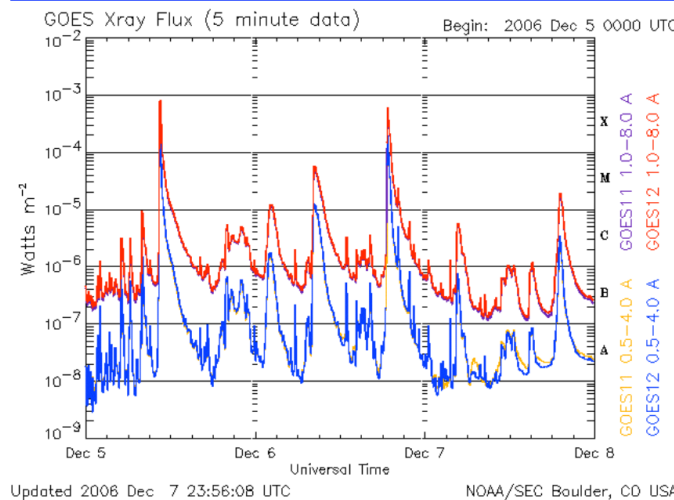


OSSE and GRANAT

Share 2001

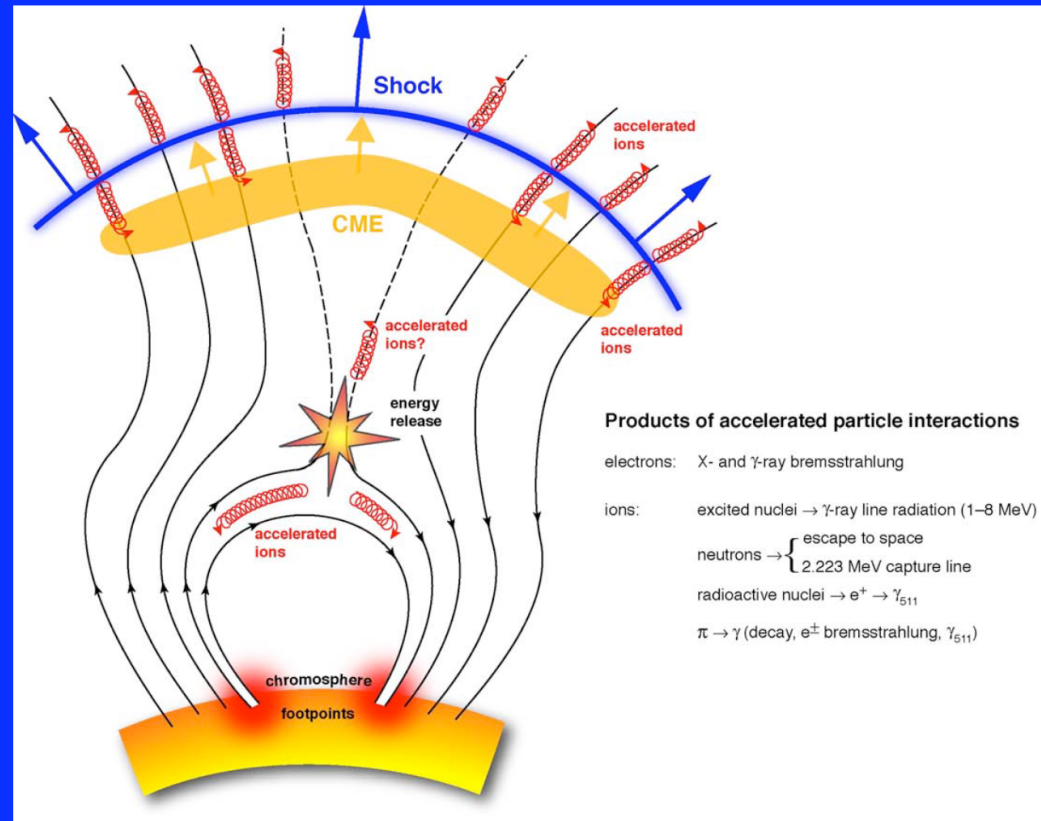
# Solar Flares in Gamma-rays

Surprises though!  
Active regions in January 2005 and December 2006  
produced  
intense X-Class Flares





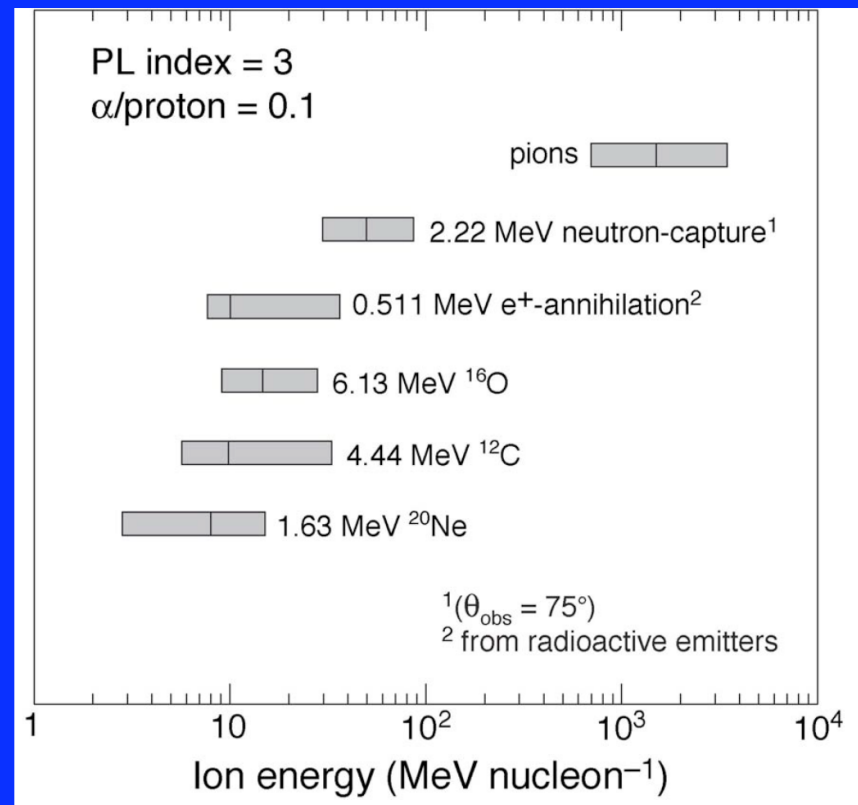
# Solar Flares in Gamma-rays



Study how particles are accelerated at the Sun and their relationship to Solar Energetic Particles (SEP) and Ground Level Events (GLE).

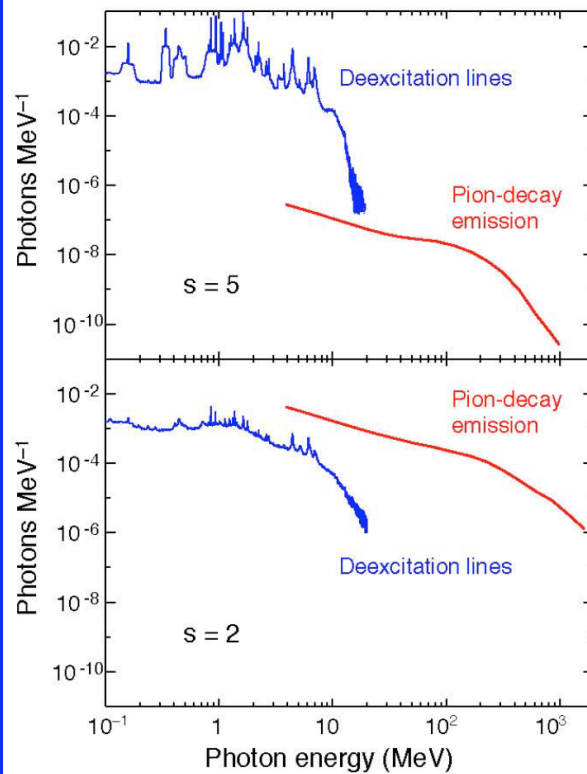
# Solar Flares in Gamma-rays

Measure the spectrum of flare-accelerated ions and electrons to energies  $> 1 \text{ GeV/nuc}$

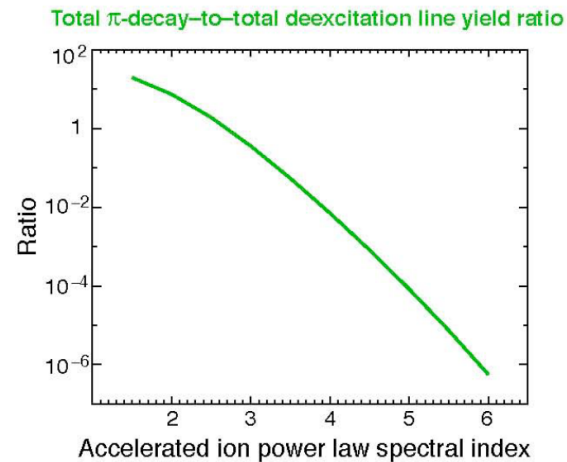


# Solar Flares in Gamma-rays

## Calculated Pion-decay Photon Spectra (cont.)



The ratio of pion-decay emission to nuclear deexcitation-line emission depends very strongly on the steepness of the accelerated-ion kinetic-energy spectrum



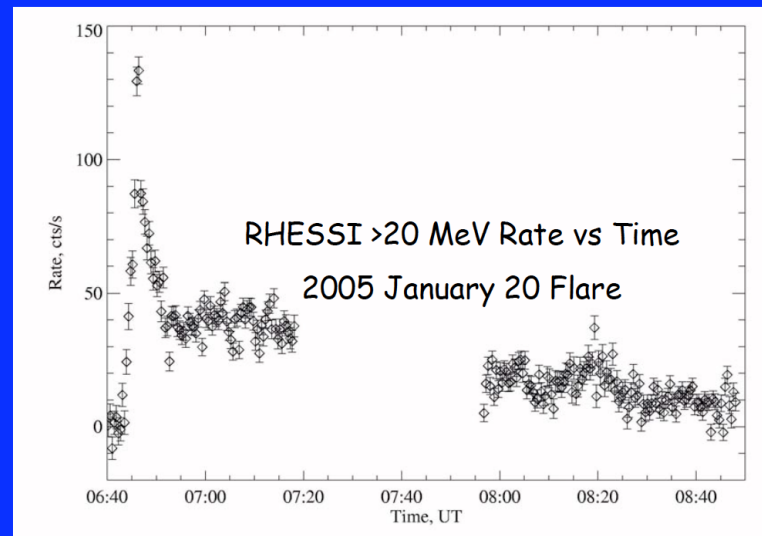
This ratio can be used to determine the accelerated-ion spectral index

Murphy, Poster 16.16

Share 2007

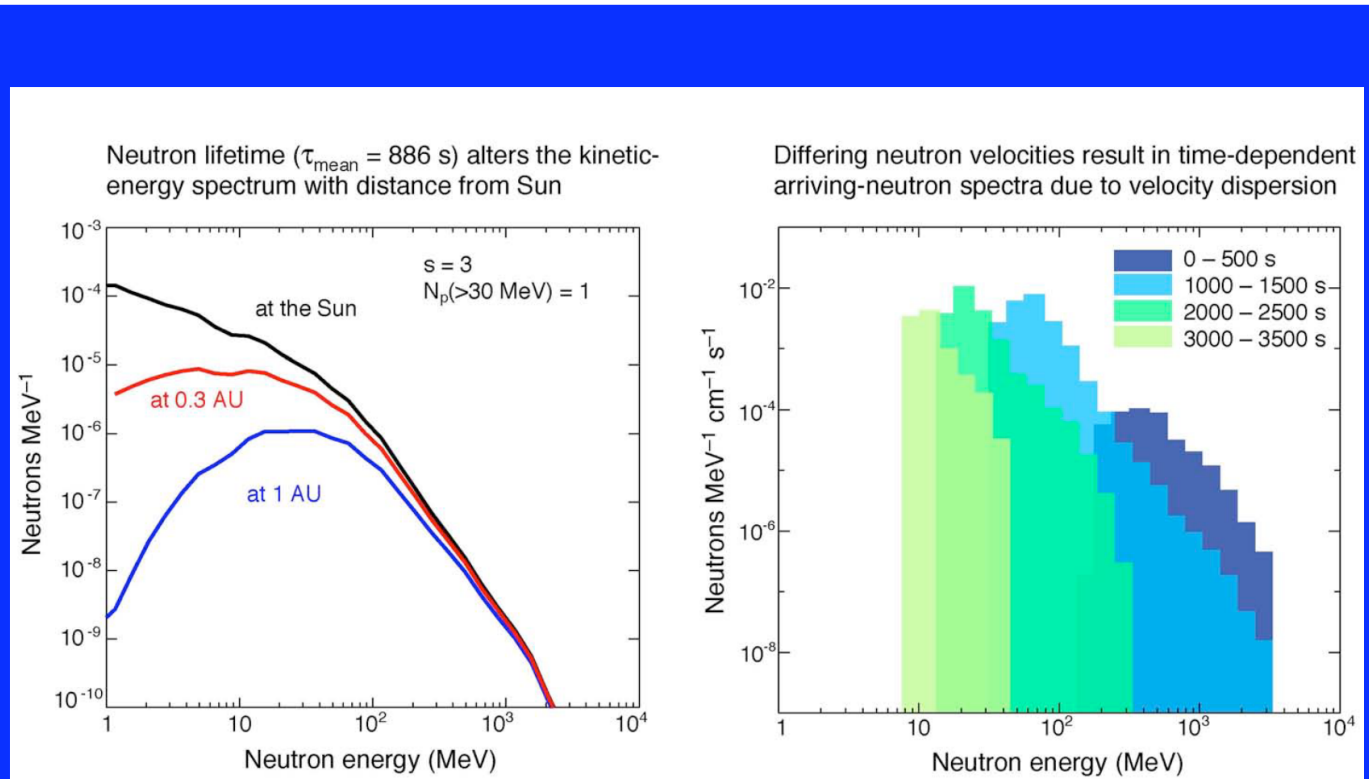
# Solar Flares in Gamma-rays

Study particle acceleration and magnetic trapping of high-energy ions from minutes to hours after flares (e.g. EGRET observation on June 11, 1991; Kanbach et al.)



LAT is  $10^4$  times more sensitive to pion radiation than RHESSI

# Solar Flares in Gamma-rays



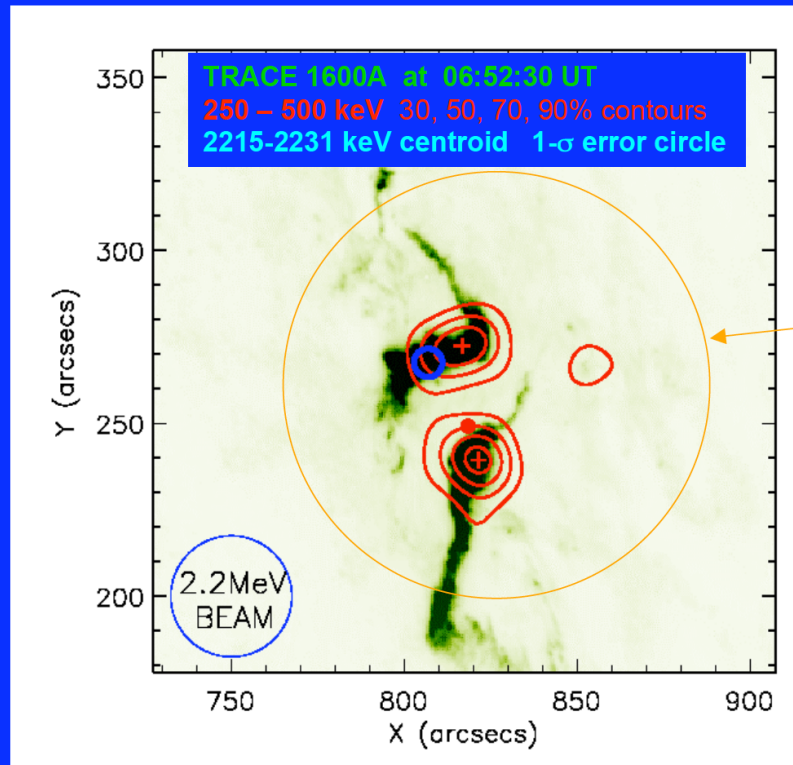
**Murphy, Poster 16.16**

**GBM will also detect an increase  
minutes after the impulsive phase of  
the flare.**

# Solar Flares in Gamma-rays

20 January 2005 06:44-06:56

RHESSI,  
Hurford et  
al. 2007



GLAST  
Location

Localize the source of  $>1$  GeV photons to  $\sim 30$  arc sec

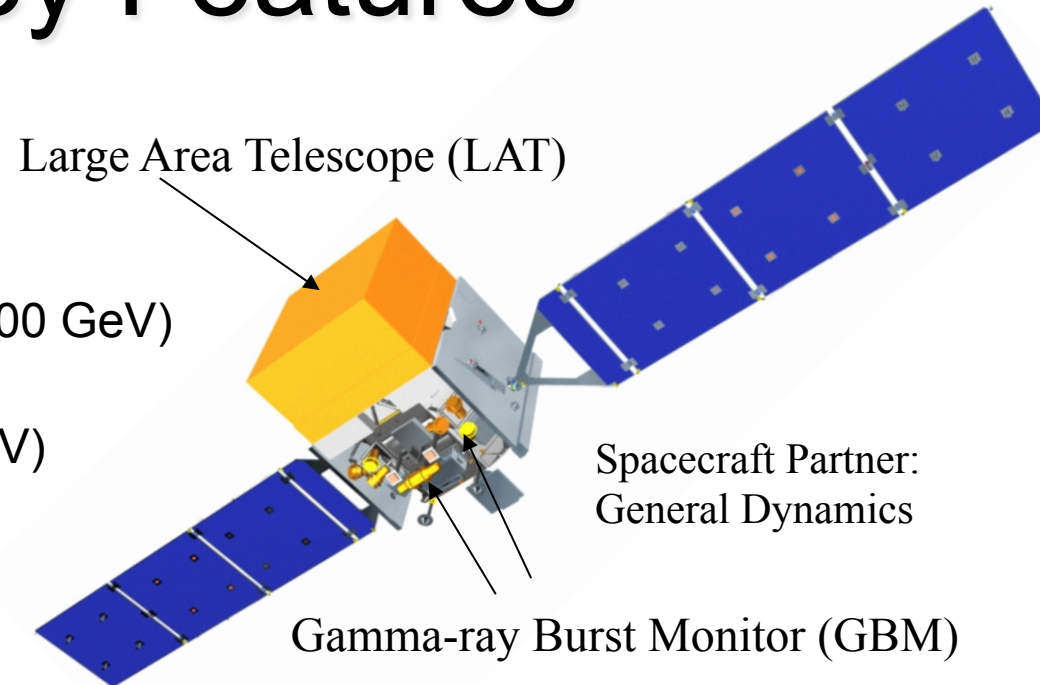
Share 2007

Astrofisica Nucleare e Subnucleare  
Laboratory for Gamma Astrophysics - 1

# Fermi Key Features

- Two instruments:

- LAT:
  - high energy (20 MeV – >300 GeV)
- GBM:
  - low energy (8 keV – 40 MeV)

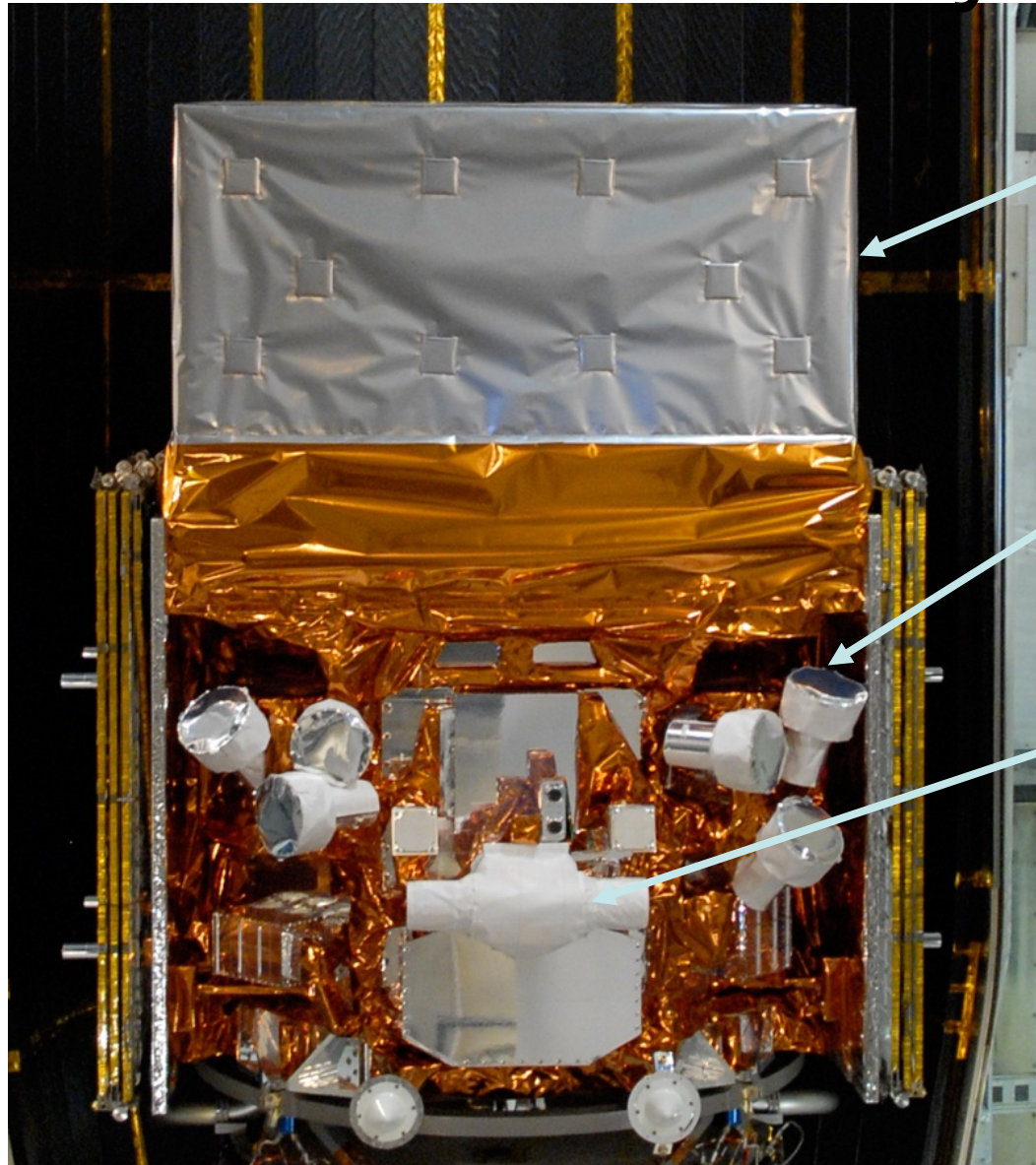


- Huge field of view

- LAT: 20% of the sky at any instant; in sky survey mode, expose all parts of sky for ~30 minutes every 3 hours. GBM: whole unocculted sky at any time.



# The Observatory



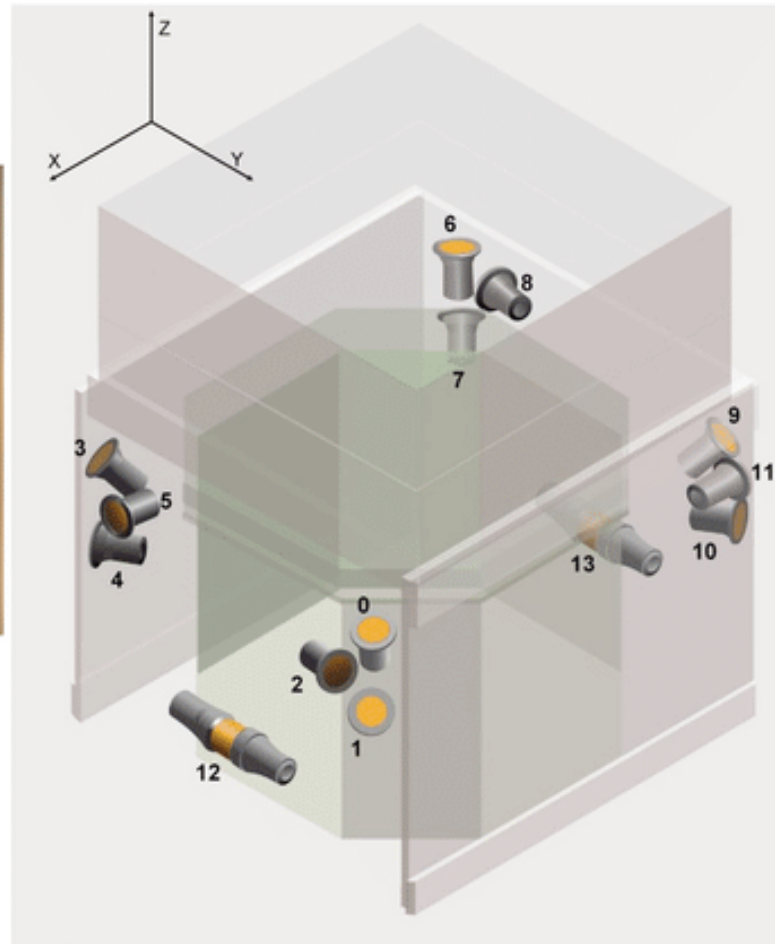
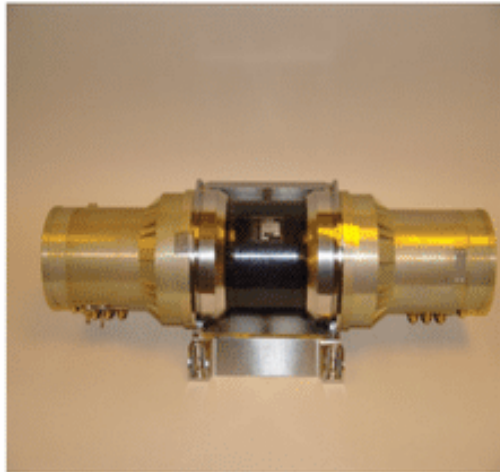
LAT

GBM  
NaI  
Detector

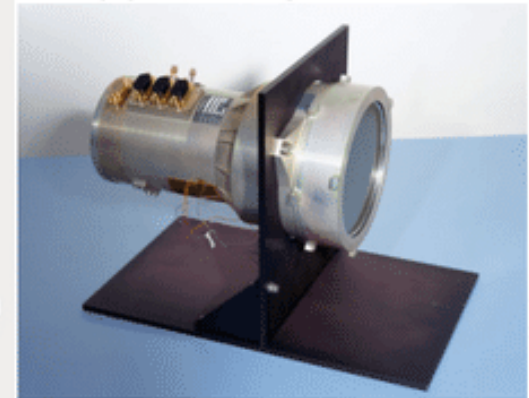
GBM  
BGO  
Detector

# Fermi/GBM detector (2008 -- ..)

BGO detector unit



Nal(Tl)-detector flight unit



# Fermi Data

## Data

- ▶ [Data Policy](#)
- ▶ [Data Access](#)
  - + [LAT Data](#)
  - + [LAT Catalog](#)
  - + [LAT Data Queries](#)
  - + [LAT Query Results](#)
  - + [LAT Weekly Files](#)
  - + [GBM Data](#)
- ▶ [Data Analysis](#)
- ▶ [Caveats](#)
- ▶ [Newsletters](#)
- ▶ [FAQ](#)

## GBM Data Products

This page lists the science data products created by the GIOC (GBM Instrument Operations Center) and provided to the FSSC.

### GBM Daily, Trigger, and Burst Data

The GBM daily, trigger, and burst data are available through the searchable interface of the HEASARC's [Browse system](#) or directly via the FTP site. See below for descriptions of the data products provided.

- [GBM Browse Tables](#)
  - [Daily Data](#)
  - [Trigger Data](#)
  - [Burst Data](#)
- [FSSC's FTP Site](#)
  - [Daily Data](#)
  - [Trigger Data](#)
  - [Burst Data](#)

<https://fermi.gsfc.nasa.gov/ssc/data/access/gbm/>

# Fermi Data

ID	Name	Description
GS-001	CTIME (daily version)	The counts accumulated every 0.256 seconds in 8 energy channels for each of the 14 detectors.
GS-002	CSPEC (daily version)	The counts accumulated every 8.192 seconds in 128 energy channels for each of the 14 detectors.
GS-003	TTE (continuous version)	Event data for each detector with a time precise to 2 microseconds, in 128 energy channels. The downlink schedule determines how many data files are produced each day. These files are being replaced by the GS-013 hourly TTE files.
GS-005	GBM gain and energy resolution history	History of the detector gains and energy resolutions; required for calculating Detector Response Matrices (DRMs).
GS-006	Fermi position and attitude history	History of Fermi's position and attitude, required for calculating DRMs.
GS-013	TTE (hourly version)	Time tagged events for each detector which occurred during the hour (including up to the last 120 seconds of events from the previous hour) with a time precise to 2 microseconds, in 128 energy channels.

<https://fermi.gsfc.nasa.gov/ssc/data/access/gbm/>

# Fermi Data

ID	Name	Description
GS-101	CTIME (burst version)	For each detector, the counts accumulated every 0.064 s in 8 energy channels
GS-102	CSPEC (burst version)	For each detector, the counts accumulated every 1024 s in 128 energy channels.
GS-103	GBM TTE (burst version)	Event data for the burst. There is one file for each detector.
GS-104	GBM DRMs	8 and 128 energy channel Detector Response Matrices (DRMs) for all 14 detectors. These files may not be produced for all triggers.
GS-105	GBM Trigger Catalog Entry	Classification of GBM trigger with some characteristics (e.g., trigger time, coordinates). This file is used to create the <a href="#">GBM Trigger Catalog</a> .
GS-107	GBM TRIGDAT	All the GBM's messages downlinked through TDRSS. These messages are the basis of the GCN Notices for the burst.
	Quicklook Plots	Lightcurves and spacecraft pointing history files in GIF and PDF format.

<https://fermi.gsfc.nasa.gov/ssc/data/access/gbm/>

# Quick Look

[Browse this table...](#)

## FERMIGBRST - Fermi GBM Burst Catalog

[HEASARC Archive](#)

### Overview

When referencing results from this online catalog, please cite [von Kienlin, A. et al. 2020](#), [Gruber, D. et al. 2014](#), [von Kienlin, A. et al. 2014](#), and [Bhat, P. et al. 2016](#).

This table lists all of the triggers observed by a subset of the 14 GBM detectors (12 NaI and 2 BGO) which have been classified as gamma-ray bursts (GRBs). Note that there are two Browse catalogs resulting from GBM triggers. All GBM triggers are entered in the [Fermi GBM Trigger Catalog](#), while only those triggers classified as bursts are entered in the Burst Catalog. Thus, a burst will be found in both the Trigger and Burst Catalogs. The Burst Catalog analysis requires human intervention; therefore, GRBs will be entered in the Trigger Catalog before the Burst Catalog. The latency requirements are 1 day for triggers and 3 days for bursts. There are four fewer bursts in the online catalog than in the Gruber et al. 2014 paper. The four missing events (081007224, 091013989, 091022752, and 091208623) have not been classified with certainty as GRBs and are not included in the general GRB catalog. This classification may be revised at a later stage.

The GBM consists of an array of 12 sodium iodide (NaI) detectors which cover the lower end of the energy range up to 1 MeV. The GBM triggers off of the rates in the NaI detectors, with some Terrestrial Gamma-ray Flash (TGF)-specific algorithms using the bismuth germanate (BGO) detectors, sensitive to higher energies, up to 40 MeV. The NaI detectors are placed around the Fermi spacecraft with different orientations to provide the required sensitivity and FOV. The cosine-like angular response of the thin NaI detectors is used to localize burst sources by comparing rates from detectors with different viewing angles. The two BGO detectors are placed on opposite sides of the spacecraft so that all sky positions are visible to at least one BGO detector.

The signals from all 14 GBM detectors are collected by a central Data Processing Unit (DPU). This unit digitizes and time-tags the detectors' pulse height signals, packages the resulting data into several different types for transmission to the ground (via the Fermi spacecraft), and performs various data processing tasks such as autonomous burst triggering.

The GRB science products are transmitted to the FSSC in two types of files. The first file, called the "beat" file, provides basic burst parameters such as duration, peak flux and fluence, calculated from 8-channel data using a spectral model which has a power-law in energy that falls exponentially above an energy  $E_{\text{Peak}}$ , known as the Comptonized model. The crude 8-channel binning and the simple spectral model allow data fits in batch mode over numerous time bins in an efficient and robust fashion, including intervals with little or no flux, yielding both values for the burst duration, and deconvolved lightcurves for the detectors included in the fit. The beat file includes two extensions. The first, containing detailed information about energy channels and detectors used in the calculations, is detector-specific, and includes the time history of the deconvolved flux over the time intervals of the burst. The second shows the evolution of the spectral parameters obtained in a joint fit of the included detectors for the model used, usually the Comptonized model described above. The beat files and their time-varying quantities contained in these two extensions are available at the HEASARC FTP site. Quantities derived from these batch fits are given in the beat primary header and presented in the Browse table, as described below. The main purpose of the analysis contained in the beat file is to produce a measure of the duration of the burst after deconvolving the instrument response. The duration quantities are:

- \* 't50' - the time taken to accumulate 50% of the burst fluence starting at the 25% fluence level.
- \* 't90' - the time taken to accumulate 90% of the burst fluence starting at the 5% fluence level.

By-products of this analysis include fluxes on various timescales and fluences, both obtained using the simple Comptonized model described above. These quantities are detailed in the Browse table using the following prefixes:

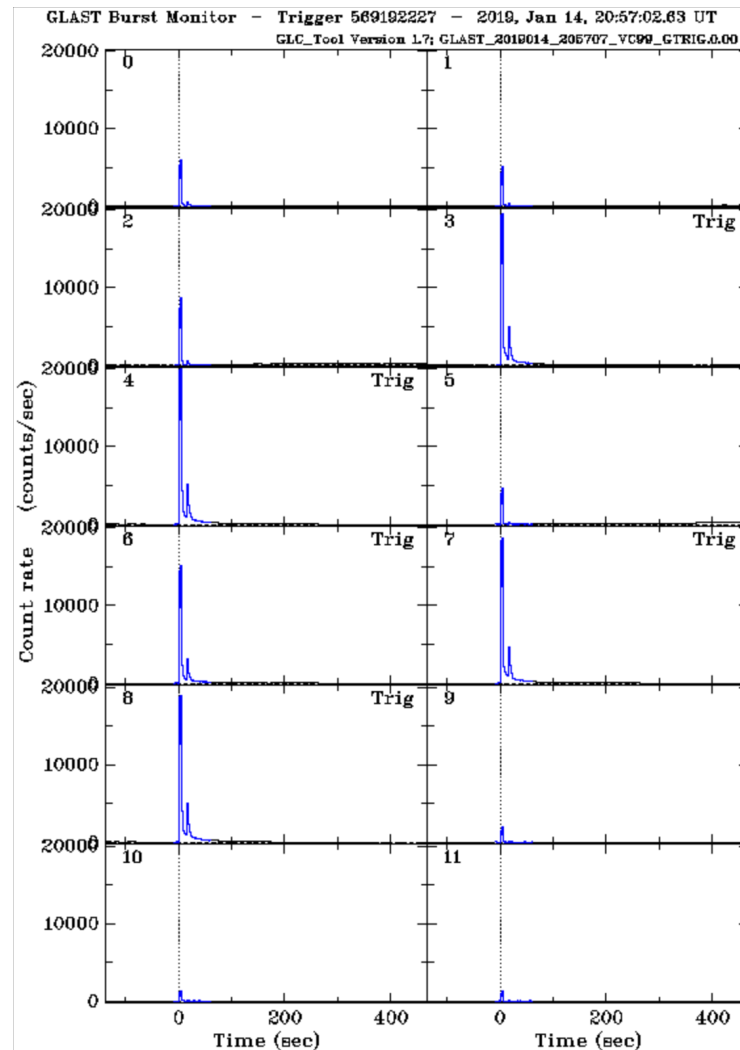
- \* 'flux' - the peak flux over 3 different timescales obtained in the batch mode fit used to calculate t50/t90.
- \* 'fluence' - the total fluence accumulated in the t50/t90 calculation.

The fluxes and fluences derived from the 8-channel data for these beat files should be considered less reliable than those in the spectral analysis files described below.

<https://heasarc.gsfc.nasa.gov/W3Browse/all/fermigbrst.html>

# Quick Look

<https://heasarc.gsfc.nasa.gov/W3Browse/all/fermigbrst.html>



# gtburst analysis

## Data

▶ [Data Policy](#)

▶ [Data Access](#)

▶ [Data Analysis](#)

- + [System Overview](#)
- + [Software Download](#)
- + [Documentation](#)
- + [Cicerone](#)
- + [Analysis Threads](#)
- + [User Contributions](#)

▶ [Caveats](#)

▶ [Newsletters](#)

▶ [FAQ](#)

## GTBURST

This tutorial provides a step-by-step guide to using the gtburst GUI for GRB and solar flare analysis of GBM and LAT data. You can also watch a [video tutorial](#)

### What it is used for?

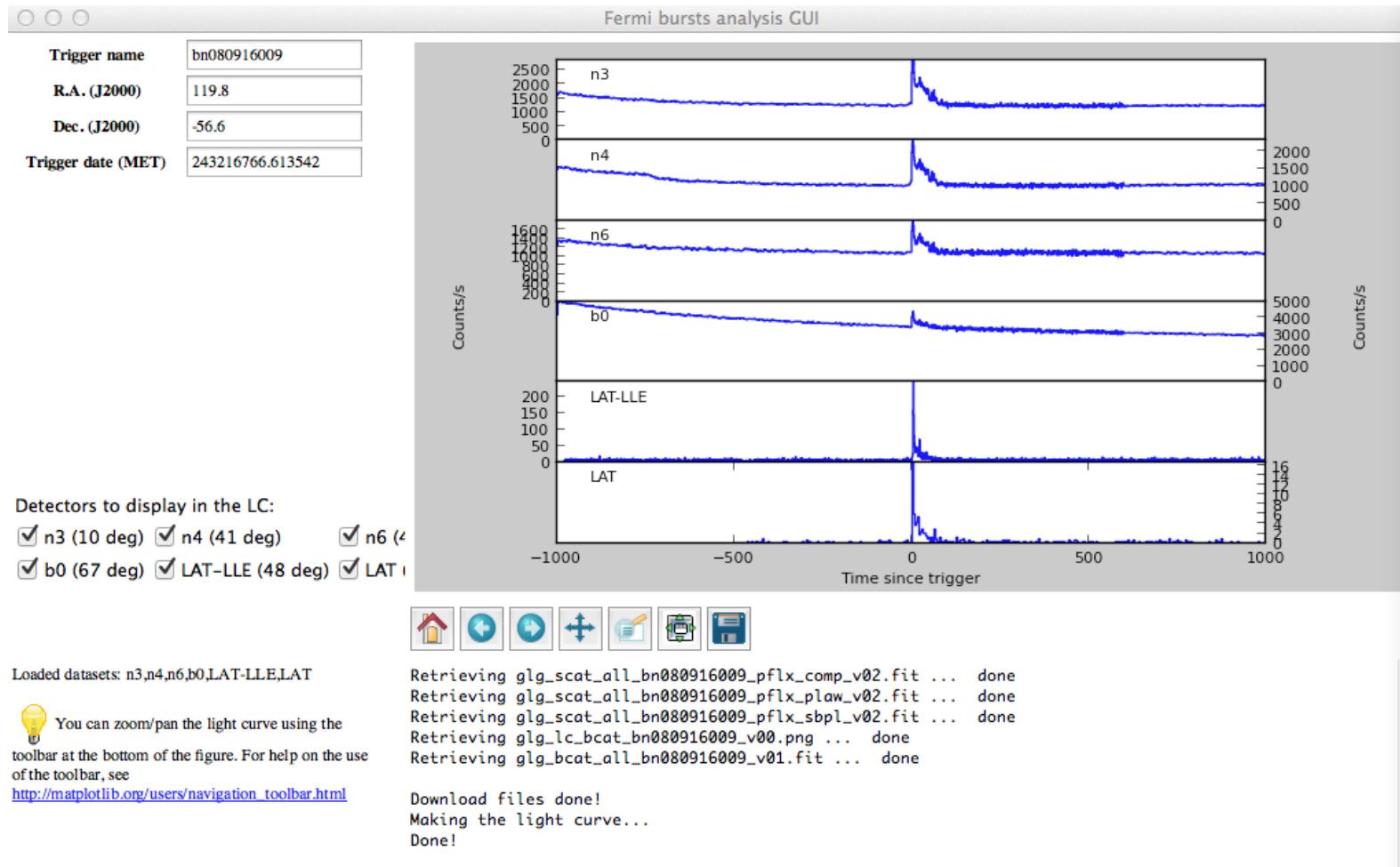
Gtburst can be used to do the following:

- **GBM data:**
  - [download data from the GBM Trigger catalog](#), select data analysis interval, and interactively fit the background
  - write out pha and rsp files for spectral analysis in either XSPEC or RMFIT
- **LLE data:**
  - download data from the Fermi [LAT Low-Energy Events Catalog](#), select data analysis interval, and interactively fit the background
  - write out pha and rsp files for spectral analysis in either XSPEC or RMFIT
- **LAT data:**
  - download photon events and spacecraft data from the [LAT Data server](#)
  - produce navigation plots to allow user to select optimal time intervals and zenith cuts
  - do photon selections based on energy, Region Of Interest (ROI), time, zenith, event class
  - produce counts maps
  - do likelihood analysis given a simple spectral model and background models
  - localization using gtfndsrc or a TS map
  - writes out pha and rsp files for spectral analysis in either XSPEC or RMFIT

<https://fermi.gsfc.nasa.gov/ssc/data/analysis/scitools/gtburst.html>

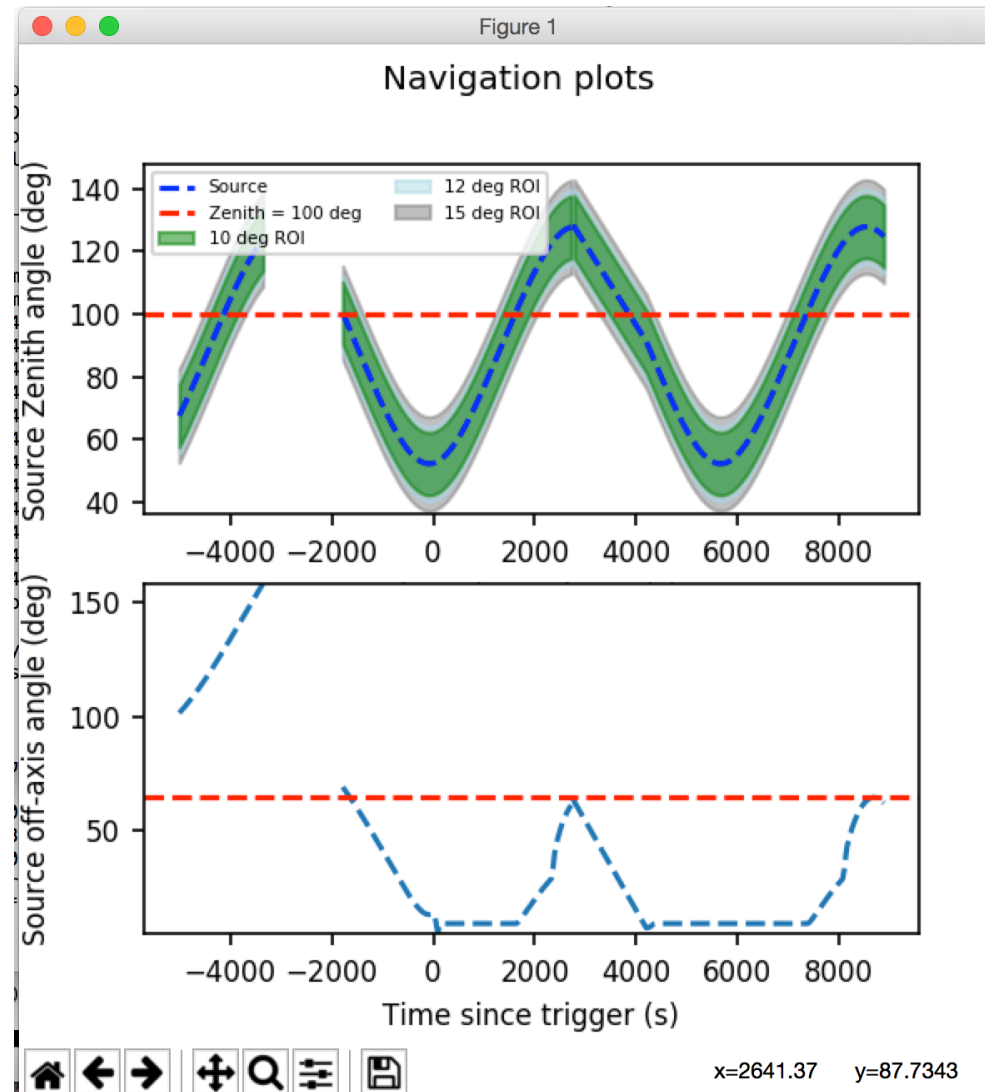


# gtburst analysis



<https://fermi.gsfc.nasa.gov/ssc/data/analysis/scitools/gtburst.html>

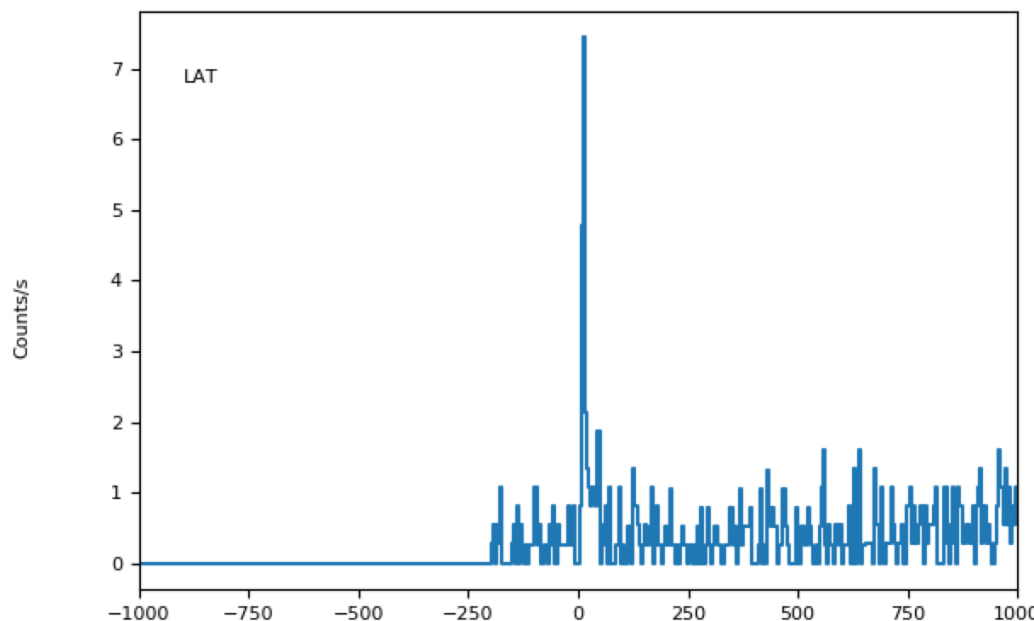
# Check the “Navigation” plot



# GRB analysis with gtburst

Fermi bursts analysis GUI

Trigger name	bn160905471
R.A. (J2000)	162.245
Dec. (J2000)	-50.801
Trigger date (MET)	494767139.912



Counts/s


LAT


Counts/s

Detectors to display in the LC:

- LAT (16 deg)

Loaded datasets: LAT

 You can zoom/pan the light curve using the toolbar at the bottom of the figure. For help on the use of the toolbar, see [http://matplotlib.org/users/navigation\\_toolbar.html](http://matplotlib.org/users/navigation_toolbar.html)



```
done.  
  
* Updating keywords in the headers of the CSPEC file...  
  
done.  
  
gtllebin done!  
Making the light curve...  
Done!
```

# RMFIT analysis

## Data

- ▶ [Data Policy](#)
- ▶ [Data Access](#)
- ▶ [Data Analysis](#)
  - + [System Overview](#)
  - + [Software Download](#)
  - + [Documentation](#)
  - + [Cicerone](#)
  - + [Analysis Threads](#)
  - + [User Contributions](#)
- ▶ [Caveats](#)
- ▶ [Newsletters](#)
- ▶ [FAQ](#)

## GBM Data Extraction and Gamma-Ray Burst Analysis

This section provides the information needed to obtain the GBM data as well as a step-by-step example of extracting and modeling a GBM Gamma-Ray Burst observation and fitting the data using the Gamma-Ray Spectral Fitting Package (RMFIT).

### Prerequisites

- RMFIT, used as a spectral analysis tool starting in Step 2 of this procedure. (See [Installing the GBM rmfFit Tool.](#))

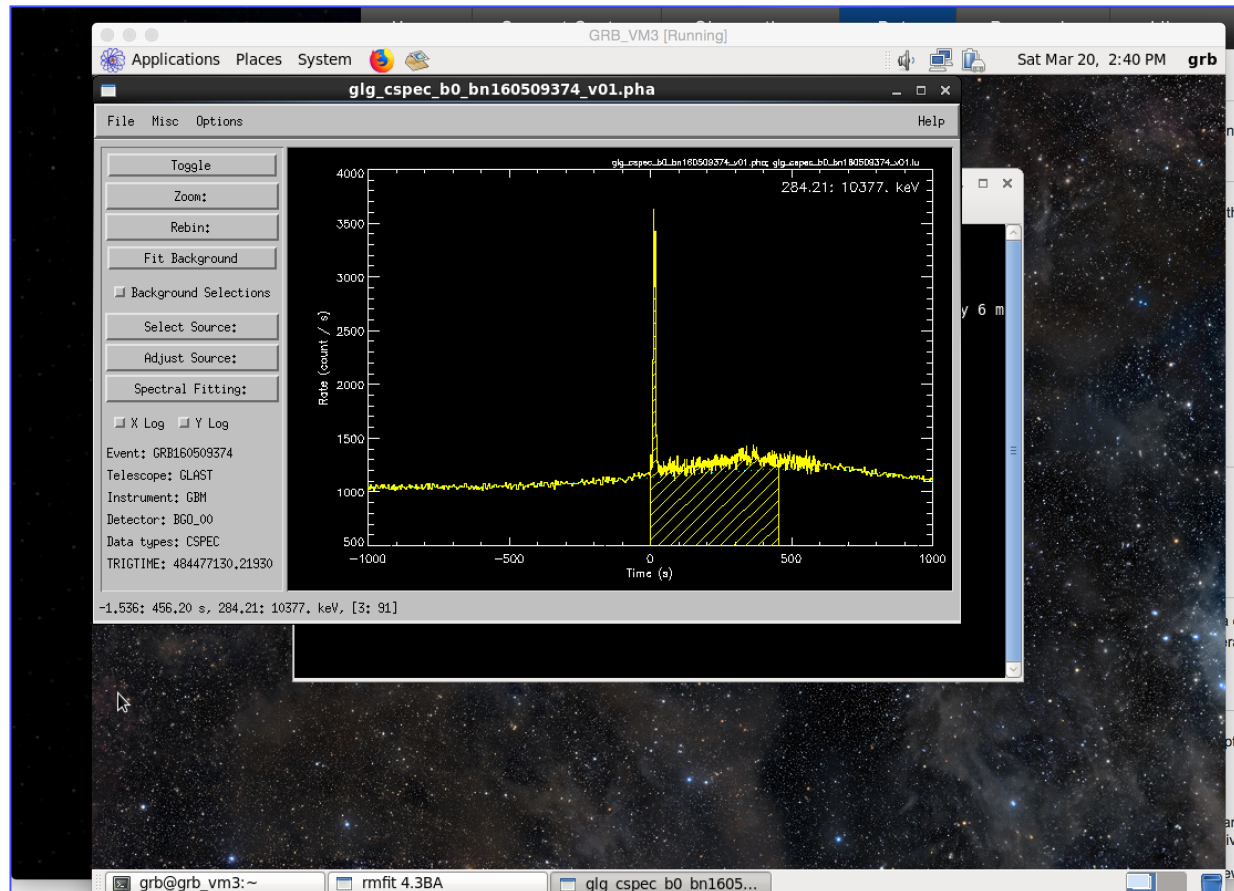
### Assumptions

It is assumed that:

- You are in your work directory.
  - Note:** For the purposes of this thread, the relevant burst properties are:
    - T0 = 00:12:45.614 UT, 16 September 2008, corresponding to 243216766.614 seconds (MET)
    - Trigger # 243216766
    - RA = 121.8 degrees (= 08h 07m 12s)
    - Dec = -61.3 degrees (= -61d 18m 00s)
- You have extracted the files used in this tutorial; these files can be found [here](#). Alternatively, you could download the GBM data for 080916C as explained below.
- For analyzing GBM data, an alternative to RMFIT is XSPEC (see [Xanadu Data Analysis for X-Ray Astronomy](#)). The standard XSPEC analysis approach assumes that the background is approximately constant through the burst prompt emission and/or is negligible when compared to the burst emission. That is, this approximation is a valid in particular for bright and/or short bursts. RMFIT incorporates an interactive time-domain background fitting capability, and in comparison with XSPEC can thus produce significantly different results.

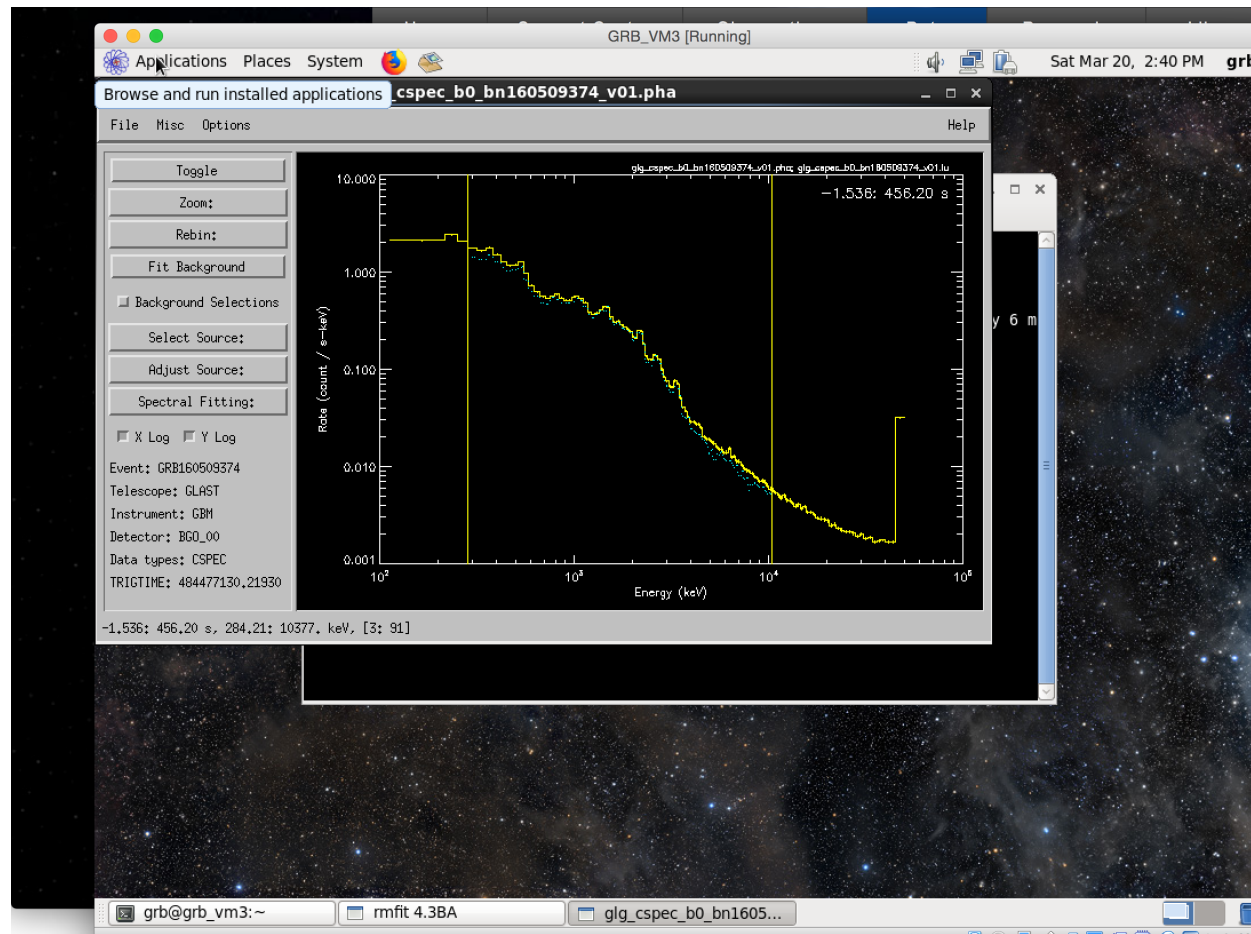
[https://fermi.gsfc.nasa.gov/ssc/data/analysis/scitools/rmfFit\\_tutorial.html](https://fermi.gsfc.nasa.gov/ssc/data/analysis/scitools/rmfFit_tutorial.html)

# RMFIT analysis



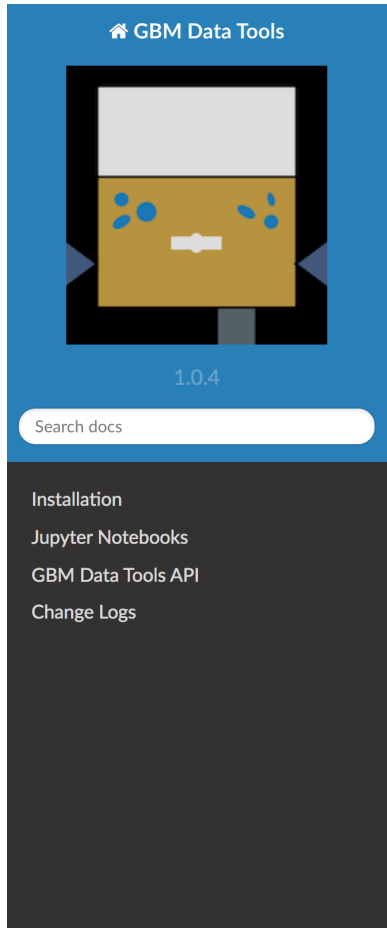
[https://fermi.gsfc.nasa.gov/ssc/data/analysis/scitools/rmfit\\_tutorial.html](https://fermi.gsfc.nasa.gov/ssc/data/analysis/scitools/rmfit_tutorial.html)

# RMFIT analysis



[https://fermi.gsfc.nasa.gov/ssc/data/analysis/scitools/rmfit\\_tutorial.html](https://fermi.gsfc.nasa.gov/ssc/data/analysis/scitools/rmfit_tutorial.html)

# GBMDataTools analysis



GBM Data Tools

1.0.4

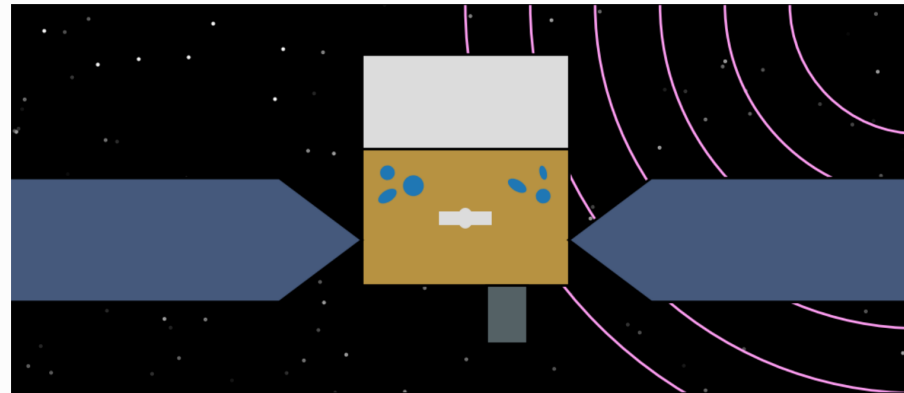
Search docs

- Installation
- Jupyter Notebooks
- GBM Data Tools API
- Change Logs

[Docs](#) » Welcome to the Fermi GBM Data Tools documentation!

[View page source](#)

## Welcome to the Fermi GBM Data Tools documentation!



*Hello, I'm Fermi. Pleased to meet you!*

The Fermi GBM Data Tools is an Application Programming Interface (API) for GBM data. The fundamental purpose of the Data Tools is to allow general users to incorporate GBM analysis into their scripts and workflows without having to sweat very many details. To this end, the Data Tools have a fairly high-level API layer allowing a user to read, reduce, and visualize GBM data with only a few lines of code. For expert users, and users who want fine control over various aspects of their analysis, the Data Tools exposes a lower-level API layer, which can also be used to generalize the GBM Data Tools to data from other like instruments.

[https://fermi.gsfc.nasa.gov/ssc/data/analysis/gbm/gbm\\_data\\_tools/gdt-docs/](https://fermi.gsfc.nasa.gov/ssc/data/analysis/gbm/gbm_data_tools/gdt-docs/)

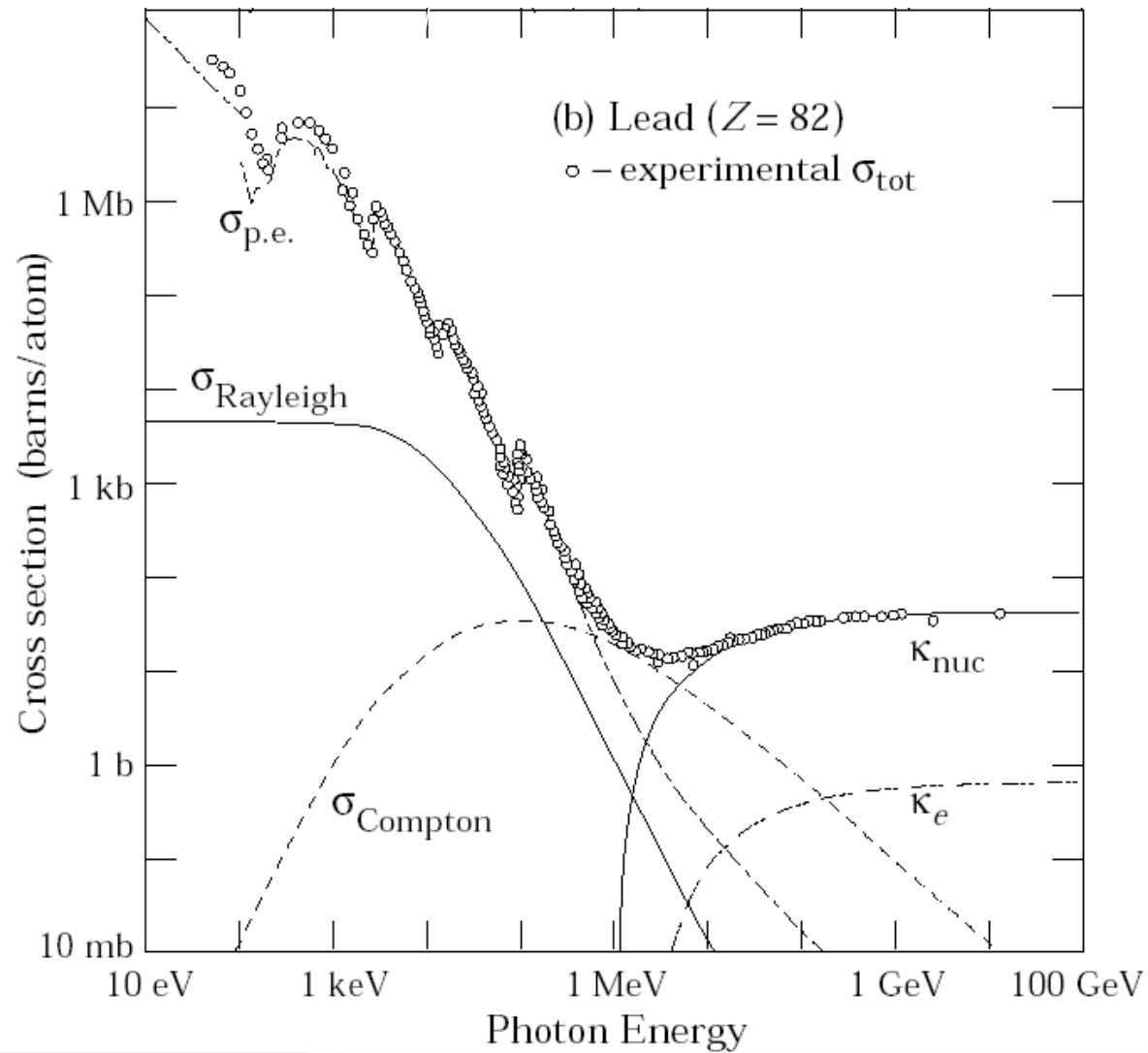
Astrofisica Nucleare e Subnucleare  
GeV Astrophysics



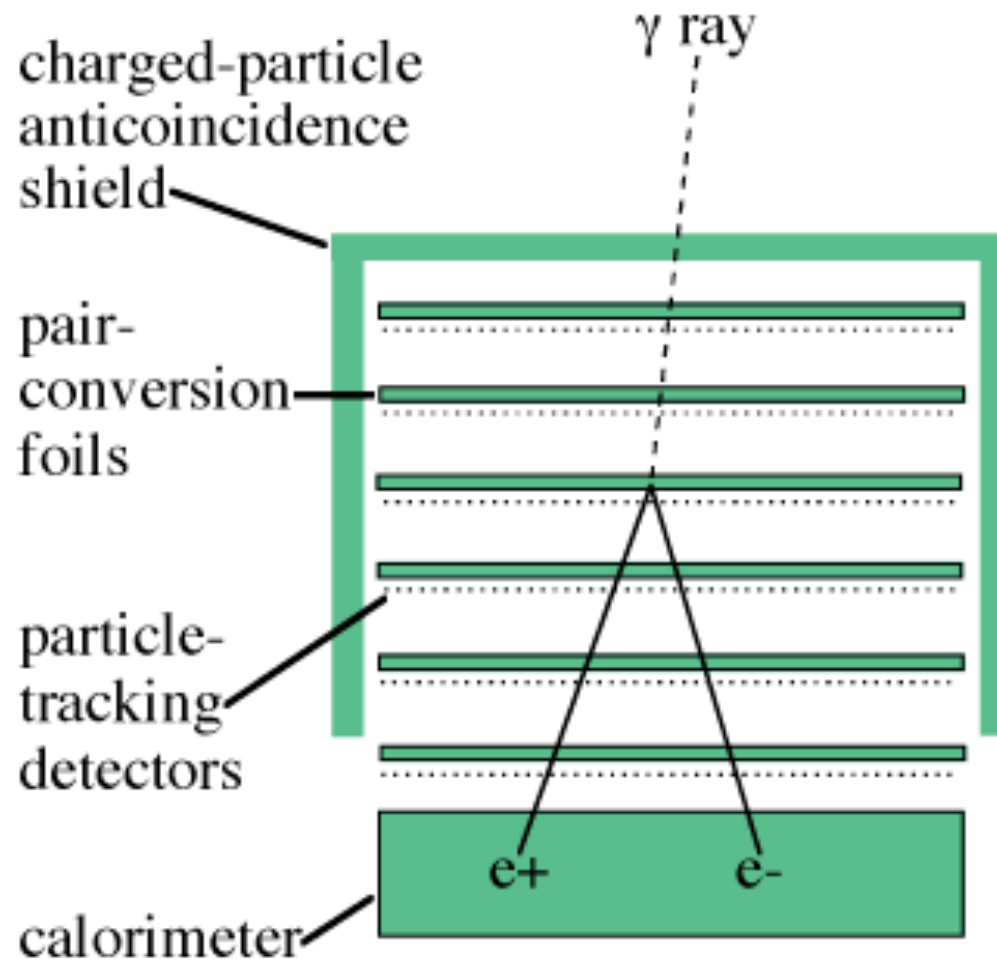
# Exercise #4

- Find the web sites of AGILE and Fermi/LAT
- Check the status of future gamma-ray detectors (CALET, DAMPE, Gamma-400(?), HERD)

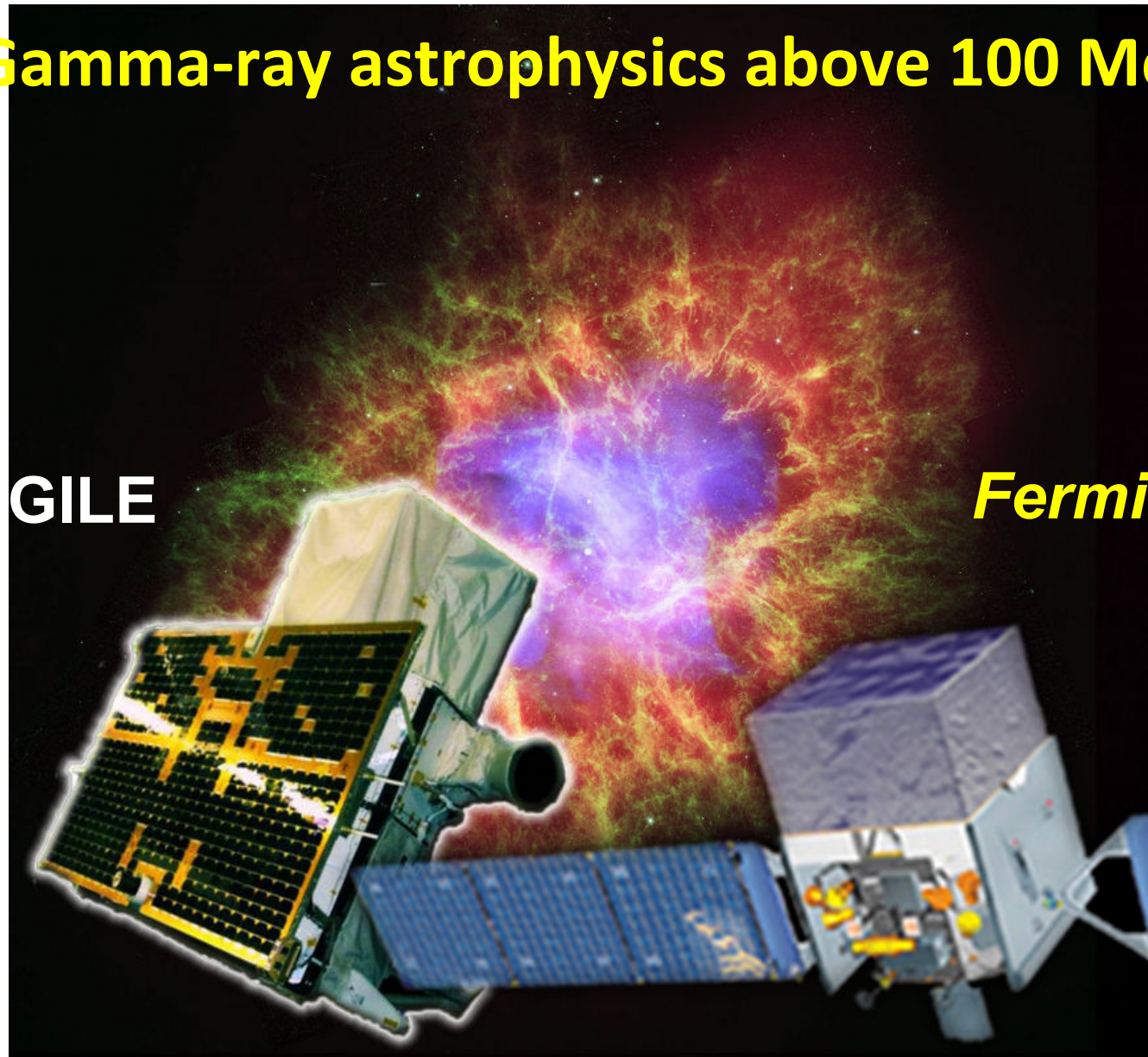
# Photon Interactions



# Detector Project



# Gamma-ray astrophysics above 100 MeV

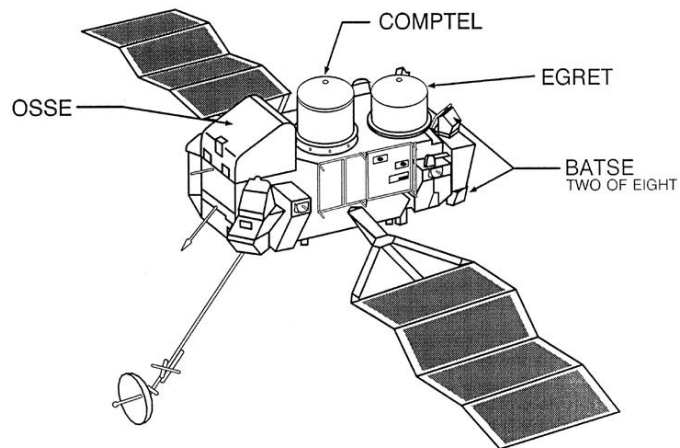


# HE Gamma-ray Astrophysics

## The EGRET legacy

# EGRET

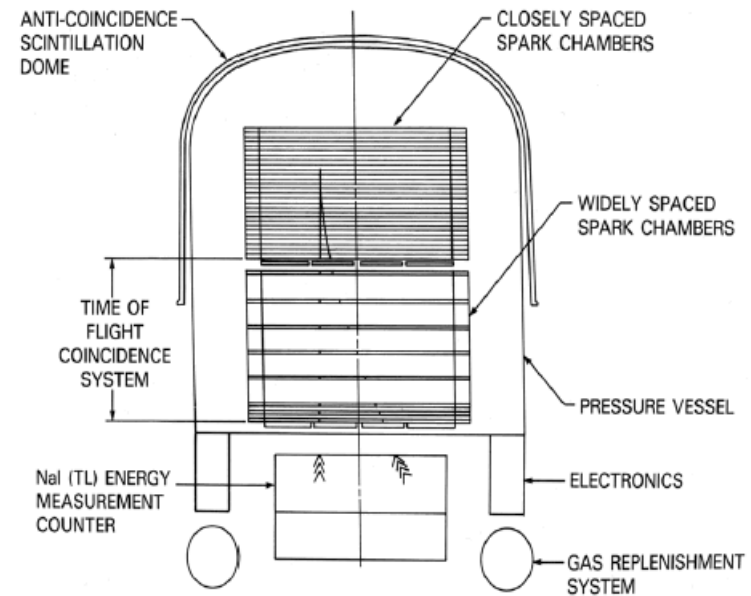
## COMPTON OBSERVATORY INSTRUMENTS



The Instruments on CGRO Cover Six Orders of Magnitude in Photon Energy



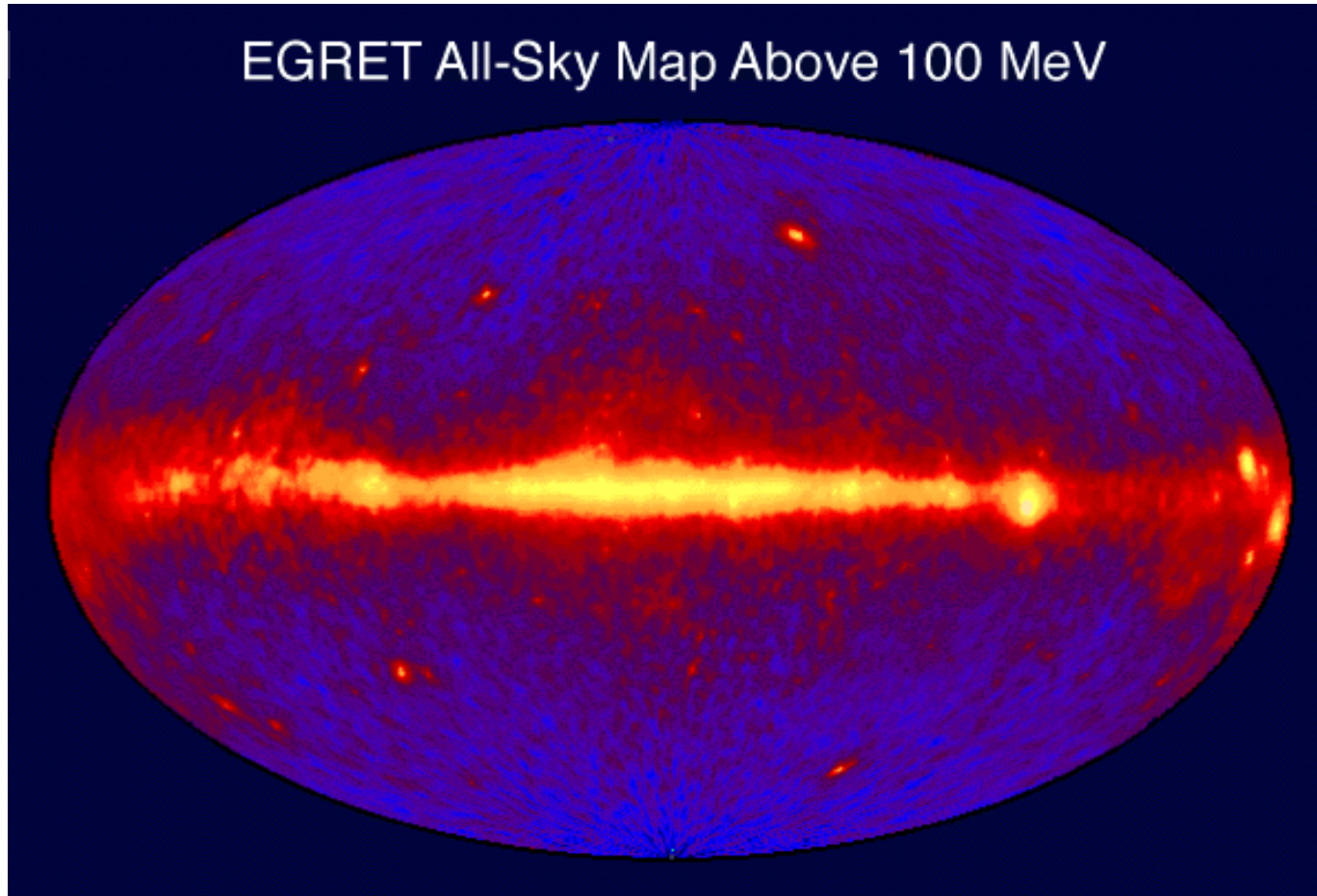
10 keV 100 keV 1 MeV 10 MeV 100 MeV 1 GeV 10 GeV 100 GeV



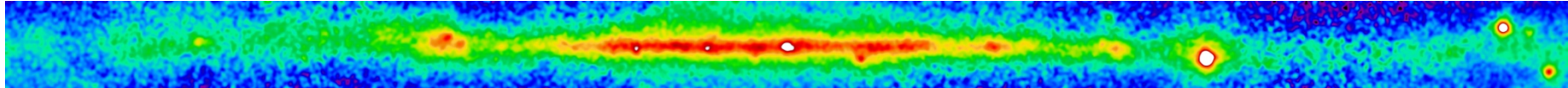
## EGRET

- 1991-2000
- 30 MeV - 30 GeV
- AGN, GRB, Unidentified Sources, Diffuse Bkg

# The HE sky from EGRET



# Analysis Topics

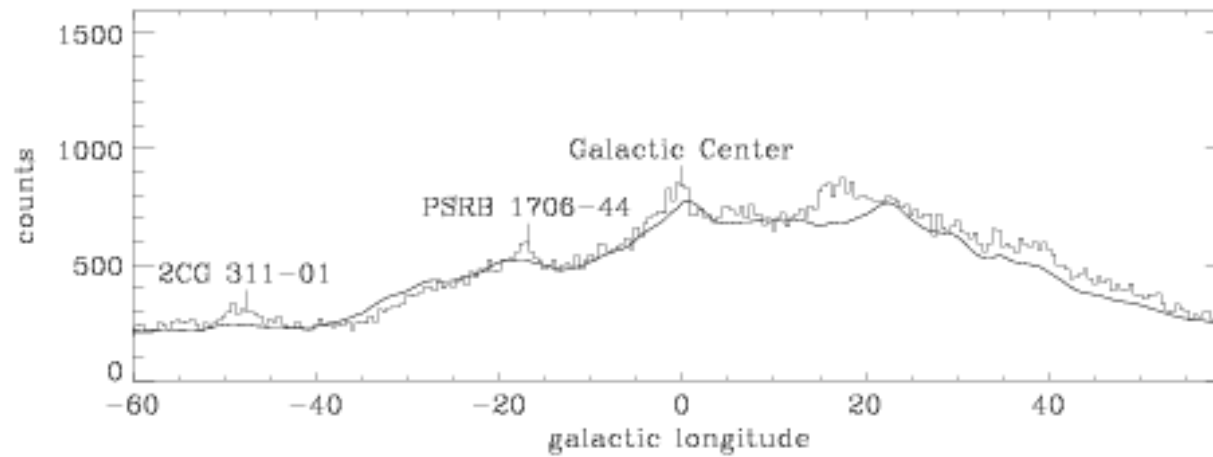
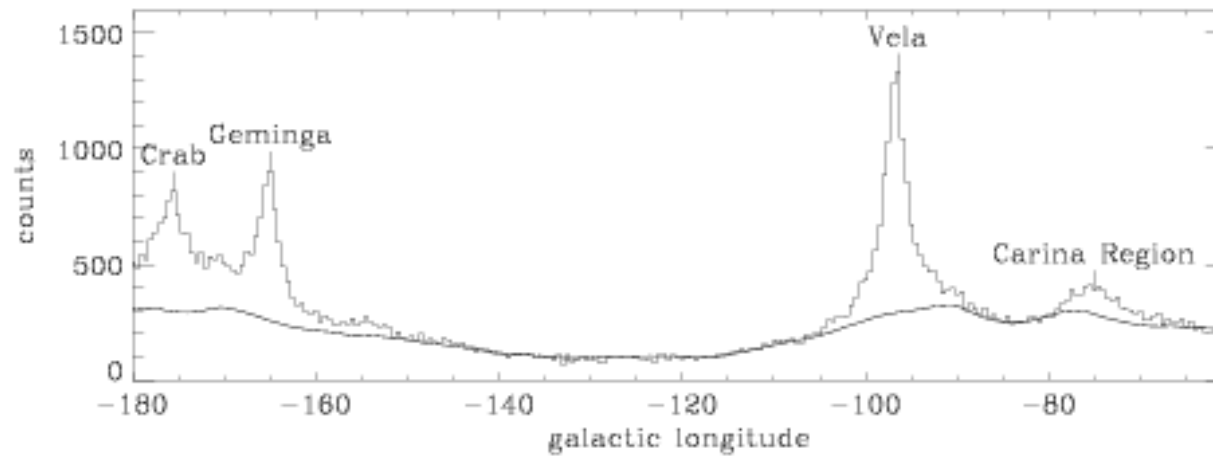


EGRET >300 MeV

- First a word about interstellar gamma-ray emission:
- Brightest at low latitudes, but detectable over the whole sky
- >60% of EGRET celestial gamma rays
- It fundamentally affects the approach to the analysis

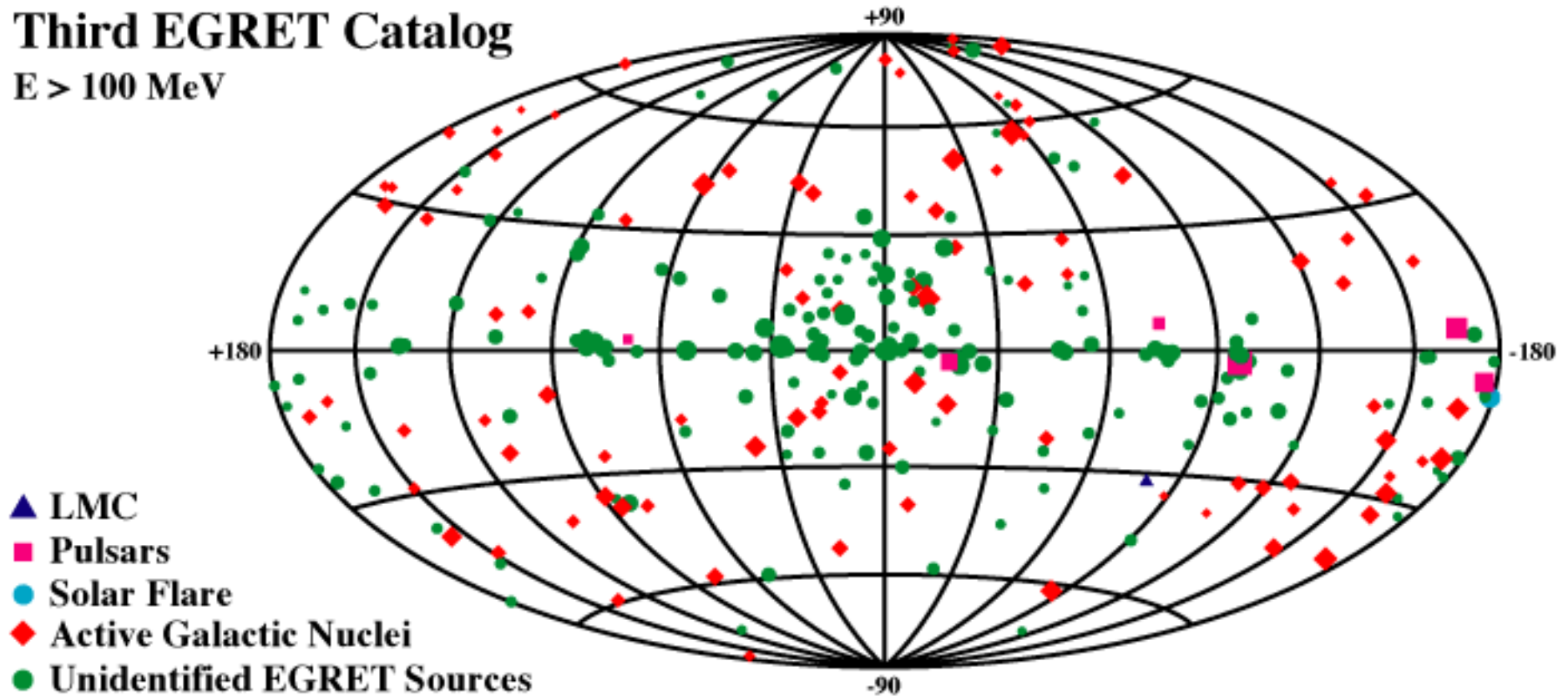


# Data Analysis



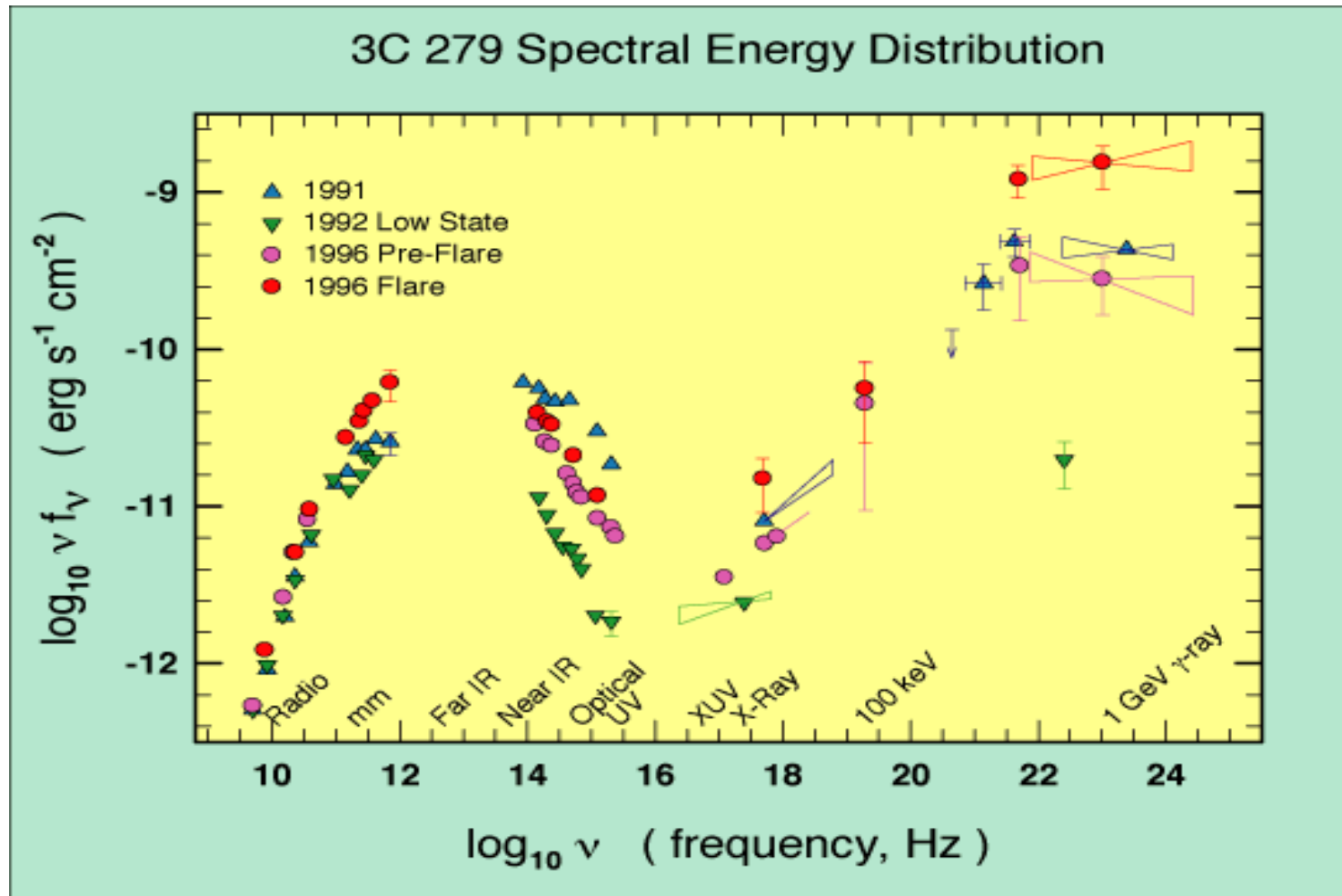
# EGRET Gamma-ray Sources

**Third EGRET Catalog**  
 $E > 100 \text{ MeV}$

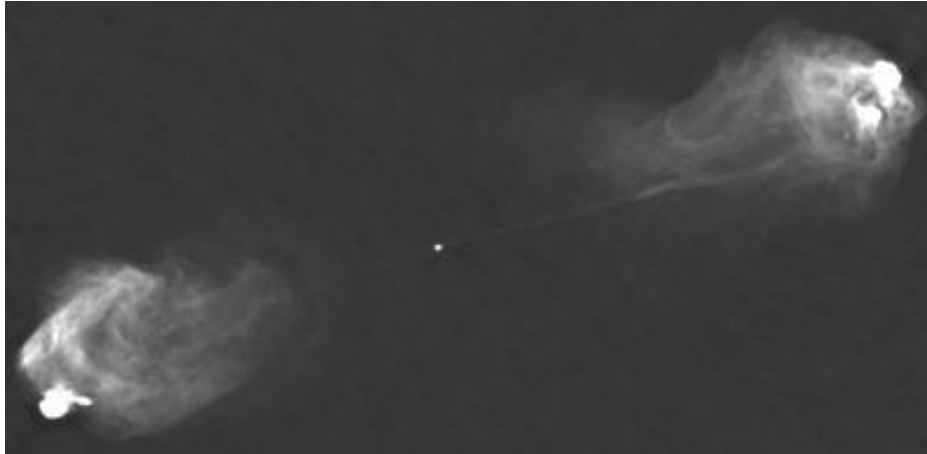


# Challenge # 1

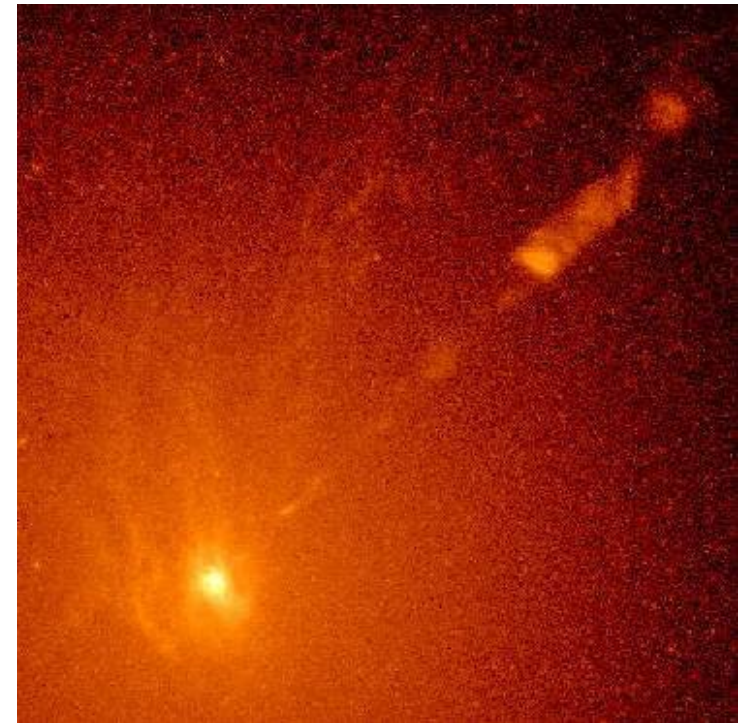
- Need simultaneous multiwavelength data to study variability and emission processes



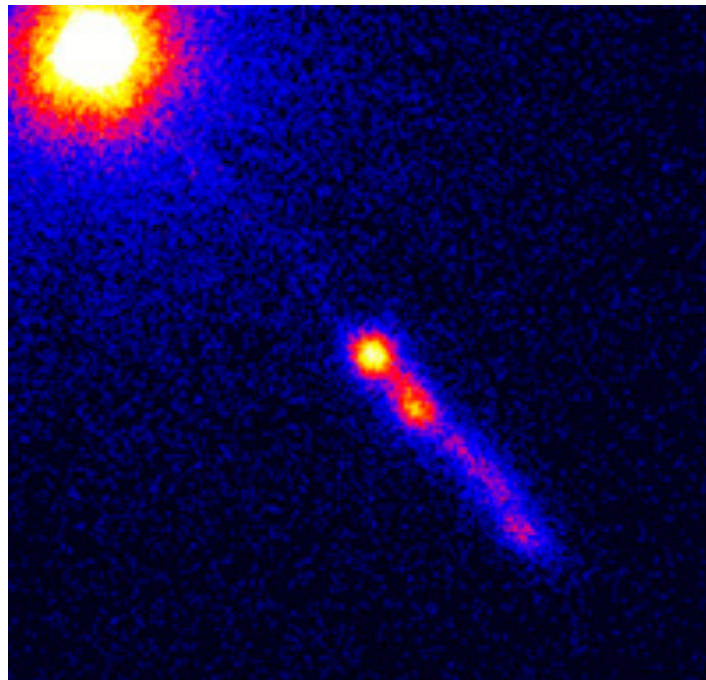
# Active Galactic Nuclei



Radio

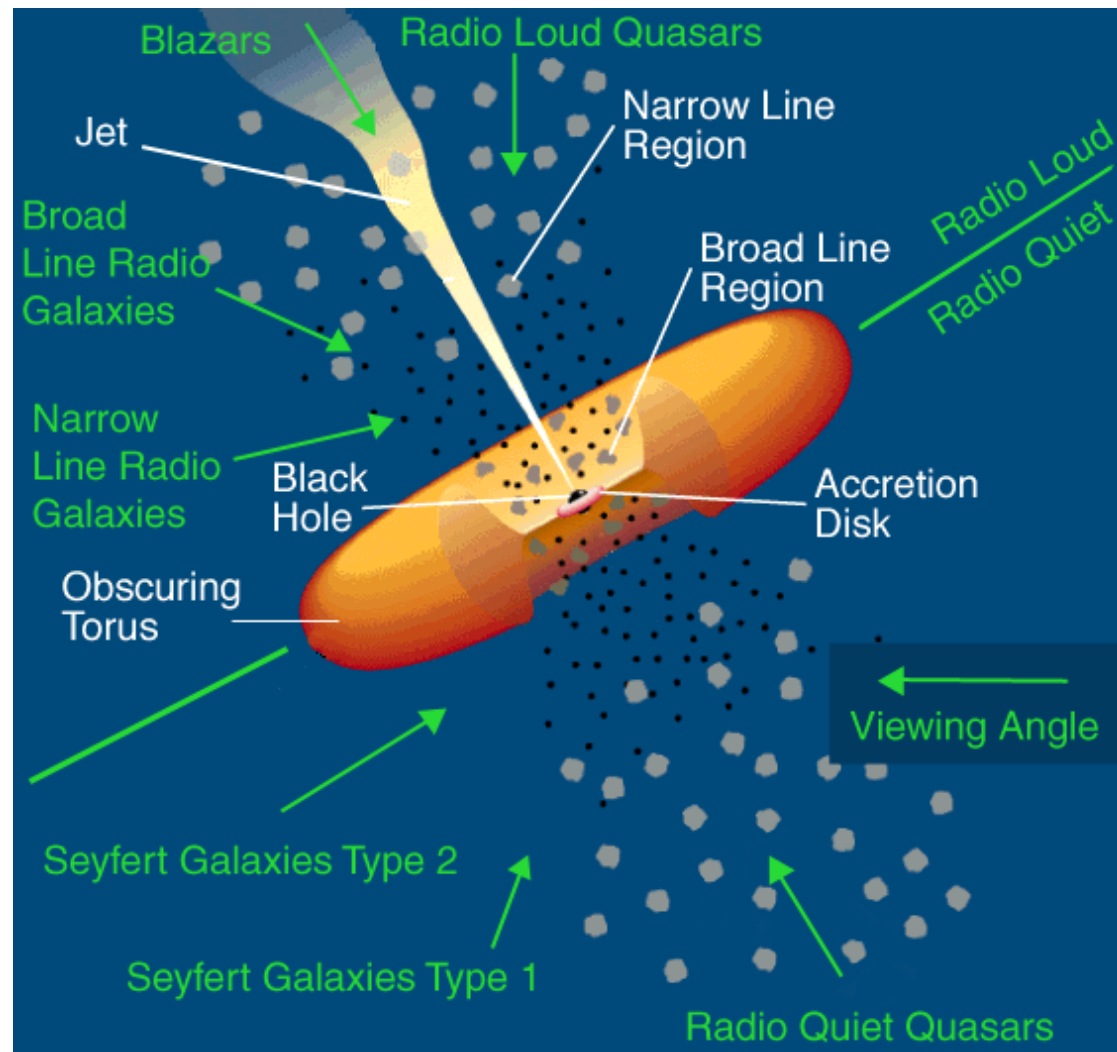


Optical

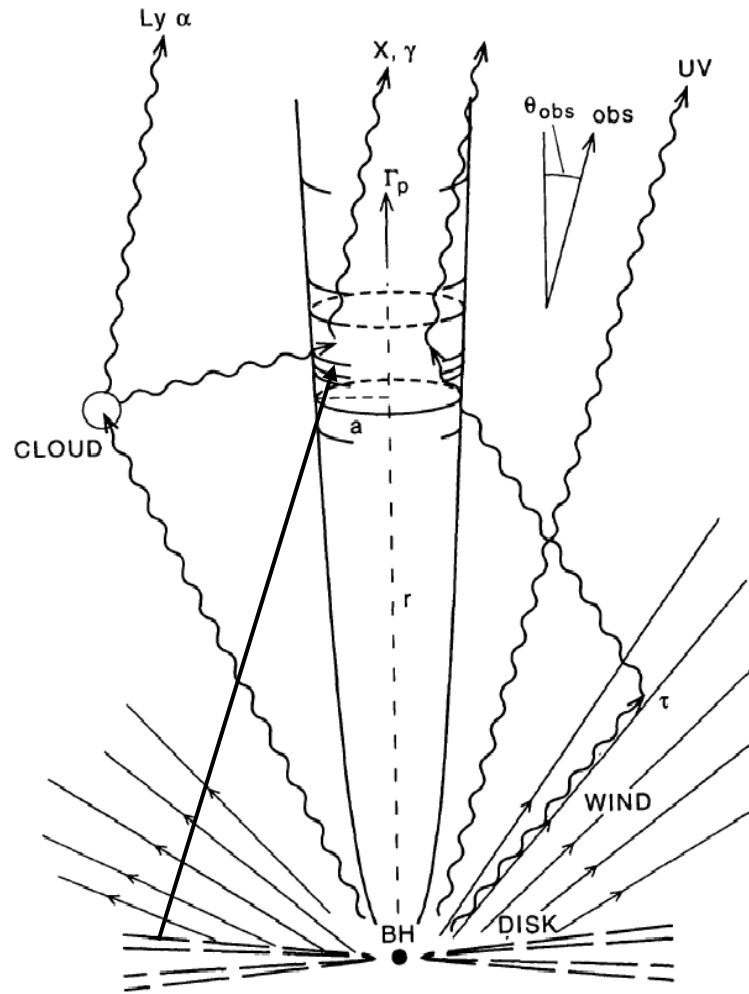


X-ray

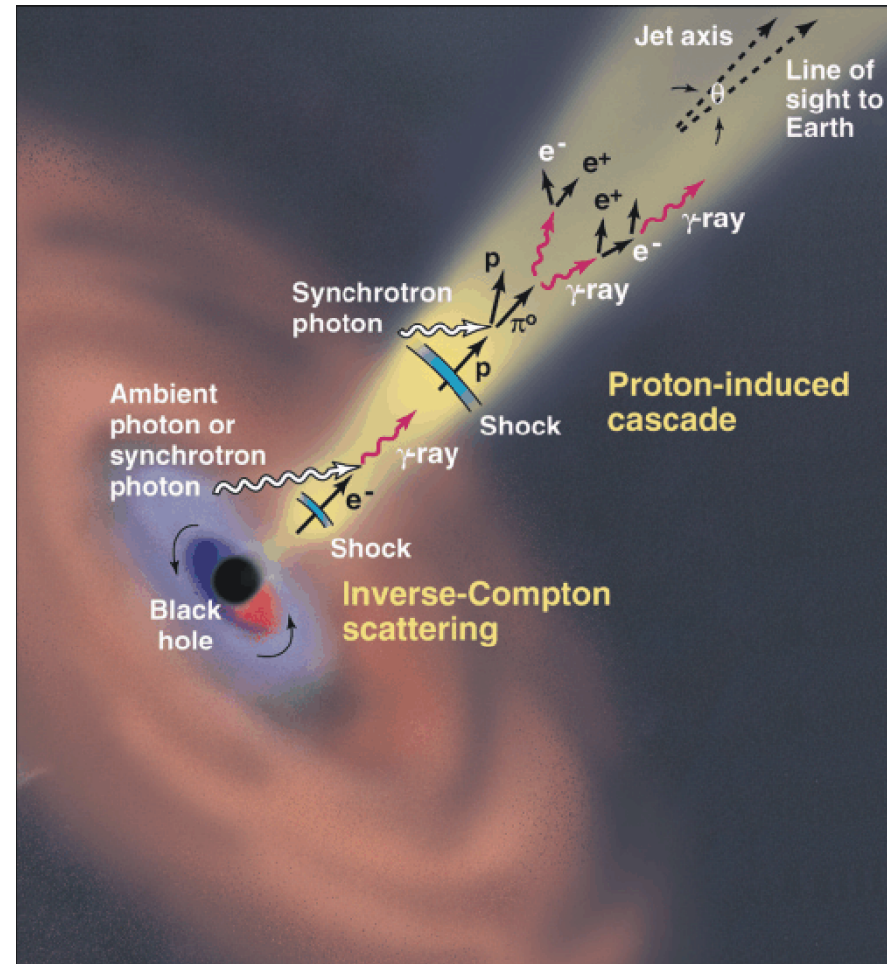
# Active Galactic Nuclei



# Models of AGN Gamma-ray Production

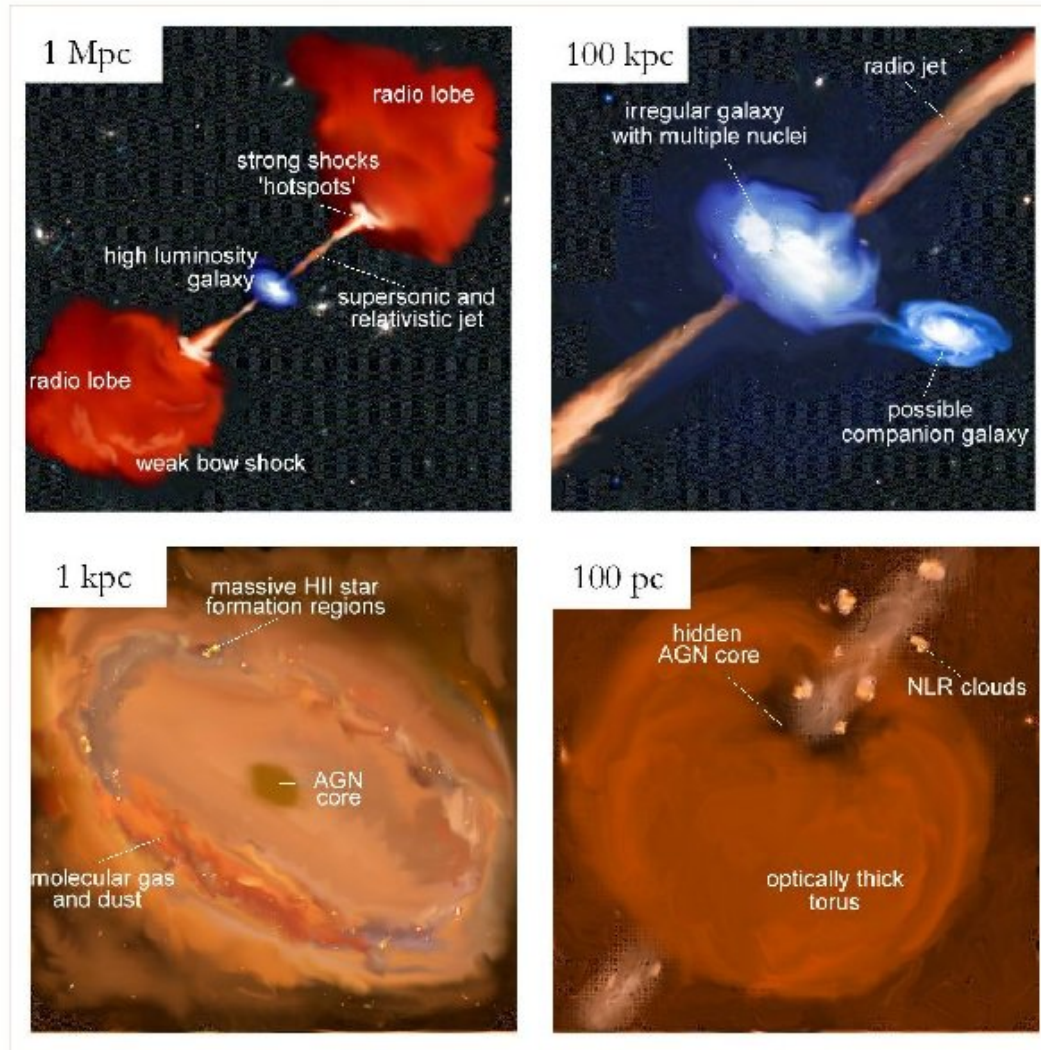


(from Sikora, Begelman, and Rees (1994))



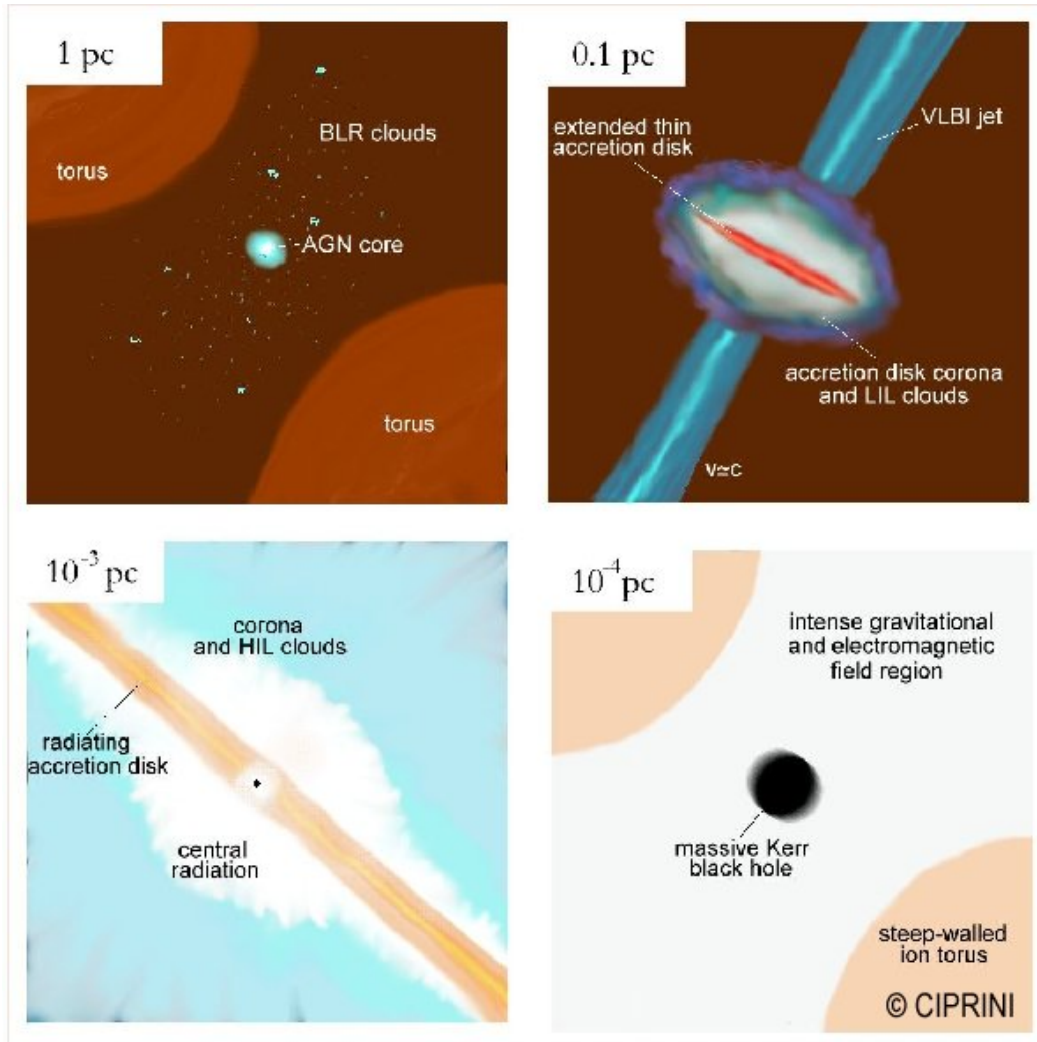
(credit: J. Buckley)

# Active Galactic Nuclei



Artistic picture by  
S.Ciprini

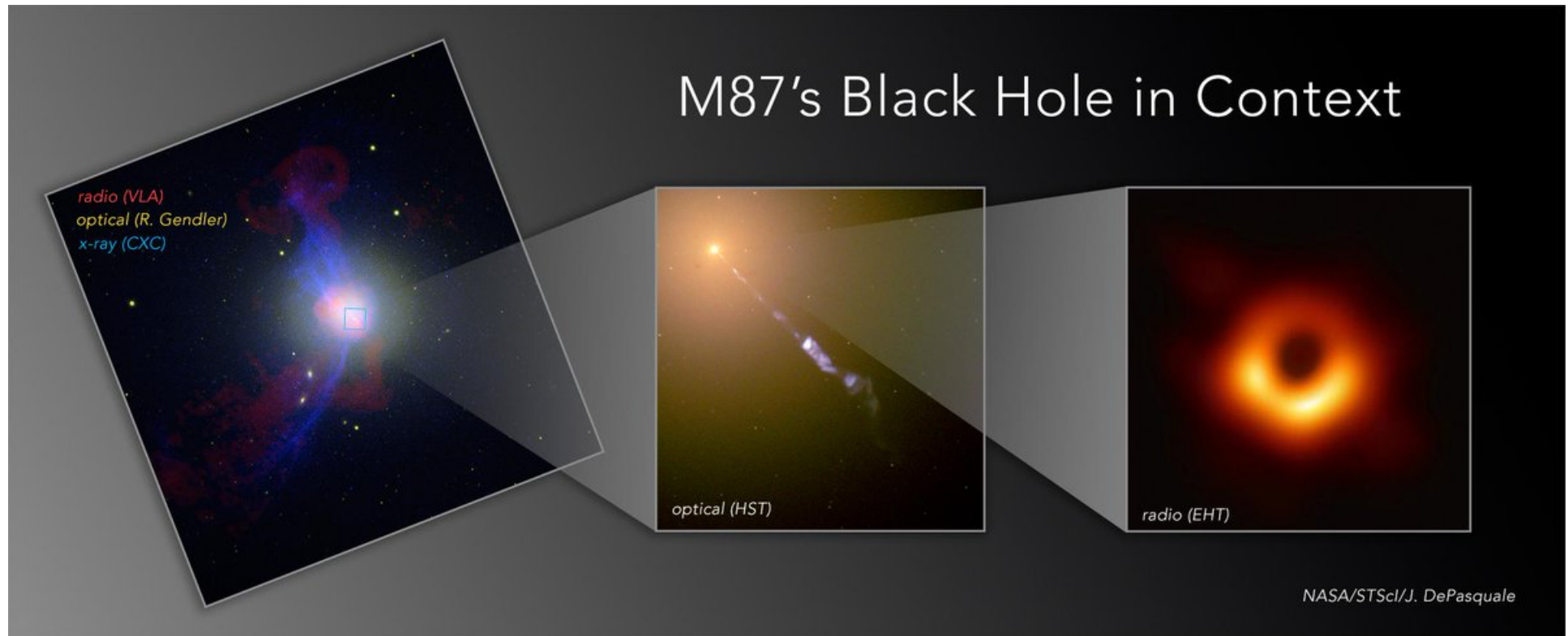
# Active Galactic Nuclei



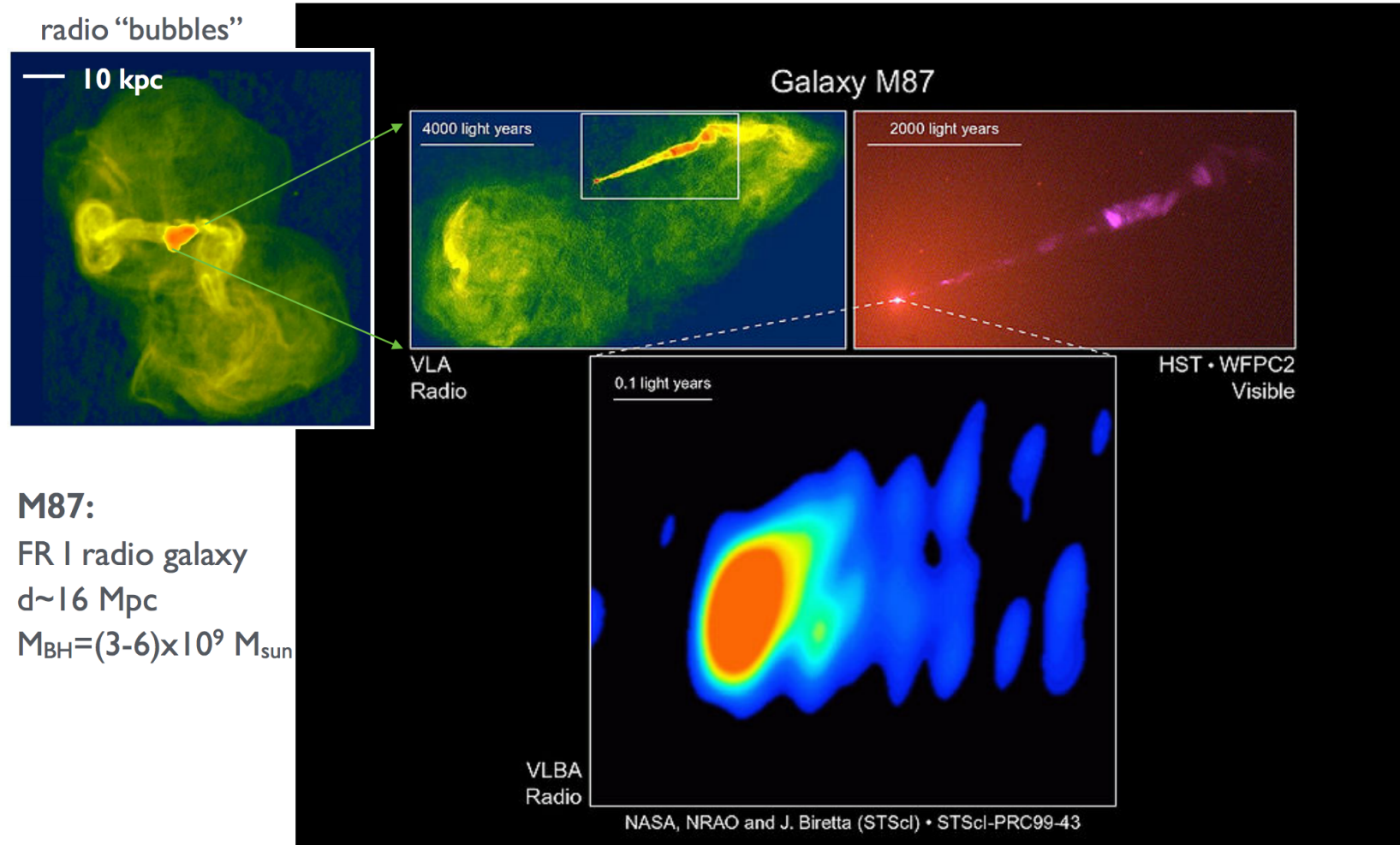
Artistic picture by  
S.Ciprini



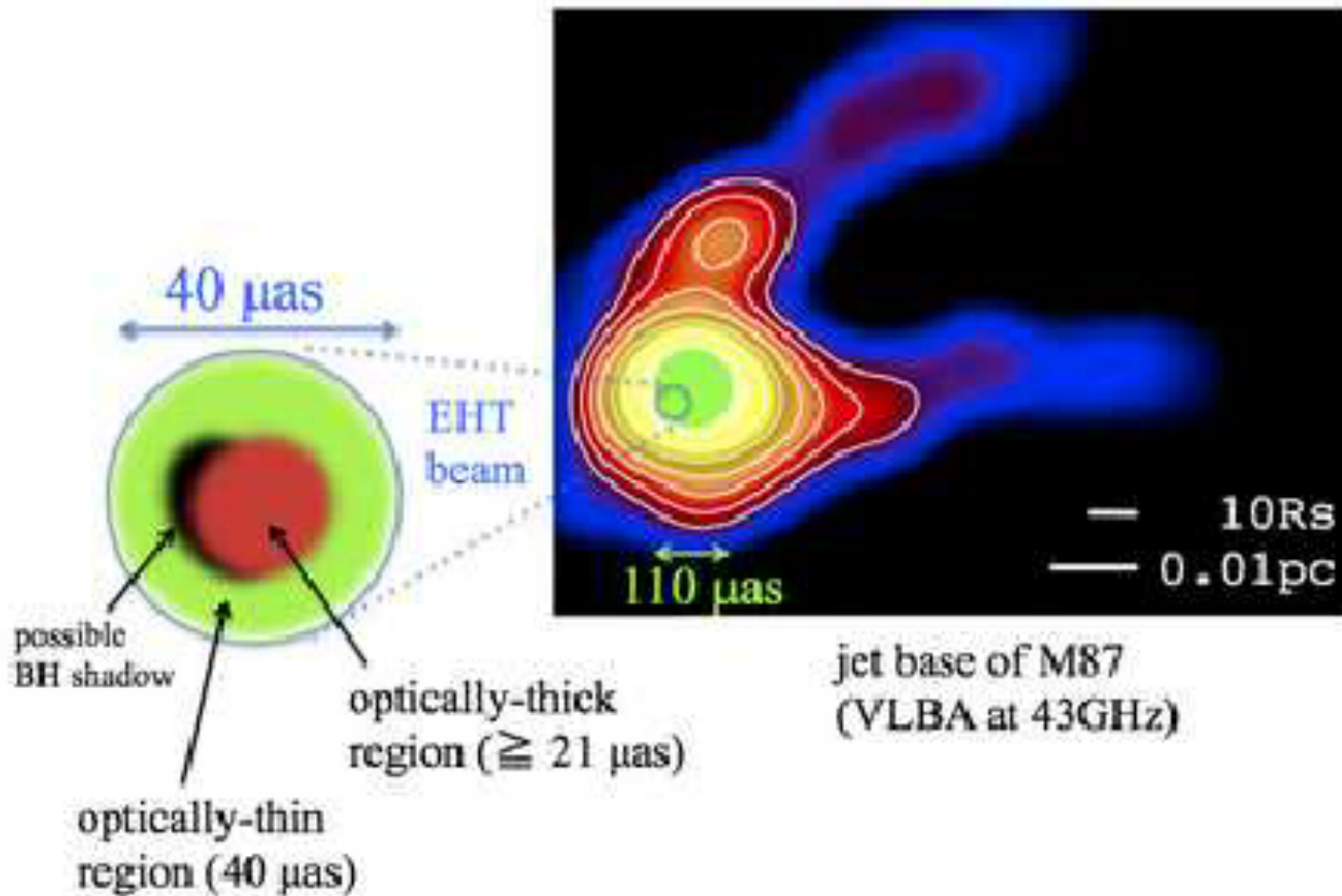
# M87 scales...



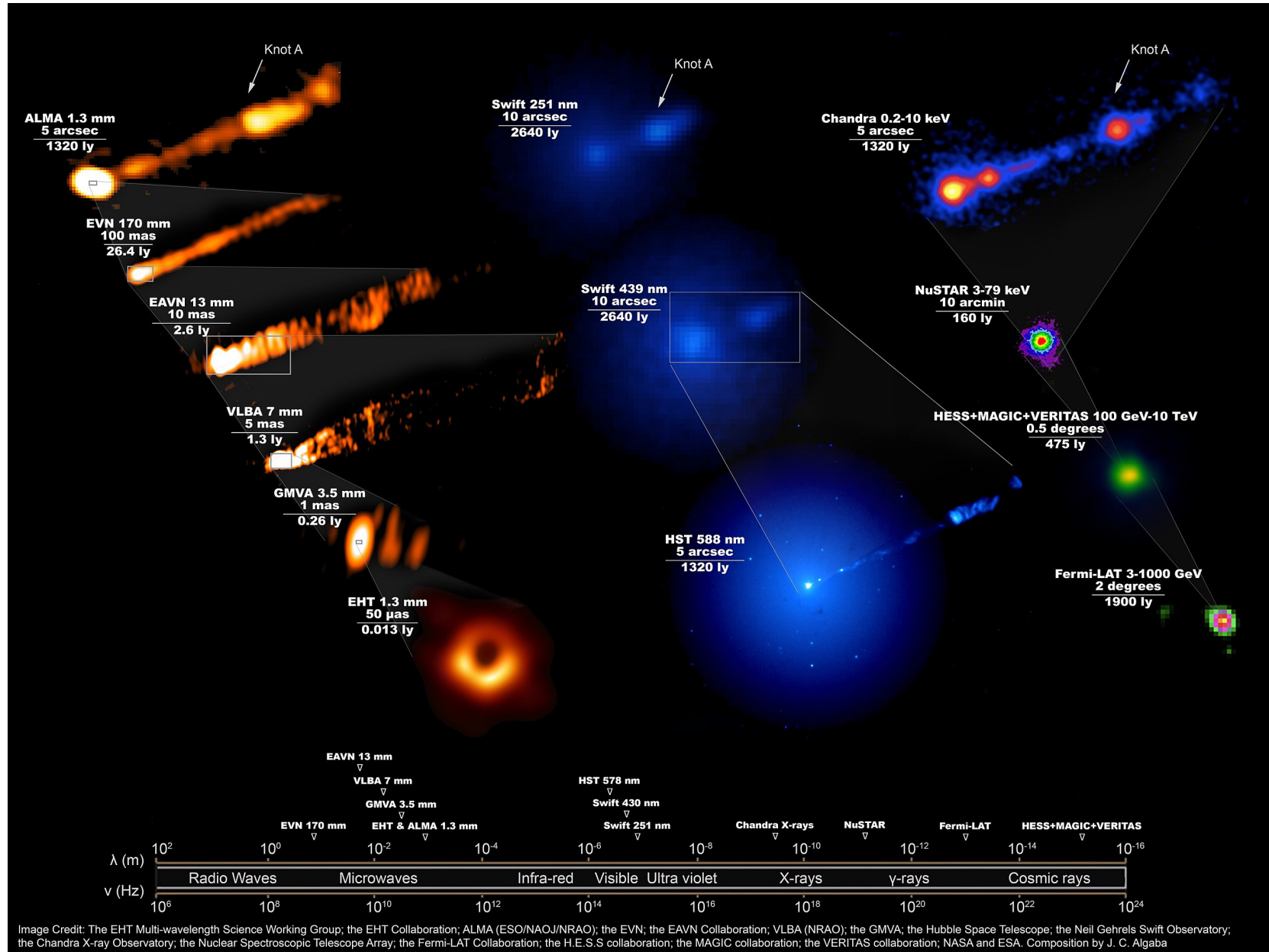
# M87 scales...



# M87 scales...



# M87 scales...



# AGN and the Extragalactic Background Light (EBL)

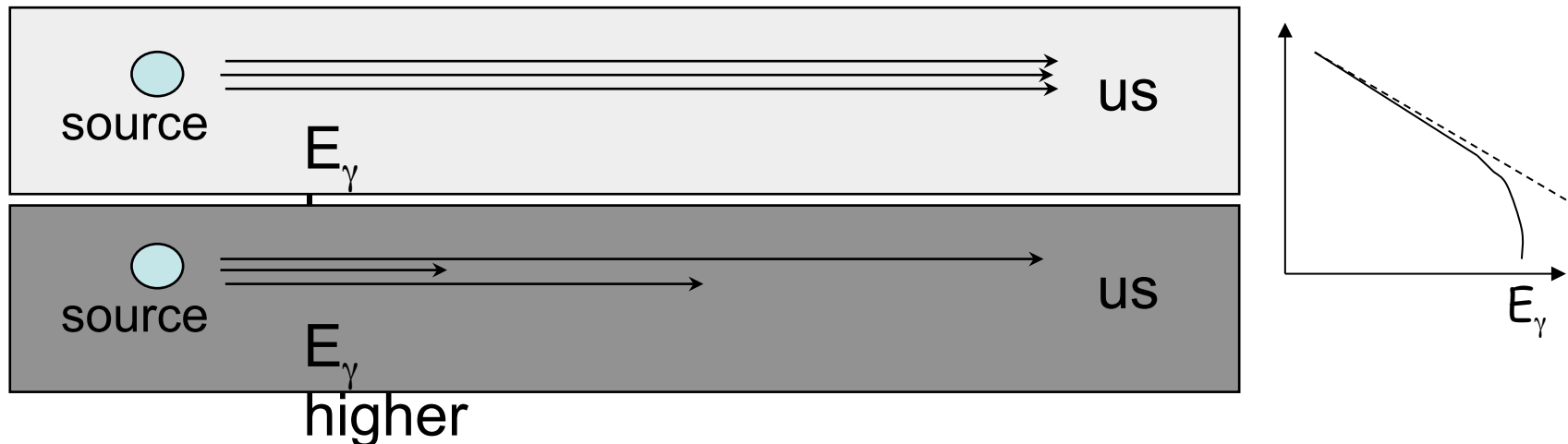


Look for roll-offs in blazar spectra due to attenuation:  
 (Stecker, De Jager & Salamon; Madau & Phinney; Macminn & Primack)

If  $\gamma\gamma$  c.m. energy  $> 2m_e$ , pair creation will attenuate flux. For a flux of  $\gamma$ -rays with energy,  $E$ , this cross-section is maximized when the partner,  $\epsilon$

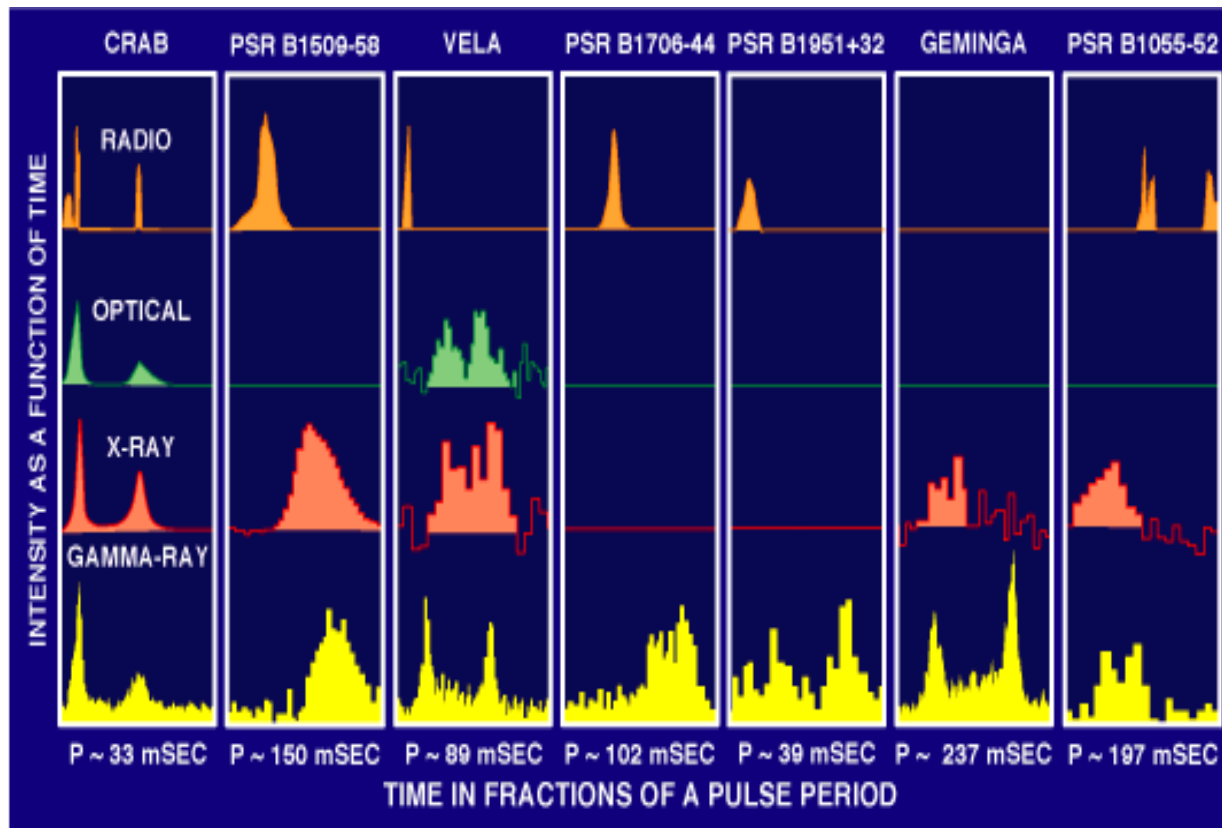
$$\epsilon \sim \frac{1}{3} \left( \frac{1 \text{ TeV}}{E} \right) eV$$

For 10 GeV- 100 GeV  $\gamma$ -rays, this corresponds to a partner photon energy in the optical - UV range. Density is sensitive to time of galaxy formation.

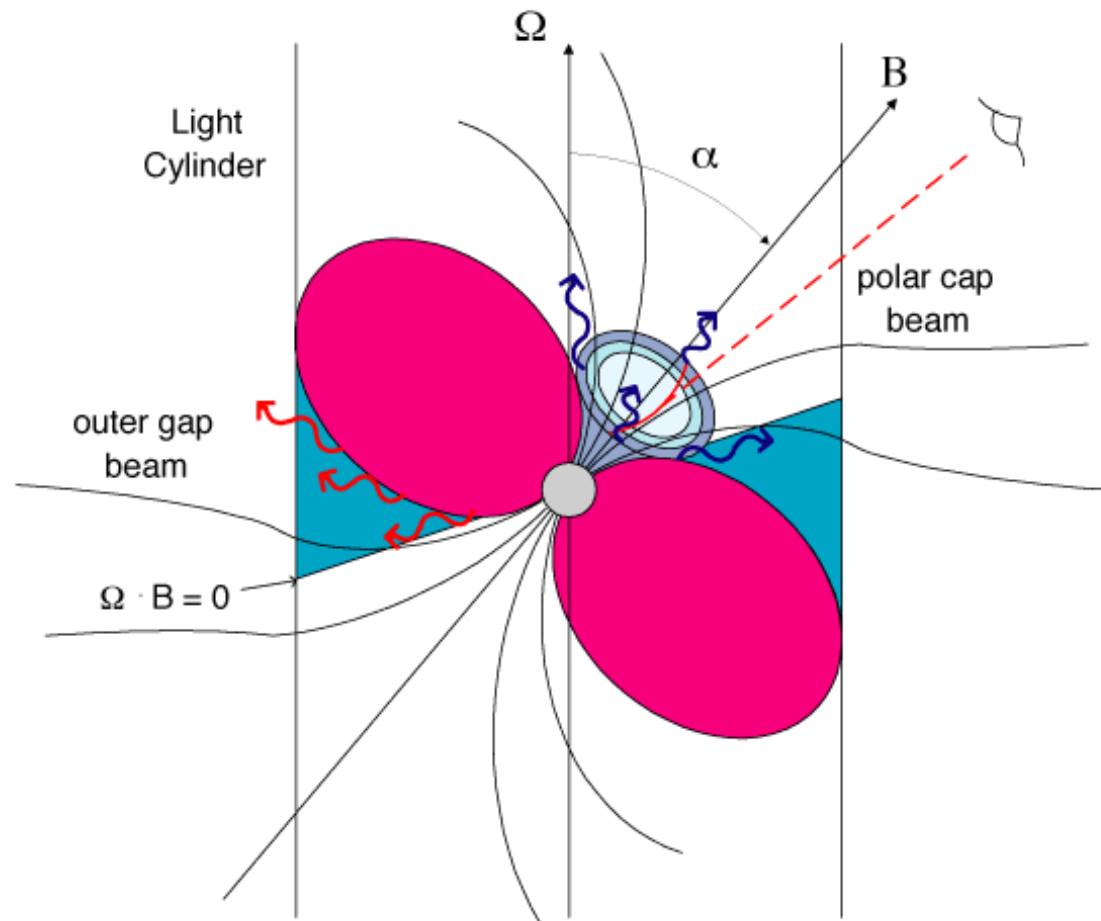


# Challenge # 2

- Need more exposure and optimal timing (and radio monitoring) to discover more gamma-ray PSRs.



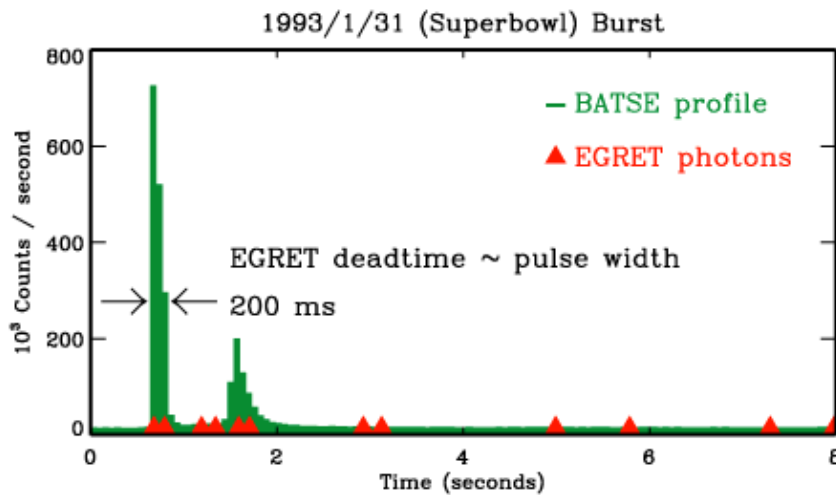
# Pulsars



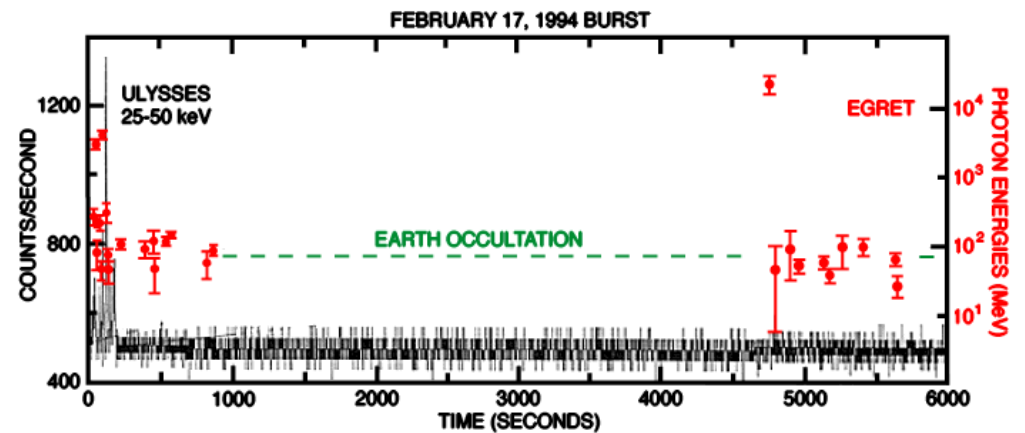
# Challenge # 3

- Need fast timing for gamma-ray detection (improving EGRET deadtime, 100 msec → 100 microsec or less).

## Prompt Emission (GRB 930131)

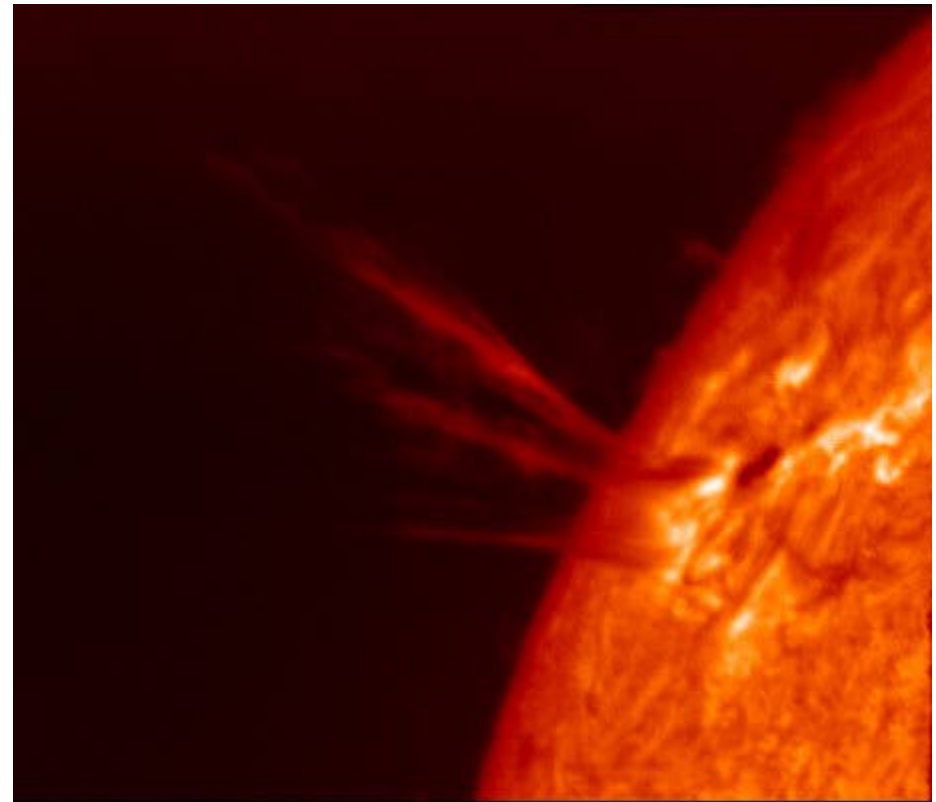
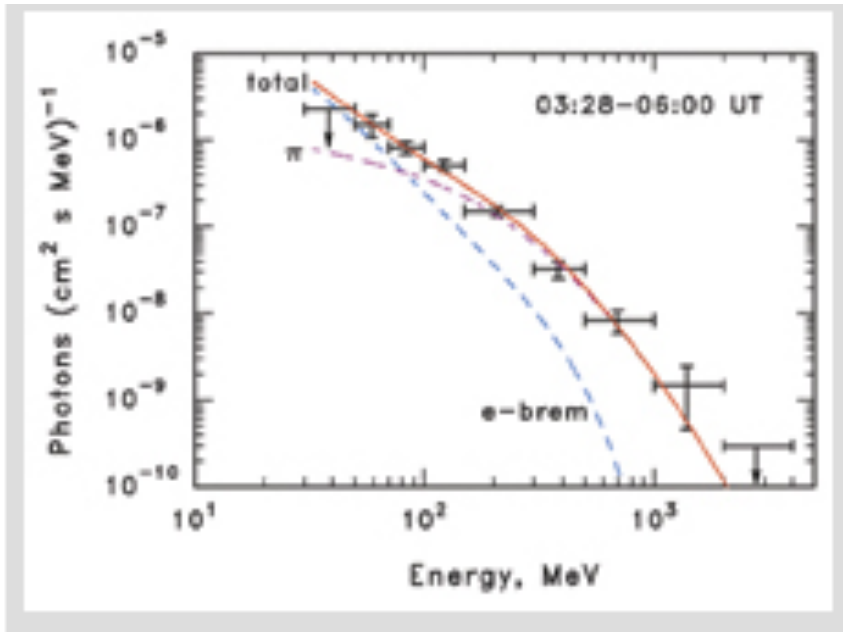


## Delayed Emission (GRB 940217)

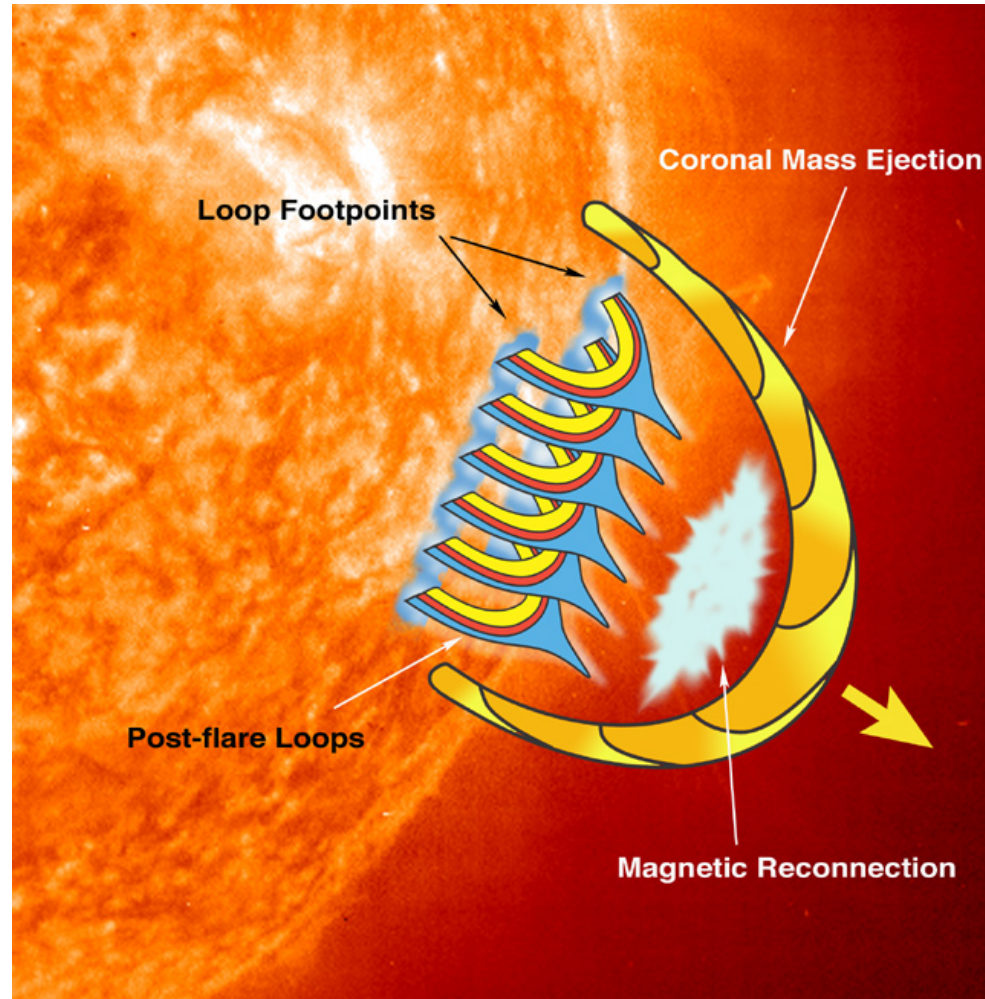




# Solar flares

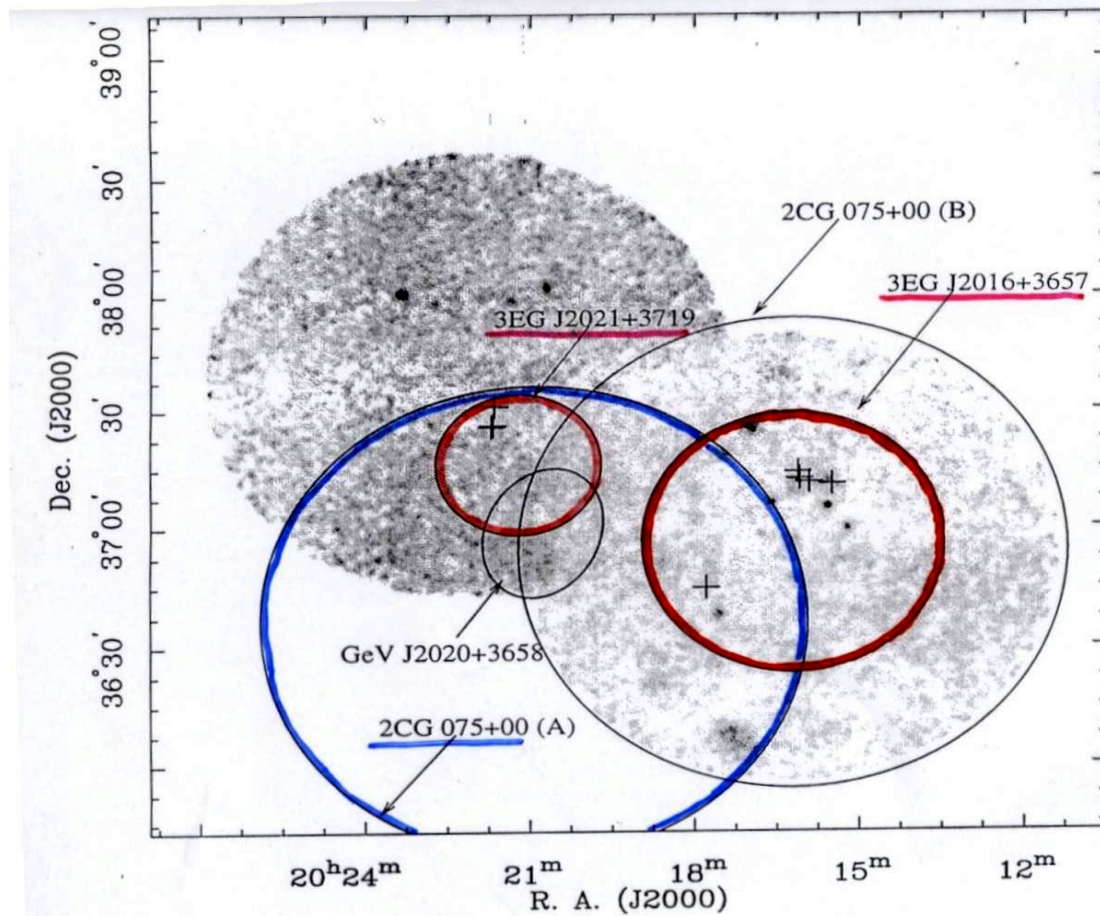


# Solar Flares

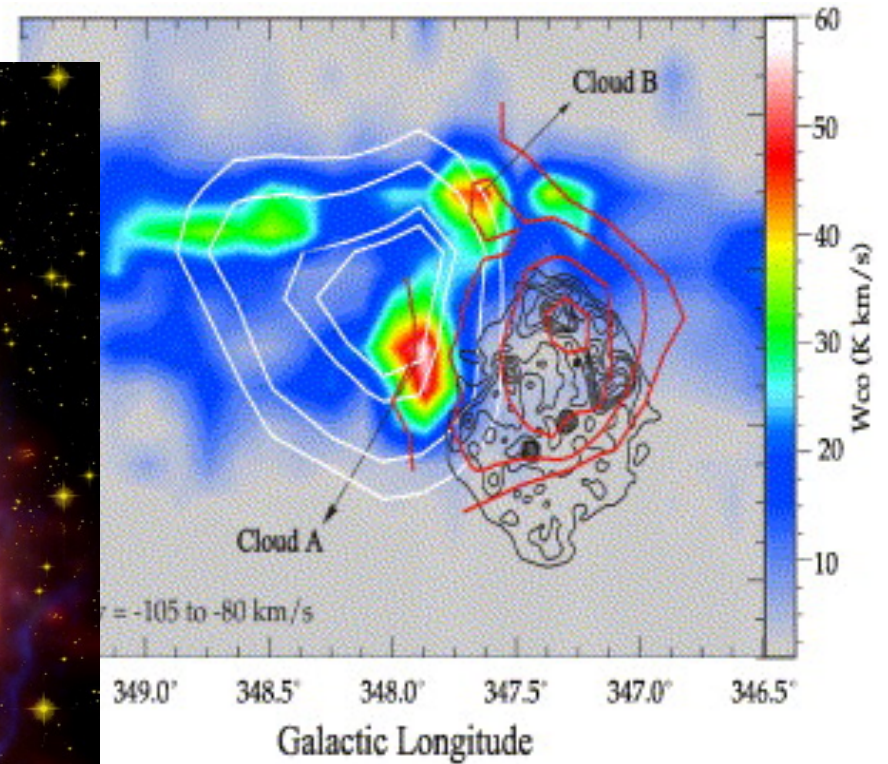
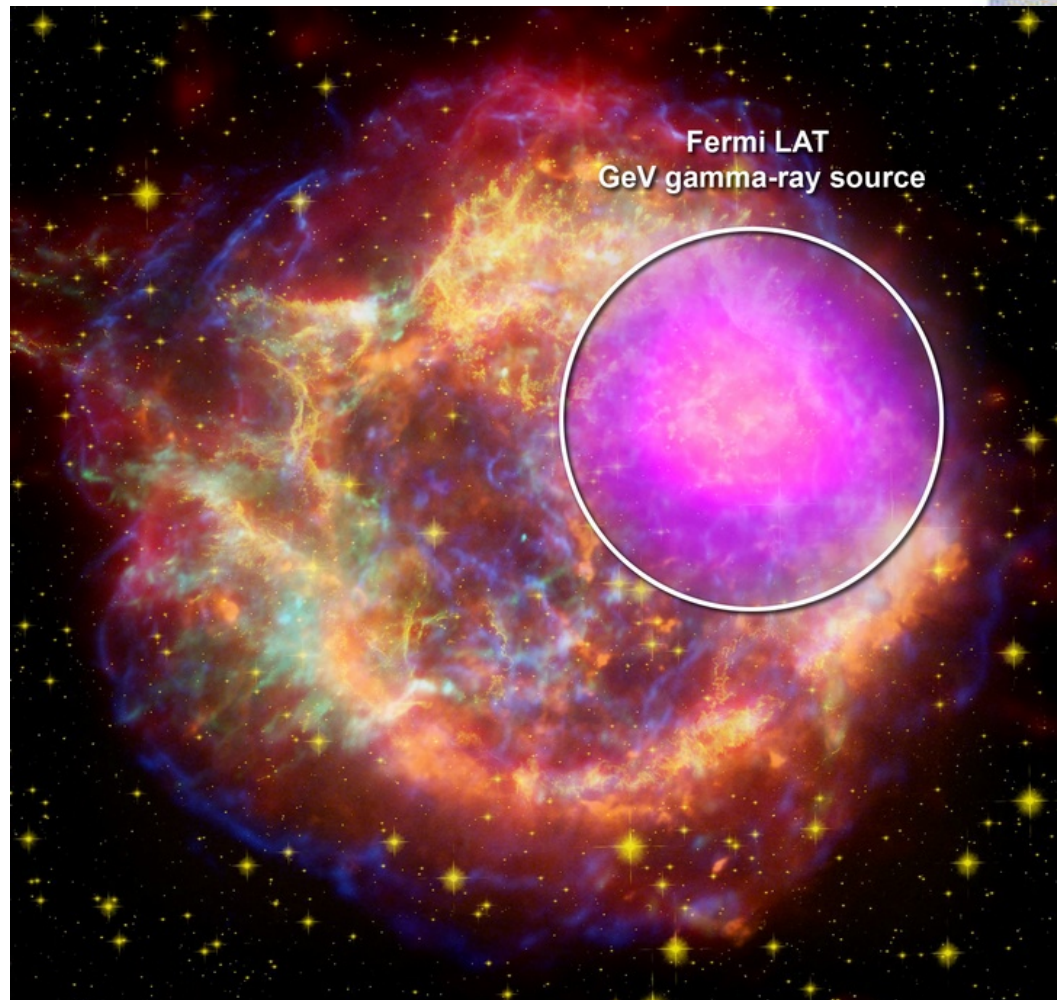


# Challenge # 4

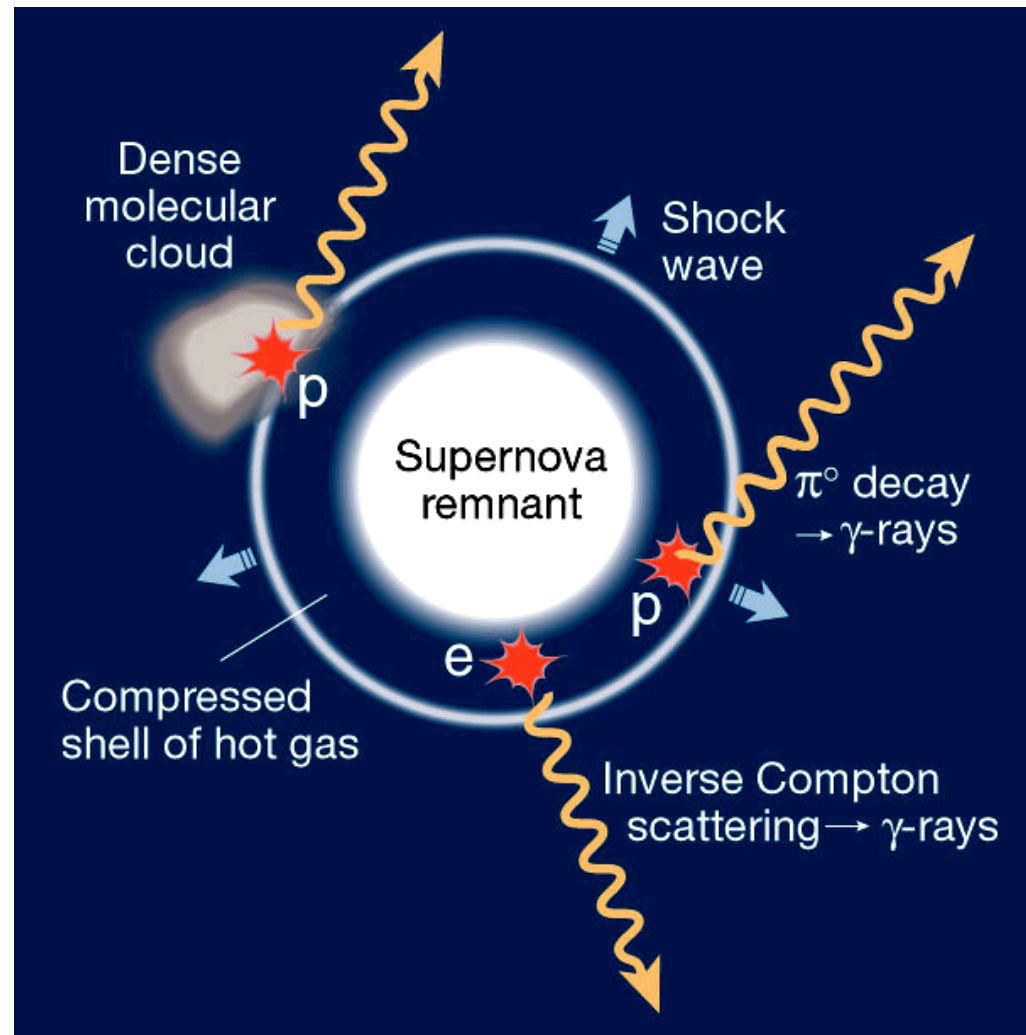
- Need arcminute positioning of gamma-ray sources (improving EGRET error box radii by a factor of 2-10).



# Supernova Remnants

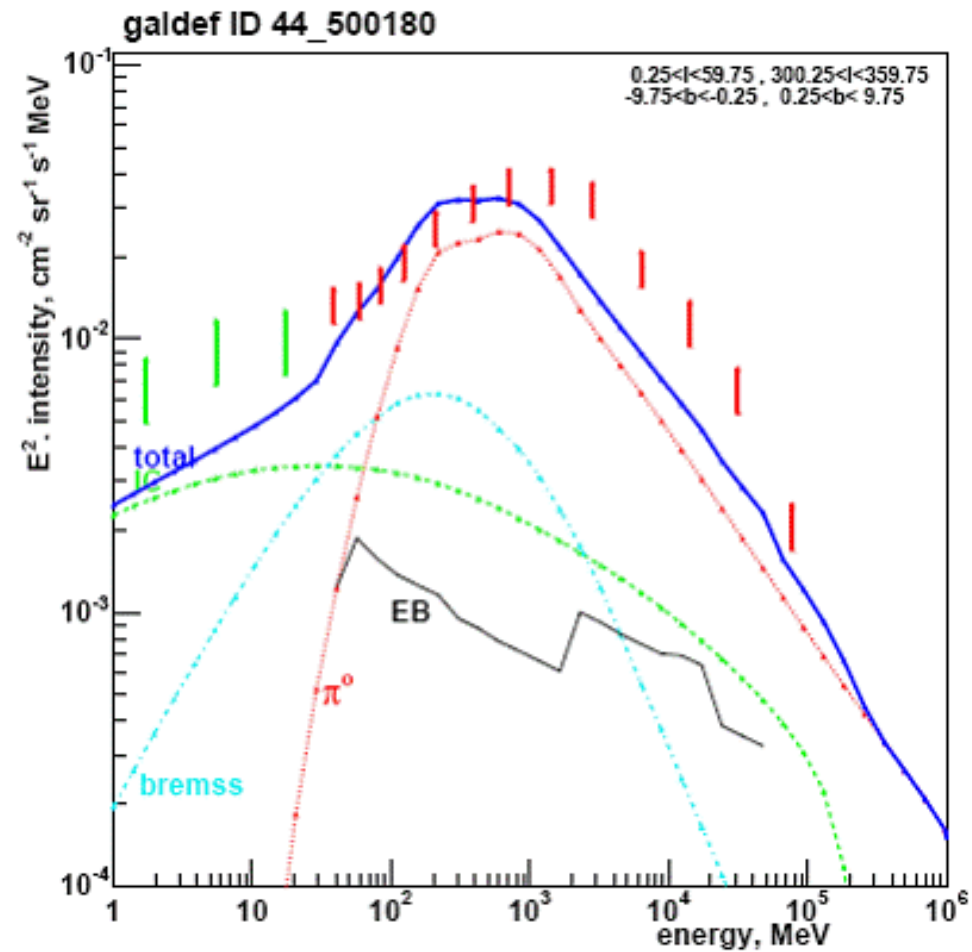


# SNR

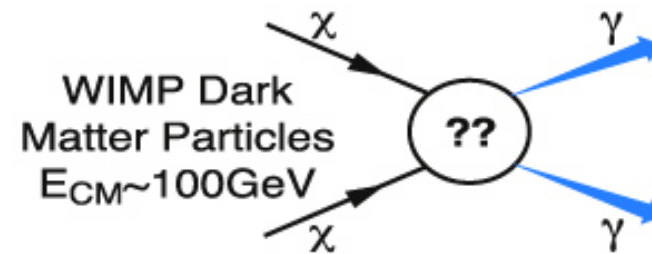
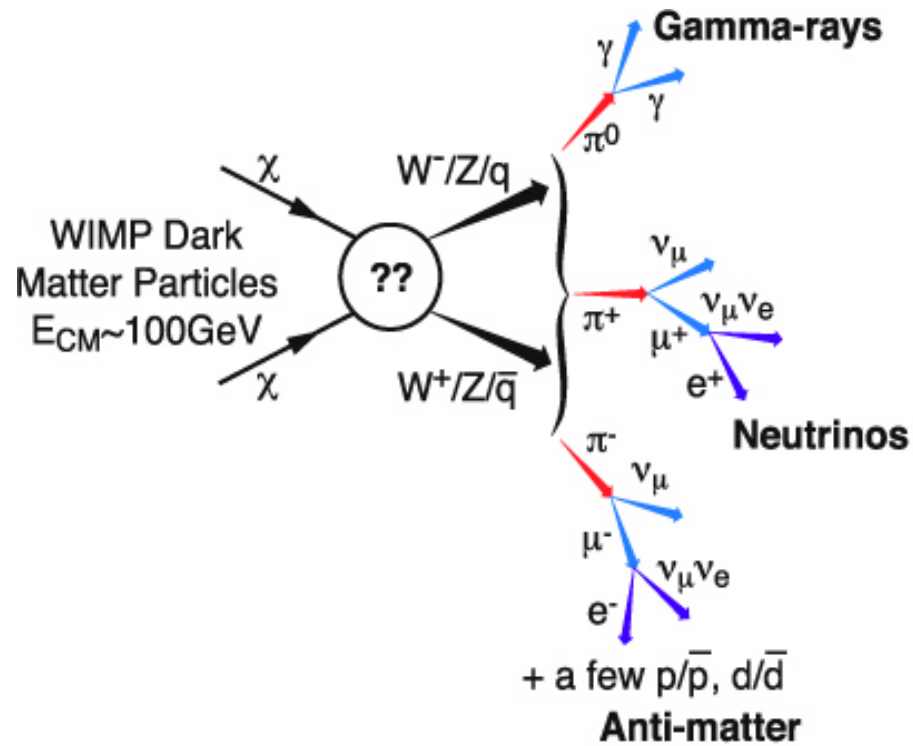


# Challenge # 5

- Need improvements in Spectral Resolution fo check for DM signals



# Dark Matter



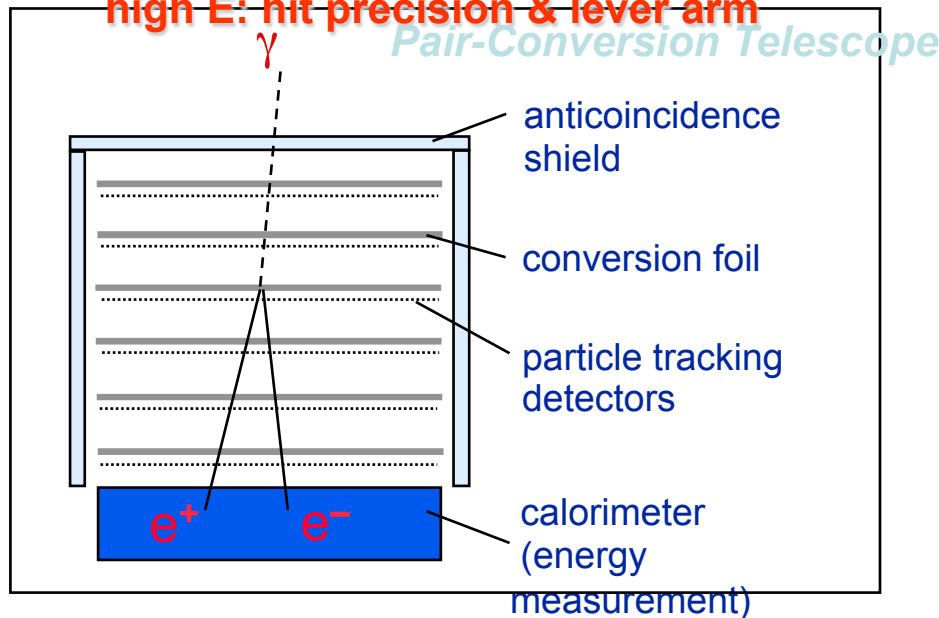
# Detector Project

- Instrument must measure the direction, energy, and arrival time of high energy photons (from approximately 20 GeV):

- photon interactions with matter in GLAST energy range dominated by pair conversion:
- limitations on angular resolution (PSF)

low E: multiple scattering => many thin layers

high E: hit precision & lever arm



## Energy loss mechanisms:

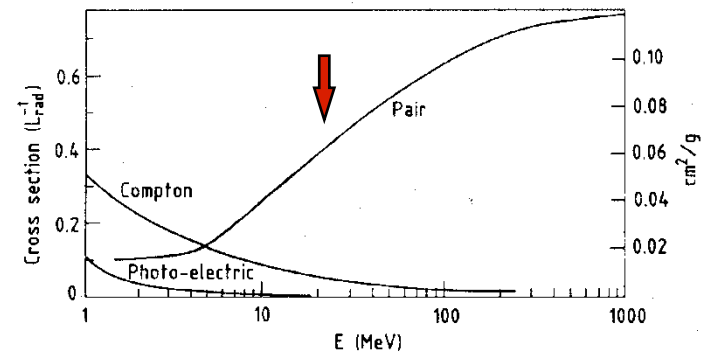


Fig. 2: Photon cross-section  $\sigma$  in lead as a function of photon energy. The intensity of photons can be expressed as  $I = I_0 \exp(-\sigma x)$ , where  $x$  is the path length in radiation lengths. (Review of Particle Properties, April 1980 edition).

- must detect  $\gamma$ -rays with high efficiency and reject the much larger ( $\sim 10^4:1$ ) flux of background cosmic-rays, etc.;
- energy resolution requires calorimeter of sufficient depth to measure buildup



# Detector Project

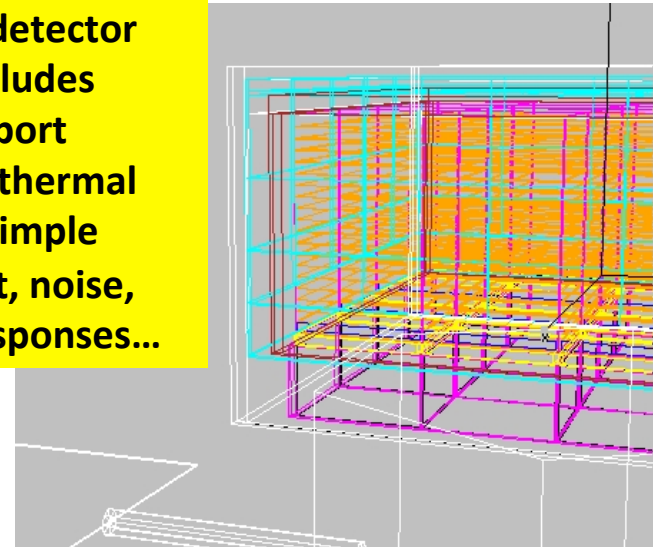
The LAT design is based on detailed Monte Carlo simulations.

Integral part of the project from the start.

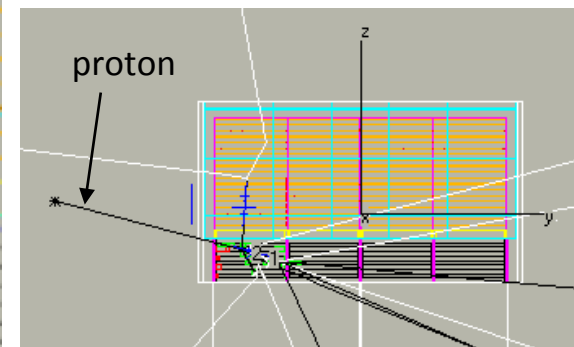
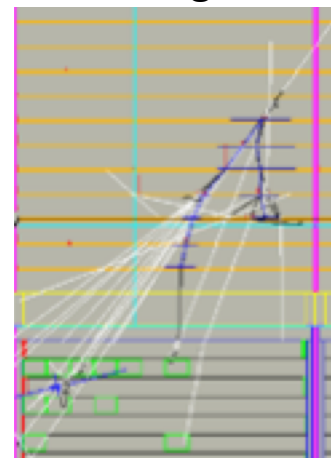
- **Background rejection**
- **Calculate effective area and resolutions (computer models now verified by beam tests). Current reconstruction algorithms are existence proofs -- many further improvements under development.**
- **Trigger design.**
- **Overall design optimization.**

Simulations and analyses are all C++, based on standard HEP packages.

Detailed detector model includes gaps, support material, thermal blanket, simple spacecraft, noise, sensor responses...

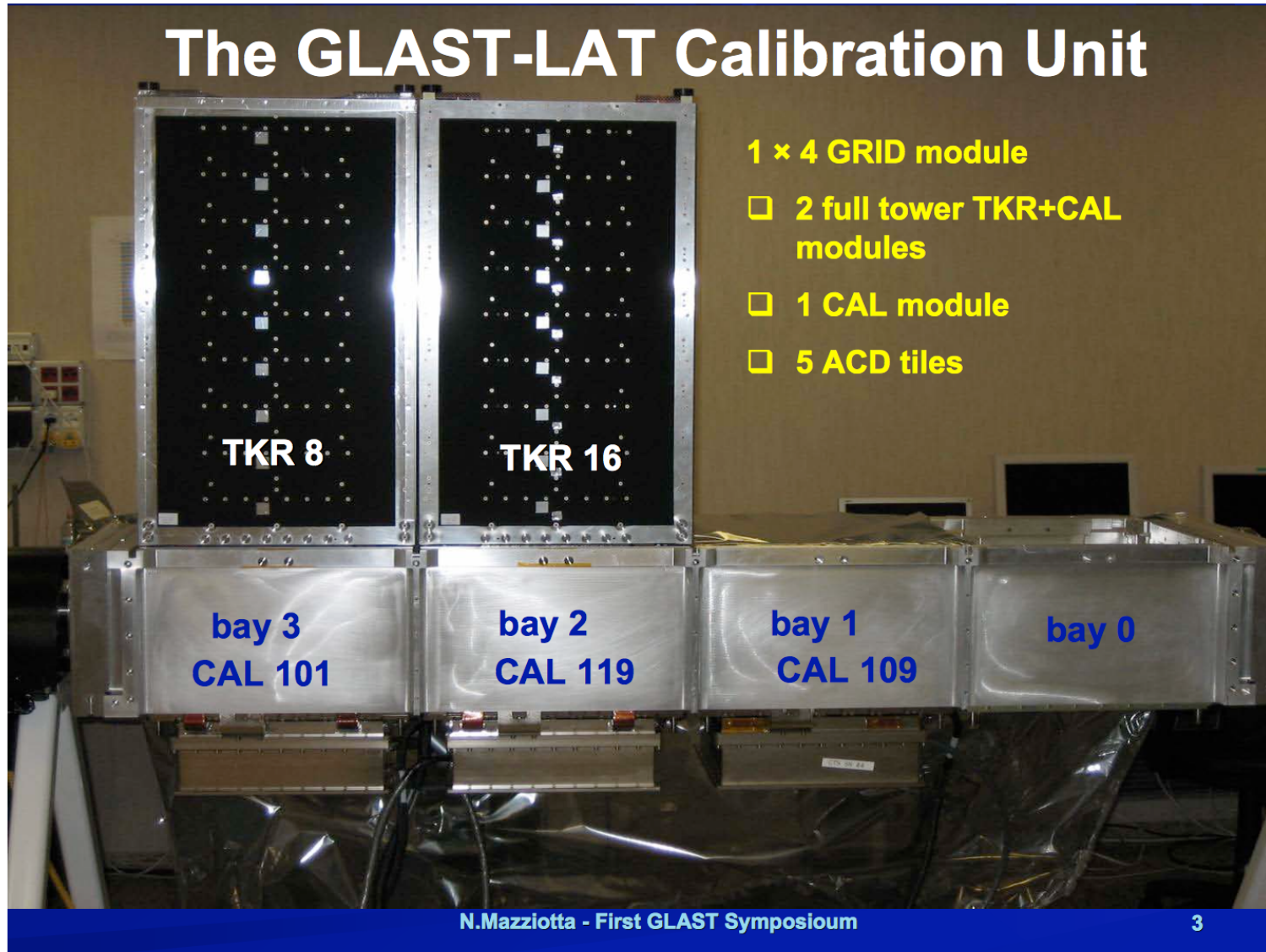


Instrument naturally distinguishes gammas from backgrounds, but details matter.



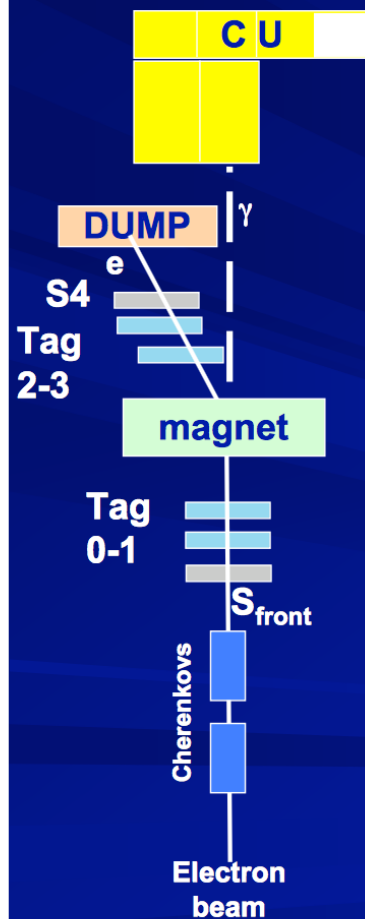
# Beam test

## The GLAST-LAT Calibration Unit



# Beam test

## Photon configuration set-up



The gamma ray beam at the CERN PS T9 line was produced by bremsstrahlung between electrons and the upstream materials. A magnet has been used to well separate electrons from photons. Finally a beam dump has been used to stop electrons.

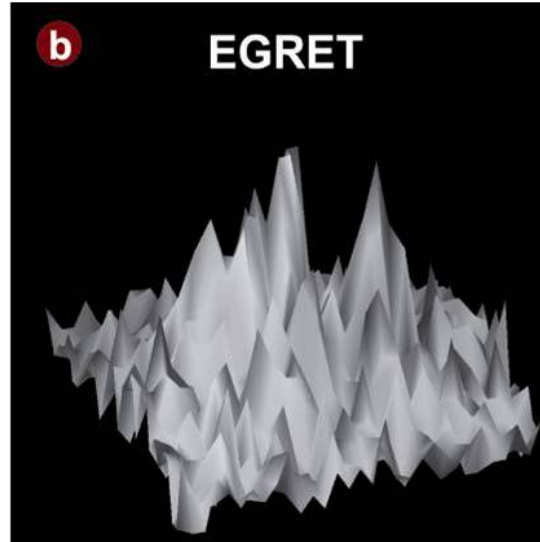
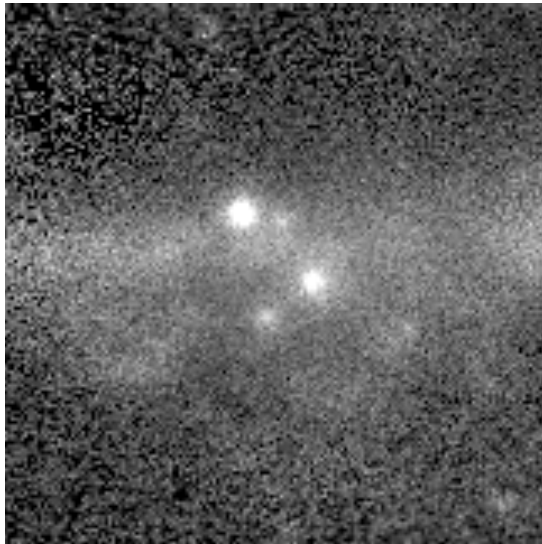
### ■ Tagged photon beam

- An external tracker (4 x-y view silicon strip detector) was used to track electrons upstream and downstream the magnet, read-out by means of an external DAQ
- Trigger on S4 & S<sub>front</sub> & Cherenkovs
- External DAQ was synchronized with the CU one, then the data have been merged with the CU one
- Different electron beam energy in the range 0.5-2.5 GeV and magnetic field intensity have been used to provide a gamma spectrum to the CU below 2 GeV

### ■ Not tagged photon beam

- Trigger on S<sub>front</sub> & Cherenkov
- Full bremsstrahlung spectrum from 2.5 GeV/c electron beam

# Technology impact -- PSF

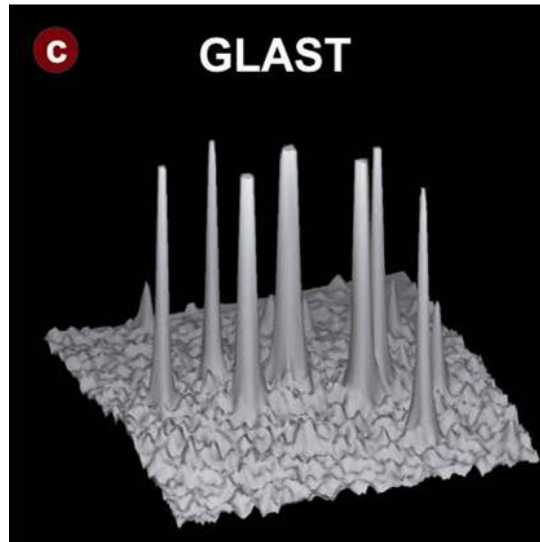
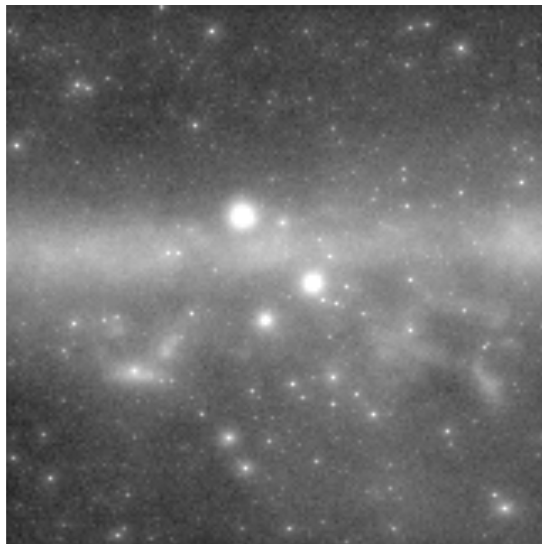


**EGRET**  
(1991-2000)  
Phases 1-5



Spark chamber

- sense electrode spacing  $\sim$ mm
- sensitive layer depth  $\sim$ cm
  - *up to 28 hit over  $>1m$*



**LAT**  
(2008-  $>2013$ )  
1-yr simulation

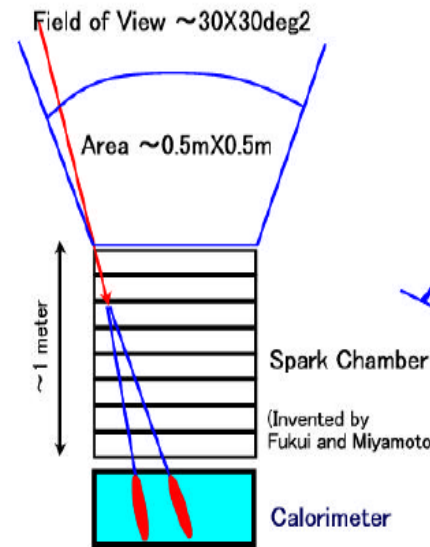
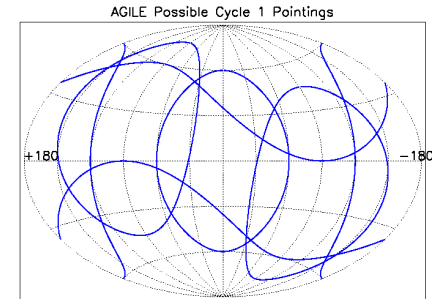
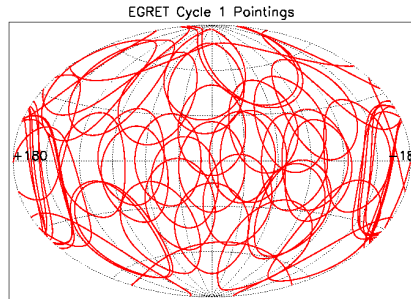
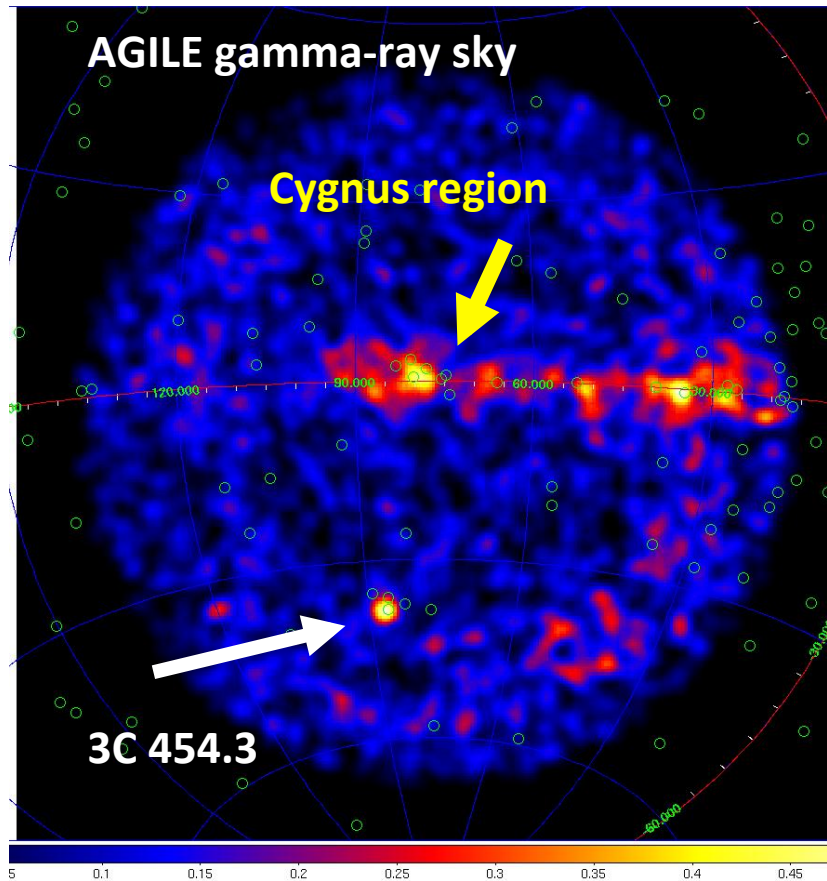


Si-strip detectors

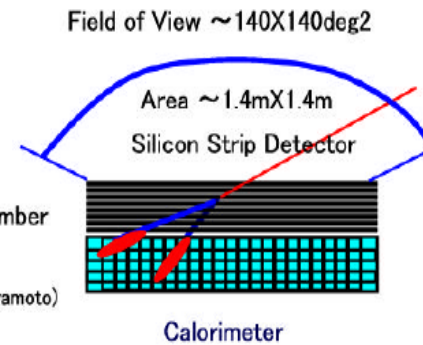
- sense electrode spacing  $\sim 0.2mm$ 
  - *better single hit resolution*
- sensitive layer depth  $\sim 0.4mm$ 
  - *up to 36 hit over  $0.8m$*
  - *converter proximity to minimize MCS*

*Cygnus region ( $15^\circ \times 15^\circ$ ),  $E_\gamma > 1 GeV$*

# Technology impact - FoV



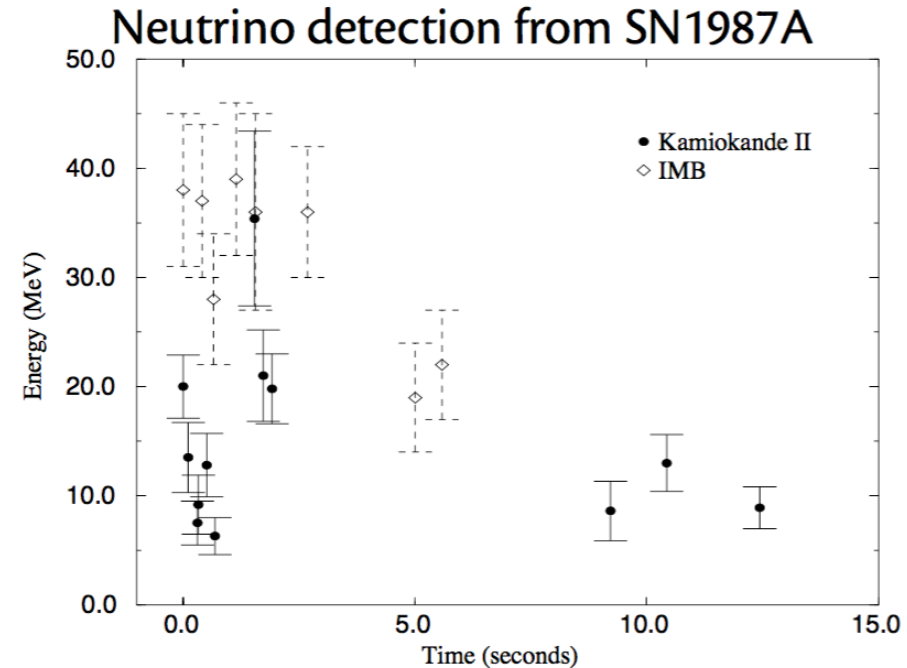
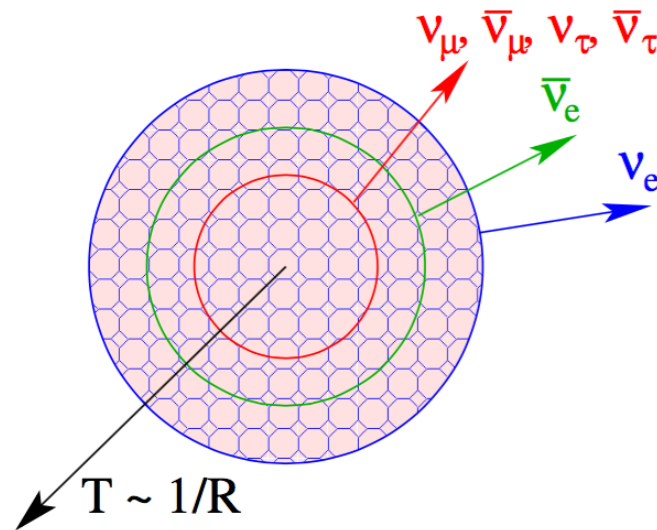
EGRET on Compton GRO



GLAST Large Area Telescope

Astrofisica Nucleare e Subnucleare  
Heavy Elements Nuclear  
Astrophysics

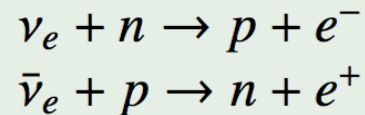
# Neutrino emission from the proto-neutron star



- Gravitational binding energy:  $E_{\text{grav}} \approx GM^2/R \sim 10^{53}$  erg.
- Neutrino emission lasts around 10 s with energies  $E_\nu \sim 10$  MeV.
- Enormous neutrino fluxes around the neutron star surface:  
 $\Phi_\nu = 10^{43} \text{ cm}^{-2} \text{ s}^{-1}$  at 20 km. Gravitational binding energy  
 nucleon  $\sim 100$  MeV.
- With  $E_\nu \sim 10$  MeV the typical neutrino-nucleon cross section is  
 $10^{-41} \text{ cm}^{-2}$ . This results in interaction times of 10 ms.

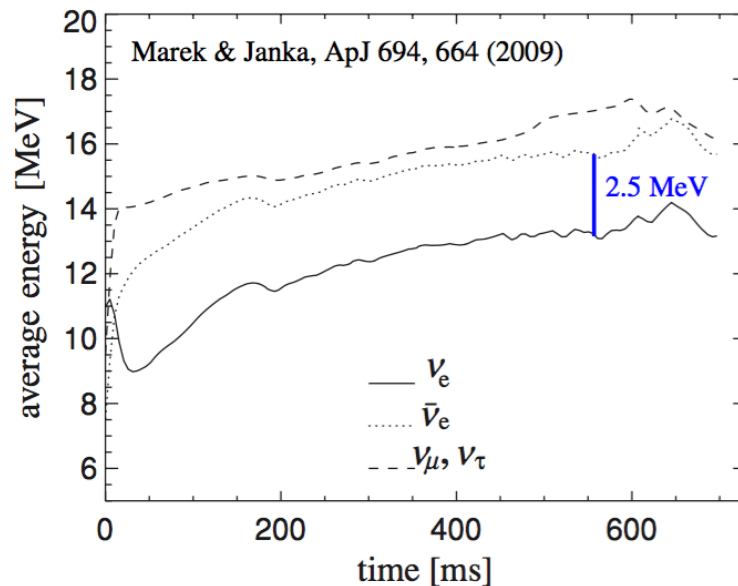
# Influence of neutrinos on nucleosynthesis

## Main processes:

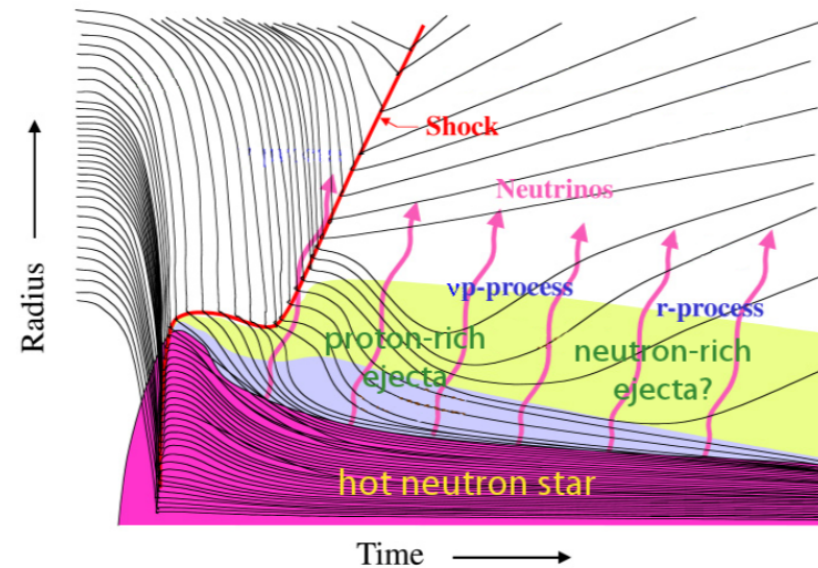


Neutrino interactions determine the proton to neutron ratio, the ejecta are proton rich if:

$$\epsilon_{\bar{\nu}_e} - \epsilon_{\nu_e} < 4(m_n c^2 - m_p c^2) \approx 5.2 \text{ MeV}$$



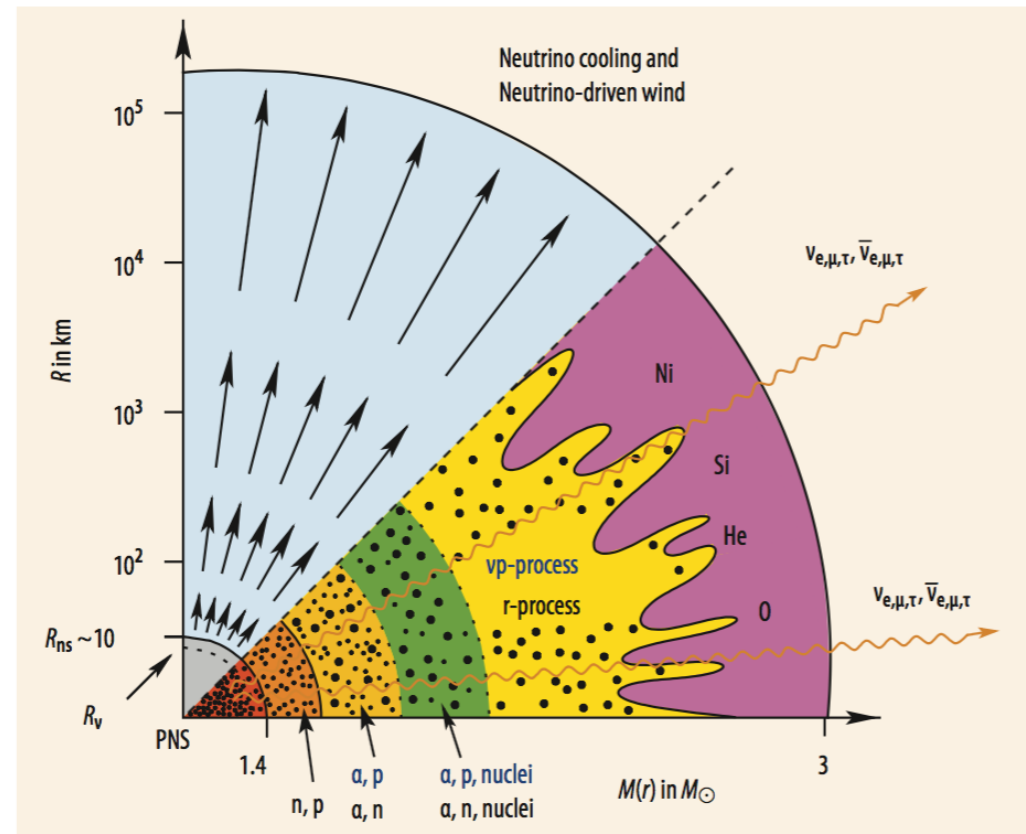
- Early times (up to 1-2 seconds): proton-rich ejecta ( $\nu p$ -process).
- Later times: neutron-rich ejecta (r-process)??





# Neutrino driven wind

- At  $T = 10$  GK starts the formation of  $\alpha$ -particles ( ${}^4\text{He}$ ).
- Between  $T = 8$  GK and  $T = 3$  GK, the formation of seeds occurs.  
Dominating reactions are:
  - $3\alpha \rightleftharpoons {}^{12}\text{C} + \gamma$   
(proton-rich ejecta)
  - $2\alpha + n \rightleftharpoons {}^9\text{Be} + \gamma$   
 ${}^9\text{Be} + \alpha \rightarrow {}^{12}\text{C} + n$   
(neutron-rich ejecta).
- At lower temperatures proton ( $\nu p$ -process) or neutron (r-process) captures take place.



GMP, Physik Journal 7, 51 (2008)

# Heavy element nucleosynthesis: the r process

Gabriel Martínez Pinedo



TECHNISCHE  
UNIVERSITÄT  
DARMSTADT

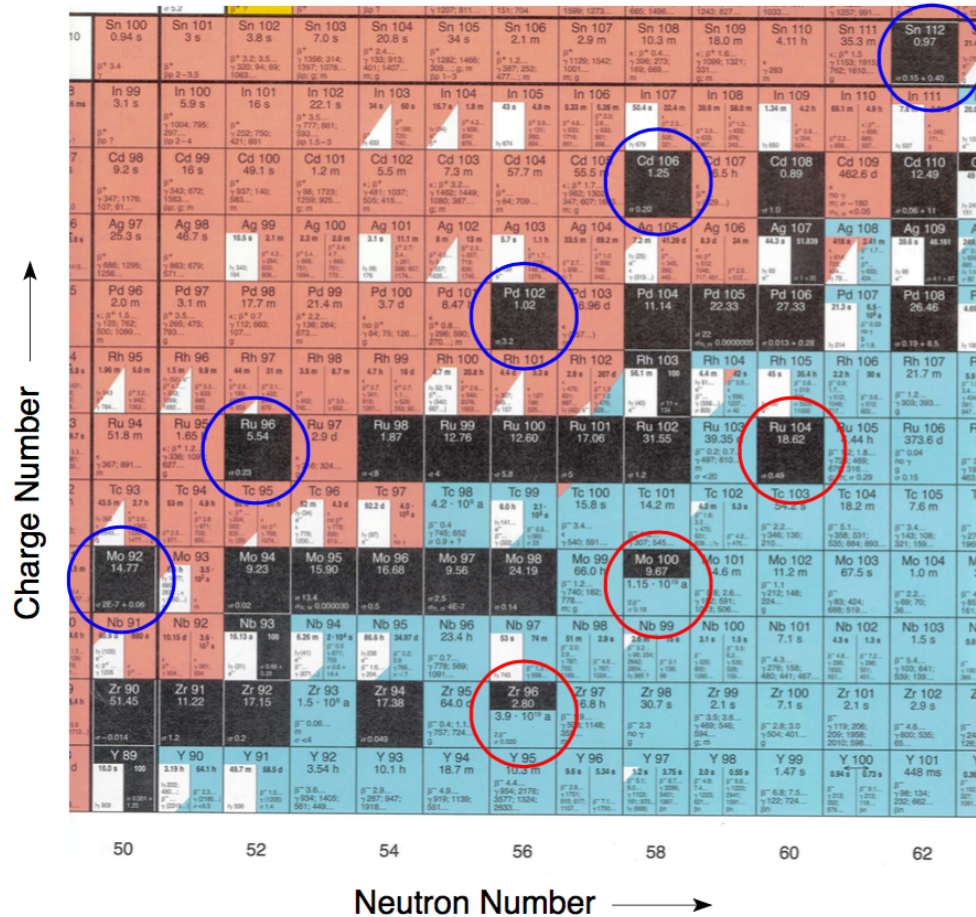
55th Karpacz Winter School of Theoretical Physics  
ChETEC COST Action CA16117 training school  
Artus Hotel, Karpacz, February 24 - March 2, 2019

**HELMHOLTZ**  
RESEARCH FOR GRAND CHALLENGES



**DFG**

# Nucleosynthesis beyond iron

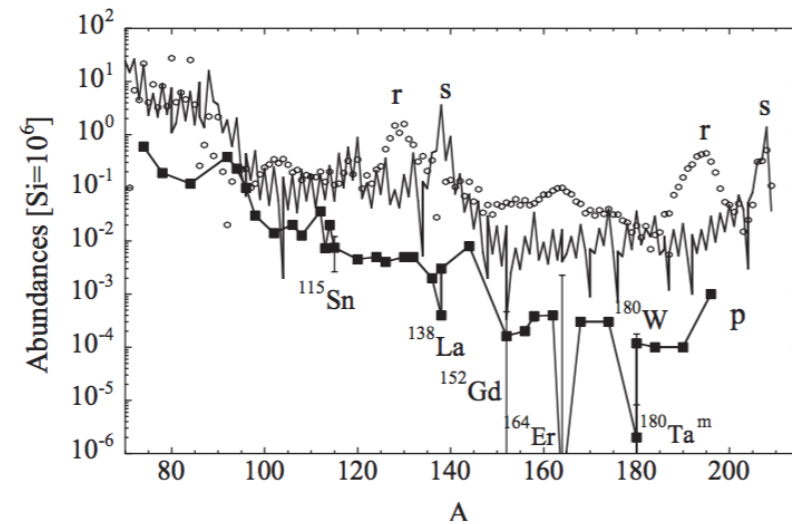
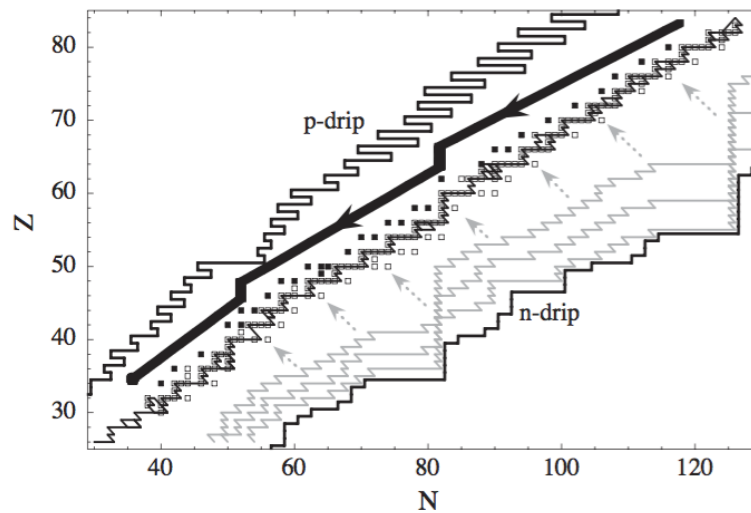


The stable nuclei beyond iron can be classified in three categories depending of their origin:

- s-process
- r-process
- p-process ( $\gamma$ -process)

# Nucleosynthesis beyond iron

Three processes contribute to the nucleosynthesis beyond iron: s-process, r-process and p-process ( $\gamma$ -process).



- s-process: relatively low neutron densities,  $n_n = 10^{10-12} \text{ cm}^{-3}$ ,  $\tau_n > \tau_\beta$
- r-process: large neutron densities,  $n_n > 10^{20} \text{ cm}^{-3}$ ,  $\tau_n < \tau_\beta$ .
- p-process: photodissociation of s-process material.

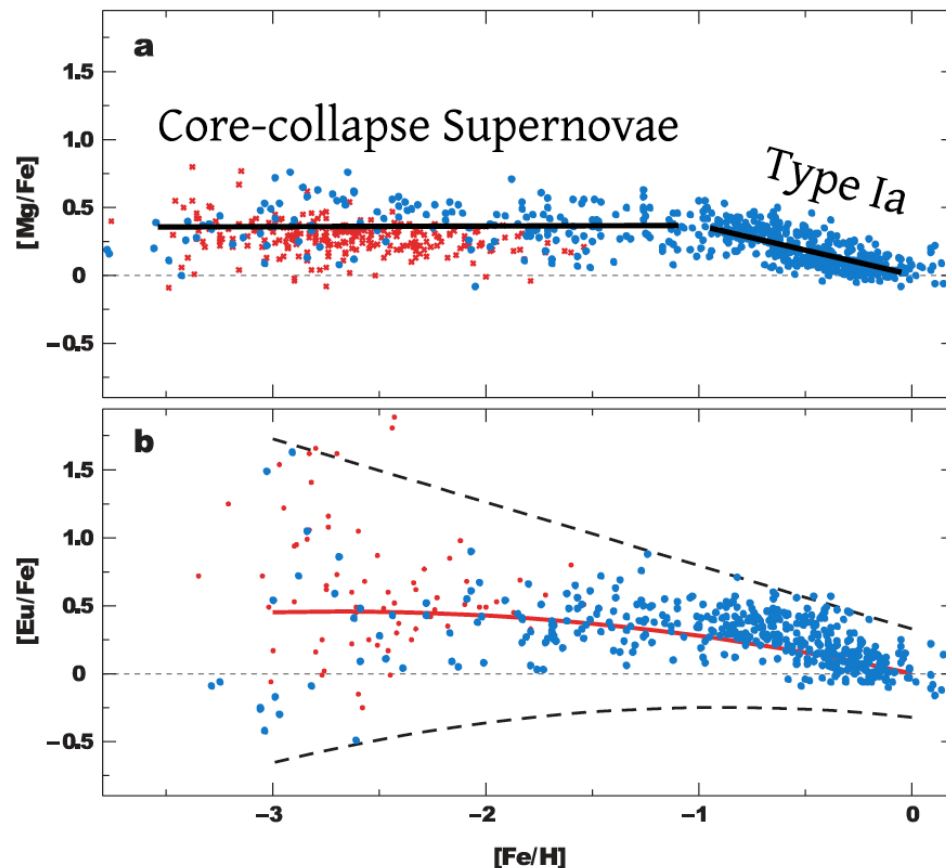




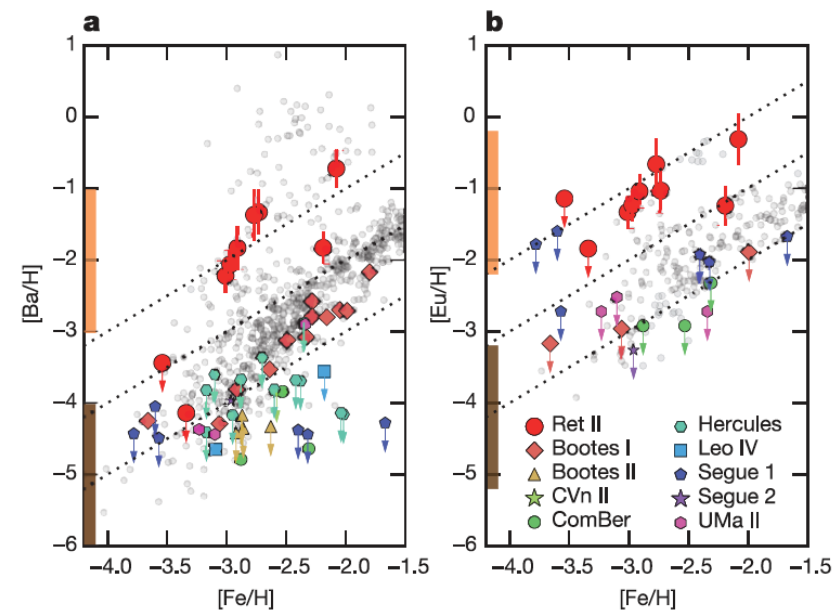


# Implications from observations

Individual stars, Milky Way Halo  
Snedden, Cowan & Gallino, 2008



Ji et al 2016 found that only 1 of 10 ultrafaint dwarf galaxies is enriched in r-process elements



R process related to rare high yield events not correlated with Iron enrichment

Similar results obtained by  $^{60}\text{Fe}$  and  $^{244}\text{Pu}$  observations in deep sea sediments (Wallner et al, 2015; Hotokezaka et al, 2015)





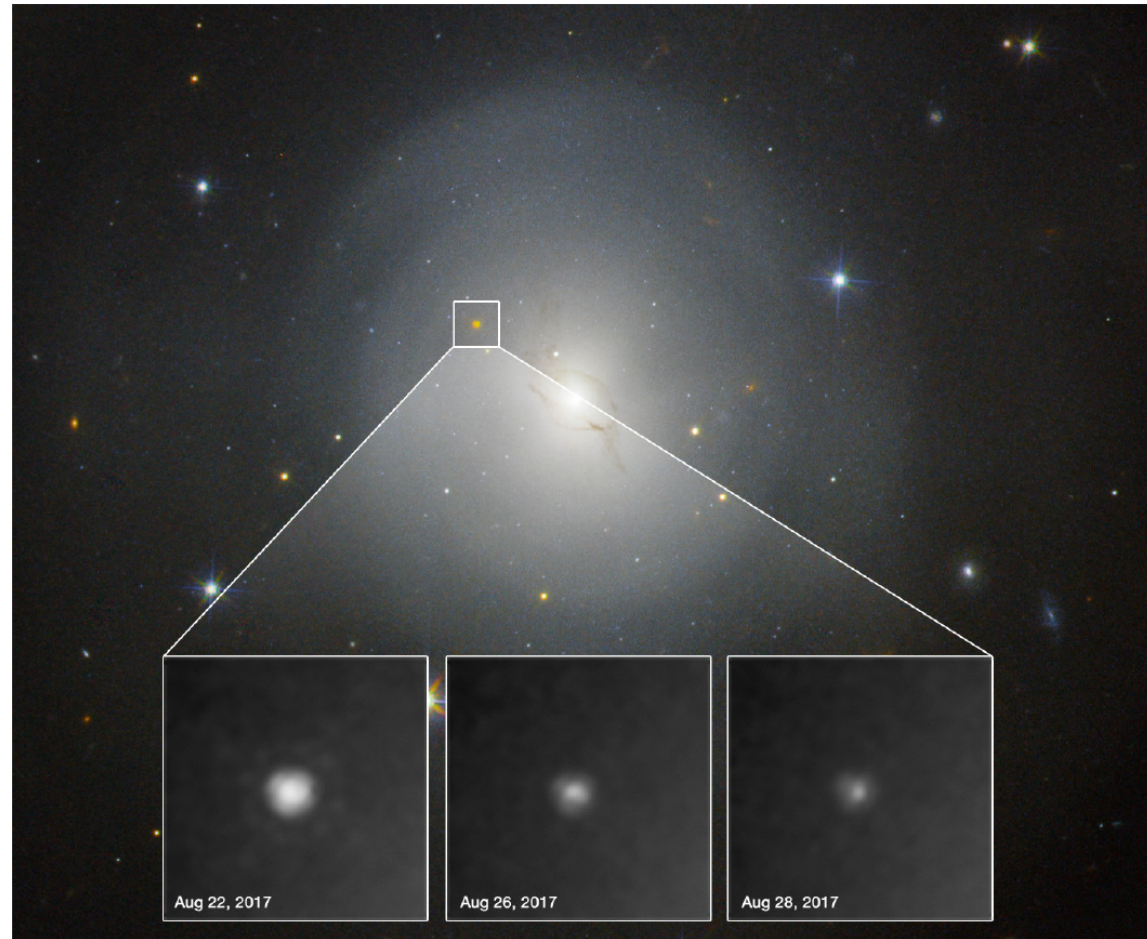






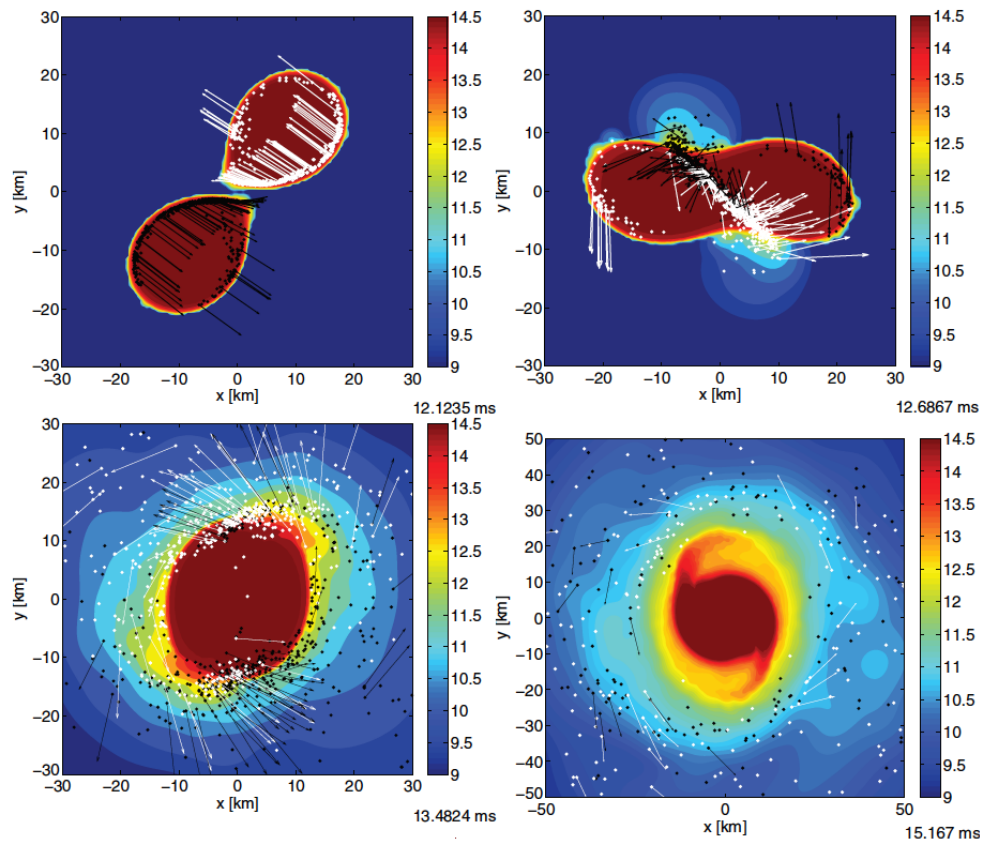
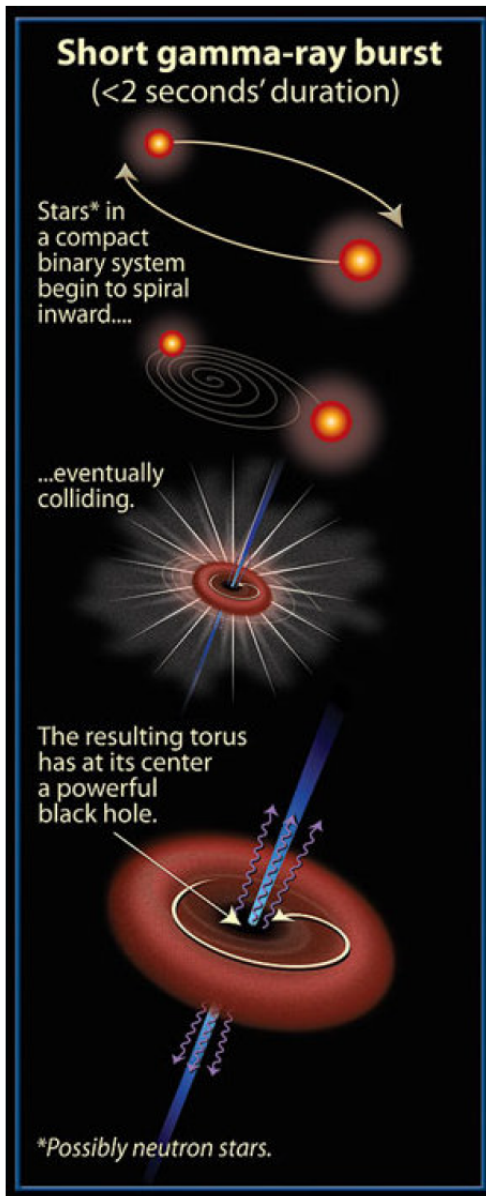
# Kilonova/Macronova luminosity

First direct signal from “in situ” r process operation.



Credit: NASA & ESA. N. Tanvir (U. Leicester), A. Levan (U. Warwick), and A. Fruchter and O. Fox (STScI)

# Neutron star mergers: Short gamma-ray bursts and r-process

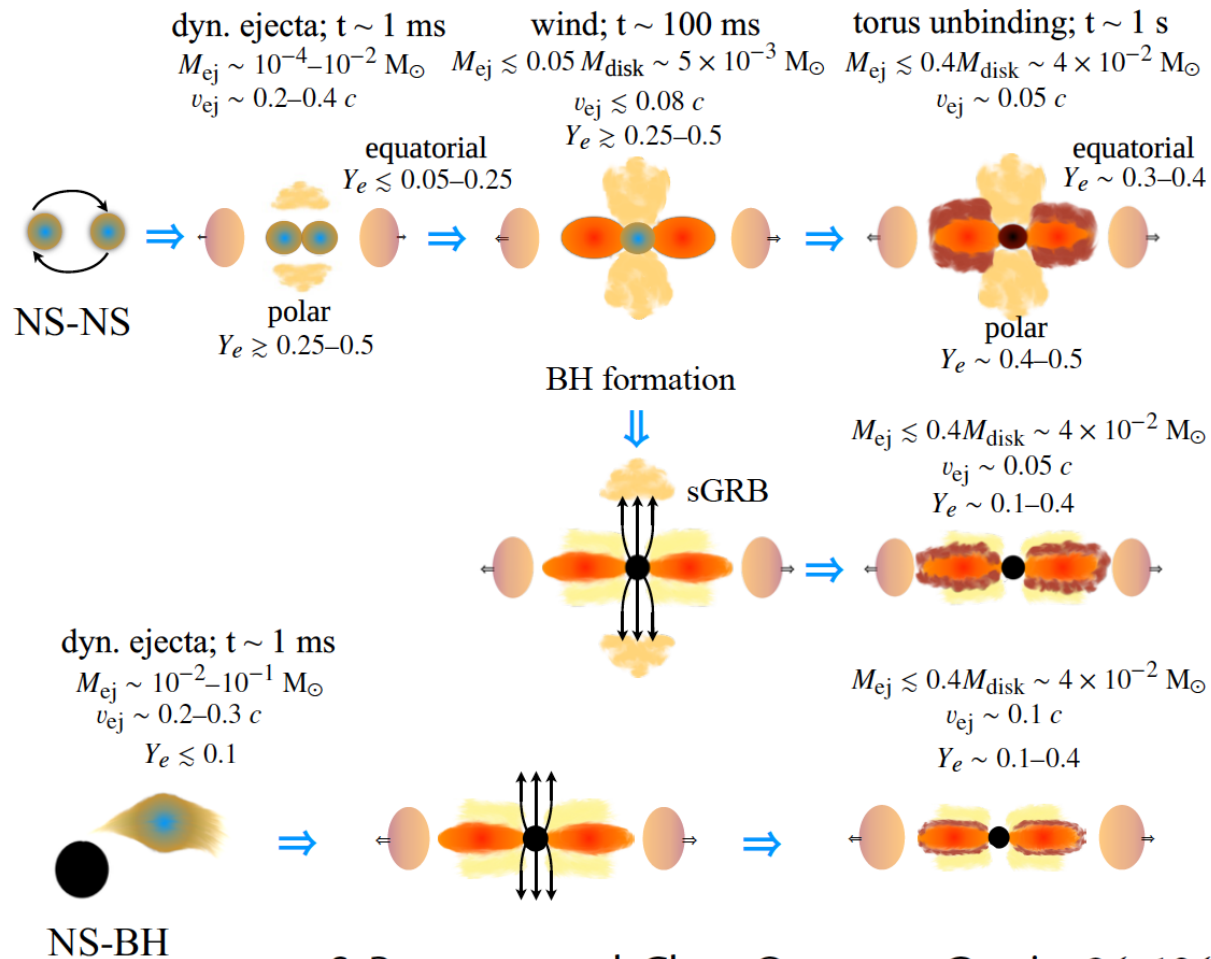


Basuswein, Goriely, Janka, ApJ 773, 78 (2013)

- Mergers are associated with short-gamma ray bursts.
- They are also promising sources of gravitational waves.
- Observational signatures of the r-process?

# Merger channels and ejection mechanism

In mergers we deal with a variety of initial configurations (neutron-star neutron-star vs neutron-star black-hole) with additional variations in the mass-ratio. The evolution after the merger also allows for further variations.

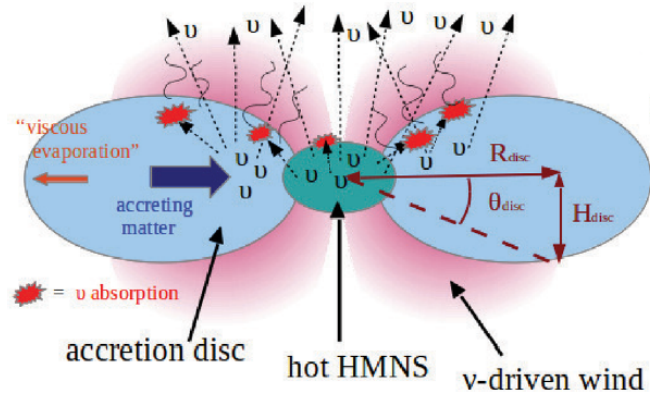




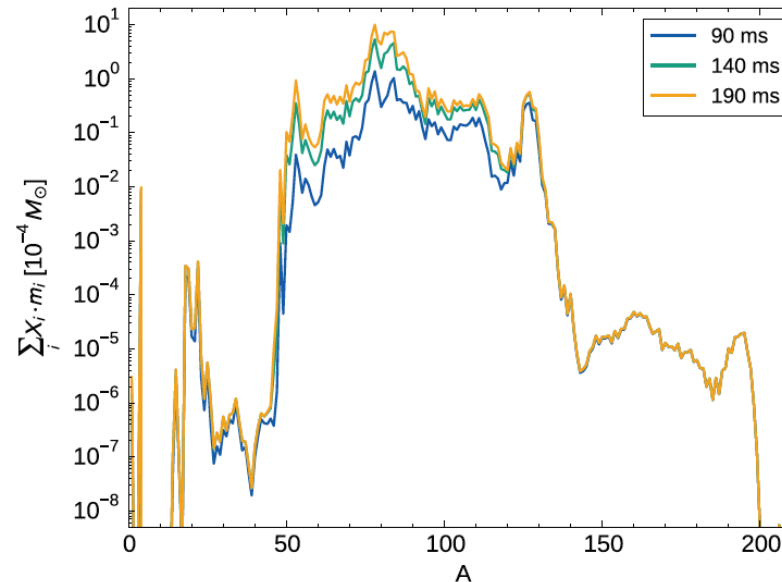


# Post-merger Nucleosynthesis (NS remnant)

An Hypermassive neutron star produces large neutrino fluxes that drive the composition to moderate neutron rich ejecta.

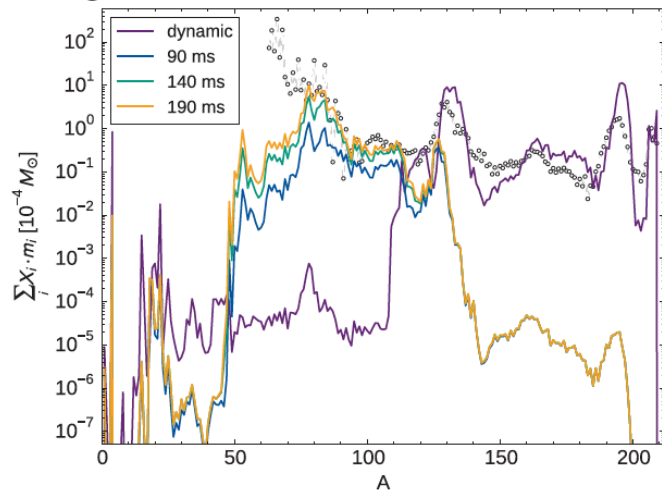


Perego, et al, MNRAS 443, 3134 (2014)



Only nuclei with  $A < 120$  are produced (no lanthanides, blue kilonova).

See also Lippuner et al, MNRAS 472, 904 (2017)

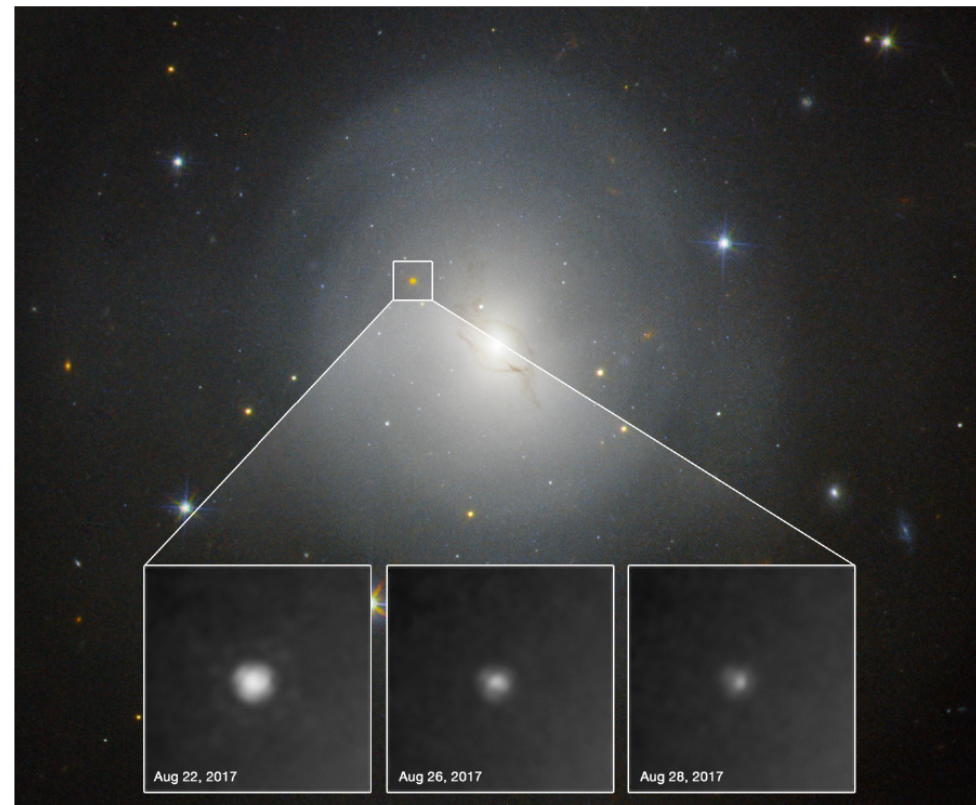


Martin, et al, ApJ 813, 2 (2015)



# AT 2017 gfo: electromagnetic signature from r process

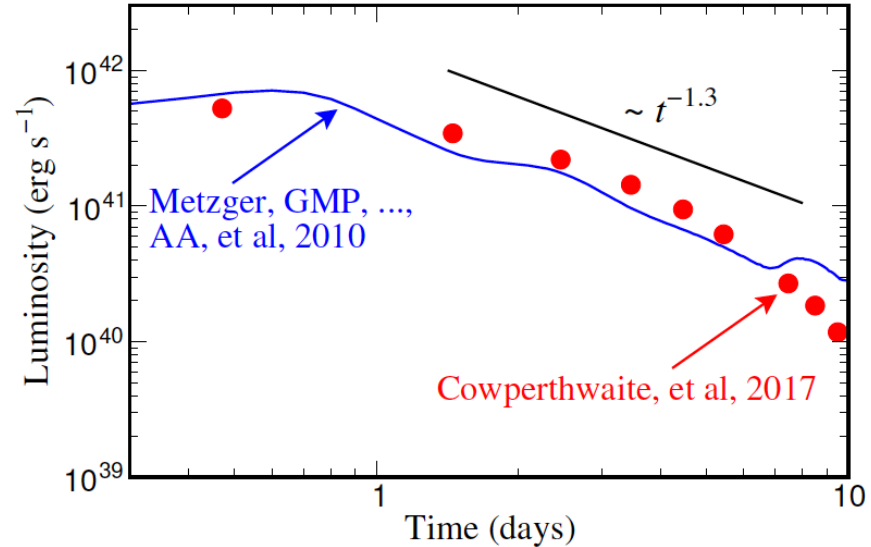
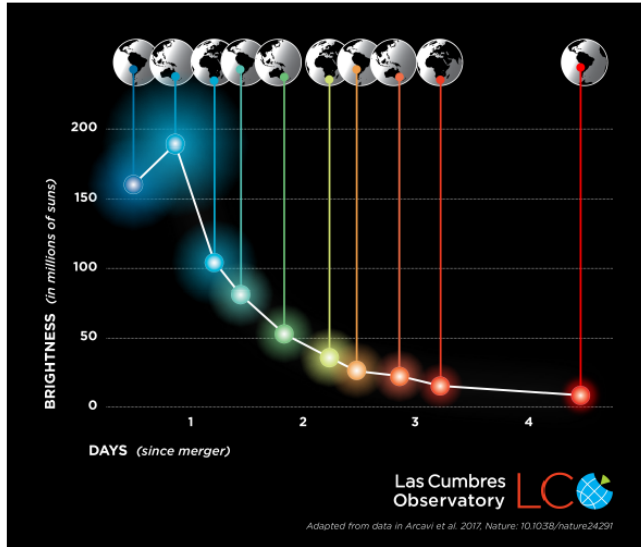
## In-situ signature of r process nucleosynthesis



NASA and ESA. N. Tanvir (U. Leicester), A. Levan (U. Warwick), and A. Fruchter and O. Fox (STScI)

- Novel fastly evolving transient
- Signature of statistical decay of freshly synthesized r process nuclei

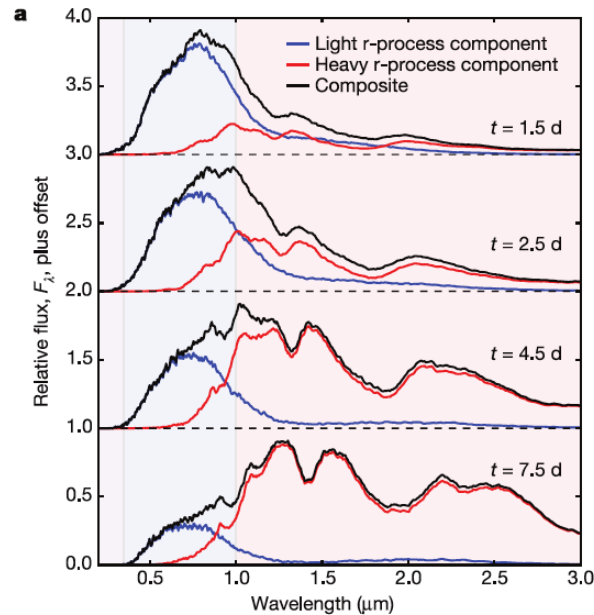
# AT 2017 gfo: interpretation



- Time evolution determined by the radioactive decay of r-process nuclei
- Two components:
  - blue dominated by light elements ( $Z < 50$ )
  - Red due to presence of Lanthanides ( $Z = 57-71$ ) and/or Actinides ( $Z = 89-103$ )
- Likely source of heavy elements including Gold, Platinum and Uranium

# Two components model

Kasen et al, Nature 551, 80 (2017)



- Blue component from polar ejecta subject to strong neutrino fluxes (light r process)

$$M = 0.025 M_{\odot}, v = 0.3c, X_{\text{lan}} = 10^{-4}$$

- Red component disk ejecta after NS collapse to a black hole (includes both light and heavy r process)

$$M = 0.04 M_{\odot}, v = 0.15c, X_{\text{lan}} = 10^{-1.5}$$

